



## University of Bradford eThesis

This thesis is hosted in [Bradford Scholars](#) – The University of Bradford Open Access repository. Visit the repository for full metadata or to contact the repository team



© University of Bradford. This work is licenced for reuse under a [Creative Commons Licence](#).

# **The use of solubility parameters to predict the behaviour of a co-crystalline drug dispersed in a polymeric vehicle**

**Approaches to the prediction of the interactions of co-crystals and their components with hypromellose acetate succinate and the characterization of that interaction using crystallographic, microscopic, thermal, and vibrational analysis**

A thesis presented by

**Abdullah Isreb**

For the degree of

**DOCTOR OF PHILOSOPHY**

Postgraduate studies in pharmaceutical innovations

The School of Pharmacy

University of Bradford



**2012**

## Abstract of the thesis

Approaches to the prediction of the interactions of co-crystals and their components with hypromellose acetate succinate and the characterization of that interaction using crystallographic, microscopic, thermal, and vibrational analysis

Abdullah Isreb

**Keywords:** co-crystals, polymer, caffeine, malonic acid, ibuprofen, nicotinamide, HPMCAS, solvent effect, solubility parameters.

Dispersing co-crystals in a polymeric carrier may improve their physicochemical properties such as dissolution rate and solubility. Additionally co-crystal stability may be enhanced. However, such dispersions have been little investigated to date. This study focuses on the feasibility of dispersing co-crystals in a polymeric carrier and theoretical calculations to predict their stability.

Acetone/chloroform, ethanol/water, and acetonitrile were used to load and grow co-crystals in a HPMCAS film. Caffeine-malonic acid and ibuprofen-nicotinamide co-crystals were prepared using solvent evaporation method. The interactions between each of the co-crystals components and their mixtures with the polymer were studied. A solvent evaporation approach was used to incorporate each compound, a mixture, and co-crystals into HPMCAS films.

Differential scanning calorimetry data revealed a higher affinity of the polymer to acidic compounds than their basic counterparts as noticed by the depression of the glass transition temperature ( $T_g$ ). Moreover, the same drug loading produced films with different  $T_g$ s when different solvents were used. Solubility parameter values (SP) of the solvents were employed to predict that effect on the depression of polymer  $T_g$  with relative success. SP values were more successful in predicting the preferential affinity of two acidic compounds to interact with the polymer. This was confirmed using binary mixtures of naproxen, flurbiprofen, malonic acid, and ibuprofen. On the other hand, dispersing basic compounds such as caffeine or nicotinamide with malonic acid in HPMCAS film revealed the growth of co-crystals. A dissolution study showed that the average release of caffeine from films containing caffeine-malonic acid was not significantly different to that of films containing similar caffeine

concentration. The stability of the caffeine-malonic acid co-crystals in HPMC-AS was prolonged to 8 weeks at 95% relative humidity and 45°C.

The theory developed in this project, that an acidic drug with a SP value closer to the polymer will dominate the interaction process and prevent the majority of the other material from interacting with the polymer, may have utility in designing co-crystal systems in polymeric vehicles.

## **Acknowledgement**

Firstly I would like to thank my supervisors, Prof. Rob Forbes and Dr. Michael Bonner for providing their support and guidance through my study.

I would like to thank my parents for their motivation and support throughout my life.

I would also like to thank all my colleagues in the University of Bradford for their support and for the amazing time we had together. I would like to give a special thanks to Dr. Debbie Fischer for motivating me and putting up with my whinging when things were not going to plan.

I would like to give a big thank to Dave Benson for being like a father providing me with help and support through the whole study.

I would like to give a big thank as well to the exam office team, Hannah, Janet, and Julie, in addition to all invigilators whom I worked with. We were like one big family.

I would like to thank the IPI staff for their support and help through the project.

Last but not least, I would like to thank Shin-Etsu for giving us the HPMCAS and for support.

## **Publications and conferences**

### **Posters**

University of Bradford open day 2010

American association for Pharmaceutical Sciences 2010

Academy of Pharmaceutical Sciences 2011

University of Bradford open day 2012

# Table of contents

LIST OF ABBREVIATIONS .....	XXIV
CHAPTER 1 .....	26
INTRODUCTION.....	26
1.1 INTRODUCTION .....	1
1.2 PHYSICAL MODIFICATION: SOLID DISPERSIONS.....	2
1.2.1 ADVANTAGES AND DISADVANTAGES OF SOLID DISPERSION TECHNIQUE .....	4
1.2.2 METHODS OF PREPARING SOLID DISPERSIONS .....	6
1.2.2.1 Melting method .....	6
1.2.2.2 Solvent evaporation method.....	7
1.3 CHEMICAL MODIFICATIONS: CO-CRYSTALLIZATION.....	8
1.3.1 METHODS OF PREPARING CO-CRYSTALS.....	10
1.3.1.1 Solvent based co-crystallization methods.....	11
1.3.1.2 Non-solvent methods.....	12
1.3.2 FACTORS THAT AFFECT THE FORMATION OF CO-CRYSTALS .....	13
1.3.3 ADVANTAGES AND DISADVANTAGES OF CO-CRYSTALS.....	14
1.3.3.1 Melting point .....	16
1.3.3.2 Stability .....	16
1.3.3.3 Solution stability .....	17
1.3.3.4 Solubility .....	17
1.3.3.5 Dissolution .....	18
1.3.3.6 Bioavailability .....	18
1.4 SOLUBILITY AND COHESION PARAMETERS.....	20
1.5 SUMMARY AND SCOPE OF THE THESIS.....	25
1.6 AIMS AND OBJECTIVES .....	25

<b>1.7 SELECTION OF MATERIALS.....</b>	<b>27</b>
<b>CHAPTER 2 .....</b>	<b>27</b>
<b>MATERIALS AND METHODS .....</b>	<b>27</b>
<b>2.1 MATERIALS.....</b>	<b>29</b>
<b>2.2 DATA ANALYSIS .....</b>	<b>30</b>
2.2.1 THERMAL ANALYSIS.....	30
2.2.1.1 TGA .....	30
2.2.1.2 DSC.....	30
2.2.2 X-RAY CRYSTALLOGRAPHY.....	32
2.2.3 VIBRATIONAL SPECTROSCOPY (FT-IR).....	32
2.2.4 MICROSCOPE ANALYSIS.....	32
2.2.4.1 SEM.....	32
2.2.4.2 Hot stage microscope .....	33
2.2.5 DISSOLUTION STATION.....	33
<b>2.3 METHODS OF PREPARATION OF MATERIALS .....</b>	<b>35</b>
2.3.1 RECRYSTALLIZATION EXPERIMENTS .....	35
2.3.2 CO-CRYSTALLIZATION EXPERIMENTS.....	35
2.3.3 PREPARATION OF FILMS CONTAINING DRUGS OR MIXTURE.....	36
2.3.4 FILMS CONTAINING CO-CRYSTALS .....	36
<b>CHAPTER 3 .....</b>	<b>28</b>
<b>RAW MATERIAL ANALYSIS AND THE STUDY OF THE SOLVENT EFFECT ON THEIR PROPERTIES.....</b>	<b>28</b>
<b>3.1 RAW MATERIAL ANALYSIS.....</b>	<b>37</b>
<b>3.2 UNPROCESSED DRUG ANALYSIS .....</b>	<b>38</b>
3.2.1 CAFFEINE .....	38
3.2.1.1 Thermal analysis .....	38
TGA and DSC.....	38



3.2.1.3 FT-IR transmission.....	41
3.2.2 MALONIC ACID.....	42
3.2.2.1 Thermal behaviour.....	42
TGA and DSC.....	42
3.2.2.3 Powder X-ray diffraction.....	44
3.2.2.4 FT-IR transmission.....	45
3.2.3 IBUPROFEN.....	47
3.2.3.1 Thermal analysis.....	47
TGA and DSC.....	47
3.2.3.2 Powder X-ray diffraction.....	48
3.2.3.3 FT-IR transmission.....	49
3.2.4 NICOTINAMIDE.....	51
3.2.4.1 Thermal analysis.....	51
TGA and DSC.....	51
3.2.4.2 Powder X-ray diffraction.....	52
3.2.4.3 FT-IR transmission.....	53
3.2.5 NAPROXEN.....	55
3.2.5.1 Thermal analysis.....	55
TGA and DSC.....	55
3.2.5.2 X-Ray.....	56
3.2.5.3 FT-IR transmission.....	57
3.2.6 FLURBIPROFEN.....	59
3.2.6.1 Thermal analysis.....	59
TGA and DSC.....	59
3.2.6.2 X-ray.....	60
3.2.7 HPMCAS.....	62
3.2.7.1 Thermal analysis.....	62
TGA and DSC.....	62
3.2.7.2 Powder X-ray diffraction.....	63

3.2.7.3 FT-IR transmission.....	64
<b>3.3 RECRYSTALLIZATION EXPERIMENTS .....</b>	<b>66</b>
3.3.1 CAFFEINE RECRYSTALLIZATION .....	66
3.3.1.1 Recrystallization using acetone/chloroform 3:2 v/v .....	66
3.3.1.2 Powder X-ray diffraction.....	69
3.3.2 RECRYSTALLIZATION WITH ETHANOL/WATER 4:1 W/W.....	71
3.3.2.1 Thermal analysis .....	71
TGA and DSC.....	71
3.3.2.2 Powder X-ray diffraction.....	72
3.3.3 RECRYSTALLIZATION OF CAFFEINE USING ACETONITRILE .....	74
3.3.3.2 Powder X-ray scan diffraction.....	75
3.3.2 RECRYSTALLIZATION OF MALONIC ACID.....	77
3.3.2.1. Thermal analysis .....	77
TGA and DSC.....	77
3.3.2.2 Powder X-ray diffraction.....	78
<b>3.4 SUMMARY AND CONCLUSION.....</b>	<b>80</b>
<b>CHAPTER 4 .....</b>	<b>36</b>
<b>PREPARATION OF CO-CRYSTALS AND THEIR CHARACTERIZATION.....</b>	<b>36</b>
<b>4.1 INTRODUCTION .....</b>	<b>81</b>
<b>4.2 CO-CRYSTALLIZATION OF CAFFEINE AND MALONIC ACID .....</b>	<b>82</b>
4.2.1 CO-CRYSTAL ANALYSIS .....	82
4.2.1.1 Thermal analysis .....	82
4.2.1.2 Powder X-ray diffraction.....	85
4.2.1.3 FT-IR transmission.....	87
<b>4.3 CO-CRYSTALLIZATION OF IBUPROFEN AND NICOTINAMIDE .....</b>	<b>88</b>
4.3.1 THERMAL ANALYSIS.....	88

TGA & DSC.....	88
4.3.2 POWDER X-RAY DIFFRACTION.....	89
4.3.3 FT-IR TRANSMISSION .....	90
<b>4.4 CO-CRYSTALLIZATION OF NICOTINAMIDE AND MALONIC ACID.....</b>	<b>92</b>
4.4.1 THERMAL ANALYSIS.....	92
TGA & DSC.....	92
4.4.2 POWDER X-RAY DIFFRACTION.....	94
4.4.3 FT-IR TRANSMISSION .....	95
<b>4.5 SUMMARY AND CONCLUSIONS.....</b>	<b>97</b>
<b>CHAPTER 5 .....</b>	<b>80</b>
<b>SOLVENT EFFECT ON THE HPMCAS PROPERTIES AND TEC-HPMCAS INTERACTION.....</b>	<b>80</b>
<b>5.1 INTRODUCTION .....</b>	<b>99</b>
<b>5.2 SOLUBILITY PARAMETERS OF THE RAW MATERIALS.....</b>	<b>99</b>
<b>5.3 THE EFFECT OF SOLVENT ON POLYMER PHYSICAL PROPERTIES (PLASTICITY).....</b>	<b>101</b>
<b>5.4 THERMAL ANALYSIS .....</b>	<b>101</b>
<b>5.5 SOLVENT EFFECT ON THE PLASTICIZER-POLYMER INTERACTION .....</b>	<b>103</b>
<b>5.6 SUMMARY AND CONCLUSION.....</b>	<b>107</b>
<b>CHAPTER 6 .....</b>	<b>98</b>
<b>PREPARATION AND CHARACTERISATION OF HPCMAS FILMS CONTAINING ACIDIC DRUGS/SPECIES....</b>	<b>98</b>
<b>6.1 INTRODUCTION .....</b>	<b>110</b>
<b>6.2 PREPARATION AND CHARACTERISATION OF HPCMAS FILMS CONTAINING A SINGLE ACIDIC DRUG/SPECIES .....</b>	<b>111</b>
6.2.1 MALONIC ACID.....	111
6.2.1.1 <i>General analysis</i> .....	112
6.2.1.2 <i>Thermal analysis</i> .....	112

<i>TGA and DSC</i> .....	112
6.2.1.3 <i>Powder X-ray diffraction</i> .....	115
6.2.1.4 <i>FT-IR transmission</i> .....	116
6.2.1.5 <i>Hot Stage Microscopy</i> .....	117
6.2.1.6 <i>SEM</i> .....	118
6.2.2 <i>IBUPROFEN</i> .....	119
6.2.2.1 <i>Thermal analysis</i> .....	119
6.2.2.2 <i>Powder X-ray diffraction</i> .....	121
6.2.2.3 <i>FT-IR transmission</i> .....	122
6.2.2.4 <i>Hot stage microscopy</i> .....	123
<b>6.3 CHARACTERISATION OF FILMS CONTAINING TWO DIFFERENT ACIDIC SPECIES/DRUGS.....</b>	<b>124</b>
6.3.1 <i>FILMS CONTAINING MALONIC ACID WITH IBUPROFEN</i> .....	124
6.3.1.1 <i>Thermal analysis</i> .....	125
6.3.1.2 <i>powder X-ray diffraction</i> .....	128
6.3.1.3 <i>FT-IR transmission</i> .....	129
6.3.1.4 <i>Hot Stage Microscopy</i> .....	130
6.3.2 <i>INVESTIGATION OF HPMCAS FILMS CONTAINING MALONIC ACID AND NAPROXEN</i> .....	131
6.3.2.1 <i>Thermal analysis</i> .....	132
6.3.2.2 <i>Powder X-ray diffraction</i> .....	134
6.3.2.3 <i>Hot Stage Microscopy</i> .....	135
6.3.3 <i>FLURBIPROFEN AS A BLOCKER OF THE ACIDIC DRUG-POLYMER INTERACTION</i> .....	137
6.3.3.1 <i>General analysis</i> .....	137
6.3.3.2 <i>Powder X-ray diffraction</i> .....	137
<b>6.4 SUMMARY AND CONCLUSION.....</b>	<b>141</b>
<b>CHAPTER 7.....</b>	<b>109</b>
<b>FILMS CONTAINING BASIC DRUGS AND THEIR PHYSICOCHEMICAL PROPERTIES.....</b>	<b>109</b>
<b>7.1 INTRODUCTION.....</b>	<b>144</b>

<b>7.2 FILMS CONTAINING CAFFEINE .....</b>	<b>145</b>
7.2.1 GENERAL ANALYSIS .....	145
7.2.2 THERMAL ANALYSIS .....	145
7.2.2.1 TGA .....	145
7.2.2.2 DSC.....	146
7.2.3 POWDER X-RAY DIFFRACTION.....	147
7.2.4 FT-IR TRANSMISSION .....	148
7.2.5 SEM .....	149
<b>7.3 FILMS CONTAINING NICOTINAMIDE.....</b>	<b>151</b>
7.3.1 THERMAL ANALYSIS.....	151
7.3.1.1 TGA analysis.....	151
7.3.1.2 DSC analysis .....	152
7.3.2 FT-IR TRANSMISSION .....	153
<b>7.4 CHARACTERISATION OF FILMS PREPARED CONTAINING ONE ACIDIC AND ONE BASIC SPECIES/DRUG .....</b>	<b>155</b>
7.4.1 FILMS CONTAINING CAFFEINE AND MALONIC ACID .....	155
7.4.1.1 Thermal analysis .....	156
TGA & DSC .....	156
7.4.1.2 Powder X-ray diffraction.....	157
7.4.1.3 FT-IR transmission.....	158
7.4.1.4 Hot stage microscopy .....	159
7.4.2 FILMS CONTAINING NICOTINAMIDE AND MALONIC ACID.....	162
7.4.2.1 Thermal analysis .....	162
7.4.2.2 Powder X-ray diffraction.....	164
7.4.2.3 FT-IR transmission.....	165
<b>7.5 SUMMARY AND CONCLUSION.....</b>	<b>166</b>
<b>MANUFACTURE AND STABILITY OF CO-CRYSTALS IN A POLYMERIC CARRIER .....</b>	<b>168</b>

<b>8.1 INTRODUCTION .....</b>	<b>169</b>
8.2 HPMCAS FILMS CONTAINING CO-CRYSTALS OF CAFFEINE AND MALONIC ACID .....	170
8.2.1 THERMAL ANALYSIS .....	170
TGA & DSC.....	170
8.2.2 Powder X-ray diffraction.....	172
8.2.2 FT-IR transmission.....	173
8.3 FILMS CONTAINING CO-CRYSTALS OF IBUPROFEN AND NICOTINAMIDE.....	176
8.3.1 Thermal analysis .....	176
TGA and DSC.....	176
8.3.2 powder X-ray diffraction.....	177
8.3.3 FT-IR transmission.....	178
8.4 THE USE OF A BLOCKING AGENT FOR IBUPROFEN-HPMCAS INTERACTION.....	180
8.4.1 General analysis.....	181
8.4.2 Thermal analysis .....	181
TGA & DSC .....	181
8.4.3 Powder X-ray diffraction.....	183
8.4.4 FT-IR transmission.....	183
8.5 DISSOLUTION TEST .....	185
8.4.6 Stability study .....	186
<b>8.5 SUMMARY AND CONCLUSIONS .....</b>	<b>189</b>
<b>CHAPTER 9 .....</b>	<b>193</b>
<b>SUMMARY, CONCLUSIONS, AND FUTURE WORK .....</b>	<b>193</b>
<b>SUMMARY AND CONCLUSION .....</b>	<b>193</b>
<b>REFERENCES.....</b>	<b>202</b>

AAKEROY, C. B. (1999) HYDROGEN-BONDING IN SOLIDS - SOME STRATEGIES AND ASPECTS OF CRYSTAL ENGINEERING. IN: SEDDON, K. R. ANDZAWOROTKO, M. (EDS.) *CRYSTAL ENGINEERING: THE DESIGN AND APPLICATION OF FUNCTIONAL SOLIDS*. (NATO ADVANCED SCIENCE INSTITUTES SERIES,

SERIES C, MATHEMATICAL AND PHYSICAL SCIENCES) VOL. 539. DORDRECHT: KLUWER ACADEMIC PUBL, PP. 303-324. ....	202
AAKEROY, C. B., ET AL. (2001) "TOTAL SYNTHESIS" SUPRAMOLECULAR STYLE: DESIGN AND HYDROGEN-BOND-DIRECTED ASSEMBLY OF TERNARY SUPERMOLECULES. <i>ANGEWANDTE CHEMIE-INTERNATIONAL EDITION IN ENGLISH-</i> , 40 (17), 3240-3242. ....	202
AAKERÖY, C. B. AND SALMON, D. J. (2005) BUILDING CO-CRYSTALS WITH MOLECULAR SENSE AND SUPRAMOLECULAR SENSIBILITY. <i>CRYSTENGCOMM</i> , 7 (72), 439-448. ....	202
ABRAMOWITZ, R. AND YALKOWSKY, S. H. (1990) MELTING POINT, BOILING POINT, AND SYMMETRY. <i>PHARMACEUTICAL RESEARCH</i> , 7 (9), 942-947. ....	202
AINOUZ, A., ET AL. (2009) MODELING AND PREDICTION OF COCRYSTAL PHASE DIAGRAMS. <i>INTERNATIONAL JOURNAL OF PHARMACEUTICS</i> , 374 (1-2), 82-89. ....	202
AKALIN, E. AND AKYUZ, S. (2006) VIBRATIONAL ANALYSIS OF FREE AND HYDROGEN BONDED COMPLEXES OF NICOTINAMIDE AND PICOLINAMIDE. <i>VIBRATIONAL SPECTROSCOPY</i> , 42 (2), 333-340. ....	202
ALMARSSON, O. AND ZAWOROTKO, M. J. (2004) CRYSTAL ENGINEERING OF THE COMPOSITION OF PHARMACEUTICAL PHASES. DO PHARMACEUTICAL CO-CRYSTALS REPRESENT A NEW PATH TO IMPROVED MEDICINES? <i>CHEMICAL COMMUNICATIONS</i> , (17), 1889-1896. ....	202
ALSHAHATEET, S. F., ET AL. (2004) CO-CRYSTALLINE HYDROGEN BONDED SOLIDS BASED ON THE ALCOHOL-CARBOXYLIC ACID-ALCOHOL SUPRAMOLECULAR MOTIF. <i>CRYSTENGCOMM</i> , 6 (3), 5-10...	202
ANDERSON, K. M., ET AL. (2008) DESIGNING CO-CRYSTALS OF PHARMACEUTICALLY RELEVANT COMPOUNDS THAT CRYSTALLIZE WITH $Z' > 1$ . <i>CRYSTAL GROWTH &amp; DESIGN</i> , 9 (2), 1082-1087.....	202
BARTON, A. F. M. (1991) <i>CRC HANDBOOK OF SOLUBILITY PARAMETERS AND OTHER COHESION PARAMETERS</i> . CRC. ....	202
BASAVOJU, S., ET AL. (2008) INDOMETHACIN-SACCHARIN COCRYSTAL: DESIGN, SYNTHESIS AND PRELIMINARY PHARMACEUTICAL CHARACTERIZATION. <i>PHARMACEUTICAL RESEARCH</i> , 25 (3), 530-541. ....	202

BASHIRI-SHAHROODI, A., ET AL. (2008) PREPARATION OF A SOLID DISPERSION BY A DROPPING METHOD TO IMPROVE THE RATE OF DISSOLUTION OF MELOXICAM. <i>DRUG DEVELOPMENT AND INDUSTRIAL PHARMACY</i> , 34 (7), 781-788. ....	202
BERRY, D. J., ET AL. (2008) APPLYING HOT-STAGE MICROSCOPY TO CO-CRYSTAL SCREENING: A STUDY OF NICOTINAMIDE WITH SEVEN ACTIVE PHARMACEUTICAL INGREDIENTS. <i>CRYSTAL GROWTH AND DESIGN</i> , 8 (5), 1697-1712. ....	202
BERTOLASI, V., ET AL. (2001) GENERAL RULES FOR THE PACKING OF HYDROGEN-BONDED CRYSTALS AS DERIVED FROM THE ANALYSIS OF SQUARIC ACID ANIONS: AMINOAROMATIC NITROGEN BASE CO-CRYSTALS. <i>ACTA CRYSTALLOGRAPHICA SECTION B</i> , 57 (4), 591-598. ....	203
BETHUNE, S. J. (2009). <i>THERMODYNAMIC AND KINETIC PARAMETERS THAT EXPLAIN CRYSTALLIZATION AND SOLUBILITY OF PHARMACEUTICAL COCRYSTALS</i> . DOCTOR OF PHILOSOPHY. THE UNIVERSITY OF MICHIGAN .....	203
BHARATE, S. S., ET AL. (2010) INTERACTIONS AND INCOMPATIBILITIES OF PHARMACEUTICAL EXCIPIENTS WITH ACTIVE PHARMACEUTICAL INGREDIENTS: A COMPREHENSIVE REVIEW. <i>JOURNAL OF EXCIPIENTS AND FOOD CHEMICALS</i> , 1.....	203
BIKIARIS, D., ET AL. (2005) PHYSICOCHEMICAL STUDIES ON SOLID DISPERSIONS OF POORLY WATER-SOLUBLE DRUGS: EVALUATION OF CAPABILITIES AND LIMITATIONS OF THERMAL ANALYSIS TECHNIQUES. <i>THERMOCHIMICA ACTA</i> , 439 (1&2), 58-67.....	203
BLAGDEN, N., ET AL. (2007) CRYSTAL ENGINEERING OF ACTIVE PHARMACEUTICAL INGREDIENTS TO IMPROVE SOLUBILITY AND DISSOLUTION RATES. <i>ADVANCED DRUG DELIVERY REVIEWS</i> , 59 (7), 617-630.....	203
BONDI, A. (1947) ON THE SOLUBILITY OF PARAFFIN-CHAIN COMPOUNDS. <i>THE JOURNAL OF PHYSICAL CHEMISTRY</i> , 51 (4), 891-903.....	203
BONDI, A. (1968) <i>PHYSICAL PROPERTIES OF MOLECULAR CRYSTALS, LIQUIDS, AND GLASSES</i> . WILEY NEW YORK. ....	203



BOTHE, H. AND CAMMENGA, H. K. (1980) COMPOSITION, PROPERTIES, STABILITY AND THERMAL DEHYDRATION OF CRYSTALLINE CAFFEINE HYDRATE. <i>THERMOCHIMICA ACTA</i> , 40 (1), 29-39. ....	203
BOUGEARD, D., ET AL. (1988) VIBRATIONAL SPECTRA AND DYNAMICS OF CRYSTALLINE MALONIC ACID AT ROOM TEMPERATURE. <i>SPECTROCHIMICA ACTA PART A: MOLECULAR SPECTROSCOPY</i> , 44 (12), 1281-1286. ....	203
BRAGA, D., ET AL. (2007) MAKING CRYSTALS FROM CRYSTALS: A SOLID-STATE ROUTE TO THE ENGINEERING OF CRYSTALLINE MATERIALS, POLYMORPHS, SOLVATES AND CO-CRYSTALS; CONSIDERATIONS ON THE FUTURE OF CRYSTAL ENGINEERING. IN: <i>39TH COURSE OF THE INTERNATIONAL SCHOOL OF CRYSTALLOGRAPHY ON ENGINEERING OF CRYSTALLINE MATERIALS PROPERTIES</i> . ERICE, ITALY: SPRINGER, PP. 131-156. ....	203
BUDAVARI, S. (2006) <i>THE MERCK INDEX: AN ENCYCLOPEDIA OF CHEMICALS, DRUGS, AND BIOLOGICALS</i> . VOL. 113. MERCK AND CO., INC. ....	203
BURKE, J. (1984) SOLUBILITY PARAMETERS: THEORY AND APPLICATION. ....	203
CAIRA, M. R., ET AL. (1995) SELECTIVE FORMATION OF HYDROGEN BONDED COCRYSTALS BETWEEN A SULFONAMIDE AND AROMATIC CARBOXYLIC ACIDS IN THE SOLID STATE. <i>JOURNAL OF THE CHEMICAL SOCIETY, PERKIN TRANSACTIONS 2</i> , (12), 2213-2216. ....	203
CAIRES, F. J., ET AL. (2009) THERMAL BEHAVIOUR OF MALONIC ACID, SODIUM MALONATE AND ITS COMPOUNDS WITH SOME BIVALENT TRANSITION METAL IONS. <i>THERMOCHIMICA ACTA</i> , 497 (1-2), 35-40. ....	203
CEBALLOS, A., ET AL. (2005) INFLUENCE OF FORMULATION AND PROCESS VARIABLES ON IN VITRO RELEASE OF THEOPHYLLINE FROM DIRECTLY-COMPRESSED EUDRAGIT MATRIX TABLETS. <i>IL FARMACO</i> , 60 (11-12), 913-918. ....	203
CHARMAN, S. A. AND CHARMAN, W. N. (2003) ORAL MODIFIED-RELEASE DELIVERY SYSTEMS. <i>DRUGS AND THE PHARMACEUTICAL SCIENCES</i> , 126, 1-10. ....	204
CHEMFINDER, C. S. C. (2004) CHEMFINDER. COM DATABASE, 2004. <i>RETRIEVED MAY-DEC</i> . ....	204

CHIARELLA, R. A., ET AL. (2007) MAKING CO-CRYSTALS THE UTILITY OF TERNARY PHASE DIAGRAMS. <i>CRYSTAL GROWTH &amp; DESIGN</i> , 7 (7), 1223-1226.....	204
CHILDS, S. L. (2008) NOVEL COCRYSTALLIZATION. GOOGLE PATENTS.....	204
CHILDS, S. L., ET AL. (2008) SCREENING STRATEGIES BASED ON SOLUBILITY AND SOLUTION COMPOSITION GENERATE PHARMACEUTICALLY ACCEPTABLE COCRYSTALS OF CARBAMAZEPINE. <i>CRYSTENGCOMM</i> , 10 (7), 856-864.....	204
CHIOU, W. L. AND RIEGELMAN, S. (1969) PREPARATION AND DISSOLUTION CHARACTERISTICS OF SEVERAL FAST RELEASE SOLID DISPERSIONS OF GRISEOFULVIN. <i>JOURNAL OF PHARMACEUTICAL SCIENCES</i> , 58 (12), 1505-1510.....	204
CHIOU, W. L. AND RIEGELMAN, S. (1971) PHARMACEUTICAL APPLICATIONS OF SOLID DISPERSION SYSTEMS. <i>JOURNAL OF PHARMACEUTICAL SCIENCES</i> , 60 (9), 1281-1302. ....	204
COLIN W, P. (2006) FORMULATION OF POORLY WATER-SOLUBLE DRUGS FOR ORAL ADMINISTRATION: PHYSICOCHEMICAL AND PHYSIOLOGICAL ISSUES AND THE LIPID FORMULATION CLASSIFICATION SYSTEM. <i>EUROPEAN JOURNAL OF PHARMACEUTICAL SCIENCES</i> , 29 (3-4), 278-287.....	204
DAMIAN, F., ET AL. (2000) PHYSICOCHEMICAL CHARACTERIZATION OF SOLID DISPERSIONS OF THE ANTIVIRAL AGENT UC-781 WITH POLYETHYLENE GLYCOL 6000 AND GELUCIRE 44/14. <i>EUROPEAN JOURNAL OF PHARMACEUTICAL SCIENCES</i> , 10 (4), 311-322.....	204
DESAI, J., ET AL. (2006) CHARACTERIZATION OF POLYMERIC DISPERSIONS OF DIMENHYDRINATE IN ETHYL CELLULOSE FOR CONTROLLED RELEASE. <i>INTERNATIONAL JOURNAL OF PHARMACEUTICS</i> , 308 (1-2), 115-123. ....	204
DONG, Z. AND CHOI, D. S. (2008) HYDROXYPROPYL METHYLCELLULOSE ACETATE SUCCINATE: POTENTIAL DRUG-EXCIPIENT INCOMPATIBILITY. <i>AAPS PHARMSCITECH</i> , 9 (3), 991-997. ....	204
DUNKEL, M. Z. (1928) CALCULATION OF INTERMOLECULAR FORCES IN ORGANIC COMPOUNDS. <i>PHYS CHEM</i> , 138, 42-54.....	204

EMEL'YANENKO, V. N. AND VEREVKIN, S. P. (2008) THERMODYNAMIC PROPERTIES OF CAFFEINE: RECONCILIATION OF AVAILABLE EXPERIMENTAL DATA. <i>THE JOURNAL OF CHEMICAL THERMODYNAMICS</i> , 40 (12), 1661-1665. ....	204
ETTER, M. C. (1990) ENCODING AND DECODING HYDROGEN-BOND PATTERNS OF ORGANIC COMPOUNDS. <i>ACCOUNTS OF CHEMICAL RESEARCH</i> , 23 (4), 120-126. ....	204
ETTER, M. C. (1991) HYDROGEN BONDS AS DESIGN ELEMENTS IN ORGANIC CHEMISTRY. <i>THE JOURNAL OF PHYSICAL CHEMISTRY</i> , 95 (12), 4601-4610. ....	204
ETTER, M. C. AND REUTZEL, S. M. (1991) HYDROGEN BOND DIRECTED COCRYSTALLIZATION AND MOLECULAR RECOGNITION PROPERTIES OF ACYCLIC IMIDES. <i>JOURNAL OF THE AMERICAN CHEMICAL SOCIETY</i> , 113 (7), 2586-2598. ....	204
FEELY, L. C. AND DAVIS, S. S. (1988) THE INFLUENCE OF POLYMERIC EXCIPIENTS ON DRUG RELEASE FROM HYDROXYPROPYLMETHYLCELLULOSE MATRICES. <i>INTERNATIONAL JOURNAL OF PHARMACEUTICS</i> , 44 (1-3), 131-139. ....	205
FISCHER, H. C. AND CHAN, W. C. W. (2007) NANOTOXICITY: THE GROWING NEED FOR IN VIVO STUDY. <i>CURRENT OPINION IN BIOTECHNOLOGY</i> , 18 (6), 565-571. ....	205
FRISCIC, T. AND JONES, W. (2007) COCRYSTAL ARCHITECTURE AND PROPERTIES: DESIGN AND BUILDING OF CHIRAL AND RACEMIC STRUCTURES BY SOLID-SOLID REACTIONS. <i>FARADAY DISCUSS.</i> , 136, 167-178. ....	205
FRIŠČIĆ, T. AND JONES, W. (2010) BENEFITS OF COCRYSTALLISATION IN PHARMACEUTICAL MATERIALS SCIENCE: AN UPDATE. <i>JOURNAL OF PHARMACY AND PHARMACOLOGY</i> , 62 (11), 1547-1559. ....	205
GAGNIERE, E., ET AL. (2009) COCRYSTAL FORMATION IN SOLUTION: IN SITU SOLUTE CONCENTRATION MONITORING OF THE TWO COMPONENTS AND KINETIC PATHWAYS. <i>CRYSTAL GROWTH &amp; DESIGN</i> , 9 (8), 3376-3383. ....	205
GHADERI, R., ET AL. (1999) PREPARATION OF BIODEGRADABLE MICROPARTICLES USING SOLUTION-ENHANCED DISPERSION BY SUPERCRITICAL FLUIDS (SEDS). <i>PHARMACEUTICAL RESEARCH</i> , 16 (5), 676-681. ....	205

GOOD, D., ET AL. (2011) DEPENDENCE OF COCRYSTAL FORMATION AND THERMODYNAMIC STABILITY ON MOISTURE SORPTION BY AMORPHOUS POLYMER. <i>CRYSTENGCOMM</i> , 13 (4), 1181-1189. ....	205
GREENHALGH, D. J., ET AL. (1999) SOLUBILITY PARAMETERS AS PREDICTORS OF MISCIBILITY IN SOLID DISPERSIONS. <i>JOURNAL OF PHARMACEUTICAL SCIENCES</i> , 88 (11), 1182-1190. ....	205
GRIESSER, U. J. AND BURGER, A. (1995) THE EFFECT OF WATER VAPOR PRESSURE ON DESOLVATION KINETICS OF CAFFEINE 4/5-HYDRATE* 1. <i>INTERNATIONAL JOURNAL OF PHARMACEUTICS</i> , 120 (1), 83-93.....	205
GRIESSER, U. J., ET AL. (1999) VAPOR PRESSURE AND HEAT OF SUBLIMATION OF CRYSTAL POLYMORPHS. <i>JOURNAL OF THERMAL ANALYSIS AND CALORIMETRY</i> , 57 (1), 45-60. ....	205
GUIDELINE, I. C. H. H. T. (2003) STABILITY TESTING OF NEW DRUG SUBSTANCES AND PRODUCTS. <i>RECOMMENDED FOR ADOPTION AT STEP, 4</i> . ....	205
HICKEY, M. B., ET AL. (2007) PERFORMANCE COMPARISON OF A CO-CRYSTAL OF CARBAMAZEPINE WITH MARKETED PRODUCT. <i>EUROPEAN JOURNAL OF PHARMACEUTICS AND BIOPHARMACEUTICS</i> , 67 (1), 112-119.....	205
HILDEBRAND, J. H. AND SCOTT, R. L. (1950) SOLUTIONS OF NONELECTROLYTES. <i>ANNUAL REVIEW OF PHYSICAL CHEMISTRY</i> , 1 (1), 75-92. ....	205
HINO, T. AND FORD, J. L. (2001) CHARACTERIZATION OF THE HYDROXYPROPYLMETHYLCELLULOSE-NICOTINAMIDE BINARY SYSTEM. <i>INTERNATIONAL JOURNAL OF PHARMACEUTICS</i> , 219 (1), 39-49. ....	205
HINO, T., ET AL. (2001) ASSESSMENT OF NICOTINAMIDE POLYMORPHS BY DIFFERENTIAL SCANNING CALORIMETRY. <i>THERMOCHIMICA ACTA</i> , 374 (1), 85-92. ....	205
HUANG, J., ET AL. (2008) DRUG-POLYMER INTERACTION AND ITS SIGNIFICANCE ON THE PHYSICAL STABILITY OF NIFEDIPINE AMORPHOUS DISPERSION IN MICROPARTICLES OF AN AMMONIO METHACRYLATE COPOLYMER AND ETHYLCELLULOSE BINARY BLEND. <i>JOURNAL OF PHARMACEUTICAL SCIENCES</i> , 97 (1), 251-262.....	205

HUBERT, S., ET AL. (2011) PROCESS INDUCED TRANSFORMATIONS DURING TABLET MANUFACTURING: PHASE TRANSITION ANALYSIS OF CAFFEINE USING DSC AND LOW FREQUENCY MICRO-RAMAN SPECTROSCOPY. <i>INTERNATIONAL JOURNAL OF PHARMACEUTICS</i> . .....	206
IBRAHIM, A. Y., ET AL. (2010) SPONTANEOUS CRYSTAL GROWTH OF CO-CRYSTALS: THE CONTRIBUTION OF PARTICLE SIZE REDUCTION AND CONVECTION MIXING OF THE CO-FORMERS. <i>CRYSTENGCOMM</i> . .....	206
JAYASANKAR, A. (2008) UNDERSTANDING THE MECHANISMS, THERMODYNAMICS AND KINETICS OF COCRYSTALLIZATION TO CONTROL PHASE TRANSFORMATIONS. ....	206
JAYASANKAR, A., ET AL. (2007) MECHANISMS BY WHICH MOISTURE GENERATES COCRYSTALS. ....	206
JAYASANKAR, A., ET AL. (2006A) COCRYSTAL FORMATION DURING COGRINDING AND STORAGE IS MEDIATED BY AMORPHOUS PHASE. <i>PHARMACEUTICAL RESEARCH</i> , 23 (10), 2381-2392. ....	206
JAYASANKAR, A., ET AL. (2006B) COCRYSTAL FORMATION DURING COGRINDING AND STORAGE IS MEDIATED BY AMORPHOUS PHASE. <i>PHARMACEUTICAL RESEARCH</i> , 23 (10), 2381-2392. ....	206
JUBERT, A., ET AL. (2006) VIBRATIONAL AND THEORETICAL STUDIES OF NON-STEROIDAL ANTI-INFLAMMATORY DRUGS IBUPROFEN [2-(4-ISOBUTYLPHENYL)PROPIONIC ACID]; NAPROXEN [6-METHOXY-[ALPHA]-METHYL-2-NAPHTHALENE ACETIC ACID] AND TOLMETIN ACIDS [1-METHYL-5-(4-METHYLBENZOYL)-1H-PYRROLE-2-ACETIC ACID]. <i>JOURNAL OF MOLECULAR STRUCTURE</i> , 783 (1-3), 34-51.....	206
KABLITZ, C. D. S. E., ET AL. (2006) DRY COATING IN A ROTARY FLUID BED. <i>EUROPEAN JOURNAL OF PHARMACEUTICAL SCIENCES</i> , 27 (2-3), 212-219. ....	206
KANG, B. K., ET AL. (2004) DEVELOPMENT OF SELF-MICROEMULSIFYING DRUG DELIVERY SYSTEMS (SMEDDS) FOR ORAL BIOAVAILABILITY ENHANCEMENT OF SIMVASTATIN IN BEAGLE DOGS. <i>INTERNATIONAL JOURNAL OF PHARMACEUTICS</i> , 274 (1-2), 65-73. ....	206
KANIG, J. L. (1964) PROPERTIES OF FUSED MANNITOL IN COMPRESSED TABLETS. <i>JOURNAL OF PHARMACEUTICAL SCIENCES</i> , 53 (2), 188-192. ....	206

KAZARIAN, S. G. AND MARTIROSYAN, G. G. (2002) SPECTROSCOPY OF POLYMER/DRUG FORMULATIONS PROCESSED WITH SUPERCRITICAL FLUIDS: IN SITU ATR-IR AND RAMAN STUDY OF IMPREGNATION OF IBUPROFEN INTO PVP. <i>INTERNATIONAL JOURNAL OF PHARMACEUTICS</i> , 232 (1-2), 81-90.....	206
KISHI, Y. AND MATSUOKA, M. (2010) PHENOMENA AND KINETICS OF SOLID-STATE POLYMORPHIC TRANSITION OF CAFFEINE. <i>CRYSTAL GROWTH &amp; DESIGN</i> , 10 (7), 2916-2920. ....	206
KONNO, H. AND TAYLOR, L. S. (2006) INFLUENCE OF DIFFERENT POLYMERS ON THE CRYSTALLIZATION TENDENCY OF MOLECULARLY DISPERSED AMORPHOUS FELODIPINE. <i>JOURNAL OF PHARMACEUTICAL SCIENCES</i> , 95 (12), 2692-2705.....	206
KRISTYÁN, S. AND PULAY, P. (1994) CAN (SEMI) LOCAL DENSITY FUNCTIONAL THEORY ACCOUNT FOR THE LONDON DISPERSION FORCES? <i>CHEMICAL PHYSICS LETTERS</i> , 229 (3), 175-180.....	206
LACOUILONCHE, F., ET AL. (1997) AN INVESTIGATION OF FLURBIPROFEN POLYMORPHISM BY THERMOANALYTICAL AND SPECTROSCOPIC METHODS AND A STUDY OF ITS INTERACTIONS WITH POLY-(ETHYLENE GLYCOL) 6000 BY DIFFERENTIAL SCANNING CALORIMETRY AND MODELLING. <i>INTERNATIONAL JOURNAL OF PHARMACEUTICS</i> , 153 (2), 167-179. ....	207
LEUNER, C. AND DRESSMAN, J. (2000) IMPROVING DRUG SOLUBILITY FOR ORAL DELIVERY USING SOLID DISPERSIONS. <i>EUROPEAN JOURNAL OF PHARMACEUTICS AND BIOPHARMACEUTICS</i> , 50 (1), 47-60.....	207
LEVY, G. (1963) EFFECT OF PARTICLE SIZE ON DISSOLUTION AND GASTROINTESTINAL ABSORPTION RATES OF PHARMACEUTICALS. <i>AMERICAN JOURNAL OF PHARMACY AND THE SCIENCES SUPPORTING PUBLIC HEALTH</i> , 135, 78.....	207
LI, Z., ET AL. (2009) A PRACTICAL SOLID FORM SCREEN APPROACH TO IDENTIFY A PHARMACEUTICAL GLUTARIC ACID COCRYSTAL FOR DEVELOPMENT. <i>ORGANIC PROCESS RESEARCH &amp; DEVELOPMENT</i> , 13 (6), 1307-1314.....	207
LIN, S. Y., ET AL. (1995) DRUG-POLYMER INTERACTION AFFECTING THE MECHANICAL PROPERTIES, ADHESION STRENGTH AND RELEASE KINETICS OF PIROXICAM-LOADED EUDRAGIT E FILMS PLASTICIZED WITH DIFFERENT PLASTICIZERS. <i>JOURNAL OF CONTROLLED RELEASE</i> , 33 (3), 375-381. .	207

LLOYD, G. R., ET AL. (1999) A CALORIMETRIC INVESTIGATION INTO THE INTERACTION BETWEEN PARACETAMOL AND POLYETHYLENE GLYCOL 4000 IN PHYSICAL MIXES AND SOLID DISPERSIONS. <i>EUROPEAN JOURNAL OF PHARMACEUTICS AND BIOPHARMACEUTICS</i> , 48 (1), 59-65.....	207
LONDON, F. (1937) THE GENERAL THEORY OF MOLECULAR FORCES. <i>TRANS. FARADAY SOC.</i> , 33 (0), 8B-26.....	207
LOPEZ, D. AND MIJANGOS, C. (1994) EFFECT OF SOLVENT ON GLASS TRANSITION TEMPERATURE IN CHEMICALLY MODIFIED POLYVINYL CHLORIDE (PVC). <i>COLLOID &amp; POLYMER SCIENCE</i> , 272 (2), 159-167. ....	207
LÓPEZ, D. AND MIJANGOS, C. (1994) EFFECT OF SOLVENT ON GLASS TRANSITION TEMPERATURE IN CHEMICALLY MODIFIED POLYVINYL CHLORIDE (PVC). <i>COLLOID &amp; POLYMER SCIENCE</i> , 272 (2), 159-167.....	207
LU, E., ET AL. (2008) A RAPID THERMAL METHOD FOR COCRYSTAL SCREENING. <i>CRYSTENGCOMM</i> , 10 (6), 665-668.....	207
MAHANTY, J. AND NINHAM, B. W. (1976) <i>DISPERSION FORCES</i> . VOL. 5. IMA.....	207
MAHESHWARI, C., ET AL. (2009A) FACTORS THAT INFLUENCE THE SPONTANEOUS FORMATION OF PHARMACEUTICAL COCRYSTALS BY SIMPLY MIXING SOLID REACTANTS. <i>CRYSTENGCOMM</i> , 11 (3), 493-500.....	207
MAHESHWARI, C., ET AL. (2009B) FACTORS THAT INFLUENCE THE SPONTANEOUS FORMATION OF PHARMACEUTICAL COCRYSTALS BY SIMPLY MIXING SOLID REACTANTS. <i>CRYSTENGCOMM</i> , 11 (3), 493-500.....	207
MANDUVA, R., ET AL. (2008) CALORIMETRIC AND SPATIAL CHARACTERIZATION OF POLYMORPHIC TRANSITIONS IN CAFFEINE USING QUASI ISOTHERMAL MTDSC AND LOCALIZED THERMOMECHANICAL ANALYSIS. <i>JOURNAL OF PHARMACEUTICAL SCIENCES</i> , 97 (3), 1285-1300.....	207
MARSAC, P., ET AL. (2009) ESTIMATION OF DRUG-POLYMER MISCIBILITY AND SOLUBILITY IN AMORPHOUS SOLID DISPERSIONS USING EXPERIMENTALLY DETERMINED INTERACTION PARAMETERS. <i>PHARMACEUTICAL RESEARCH</i> , 26 (1), 139-151. ....	207

MAYERSOHN, M. AND GIBALDI, M. (1966) NEW METHOD OF SOLID STATE DISPERSION FOR INCREASING DISSOLUTION RATES. <i>JOURNAL OF PHARMACEUTICAL SCIENCES</i> , 55 (11), 1323-1324. ...	208
MCMAMARA, D., ET AL. (2006) USE OF A GLUTARIC ACID COCRYSTAL TO IMPROVE ORAL BIOAVAILABILITY OF A LOW SOLUBILITY API. <i>PHARMACEUTICAL RESEARCH</i> , 23 (8), 1888-1897. ....	208
MIRZA, S., ET AL. (2008) CO-CRYSTALS: AN EMERGING APPROACH TO IMPROVING PROPERTIES OF PHARMACEUTICAL SOLIDS. IN: <i>19TH HELSINKI DRUG RESEARCH</i> . HELSINKI, FINLAND: ELSEVIER SCIENCE BV, PP. S16-S17. ....	208
MOHAMMAD, M. A., ET AL. (2011) HANSEN SOLUBILITY PARAMETER AS A TOOL TO PREDICT COCRYSTAL FORMATION. <i>INTERNATIONAL JOURNAL OF PHARMACEUTICS</i> . ....	208
MURDANDE, S. B., ET AL. (2011) SOLUBILITY ADVANTAGE OF AMORPHOUS PHARMACEUTICALS, PART 3: IS MAXIMUM SOLUBILITY ADVANTAGE EXPERIMENTALLY ATTAINABLE AND SUSTAINABLE? <i>JOURNAL OF PHARMACEUTICAL SCIENCES</i> . ....	208
NAKAYAMA, S., ET AL. (2009) STRUCTURE AND PROPERTIES OF IBUPROFEN-HYDROXYPROPYL METHYLCELLULOSE NANOCOMPOSITE GEL. <i>POWDER TECHNOLOGY</i> , IN PRESS, CORRECTED PROOF.	208
OGUCHI, T., ET AL. (2000) SPECIFIC COMPLEXATION OF URSODEOXYCHOLIC ACID WITH GUEST COMPOUNDS INDUCED BY CO-GRINDING. <i>PHYSICAL CHEMISTRY CHEMICAL PHYSICS</i> , 2 (12), 2815-2820. ....	208
PADRELA, L., ET AL. (2010) SCREENING FOR PHARMACEUTICAL COCRYSTALS USING THE SUPERCRITICAL FLUID ENHANCED ATOMIZATION PROCESS. <i>THE JOURNAL OF SUPERCRITICAL FLUIDS</i> , 53 (1-3), 156-164. ....	208
PADRELA, L., ET AL. (2009) FORMATION OF INDOMETHACIN-SACCHARIN COCRYSTALS USING SUPERCRITICAL FLUID TECHNOLOGY. <i>EUROPEAN JOURNAL OF PHARMACEUTICAL SCIENCES</i> , 38 (1), 9-17. ....	208
PAN, R. N., ET AL. (2000) ENHANCEMENT OF DISSOLUTION AND BIOAVAILABILITY OF PIROXICAM IN SOLID DISPERSION SYSTEMS. <i>DRUG DEVELOPMENT AND INDUSTRIAL PHARMACY</i> , 26 (9), 989-994.	208



PATEL, T., ET AL. ENHANCEMENT OF DISSOLUTION OF FENOFIBRATE BY SOLID DISPERSION TECHNIQUE. <i>INTERN J RES PHARM SCI</i> , 1 (2), 127-132.....	208
PATRA, B. B. AND SAMANTRAY, B. (2011) <i>ENGINEERING CHEMISTRY I</i> . PEARSON EDUCATION INDIA. .....	208
PATRICK, J. J., ET AL. (1998) CHARACTERIZATION OF IMPURITIES FORMED BY INTERACTION OF DULOXETINE HCL WITH ENTERIC POLYMERS HYDROXYPROPYL METHYLCELLULOSE ACETATE SUCCINATE AND HYDROXYPROPYL METHYLCELLULOSE PHTHALATE. <i>JOURNAL OF PHARMACEUTICAL SCIENCES</i> , 87 (1), 81-85. ....	208
PEDIREDDI, V. R., ET AL. (1996) CREATION OF CRYSTALLINE SUPRAMOLECULAR ARRAYS: A COMPARISON OF CO-CRYSTAL FORMATION FROM SOLUTION AND BY SOLID-STATE GRINDING. <i>CHEMICAL COMMUNICATIONS</i> , (8), 987-988.....	208
POKHARKAR, V. B., ET AL. (2006) DEVELOPMENT, CHARACTERIZATION AND STABILIZATION OF AMORPHOUS FORM OF A LOW TG DRUG. <i>POWDER TECHNOLOGY</i> , 167 (1), 20-25. ....	208
PORTER III, W. W., ET AL. (2008) POLYMORPHISM IN CARBAMAZEPINE COCRYSTALS. <i>CRYSTAL GROWTH AND DESIGN</i> , 8 (1), 14-16. ....	208
PUTTIIPATKHACHORN, S., ET AL. (2001) DRUG PHYSICAL STATE AND DRUG-POLYMER INTERACTION ON DRUG RELEASE FROM CHITOSAN MATRIX FILMS. <i>JOURNAL OF CONTROLLED RELEASE</i> , 75 (1-2), 143-153.....	209
REDDY, L. S., ET AL. (2008) COCRYSTALS AND SALTS OF GABAPENTIN: PH DEPENDENT COCRYSTAL STABILITY AND SOLUBILITY. <i>CRYSTAL GROWTH AND DESIGN</i> , 9 (1), 378-385.....	209
REMENAR, J. F., ET AL. (2003) CRYSTAL ENGINEERING OF NOVEL COCRYSTALS OF A TRIAZOLE DRUG WITH 1, 4-DICARBOXYLIC ACIDS. <i>J. AM. CHEM. SOC</i> , 125 (28), 8456-8457.....	209
RIEDEL, A. AND LEOPOLD, C. S. (2005) DEGRADATION OF OMEPRAZOLE INDUCED BY ENTERIC POLYMER SOLUTIONS AND AQUEOUS DISPERSIONS: HPLC INVESTIGATIONS. <i>DRUG DEVELOPMENT AND INDUSTRIAL PHARMACY</i> , 31 (2), 151-160. ....	209

RODIER, E., ET AL. (2005) A THREE STEP SUPERCRITICAL PROCESS TO IMPROVE THE DISSOLUTION RATE OF EFLUCIMIBE. <i>EUROPEAN JOURNAL OF PHARMACEUTICAL SCIENCES</i> , 26 (2), 184-193. ....	209
RODRÍGUEZ-HORNEDO, N., ET AL. (2006) REACTION CRYSTALLIZATION OF PHARMACEUTICAL MOLECULAR COMPLEXES. <i>MOLECULAR PHARMACEUTICS</i> , 3 (3), 362-367.....	209
SANDER, J. R. G., ET AL. (2010) PHARMACEUTICAL NANO-COCRYSTALS: SONOCHEMICAL SYNTHESIS BY SOLVENT SELECTION AND USE OF A SURFACTANT. <i>ANGEWANDTE CHEMIE</i> , 122 (40), 7442-7446.....	209
SCHULTHEISS, N. AND NEWMAN, A. (2009) PHARMACEUTICAL COCRYSTALS AND THEIR PHYSICOCHEMICAL PROPERTIES. <i>CRYSTAL GROWTH &amp; DESIGN</i> , 9 (6), 2950-2967.....	209
SEKIGUCHI, K., ET AL. (1964) STUDIES ON ABSORPTION OF EUTECTIC MIXTURE. II. ABSORPTION OF FUSED CONGLOMERATES OF CHLORAMPHENICOL AND UREA IN RABBITS. <i>CHEMICAL &amp; PHARMACEUTICAL BULLETIN</i> , 12, 134. ....	209
SEKIGUCHI KEIJI AND OBI NOBORU (1961) STUDIES ON ABSORPTION OF EUTECTIC MIXTURE. I. A COMPARISON OF THE BEHAVIOR OF EUTECTIC MIXTURE OF SULFATHIAZOLE AND THAT OF ORDINARY SULFATHIAZOLE IN MAN. <i>CHEMICAL &amp; PHARMACEUTICAL BULLETIN</i> , 9 (11), 866-872.....	209
SEO, A., ET AL. (2003) THE PREPARATION OF AGGLOMERATES CONTAINING SOLID DISPERSIONS OF DIAZEPAM BY MELT AGGLOMERATION IN A HIGH SHEAR MIXER. <i>INTERNATIONAL JOURNAL OF PHARMACEUTICS</i> , 259 (1&2), 161-171. ....	209
SHAN, N., ET AL. (2002) MECHANOCHEMISTRY AND CO-CRYSTAL FORMATION: EFFECT OF SOLVENT ON REACTION KINETICS. <i>CHEMICAL COMMUNICATIONS</i> , 2002 (20), 2372-2373. ....	209
SHAN, N. AND ZAWOROTKO, M. J. (2008) THE ROLE OF COCRYSTALS IN PHARMACEUTICAL SCIENCE. <i>DRUG DISCOVERY TODAY</i> , 13 (9-10), 440-446. ....	209
SHIN-ETSU (2005) <i>SHIN-ETSU AQOAT</i> .....	209
SONG, J. S. AND SOHN, Y. T. (2011) CRYSTAL FORMS OF NAPROXEN. <i>ARCHIVES OF PHARMACAL RESEARCH</i> , 34 (1), 87-90.....	209

STANTON, M. K., ET AL. (2009) DRUG SUBSTANCE AND FORMER STRUCTURE PROPERTY RELATIONSHIPS IN 15 DIVERSE PHARMACEUTICAL CO-CRYSTALS. <i>CRYSTAL GROWTH AND DESIGN</i> , 9 (3), 1344-1352. ....	209
STOTT, P. W., ET AL. (1998) TRANSDERMAL DELIVERY FROM EUTECTIC SYSTEMS: ENHANCED PERMEATION OF A MODEL DRUG, IBUPROFEN. <i>JOURNAL OF CONTROLLED RELEASE</i> , 50 (1-3), 297-308. .....	210
STROYER, A., ET AL. (2006) SOLID STATE INTERACTIONS BETWEEN THE PROTON PUMP INHIBITOR OMEPRAZOLE AND VARIOUS ENTERIC COATING POLYMERS. <i>JOURNAL OF PHARMACEUTICAL SCIENCES</i> , 95 (6), 1342-1353. ....	210
TANNO, F., ET AL. (2004) EVALUATION OF HYPROMELLOSE ACETATE SUCCINATE (HPMCAS) AS A CARRIER IN SOLID DISPERSIONS. <i>DRUG DEVELOPMENT AND INDUSTRIAL PHARMACY</i> , 30 (1), 9-17. .	210
TIMKO, R. J. AND LORDI, N. G. (1979) THERMAL CHARACTERIZATION OF CITRIC ACID SOLID DISPERSIONS WITH BENZOIC ACID AND PHENOBARBITAL. <i>JOURNAL OF PHARMACEUTICAL SCIENCES</i> , 68 (5), 601-605. ....	210
TRASK, A. V. AND JONES, W. (2005A) CRYSTAL ENGINEERING OF ORGANIC COCRYSTALS BY THE SOLID- STATE GRINDING APPROACH. IN: <i>ORGANIC SOLID STATE REACTIONS</i> . (TOPICS IN CURRENT CHEMISTRY) VOL. 254. BERLIN: SPRINGER-VERLAG BERLIN, PP. 41-70. ....	210
TRASK, A. V. AND JONES, W. (2005B) CRYSTAL ENGINEERING OF ORGANIC COCRYSTALS BY THE SOLID- STATE GRINDING APPROACH .....	210
ORGANIC SOLID STATE REACTIONS. IN: TODA, F. (ED.) (TOPICS IN CURRENT CHEMISTRY) VOL. 254. SPRINGER BERLIN / HEIDELBERG, PP. 131-131. ....	210
TRASK, A. V., ET AL. (2005) PHARMACEUTICAL COCRYSTALLIZATION: ENGINEERING A REMEDY FOR CAFFEINE HYDRATION. <i>CRYSTAL GROWTH &amp; DESIGN</i> , 5 (3), 1013-1021. ....	210
TRASK, A. V., ET AL. (2006) PHYSICAL STABILITY ENHANCEMENT OF THEOPHYLLINE VIA COCRYSTALLIZATION. <i>INTERNATIONAL JOURNAL OF PHARMACEUTICS</i> , 320 (1-2), 114-123. ....	210

VAN DEN MOOTER, G., ET AL. (2006) EVALUATION OF INUTEC SP1 AS A NEW CARRIER IN THE FORMULATION OF SOLID DISPERSIONS FOR POORLY SOLUBLE DRUGS. <i>INTERNATIONAL JOURNAL OF PHARMACEUTICS</i> , 316 (1-2), 1-6.....	210
VAN DROOGE, D. J., ET AL. (2006) CHARACTERIZATION OF THE MOLECULAR DISTRIBUTION OF DRUGS IN GLASSY SOLID DISPERSIONS AT THE NANO-METER SCALE, USING DIFFERENTIAL SCANNING CALORIMETRY AND GRAVIMETRIC WATER VAPOUR SORPTION TECHNIQUES. <i>INTERNATIONAL JOURNAL OF PHARMACEUTICS</i> , 310 (1-2), 220-229. ....	210
VARIANKAVAL, N., ET AL. (2006) PREPARATION AND SOLID-STATE CHARACTERIZATION OF NONSTOICHIOMETRIC COCRYSTALS OF A PHOSPHODIESTERASE-IV INHIBITOR AND L-TARTARIC ACID. <i>CRYSTAL GROWTH &amp; DESIGN</i> , 6 (3), 690-700.....	210
VASCONCELOS, T. AND COSTA, P. (2007) DEVELOPMENT OF A RAPID DISSOLVING IBUPROFEN SOLID DISPERSION.....	210
VASCONCELOS, T. F., ET AL. (2007) SOLID DISPERSIONS AS STRATEGY TO IMPROVE ORAL BIOAVAILABILITY OF POOR WATER SOLUBLE DRUGS. <i>DRUG DISCOVERY TODAY</i> , 12 (23-24), 1068-1075. ....	210
VERRECK, G., ET AL. (2005) THE EFFECT OF PRESSURIZED CARBON DIOXIDE AS A TEMPORARY PLASTICIZER AND FOAMING AGENT ON THE HOT STAGE EXTRUSION PROCESS AND EXTRUDATE PROPERTIES OF SOLID DISPERSIONS OF ITRACONAZOLE WITH PVP-VA 64. <i>EUROPEAN JOURNAL OF PHARMACEUTICAL SCIENCES</i> , 26 (3-4), 349-358. ....	210
VIPPAGUNTA, S. R., ET AL. (2007) FACTORS AFFECTING THE FORMATION OF EUTECTIC SOLID DISPERSIONS AND THEIR DISSOLUTION BEHAVIOR. <i>JOURNAL OF PHARMACEUTICAL SCIENCES</i> , 96 (2), 294-304.....	211
VISHWESHWAR, P., ET AL. (2006) PHARMACEUTICAL CO-CRYSTAL. <i>JOURNAL OF PHARMACEUTICAL SCIENCES</i> , 95 (3), 499-516.....	211
VOGURI, R. S. (2010). <i>CO-CRYSTALLISATION OF <math>\alpha,\omega</math>-DICARBOXYLIC ACIDS WITH NICOTINAMIDE AND ISONICOTINAMIDE</i> . MSc. UNIVERSITY OF BIRMINGHAM. ....	211

VOGURI, R. S. (SEP 2010A). <i>CO-CRYSTALLISATION OF A,<math>\Omega</math>-DICARBOXYLIC ACIDS WITH NICOTINAMIDE AND ISONICOTINAMIDE</i> . MSc. UNIVERSITY OF BIRMINGHAM. ....	211
VOGURI, R. S. (SEP 2010B). <i>CO-CRYSTALLISATION OF A,<math>\Omega</math>-DICARBOXYLIC ACIDS WITH NICOTINAMIDE AND ISONICOTINAMIDE</i> . MASTER OF RESEARCH. UNIVERSITY OF BIRMINGHAM. ....	211
WANG, C., ET AL. (2007) EFFECT OF DRUG-POLYMER INTERACTION ON DRUG DIFFUSION THROUGH POLYMERIC MEMBRANES. <i>JOURNAL OF MEDICAL AND BIOLOGICAL ENGINEERING</i> , 27 (1), 35.....	211
WANG, X., ET AL. (2005) SOLID STATE CHARACTERISTICS OF TERNARY SOLID DISPERSIONS COMPOSED OF PVP VA64, MYRJ 52 AND ITRACONAZOLE. <i>INTERNATIONAL JOURNAL OF PHARMACEUTICS</i> , 303 (1), 54-61.....	211
WARD, S. C., ET AL. (2003) SYSTEMATIC STUDY INTO THE SALT FORMATION OF FUNCTIONALISED ORGANIC SUBSTRATES. <i>SCHOOL OF CHEMISTRY, UNIVERSITY OF SOUTHAMTON, SO 17BJ, UK SCHOOL MATHEMATICS, UNIVERSITY OF SOUTHAMTON, SO 17BJ, UK</i> . ....	211
WHELAN, M. R., ET AL. (2002) SIMULTANEOUS DETERMINATION OF IBUPROFEN AND HYDROXYPROPYLMETHYLCELLULOSE (HPMC) USING HPLC AND EVAPORATIVE LIGHT SCATTERING DETECTION. <i>JOURNAL OF PHARMACEUTICAL AND BIOMEDICAL ANALYSIS</i> , 30 (4), 1355-1359. ....	211
YAMAGUCHI, H. AND TOMINAGA, T. (2006) FINE PARTICLES OF POORLY WATER-SOLUBLE DRUG HAVING ENTERIC MATERIAL ADSORBED ON PARTICLE SURFACE. GOOGLE PATENTS. ....	211
YAMAGUCHI, H. AND TOMINAGA, T. (2008) MICROPARTICLE OF HARDLY-SOLUBLE SUBSTANCE HAVING ENTERIC BASE MATERIAL ADSORBED ON THE SURFACE OF THE SUBSTANCE. EP PATENT 1,923,051. ....	211
YOSHIHASHI, Y., ET AL. (2006) ESTIMATION OF PHYSICAL STABILITY OF AMORPHOUS SOLID DISPERSION USING DIFFERENTIAL SCANNING CALORIMETRY. <i>JOURNAL OF THERMAL ANALYSIS AND CALORIMETRY</i> , 85 (3), 689-692.....	211
APPENDIX I (TGA).....	212
APPENDIX II (DSC) .....	218
APPENDIX III (POWDER X-RAY DIFFRACTION) .....	231

APPENDIX IV (FT-IR TRANSMISSION).....	233
APPENDIX V (SEM) .....	238
APPENDIX VI (DISSOLUTION TEST) .....	239
APPENDIX VII (STABILITY STUDY) .....	241

## List of abbreviations

API:	Active Pharmaceutical Ingredient.
CMX:	Caffeine and Malonic acid Co-crystals.
CMXH:	Caffeine and Malonic acid inside a film of HPMCAS.
CSD:	Cambridge Structure Database.
DSC:	Differential Scanning Calorimetry.
HPMCAS:	Hydroxypropyl methylcellulose acetate succinate Hypromellose Acetate Succinate
HSM	Hot Stage microscopy.
INX	Ibuprofen nicotinamide co-crystals
INX-MH	Ibuprofen nicotinamide co-crystals in a film with malonic acid as a blocker
PXRD	Powder X-Ray Diffractometry.
SEM:	Scanning Electron Microscopy
SP	Solubility Parameter
TGA	Thermo-Gravimetric Analysis

UV

Ultra violet

## **Chapter 1**

### **Introduction**



## **1.1 Introduction**

The improvement in drug solubility and dissolution rate is considered one of the main targets in drug formulation. This improvement can give rise to a better bioavailability of the drug. There are many approaches that can be used to serve this purpose. These approaches can be divided into physical modifications and chemical modifications.

Changing the physical properties of the active pharmaceutical ingredients (API) can be performed by using one of the various methods that are well documented in the literature such as reducing the particle size, modifying the crystal habit, using polymorphs, and dispersing the drug in carriers. On the other hand, chemical modification includes a variety of methods such as using the salt form of the drug or using the co-crystalline form in addition to others.

Using a combination of these aforementioned methods might further improve the solubility and the dissolution rate for drugs and is the underpinning strategy of this thesis.

## 1.2 Physical modification: solid dispersions

The solid dispersion approach is one of the techniques used to enhance the dissolution rate and the solubility of the poorly soluble drugs (Bashiri-Shahroodi et al., 2008 , Patel et al., Pan et al., 2000). A solid dispersion can be simply defined as the molecular mixture of a poorly soluble drug and a hydrophilic polymer. Both materials are in their solid-state. A solid dispersion was first defined by (Mayersohn and Gibaldi, 1966). A solid dispersion is similar to a eutectic system regarding the improvement on the dissolution and the solubility of the poorly soluble drugs. However, solid dispersions are usually formed as a result of the interaction between the drug and the polymer. This interaction helps to slow or stop the rate of growth of drug crystals and in certain cases it helps to convert the drug into an amorphous material. Reducing the size of the drug has a great effect on dissolution rate as it increases the contact surface between the drug and the dissolution media.

Solid dispersions can be divided into three generations (Vasconcelos et al., 2007) that are summarized in figure 1.1.

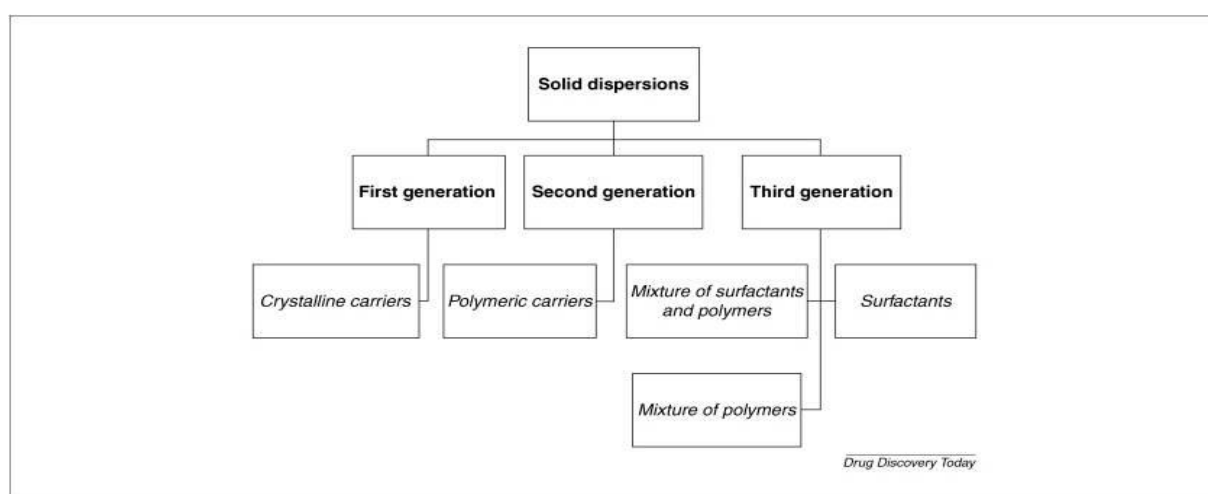


Figure 1.1 types of solid dispersions obtained from (Vasconcelos et al., 2007).

The first generation was noted by Sekiguchi and Obi in 1961. They prepared a eutectic mixture of several drugs and urea (used as a carrier). This mixture resulted in improving the dissolution rate of the drugs. However, the preparation of solid dispersions was improved later by using a molecular dispersion instead of eutectic mixture in preparing the solid dispersion (Levy, 1963, Kanig, 1964). The second generation is characterized by the use of an amorphous carrier as an opposite to the first generation that is using a crystalline carrier for the drug. In this case, the drug is molecularly dispersed within the amorphous carrier. Amorphous solid dispersions can be classified according to the molecular interaction of the drug and the carrier into: solid solutions, solid suspension, or a mixture of both.

Amorphous solid solutions are characterized by the complete miscibility of the drug and the amorphous polymeric carrier resulting in a homogenous molecular interaction between them. This type is considered to be homogenous on the molecular level (Van Drooge et al., 2006).

Amorphous solid suspensions occur when the drug has a limited solubility in the amorphous carrier or it has an extremely high melting point (Chiou and Riegelman, 1971). Unlike the solid solution, this type of solid dispersion is composed of two phases. When the drug is dissolved and suspended in the amorphous carrier, a heterogeneous structure is obtained with mixed properties of amorphous solid solution and suspension and amorphous solid suspension (Van Drooge et al., 2006).

The third generation of the solid dispersion is obtained with the use of a surface active agent in addition to the amorphous carrier. The third generation solid

dispersion is intended to provide the highest degree of bioavailability and stability for poorly soluble drugs in their amorphous form.

The solubility improvement from the physical modification of the drug resulted from reducing drug's particle size, solubilising it in a water soluble carrier, providing a better wettability, and to a certain limit producing an amorphous drug (Damian et al., 2000).

### **1.2.1 Advantages and disadvantages of solid dispersion technique**

Physical modification of the drug is better than chemical modification as the product is not considered as a new chemical entity that needs to go through a clinical trial test before it goes to the market (Charman and Charman, 2003) in (Vasconcelos et al., 2007). However, recent discoveries unveiled the toxicity of some physically modified drugs. Therefore, they have to go through some of the clinical trial tests before being released into the market (Fischer and Chan, 2007).

The main advantage for the solid dispersion technique is the improvement in drugs bioavailability without the need to spend a lot of efforts in their preparation.

The advantages of dispersing the drug in a solid carrier can be summarized in the following points:

#### **1- Reducing drug particle size**

A high surface area is formed as a result of reducing the drug particle size. This reduction can be up to the molecular level and is accompanied by dispersing

the drug in a highly water soluble carrier that will further enhance the release of the drug particles. Consequently, this will improve its bioavailability (Leuner and Dressman, 2000 , Bikiaris et al., 2005).

## **2- Improving the wettability of the drug**

The improvement of drug wettability by solid dispersion of the drug was noticed to be independent of the surface activity of the carrier (Vasconcelos et al., 2007). However, a carrier with a surface activity will provide a significant increase in the wettability of the drug by direct dissolution or co-solvent effect (Kang et al., 2004 , Leuner and Dressman, 2000 , Colin W, 2006).

## **3- Increasing particles porosity**

Drug particles in solid dispersion were found to have a higher degree of porosity (Vasconcelos and Costa, 2007). Therefore, these solid dispersed drugs have a better release profile (Ghaderi et al., 1999).

## **4- Production of amorphous drugs**

When the drug is dissolved in the polymeric carrier, it may convert into its amorphous state. This conversion will provide the drug with a higher solubility and dissolution rate that characterize the amorphous materials (Lloyd et al., 1999).

On the other hand, there are few disadvantages for the solid dispersion technique. The low physical and chemical stability of the amorphous form of the drug is considered one of the major drawbacks that prevent the wide use of this

technique. In addition to that, most of the polymers that are used in this technique can absorb moisture. Consequently, this may give rise to a phase separation, crystal growth, or conversion of a meta-stable crystalline form into a more stable one resulting in decreasing the solubility and dissolution rate (Van den Mooter et al., 2006 , Wang et al., 2007 , Wang et al., 2005).

Another disadvantage of solid dispersions is their poor ease of scale-up for industrial manufacturing (Vasconcelos et al., 2007).

### **1.2.2 Methods of preparing solid dispersions**

Solid dispersions can be prepared using one of the two methods: melting and solvent evaporation.

#### **1.2.2.1 Melting method**

The melting method is the first method to be discovered for the preparation of solid dispersions. The first generation of solid dispersion was prepared using the melting of the urea with other drugs to form an eutectic mixture (Sekiguchi Keiji and Obi Noboru, 1961). Both drug and carrier are melted and mixed to form the new phase. A common adaptation of this technique was conducted by suspending the drug into a previously melted carrier, instead of melting both drug and carrier (Vippagunta et al., 2007). This in turn results in the ability to reduce the processing temperature.

After melting the drug and the carrier, a cooling step is performed by either using an ice bath agitation (Sekiguchi et al., 1964), stainless steel thin layer spreading followed by a cold draught (Chiou and Riegelman, 1969), or using dry

ice or liquid nitrogen (Ceballos et al., 2005 , Timko and Lordi, 1979) in addition to a few other less commonly employed methods.

The high temperature needed to melt both drug and its carrier may cause the degradation of some drugs. This can be considered as one of the disadvantages for this method. Therefore, some improvements to this method were implied by using mechanical forces as in hot melt extrusion or melt agglomeration (Verreck et al., 2005 , Seo et al., 2003).

#### **1.2.2.2 Solvent evaporation method**

This method consists of dissolving the drug and the carrier in a proper solvent. After that, the solvent evaporates and leave behind the dispersed drug in the carrier (Rodier et al., 2005). Evaporating the solvent can be carried out through vacuum drying (Yoshihashi et al., 2006), using some heat (Desai et al., 2006), slow evaporation at low temperature (Yoshihashi et al., 2006), spray drying (Pokharkar et al., 2006), freeze drying (Van Drooge et al., 2006).

Using a low temperature over the whole preparation process is considered the main advantages of this method over the melt approach.

As previously mentioned, the solid dispersion is considered one of the physical modifications to improve the dissolution rate and therefore the bioavailability of the drug. On the other hand, chemical modifications, such as co-crystal formation, can be used to alter the solubility and the dissolution rate of drugs. However, these modifications are harder to achieve and may need to go through a clinical trial tests to insure their potency and safety.

### 1.3 Chemical modifications: co-crystallization

Co-crystal formation is a new technique introduced recently to improve the physicochemical properties of APIs. This technique is based on the combination of two materials together in order to obtain a hybrid compound that has mixed properties of both. There is no unified definition of co-crystals in literature. Some workers have defined them as a combination of multiple components that are solid at room temperature (Aakeröy and Salmon, 2005 , Shan and Zaworotko, 2008 , Almarsson and Zaworotko, 2004). This definition excluded combinations that contain solvent (solvates) or gas molecules as a constituent of the co-crystal. Others have included those divisions in the definition of the co-crystals. Therefore, it is better to define co-crystals as crystalline forms that contain more than one compound in the crystal (Schultheiss and Newman, 2009).

Co-crystals differ from salts in that they are made of polar compounds rather than ionisable compounds as in salts. This suggests that the bonds that link the constituent particles are hydrogen bond, Vander Waals or  $\pi$ - $\pi$  bonds (Aakeröy and Salmon, 2005 , Etter, 1991 , Friščić and Jones, 2010 , Bertolasi et al., 2001 , Aakeroy, 1999 , Aakeroy et al., 2001).

There is no clear boundary that separates co-crystals and salts. It is difficult to differentiate between both as the difference depends mainly on the extent of proton transfer from one molecule to the other or in other words, the bond length (Schultheiss and Newman, 2009). However, there has been suggestions to use the rule of three to differentiate between salts and co-crystals (Ward et al., 2003). This rule states that a PKa difference of three or more between the individual components of the system will cause it to be considered a salt and



less than three will make it a co-crystal (Variankaval et al., 2006 , Ward et al., 2003 , Alshahateet et al., 2004 , Ainouz et al., 2009).

In order to predict the co-crystal formation between two materials a phase diagram is drawn. A ternary phase diagram is classically employed and it is a triangle that has each angle representing one of the components in the co-crystals with the third angle representing the solvent used in preparing the co-crystal. The solubility of each of the two components in the solvent is defined on the triangle and the stoichiometric ratio for co-crystal formation is represented on the third side. This helps to give some idea about the amount required from each of the components and the amount required from the solvent in order for the co-crystals to be formed (figure 1.2).

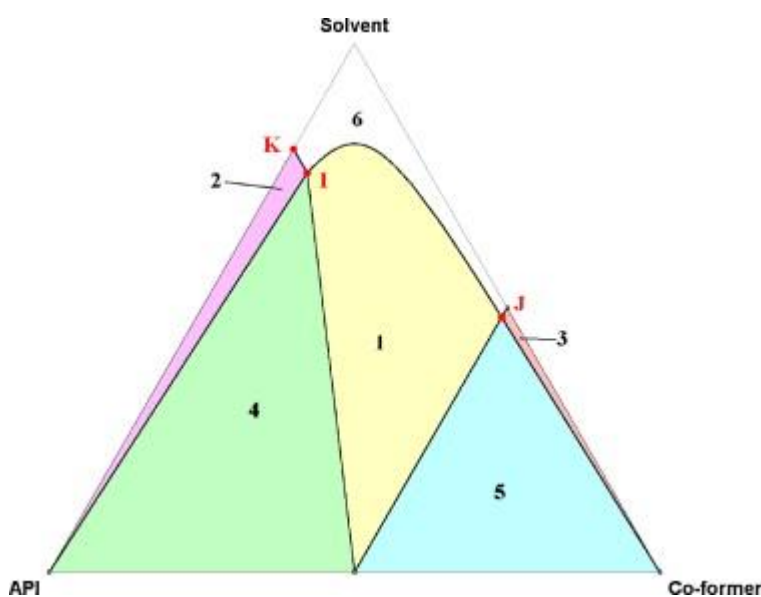


Figure 1.2. General ternary phase diagram(Ainouz et al., 2009). Phase 1: co-crystals formation zone, 2: API+solvent, 3: co-former+solvent, 4: API+co-crystals, 5:co-former+co-crystals, and 6: solution of the mixture.

A ternary phase diagram simplifies the relation between the API, co-crystal former and the solvent. It shows the optimal ratios of co-crystal formers and

solvent. The optimal mixing ratio in figure 1.1 is 1:1 molar ratio of API/co-crystal former.

Generally speaking, co-crystal's properties are usually the average of their component's properties. This means that mixing poorly soluble drugs with a highly soluble entity will result in improving the solubility of the API. Co-crystallization allows changing the physical properties of drugs without any covalent chemical modification.

### **1.3.1 Methods of preparing co-crystals**

Co-crystals can be prepared by solvent or solid based methods. The solvent methods include slurry conversion, anti-solvent addition, solvent evaporation, cooling crystallization and precipitation. The solid-based methods include grinding (dry and wet), melt crystallization, and sonication (wet and dry). In addition to that, there are other methods to prepare co-crystals such as the Kofler method, and the use of moisture amongst others (Maheshwari et al., 2009b , Lu et al., 2008 , Jayasankar et al., 2007).

Co-crystal properties might differ depending on the production technique. Furthermore, co-crystals might only be possible to form using one or two techniques but not others. In addition, one method might produce a polymorphic form of one of the components and this will result in a different final co-crystal.

### **1.3.1.1 Solvent based co-crystallization methods**

#### **1.3.1.1.1 Solution co-crystallization**

The co-crystal components must have similar solubility patterns in the solvent used in the process. If not, the component with the lowest solubility will precipitate first without interacting with other components. Similar solubility of the compounds is not the only condition for this method. Polymorphism plays a role in co-crystal formation in this method. The ability of the compound to form intermolecular bonds plays a role as well (Trask et al., 2005 , Trask et al., 2006 , Chiarella et al., 2007 , Gagniere et al., 2009).

#### **1.3.1.1.2 Slurry conversion**

In this technique solvents are added to the co-crystals components and the resulting suspension is stirred for few days. Afterward, the solvent is decanted and the solid materials dried under the flow of nitrogen gas (Rodríguez-Hornedo et al., 2006 , Porter Iii et al., 2008 , Hickey et al., 2007 , Li et al., 2009).

#### **1.3.1.1.3 Anti solvent addition**

Anti solvent addition is based on the precipitation or re-crystallization of co-crystal formers with the API. An example of this method is the preparation of co-crystals of aceclofenac using chitosan (Padrela et al., 2009 , Trask and Jones, 2005a , Padrela et al., 2010 , Sander et al., 2010).

### **1.3.1.2 Non-solvent methods**

#### **1.3.1.2.1 Grinding**

Co-crystal formation can be achieved by mechanical activation of materials by a mechanical process (grinding). Grinding can be carried out without the addition of a solvent (dry grinding) or with the addition of small amount of solvent (wet-grinding). The amount of added solvent is only enough to wet and partially dissolve parts of the components but not enough to dissolve them completely. The grinding technique depends on the input of mechanical forces to the system that will result in breaking down the crystals and forcing them together in order to create a link or a bond (Trask et al., 2005 , Shan et al., 2002 , Braga et al., 2007). The use of a small amount of a solvent is meant to aid such bond breaking and bond formation by partially dissolving the particles. Co-crystals have been widely formed by dry or wet grinding (Trask et al., 2006 , Etter, 1990 , Etter, 1991 , Etter and Reutzel, 1991 , Caira et al., 1995 , Pedireddi et al., 1996 , Oguchi et al., 2000 , Trask and Jones, 2005b , Jayasankar et al., 2006a , Childs et al., 2008).

The formation of co-crystals passes through the formation of amorphous materials or a disordered phase formed by the reactants. As the process continues, the amorphous reactants convert into co-crystals. This conversion was monitored in the formation of anhydrous carbamazepine and saccharin (Jayasankar et al., 2006b). Although co-crystals usually require some energy to form, some co-crystals formed spontaneously after being stored together with no input of any kind of force. This was the case in the formation of carbamazepine-nicotinamide and carbamazepine-saccharin co-crystals (Maheshwari et al., 2009a).

Co-crystals obtained from grinding are usually similar to those obtained from solution co-crystallization. This indicates that the hydrogen bonds formed between the crystals by these two methods are not idiosyncratic. However, there are few exceptions to this rule. Some co-crystals can be prepared by either solvent-based processes or solid-state grinding. An example is the co-crystallization of 2,4,6-trinitrobenzoic acid and indole-3-acetic acid. On the other hand, some co-crystals cannot be prepared by grinding. This might be due to the inability of the grinding technique to generate suitable co-crystal arrangements rather than the stability of the initial phases. The addition of small amount of solvent during the grinding process has been shown to enhance the kinetics and facilitate co-crystal formation (Maheshwari et al., 2009a).

### **1.3.2 Factors that affect the formation of co-crystals**

There are some factors that might influence the quality and the outcome yield of co-crystallization processes. These factors can be divided according to the method of manufacturing and the mechanism behind the formation. Solvent-related methods are characterized by the obvious effect of the nature of the solvent used in the experiment. The type of solvent might play a significant role in enhancing or blocking the formation of co-crystals. The formation of co-crystals in solvent-dependent methods (wet-methods) depends on dissolving the co-crystal formers in a solvent to break down the bond between similar molecules and allow the different type of molecule to meet up and form a bond. If the solvent used in this experiment does not have the adequate strength to dissolve those particles. This might cause interference to the whole formation

process. If the solvent was too strong and formed a bond with one of the materials, it might block the formation of the co-crystal bond.

On the other hand, dry co-crystallization methods are affected by other factors. Grinding for example uses mechanical forces to break similar crystals apart. This technique reduces the size of the crystals and consequently increases the surface free energy and the surface charges. This might trigger the formation of co-crystals. On the other hand any electrostatic charge that results from the grinding may cause the particles to aggregate and prevent the formation of co-crystals.

Melting the materials is another technique used to form co-crystals. However, some drugs can be adversely affected by the increase in temperature. The heating of such drugs can result in the degradation of these drugs and consequent loss of pharmacological activity.

### **1.3.3 Advantages and disadvantages of co-crystals**

The main disadvantage of the co-crystals is their short-term physical stability. This has resulted in keeping the co-crystals out of the market so far.

Co-crystallization means an improvement of physical properties without changing drugs chemically. In contrast to salt formation co-crystallization is applicable for a larger number of APIs. This is because most of the APIs are polar in nature, while the formation of a salt requires the ionization of the compounds. In addition to that, co-crystal formation does not require full ionization of the molecules involved. The polar nature of most APIs makes co-

crystallization potentially a much more widely preferable technique over salt formation.

Moreover, there is a wider range of molecules that can be used as co-crystal formers compared to salt formers (Mirza et al., 2008).

Many physicochemical properties can be manipulated through co-crystal formation these includes hygroscopicity, melting point, stability, bioavailability, and dissolution rate. These changes makes co-crystals better than their parent drugs for the pharmaceutical field.

### **1.3.3.1 Melting point**

The melting point of a compound is related to aqueous solubility and vapour pressure (Abramowitz and Yalkowsky, 1990). The melting point of a co-crystal can be either lower than one of their constituents or in some cases lower than the melting point of all the constituents (Rodríguez-Hornedo et al., 2006 , Jayasankar, 2008 , Childs, 2008 , Reddy et al., 2008 , Maheshwari et al., 2009b). Characterization of co-crystals using differential scanning calorimeter (DSC) to determine their melting point can be a useful tool to check the formation of co-crystals and to provide an overall idea about the percentage of co-crystal formation (Schultheiss and Newman, 2009).

### **1.3.3.2 Stability**

Drug stability is considered to be one of the main issues during the formulation of the drug and for choosing the crystal form to be used in formulation. The stability of the co-crystals is determined by the ability of the co-crystals to stay intact without breaking the bond in between the constituent compounds. The resistance of drug to moisture stress is an important consideration in stability study.

The effect of moisture on the stability of the co-crystals has not been thoroughly investigated. Some crystals were found to interact and form co-crystals under high relative humidity atmospheres (Jayasankar et al., 2007). However, not all co-crystals can be formed by moisture interaction. Whilst moisture can theoretically act as a solvent it can also act to break co-crystal bonds. There is little if any information in the open literature to prove or disprove this point.



Some studies, however, have shown that co-crystals are less hygroscopic than their parent drugs (Basavoju et al., 2008 , Schultheiss and Newman, 2009).

#### **1.3.3.3 Solution stability**

This property is an important characteristic for the dissolution of the co-crystals in the GI tract (Schultheiss and Newman, 2009 , Stanton et al., 2009 , Jayasankar, 2008).

#### **1.3.3.4 Solubility**

Solubility is considered as one of the main issues in the bioavailability of drugs. There is a large number of drugs that have either poor or low solubility in simulated aqueous GI tract solutions. Co-crystals formation may improve the solubility of drugs. However, co-crystals can be formed with neutral drugs while salts formation requires the ionization of the drugs.

Many studies were carried out on co-crystal systems to compare their solubility and their dissolution to the parent API. The result was a large difference between the co-crystals formation and the raw drug. However, they showed that co-crystals are not as good as salts in improving the solubility or the dissolution rate (Bethune, 2009).

A study of three co-crystal systems for itraconazole showed that two of the three gave an enhanced solubility similar to the amorphous form of itraconazole (Remenar et al., 2003).

### **1.3.3.5 Dissolution**

The dissolution step can be the rate limiting step towards the bioavailability of the drugs. The dissolution of the drug depends on many factors. Co-crystals improve the dissolution rate of drugs (Anderson et al., 2008). The dissolution rate is enhanced due to the combining of the drug with a highly soluble entity (co-crystal former). This interaction may help to reduce relative lattice energy compared to that of the API.

### **1.3.3.6 Bioavailability**

The bioavailability of a drug is the measurement of the amount of unchanged drug that reaches the systemic circulation and then the site of action. Different forms of the same drug can result in different bioavailability patterns. Thus, choosing the right form of the drug is crucial in the pharmaceutical formulation field.

McNamara studied the co-crystals of 2-[4-(4-chloro-2-fluorophenoxy)phenyl]pyrimidine-4-carboxamide with glutaric acid and identified that co-crystals have a dissolution rate 18 times higher than that of the pure API (McNamara et al., 2006).

The study of the solid dispersion and the co-crystals showed that they both either started as or they are a part of eutectic systems. Thus, the study of eutectic mixture and the prediction of compounds miscibility may provide a better understanding for both systems.

A eutectic mixture is defined as “a mixture of elements or chemical compounds in definite proportions which is crystallized from melt or solution simultaneously

at a lower temperature than any other composition” (Patra and Samantray, 2011). The behaviour and miscibility of compounds forming eutectic mixtures were studied and documented in the literature. A relation was found between the ability of the compounds to be miscible and form an eutectic mixture and their chemical structure (Stott et al., 1998). A new theoretical rule was investigated to allow the prediction of eutectic mixtures formation. This rule depends on the solubility and cohesion parameters of these compounds to predict the feasibility of eutectic mixture formation.

## 1.4 Solubility and cohesion parameters

The chemical structure of any material and the arrangement of the atoms in that material play a crucial role in the interaction with other materials. The type of functional groups, their orientation in the space, and the existence of any adjacent electron withdrawing or donating groups will have a huge impact on the polarity of the molecule. This effect can influence the intensity of the bond to be formed between the two compounds. The polarity participates in the formation of the intermolecular bonds such as the bonding between water molecules. Such interactions have a huge effect on the physical and the chemical properties of the compounds. Hildebrand studied the effect of the different groups and the volume occupied by these groups on the capability of solvents to form bonds and to be miscible with each others.

The effect of the volume that is occupied by these groups can be explained by the effect of steric hindrance. If the groups are too bulky then the large volume of them will interfere with the formation of any bond with the functional groups. Hildebrand has worked on the interaction between solvents and devised an equation to predict the miscibility of liquids. According to Hildebrand the solubility parameter of a solvent is calculated by the square root of its cohesive energy density. The equation takes into consideration the effect of each group separately.

$$\delta = \sqrt{\frac{\Delta H_v - RT}{V_m}}$$

(equation 1.1(Hildebrand and Scott, 1950))

Where  $\Delta H_v$  is the heat of vaporization, R is the gas constant, T temperature, and  $V_m$  molar volume.

Hildebrand suggested that liquids with solubility parameter difference of 7 or less are miscible and can form a homogeneous monophasic mixture. The use of solubility parameters was expanded to predict the miscibility of solids in order to form an eutectic mixture (Greenhalgh et al., 1999).

The limitation of this equation comes from the fact that it can be applied only on the associated solutions. There are some other factors that can be taken into consideration such as the ability of the compound to form internal bonding. On the other hand, Hansen suggested another equation to calculate the solubility parameter for the solvents based on the principle of "like dissolves like". Each molecule has three parameters named  $\delta_d$  which calculates the dispersion energy,  $\delta_p$  calculates the polarity energy, and  $\delta_h$  which calculates the energy from the hydrogen bond formed by two molecules.

The dispersion forces arise from the effect of positive nucleus and a negative electron. The effect of the dispersion can be explained with London theory (Kristyán and Pulay, 1994, London, 1937, Mahanty and Ninham, 1976). The effect of non-polar dispersive interaction between unlike molecules provides a contribution to the cohesion pressures. On the other hand, the polarity force arises from the effect of two factors: the orientation and the induction of the contributing groups. The orientation factor results from the dipole-dipole or Keesom interaction, which occurs between molecules possessing a permanent dipole moment. The induction effect arises from the "dipole induced dipole

occurring between molecules with permanent dipole moments and other neighbouring molecules, whether polar or not and resulting in an induced non-uniform charge distribution” (Barton, 1991). The last factor in the equation is the effect of the hydrogen bonding. The effect of the hydrogen bonding depends to a large extent to the degree of acidity or the basicity of the compounds to form the bond between each others. It is mainly related to the ability of each system to donate or accept an electron.

The summation of the three energies gives the relative energy difference of the compound. This parameter will determine the solubility of the molecules if they dissolve into each other or if they do not. Although the Hansen equation can be applied to a wider range of molecules, there are a few variables that it does not include to compute the solubility parameter of the compound.

The solubility parameter of a compound can be calculated according to a more comprehensive equation that calculates the effect of the group molar cohesive energy divided over the molar volume. Dunkle was the first to introduce an equation to estimate the group molar vaporization enthalpy. He showed that liquid molar vaporization enthalpies at a given temperature can be estimated by the summation of the group contributions (Dunkel, 1928). Bondi has managed to estimate the contributions to the enthalpy of vaporization extrapolated to zero Kelvin (Bondi, 1947 , Bondi, 1968).

The solubility parameter of the compounds used in this thesis were calculated based on the simple version of the group contribution method of Hildebrand equation that is explained with the required tables in the “Handbook of solubility parameters and other cohesion parameters, chapter 6” (Barton, 1991). The

effect of internal cycle formation has not been taken under consideration as it does not have significant impact on the calculated results on the molecules used in this study.

As previously mentioned, an attempt was carried out to link the solubility parameter values of compounds to their miscibility and their ability to form eutectic mixture (Stott et al., 1998) which is considered as a solid dispersion system. These attempts found that in most of the cases two compounds should form eutectic mixture when the difference in their solubility parameter values is less than  $7 \text{ MPa}^{1/2}$ . However, the same study reveals the existence of some compounds that are considered to be exception for this rule.

On the other hand, there were some attempts as well to predict the co-crystal formation of two or more compounds through their solubility parameter values difference (Mohammad et al., 2011). These attempts were based on the fact that the co-crystals are eutectic mixtures in origin. It was expected that two compounds are able to form co-crystals when their SP value difference is no more than  $7 \text{ MPa}^{1/2}$ . However, this rule is not applicable in all the cases.

Ibuprofen *RS/S* and nicotinamide are known to form a co-crystalline system (Berry et al., 2008). The solubility parameter of ibuprofen is  $19.5 \text{ MPa}^{1/2}$  and nicotinamide is  $27.52 \text{ MPa}^{1/2}$ . The difference is  $8.02 \text{ MPa}^{1/2}$  yet they form co-crystals.

There is a dearth of information about the behaviour of co-crystals in polymeric films. The one recently made available study followed the growth of carbamazepine-nicotinamide co-crystals from a mixture that contains polyvinyl pyrrolidone. The moisture absorbed by the polymer dissolved the two drugs and

bring them together to form co-crystals. A stability study of that system showed that the co-crystals were partially unstable (Good et al., 2011).

The above experiment represents the available literature for the study of loading co-crystals in a polymeric film. It also draws attention to the fact that dispersing the co-crystals in a polymeric carrier might improve their stability.



## **1.5 Summary and scope of the thesis**

The improvement of the dissolution rate and the solubility of APIs are expected to greatly reflect on improving the bioavailability of drugs. These improvements can be achieved by physical (such as solid dispersions) or chemical (such as co-crystallization) modifications for the API. Combining both types of modifications is expected to improve the physicochemical properties of the API even more. There was only one attempt in the literature to load co-crystals inside a polymeric film. Therefore, there is almost no information about the possible behaviour of co-crystals in a polymeric carrier, their ease of formation and their stability and properties. This combination can be used in future for either transdermal or oral use.

## **1.6 Aims and objectives**

The aim of this project is to investigate the possibility of combining both physical and chemical modification of an API and to discover the effect of such combination on resultant properties. In addition, the preparation media effect was studied through the use of different solvent systems. An important sub-aim of this project was to probe whether a theoretical basis could be developed for the ease of formation and stability of co-crystals in polymeric films by utilising compounds that have a theoretical affinity to interact with the polymer rather than interacting with each other to form co-crystals. This affinity was estimated through the use of the solubility and cohesion parameters of the starting materials.

In order to fulfil the aim of this thesis, a number of objectives need to be met.

These objectives are as follows:

- To identify suitable co-crystal forming starting materials and to analyse the materials and their physicochemical properties when recrystallized using various solvent systems.
- To produce the selected co-crystals using a variety of solvent systems to monitor any morphology or behaviour change and to study the interaction between the materials in advance of their incorporation within a polymeric film matrix.
- To study the effect of various solvent systems on the physicochemical properties of the pure polymeric film.
- To investigate the effect of adding each single co-crystal component on the physicochemical properties of the film using various solvent systems.
- To study the effect of adding two materials simultaneously to the polymer using different solvent systems.
- To identify whether any novel co-crystal systems form in the polymeric vehicle for the use in transdermal or oral drug delivery.
- To identify a rational approach as to whether a co-crystal can be successfully incorporated into a polymer. Specifically to investigate the use of solubility parameters to predict the behaviour of a co-crystalline drug dispersed in a polymeric vehicle
- To explore whether additives can be used to enhance the stability and ease of formation of co-crystals within a polymeric film.

## 1.7 Selection of materials

Caffeine-malonic acid and ibuprofen-nicotinamide were used as model co-crystal systems as they are cheap, and relatively non-toxic. In addition to that, both co-crystals are easy to prepare and their properties have been extensively studied (Bothe and Cammenga, 1980). Caffeine, malonic acid, and nicotinamide are water soluble (1 g/46 ml, 1 g/0.65 ml, and 1 g/1 ml water respectively) while ibuprofen is sparingly soluble in water (<1mg/ml) (Budavari, 2006). Thus, the two systems are expected to interact with the polymer in different ways.

Hypromellose Acetate Succinate (HPMCAS) was used because it is cheap, relatively non-toxic, dissolves in many common solvents and for its enteric coating property. This latter is particularly useful as ibuprofen is known to cause stomach ulcer.

On the other hand, the solvent systems used in the preparation step are either mentioned in the literature for their capability of providing the required properties or adapted from the literature and modified to serve the purpose of its use. The three systems mentioned in the literature are:

- **Chloroform/methanol 30:1 v/v** was used in the production of caffeine/malonic acid co-crystals (Trask et al., 2005). Chloroform is a good solvent for both caffeine and malonic acid and spiking it with methanol gives the required polarity to the mixture. This improves the solubility of the raw material and the formation of co-crystals.
- **Ethanol/water 4:1 w/w** was used for its capability of dissolving the polymer (HPMCAS) (Shin-Etsu, 2005).

- **Acetonitrile** is the solvent of choice for producing ibuprofen-nicotinamide co-crystals (Berry et al., 2008). However, there was no data regarding the solubility of HPMCAS in acetonitrile.

Other solvent systems will be developed as required.

## **Chapter 2**

### **Materials and methods**

## 2.1 Materials

Materials used in the thesis are summarised in the following table.

<b>Material</b>	<b>supplier</b>	<b>Batch number</b>	<b>Purity</b>
Caffeine	Fluka	1381891 10808p01	99%
malonic acid	Sigma-Aldrich	S43239-487	98%
Ibuprofen	Sigma-Aldrich	026H1368	98%
Nicotinamide	Sigma-Aldrich	079K1404	98%
Naproxen	Sigma-Aldrich	078K1629	99%
Flurbiprofen	Sigma-Aldrich	070M1445V	97%
HPMCAS	Shin-Etsu	9073188	NA
Triethyl citrate	Aldrich	18621AB	99%

Table 2.1. Materials used in the thesis.

The solvents used were:

Acetone, acetonitrile, ethanol, chloroform, methanol, and distilled water. All the solvents were laboratory grade and purchased from Fischer scientific (Loughborough, UK).

## **2.2 Data analysis**

### **2.2.1 Thermal analysis**

#### **2.2.1.1 TGA**

A Thermal Analysis TGA Q5000 (TA instruments, Elstree, Hertfordshire, UK) was used to measure the thermal profile for the samples and in order to measure the residual solvent and moisture content.

The TGA was calibrated in two steps. The first step includes the calibration for temperature. For this purpose, a sample of nickel was heated in the TGA. The cure point of nickel (627 K or 354°C) is used as a reference value for calibrating the temperature scale.

On the second step of calibration, 25 mg and 125 mg standard weights are used to perform the mass calibration of the TGA.

The thermal profiles for samples (powder, crystals, or films) were obtained by taring the TGA using the supplied software. After that, a sample of approximately 5 mg was placed inside the aluminum pan. The sample was heated from room temperature (around 25°C) to 300°C for unprocessed materials, recrystallized crystals, and co-crystals. Films were heated to 600°C. All the measurements were performed with a heating rate of 10°C/min.

#### **2.2.1.2 DSC**

A Thermal Analysis DSC Q2000 (TA instruments, Elstree, Hertfordshire, UK) was used to scan the samples and measure their melting enthalpy.

Aluminum lid and pan were used for scanning unprocessed materials except for caffeine were Tzero™ hermetic pan and lid used for the analysis process. The

DSC was calibrated once a month using around 1 mg of indium. The onset temperature of the melting peak (156.6°C) was used to calibrate the DSC. Triplicates of 3-7 mg each were weighed and filled in a pan closed with a pin-holed lid. Raw materials and the recrystallized ones were scanned from room temperature to above their melting point with a heating rate of 10°C (caffeine 240°C, malonic acid 150°C, ibuprofen 120°C, nicotinamide 135°C, naproxen 165°C, and flurbiprofen 135°C). One sample of caffeine and recrystallized caffeine were scanned from room temperature to 240°C, then cooled to 0°C, after that the samples were reheated again to 240°C. The heating rate for that sequence was 10°C/min.

HPMCAS and all the films were scanned in a different pattern. The sample were first heated to 100°C with a rate of 10°C/min. then the sample were kept on an isothermal step at 100°C for 5 minutes in order to dry the sample off. After that, the sample was cooled to 0°C (films with 25% crystal concentration or above were cooled to -20°C at the same rate. The temperature was kept at 0°C or -20°C for 5 minutes. Then the sample was heated again to 120°C with the same rate. Tg and melting points values were collected using the second run to avoid discrepancies due to the moisture content and the thermal history of the sample. For films containing ibuprofen the first run was used to measure the melting point as ibuprofen crystals were dissolving during the drying off step producing an amorphous system.



### **2.2.2 X-ray crystallography**

A Bruker D8 diffractometer (Bruker Corporation, Bruker AXS, Cambridge, UK) was used to scan the samples. The wavelength of the X-ray was 0.154 nm using Cu source. The voltage used was 40KV. Filament emission was 30 mA. The samples were either packed into a deep sample holder and pressed to have a flat surface and equal distribution, or sprayed over a flat surface sample holder. Samples were scanned from 5-50° (2 $\theta$ ) using 0.01° step width and a 1 second time count. The receiving slit was 1° and the scatter slit 0.2°.

### **2.2.3 Vibrational spectroscopy (FT-IR)**

The samples were scanned using Digilab UMA 400 (DIGILAB, London, UK) was set to a scan speed of 20 KHz. Scan resolution was 4cm<sup>-1</sup> and the sensitivity 1 transmission %. The accumulation of 128 scans was used and the samples were scanned from 4000 cm<sup>-1</sup> to 600cm<sup>-1</sup>.

### **2.2.4 Microscope analysis**

#### **2.2.4.1 SEM**

Using the FEI QUANTA 400 SEM, (Oxford instruments, UK), INCAx-sight, with aluminum stubs and carbon tabs (12 mm Dia, FK100) samples were scanned for their topography and appearance. Samples often showed high electrostatic charge. In order to get rid of the charge, samples were coated with carbon dust using a coating machine (EMITECH K450, Quorumtech, the carbon thickness produced was 15 nm). The SEM chamber was subjected to a high pressure vacuum and high voltage was used for scan.

#### **2.2.4.2 Hot stage microscope**

Crystals and films were scanned using a hot stage microscope (Zeiss, Thornwood, USA) equipped with Axiocam MRC 5 Zeiss, Tv2/3" c, 0.63x, 1069-414 camera. The stage was connected to a heating unit (Linkam, Guildford, Surrey, UK). Cross polarized light was used to identify the crystals and co-crystals. However, in some samples normal bi-focal used to observe the crystals as the films were thick and the light was barely passing by. Samples were heated using a heating rate of 5°C/min. Images were obtained when any change was observed.

#### **2.2.5 Dissolution station**

A USP basket method was followed to scan samples taken from the dissolution bath. Films containing drug (caffeine, ibuprofen), co-crystals (caffeine-malonic acid, ibuprofen-nicotinamide), films containing drug and a blocking agent (ibuprofen and malonic acid), and films containing co-crystals and a blocking agent were scanned in the dissolution bath by either using a small part of the film that can fit inside the stirring basket (caffeine and malonic acid) or by breaking the film and loading the pieces inside the basket (films containing ibuprofen, ibuprofen and malonic acid, ibuprofen co-crystals, and ibuprofen co-crystals with a blocker). The basket was set to revolve at rate of 100 RPM. The dissolution vessel was connected with two rubber tubes to a peristaltic pump operating at a rate of 25 RPM. The tubes were connected to a closed UV cell in order to perform a continuous scanning for the dissolution media. The dissolution vessel was filled with pH 7.4 phosphate buffer solution maintained at a temperature of 37°C.

The flow through the tube was measured for 2 hrs in order to measure the drug release from the film. The samples were measured with a Jenway 6800 UV/VIS Spectrophotometer (Bibby Scientific Limited, Staffordshire, UK). The data were analysed using a program (Flight Deck version 1.0) and concentration v/s time curve were plotted. The release percentage was used instead of the released concentration in order to ease the comparison and eliminate the difference in samples concentrations.

## **2.3 Methods of preparation of materials**

### **2.3.1 Recrystallization experiments**

Solvent evaporation was used as a technique to prepare the recrystallised form. The raw materials were dissolved separately in acetone/chloroform, ethanol/water, and acetonitrile. Caffeine was recrystallised with chloroform/methanol as well as the previous solvents. After dissolving the raw materials in the solvents, the solution was stirred and an extra amount of the solute was added to ensure saturation. The solution was poured into a petri-dish and it was left in a fume cupboard to allow the solvent to evaporate. The crystals were collected and stored in re-sealable plastic bags under room temperature (18°-25°).

### **2.3.2 Co-crystallization experiments**

Caffeine and malonic acid co-crystals were prepared by dissolving them in their stoichiometric molar ratio of 2:1 mol/mol caffeine/malonic acid in one of the previously mentioned solvents and solvent allowed to evaporate under ambient conditions.

143 mg caffeine and 380 mg malonic acid were added to 40 ml acetonitrile, 31 ml chloroform/methanol, 50 ml acetone/chloroform, 50 ml ethanol/water. The mixture was stirred until all the particles dissolved. The solution was poured in a petri-dish and it was left in a fume cupboard to allow the solvent to evaporate. The co-crystals were collected and stored in re-sealable plastic bags under room temperature (18°-25°).

### **2.3.3 Preparation of films containing drugs or mixture**

Films containing one or more types of crystals were prepared by dissolving various amounts of the crystals in one of the solvents. The solution was stirred until all the particles dissolved. 4 g of HPMCAS were added to the solution gradually with continuous stirring. The solution was cast into a petri-dish with an acetate sheet covering its base. The films were placed in a fume cupboard to allow the solvent to evaporate.

Films were separated from the acetate sheet and stored in re-sealable plastic bags and stored under room temperature (18°-25°) in a desiccator.

### **2.3.4 Films containing co-crystals**

Films containing co-crystals were prepared by dissolving 4 g of HPMCAS in either 40 ml of acetonitrile or 50ml of acetone/chloroform 3:2 v/v. The solution was stirred for 1-1.5 hours using a magnetic stirrer to allow the viscosity to increase. 500 mg of caffeine-malonic acid co-crystals or 500 mg of ibuprofen-nicotinamide were crushed using a mortar and pestle in order to reduce the particle size of the co-crystals then it was added gradually to the solution of the polymer. The solution was stirred for 2 minutes and then it was cast into a petri-dish with an acetate sheet covering its base. The petri-dish was left for 2 weeks in a fume cupboard to allow the solvent to evaporate completely. Films were stored under room temperature (18°-25°) in a desiccator.

## **Chapter 3**

**Raw material analysis and the study of the solvent effect on  
their properties**

### **3.1 Raw material analysis**

The main aim of the thesis is to study the interaction between a co-crystal and a polymeric vehicle and the impact of such interaction on the physicochemical properties of the dosage form. Therefore it is imperative to start by first characterizing the unprocessed materials to be able to identify any changes that might arise when those materials interact with each other. Moreover, in order to produce the co-crystals alone or when interacting with the polymer, the starting components have to be dissolved or dispersed into a solvent system before they are recrystallized from the solvent. Hence, it is important to understand the effect of these solvent systems on the physical and chemical properties of the starting materials to differentiate between the effect of the solvent system and the effect of the interactions of the components when they are mixed together.

For the above reasons, this chapter will investigate some of the physicochemical properties of the unprocessed materials: caffeine, malonic acid, ibuprofen, nicotinamide, and HPMCAS. It will also study the effect of recrystallizing these materials using ethanol/water and acetonitrile.

A third solvent system was added after few studies that are related to the solubility of the previous drugs. This system is acetone/chloroform 3:2 v/v.

The study of the solvent effect on the raw materials requires the knowledge of raw materials properties and hence the unmodified drugs were analyzed at first.

## 3.2 Unprocessed drug analysis

### 3.2.1 Caffeine

Caffeine (1, 3, 7 trimethyl-3, 7 dihydro-1H-purine-2, 6-dione) is a natural alkaloid found in tea leaves,

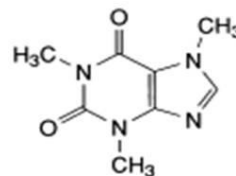


Figure 3.1. Caffeine structure

coffee beans, and cocoa beans. It was synthesized first by E. Fischer at 1882 (figure 3.1). It sublimes at 178°C and melt at 238°C. Fast sublimation can be obtained at 160-165°C at 1mm Hg pressure. It has a hexagonal prism shape. It dissolves freely in alcohol and water/ alcohol mixtures. It can interact with water to give a monohydrate derivative (Chemfinder, 2004). Caffeine has 2 polymorphs I and II with a transition point of 141±2°C. Caffeine is considered as a CNS and respiratory tract stimulant.

#### 3.2.1.1 Thermal analysis

##### TGA and DSC

Unprocessed caffeine was scanned in order to measure the thermal degradation profile of the drug and its melting point. TGA and DSC tests were carried out according to the method described in section 2.2.1.1 and 2.2.1.2 Tzero™ hermetic pans and lids were used for DSC test in order to contain caffeine sublimation. The results are shown in figure 3.2.



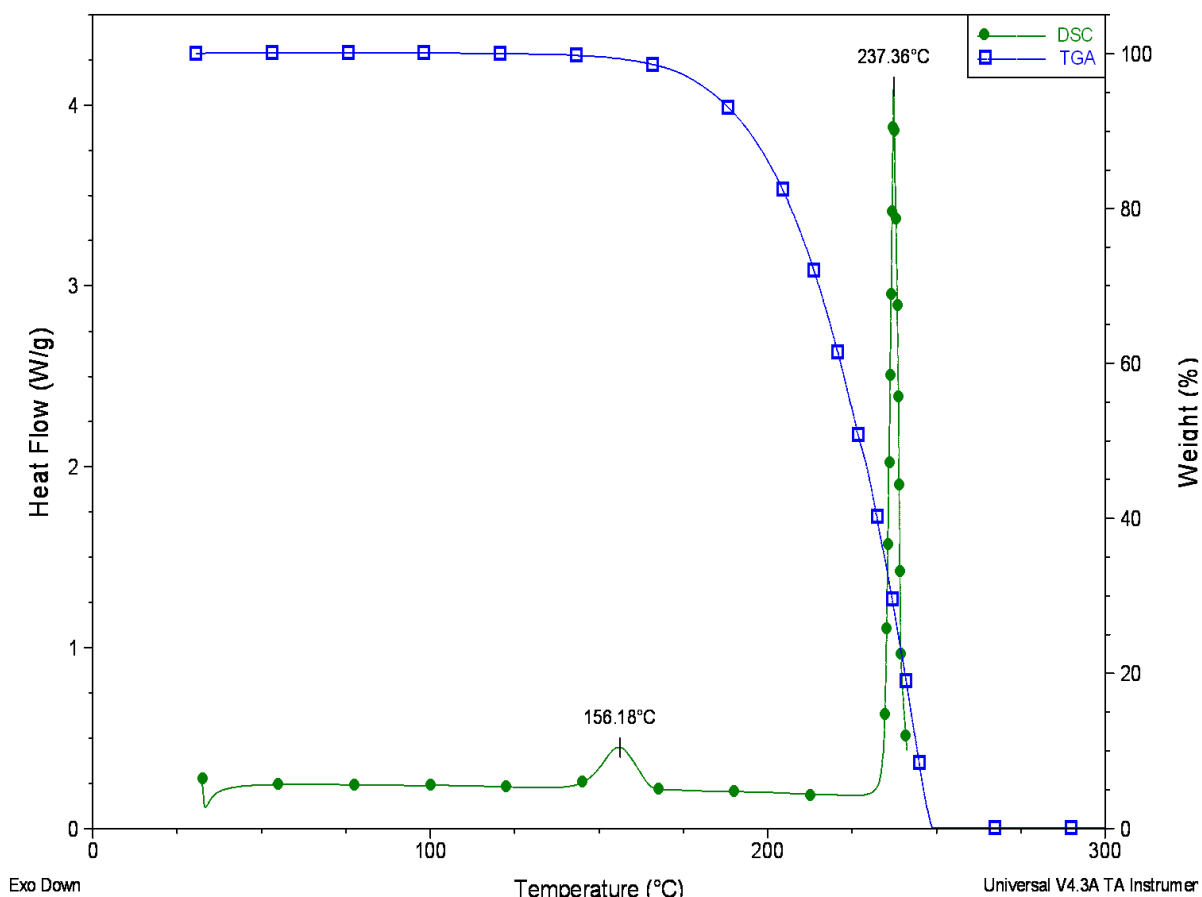


Figure 3.2. Representative TGA (blue) and DSC (green) thermal profiles of unprocessed caffeine powder.

Figure 3.2 shows that the TGA profile reveals an onset of weight loss due to sublimation/degradation at around 160°C. Meanwhile, the DSC curve shows an endothermic broad peak at 158°C which was correlated to the sublimation of caffeine (Hubert et al., 2011). The peak at 237°C corresponds to the theoretical value of the melting point of caffeine. However, it has to be noted that at the melting point of caffeine only 28% of the weight was left according to the TGA curve. This is due to caffeine sublimation

### 3.2.1.2 Powder X-ray diffraction

Caffeine was analyzed using powder x-ray diffraction in order to verify the crystal lattice structure of the compound. The measured diffraction was

compared to that obtained from the Cambridge Structure Database (CSD) library for the anhydrous and monohydrate forms of caffeine (figure 3.3).

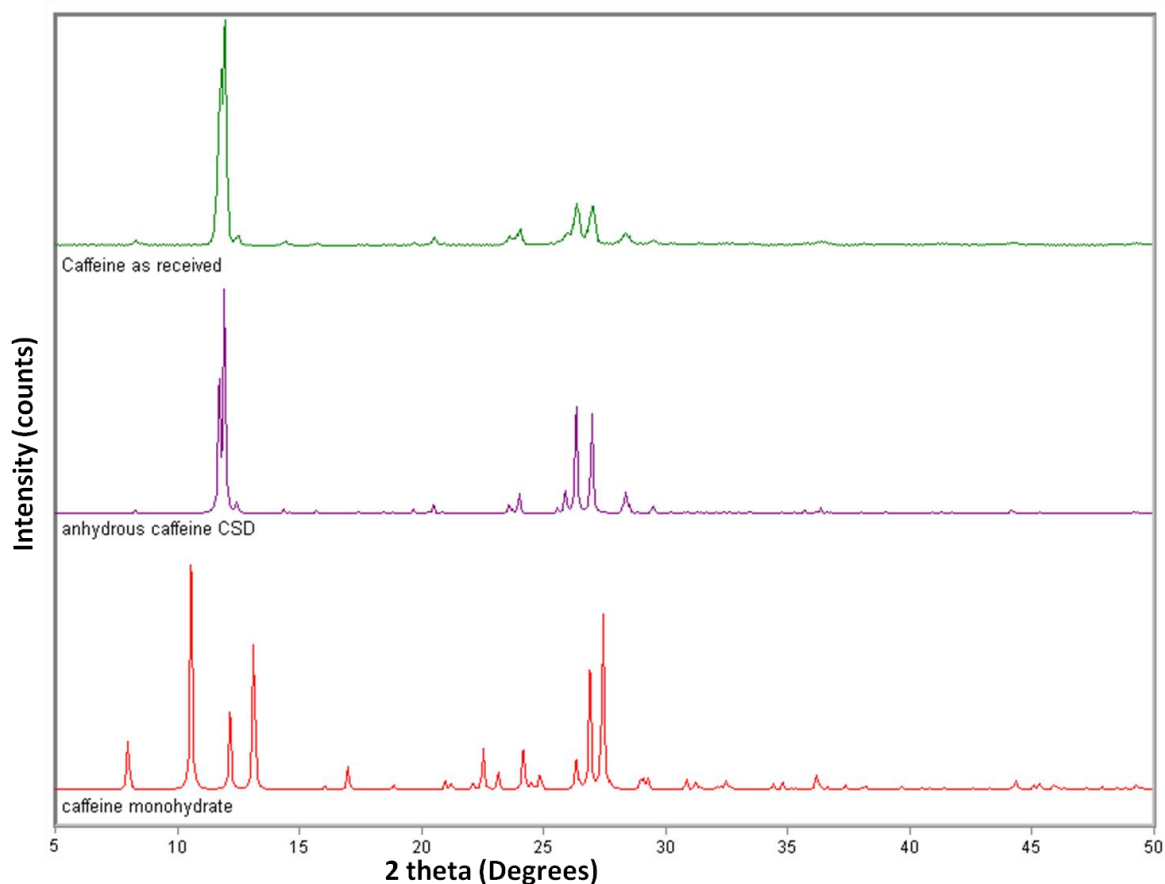


Figure 3.3. Representative X-ray diffraction patterns of caffeine monohydrate CSD (bottom), anhydrous caffeine CSD (middle), and caffeine as received (top).

X-ray diffraction of anhydrous caffeine is characterized by a weak intensity single peak at  $8^\circ$  and another strong intensity peak at  $11^\circ$ . On the other hand, monohydrated caffeine is characterized by the existence of three peaks at  $10^\circ$ ,  $12^\circ$ , and  $13^\circ$ . In addition to a strong intensity peak that exists at  $8^\circ$ . The scan of caffeine as received in figure 3.3 shows a weak intensity peak at  $8^\circ$  and a strong single peak at  $11^\circ$ . This means that the diffraction pattern of caffeine received from Sigma-Aldrich corresponds well to that of anhydrous caffeine. Moreover, a further investigation reveals that the caffeine polymorph I has a single diffraction peak at  $26.8^\circ$  in comparison to polymorph II that reveals two

peaks at  $26.3^\circ$  and  $27^\circ$  (Kishi and Matsuoka, 2010). The unprocessed caffeine diffraction pattern contain two peaks at  $26.3^\circ$  and  $26.9^\circ$  indicating that it is type II polymorph.

### 3.2.1.3 FT-IR transmission

Caffeine was scanned with FT-IR spectroscopy as detailed in section 2.2.3. The results are represented in figure 3.4. The spectrum reveals three characteristic peaks at 3133 (N-H), 1700 (C=N), and 958 (N-H)  $\text{cm}^{-1}$ . These peaks are significant since the nitrogen atom in that bond is expected to form a hydrogen bond when co-crystals of caffeine are formed. If such a hydrogen bond is formed then it will be manifested by a shift in one of those three peaks.

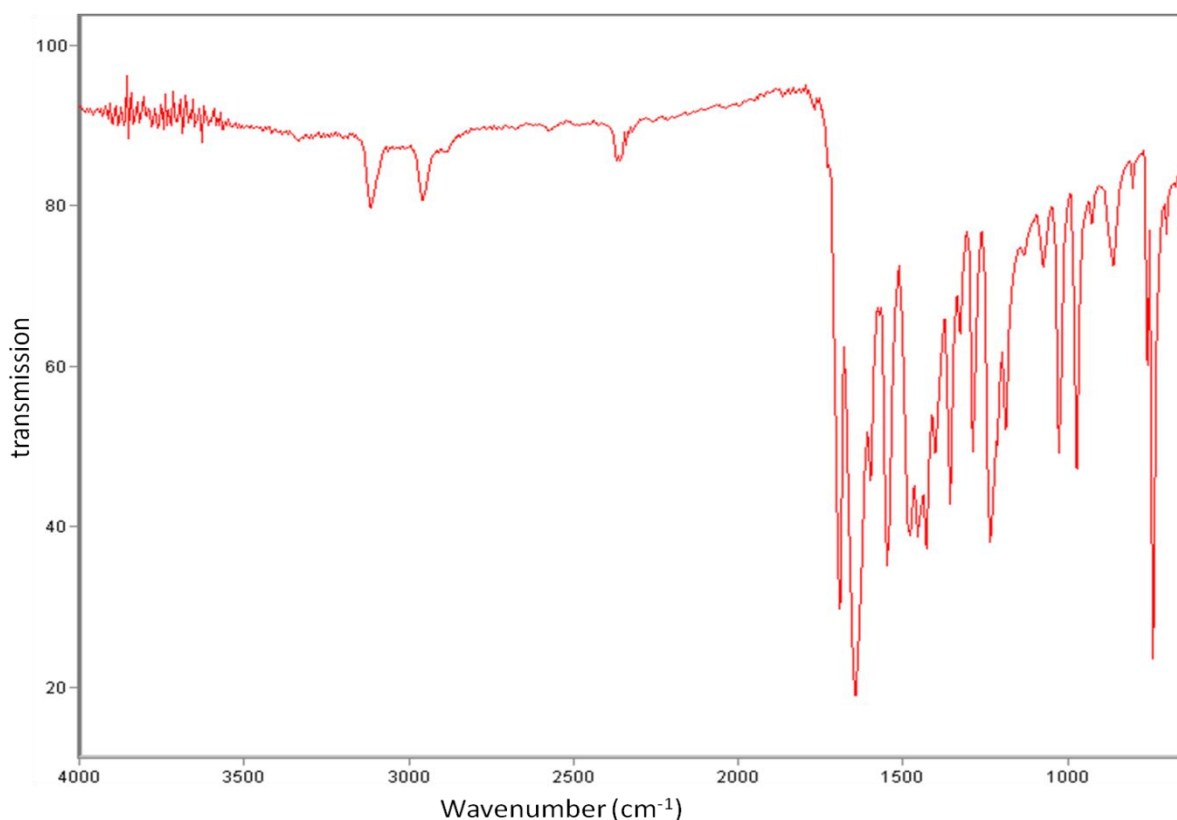


Figure 3.4, Representative FT-IR spectrum of caffeine as received.

### 3.2.2 Malonic acid

Malonic acid or propanedioic acid is a dicarboxylic acid. It has the structure of  $\text{CH}_2(\text{COOH})_2$  (figure 3.5).

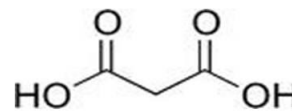


Figure 3.5. Malonic acid structure

It has a molecular weight of 104.06146 [g/mol]. It forms crystals that melt at 135°C (Sigma-Aldrich). It is freely soluble in water and alcohol. It is used in the manufacturing of barbiturates.

Malonic acid is used as a co-crystal former with caffeine to protect caffeine from hydration.

#### 3.2.2.1 Thermal behaviour

##### TGA and DSC

Thermal behaviour of malonic acid was characterized using TGA and DSC (method section 2.2.1.1 and 2.2.1.2). The thermal profile scan revealed the degradation profile of malonic acid and its melting temperature (figure 3.6). A triplicate scan was carried out to ensure accuracy (figure Appendix II.1).

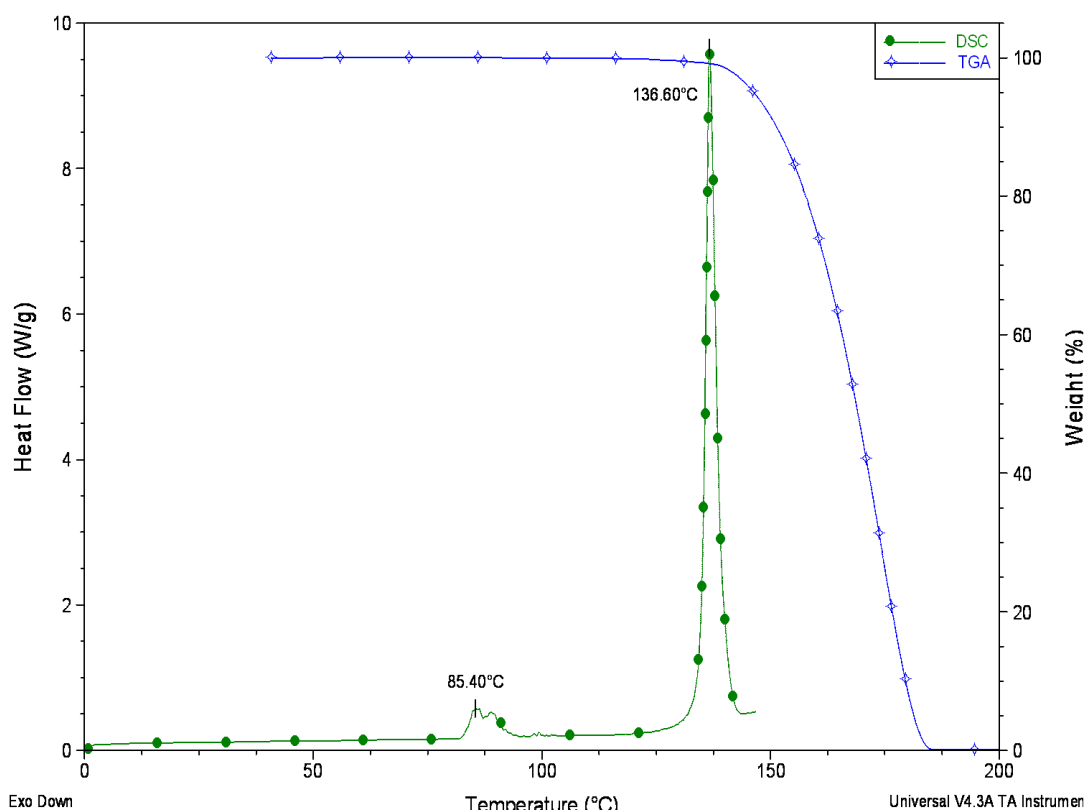


Figure 3.6. A representative TGA and DSC thermal profile of malonic acid as received

The thermal degradation of malonic acid was observed to commence at 140°C on the TGA profile. The DSC profile shows two endothermic peaks. The first peak, at 136.6°C, can be correlated with the melting and / or decomposition point of malonic acid as it is similar to the theoretical value provided in Sigma-Aldrich database (132-135°C). The difference between the two values may be related to the thermal lag due to the packing of the crystals in the DSC pan. The peak at 84°C was not mentioned in Sigma-Aldrich Database. (Caires et al., 2009) analysed the thermal behaviour of malonic acid using TGA, X-ray, and FT-IR and they found that malonic acid has a solid phase transition peak at 110°C (heating rate 20°/min) with melting point of 145°C and decomposition of 215°C. (Bougeard et al., 1988) also analysed malonic acid thermally. They identified the solid phase transition peak from  $\beta$  to  $\alpha$  at ca 360 K (87°C) with heating rate of 10°C/min. The latter result is only 2°C different to the result

obtained in the current and this difference might be related to the hygroscopicity or traces of impurity in malonic acid sample or an instrumental differences.

### **3.2.2.3 Powder X-ray diffraction**

A malonic acid diffraction pattern using the powder x-ray diffractometer was performed in order to identify the polymorph type of malonic acid. Unlike caffeine, malonic acid has a one diffraction pattern provided by the CSD software. (Caires et al., 2009) provide the X-ray data for the two polymorphs. A comparison of the diffraction pattern provided by him shows that the diffraction pattern of  $\alpha$  polymorph has two peaks at  $17^\circ$  and  $18^\circ$  in comparison to one peak at  $17^\circ$  for  $\beta$  polymorph. In addition  $\beta$  polymorph showed a diffraction peak at  $27^\circ$  with no similar peak in  $\alpha$  polymorph. Figure 3.7 reveals that the diffraction pattern obtained by scanning malonic acid shows peaks at  $17^\circ$ ,  $18^\circ$  and  $27^\circ$ . Thus the starting malonic acid sample used in this study is believed to contain both polymorphs.

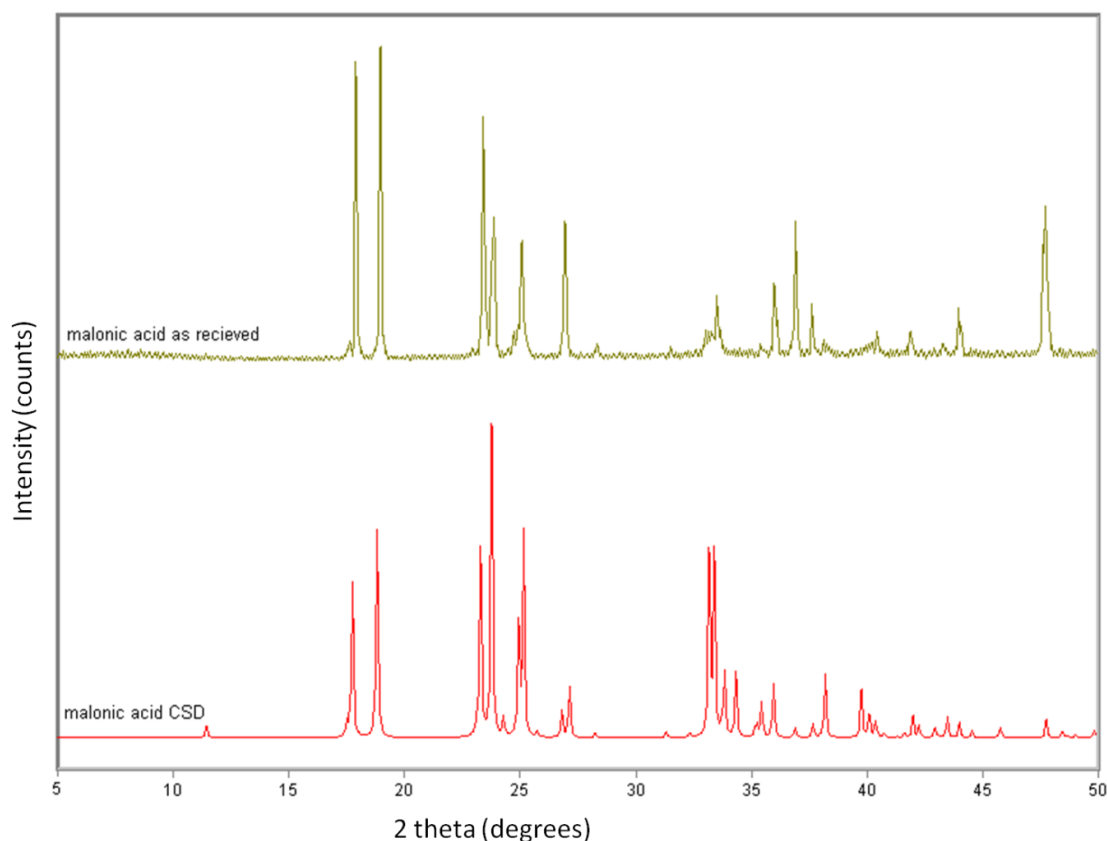


Figure 3.7. Representative powder X-ray diffraction pattern of malonic acid as received (top) and a reference pattern for malonic acid from CSD (bottom).

### 3.2.2.4 FT-IR transmission

Malonic acid is a complicated compound to analyze with FT-IR. It has two mirror-image carboxylate groups attached to  $\text{CH}_2$  center as shown in figure 3.5. Malonic acid was analyzed using FT-IR according to the method described in section 2.2.3. The results, shown in figure 3.8 reveals a characteristic peak at  $1700\text{ cm}^{-1}$ . this peak can be correlated to the  $\text{C}=\text{O}$  and  $\text{O}-\text{H}$  bands (Bougeard et al., 1988). Both functional groups are expected to be involved in hydrogen bond formation. If such a hydrogen bond is formed then we would expect a shift in that peak in the FT-IR spectrum.

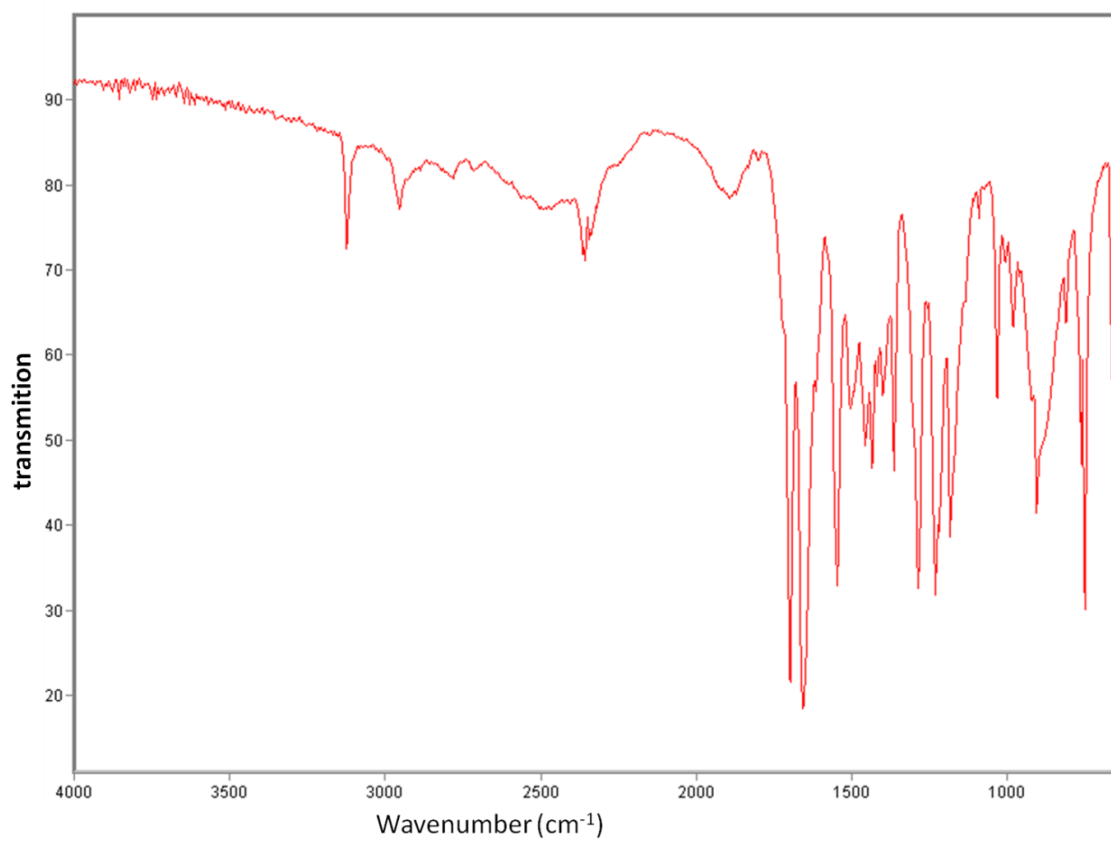


Figure 3.8. A representative of FT-IR spectrum of malonic acid as received.



### 3.2.3 Ibuprofen

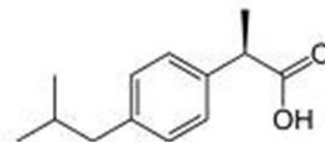


Figure 3.9. Ibuprofen structure

Ibuprofen or  $\alpha$ -methyl-4-(2-methylpropyl)

benzeneacetic acid is a non steroidal anti inflammatory drug (see figure 3.9). It has an analgesic antipyretic activity as well. Ibuprofen has a molecular weight of 206.28 g/mol and a melting point of 75-77°C. It is a colorless crystalline stable solid. Ibuprofen exists as *S*, *R*, or *R/S* racemate isomer. The *S* isomer is more active than the *R* isomer.

Ibuprofen (*S*, *RS*) is known to form a co-crystal with nicotinamide (Berry et al., 2008).

#### 3.2.3.1 Thermal analysis

##### TGA and DSC

A thermal degradation profile and change of the enthalpy of ibuprofen was recorded using TGA and DSC following the methods described in sections 2.2.1.1 and 2.2.1.2. TGA thermal profile in figure 3.10 shows that the thermal degradation of ibuprofen begins at around 150°C. The DSC scan shows a sharp endothermic peak at 76°C. This peak matches the melting point of ibuprofen (section 3.1.3). A triplicate scan is shown in Appendix All.2.

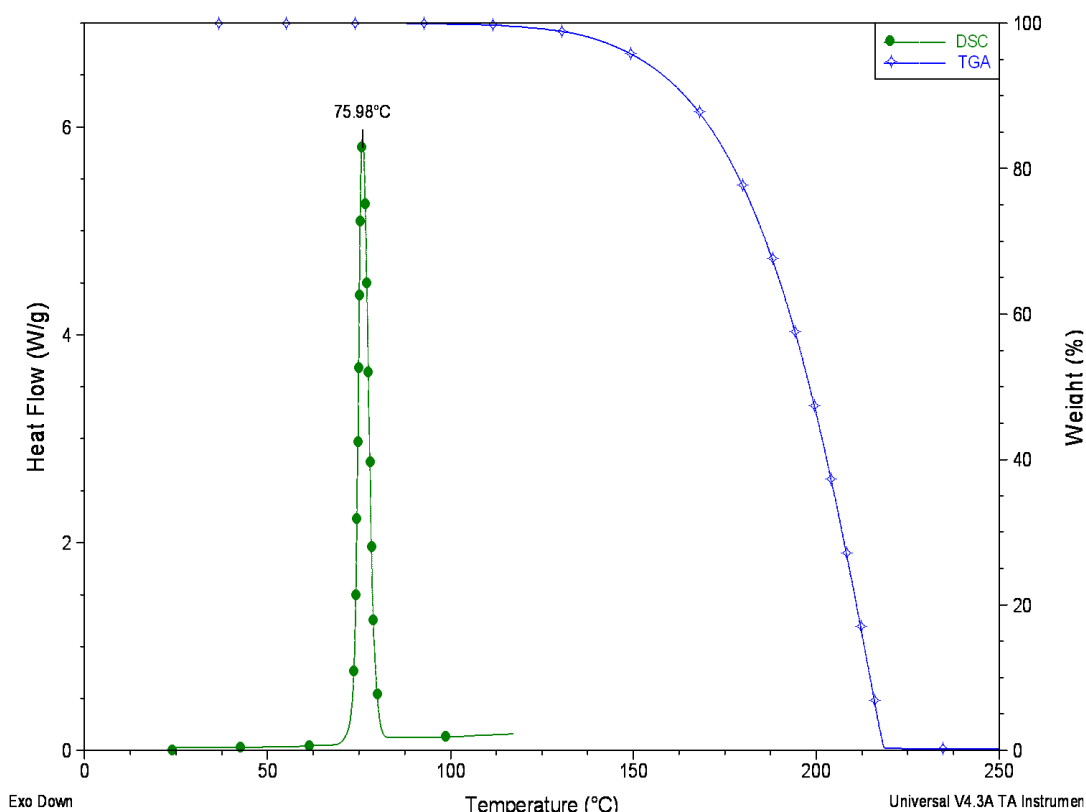


Figure 3.10. A representative of TGA and DSC thermal profile of unprocessed ibuprofen.

### 3.2.3.2 Powder X-ray diffraction

Ibuprofen has three isomers (*R*, *S*, and *RS* racemate). *S* and *R/S* isomers can form co-crystals with nicotinamide (Berry et al., 2008). In this study, ibuprofen was analyzed with PXRD using the method described in section 2.2.2. The results were compared with those obtained from CSD software (Mercury 3.0) (figure 3.11). Standard diffraction pattern of *RS*-ibuprofen shows a peak at 6°. On the other hand, *S* isomer has two peaks at 7° and 7.7° that do not appear in the racemate pattern. Figure 3.11 shows that the diffraction obtained for unprocessed ibuprofen using the method in section 2.2.2 has a high intensity peak at 6° with no sign for peaks at 7° or 7.7°. Therefore, it can be concluded that the unprocessed ibuprofen is a racemate form.

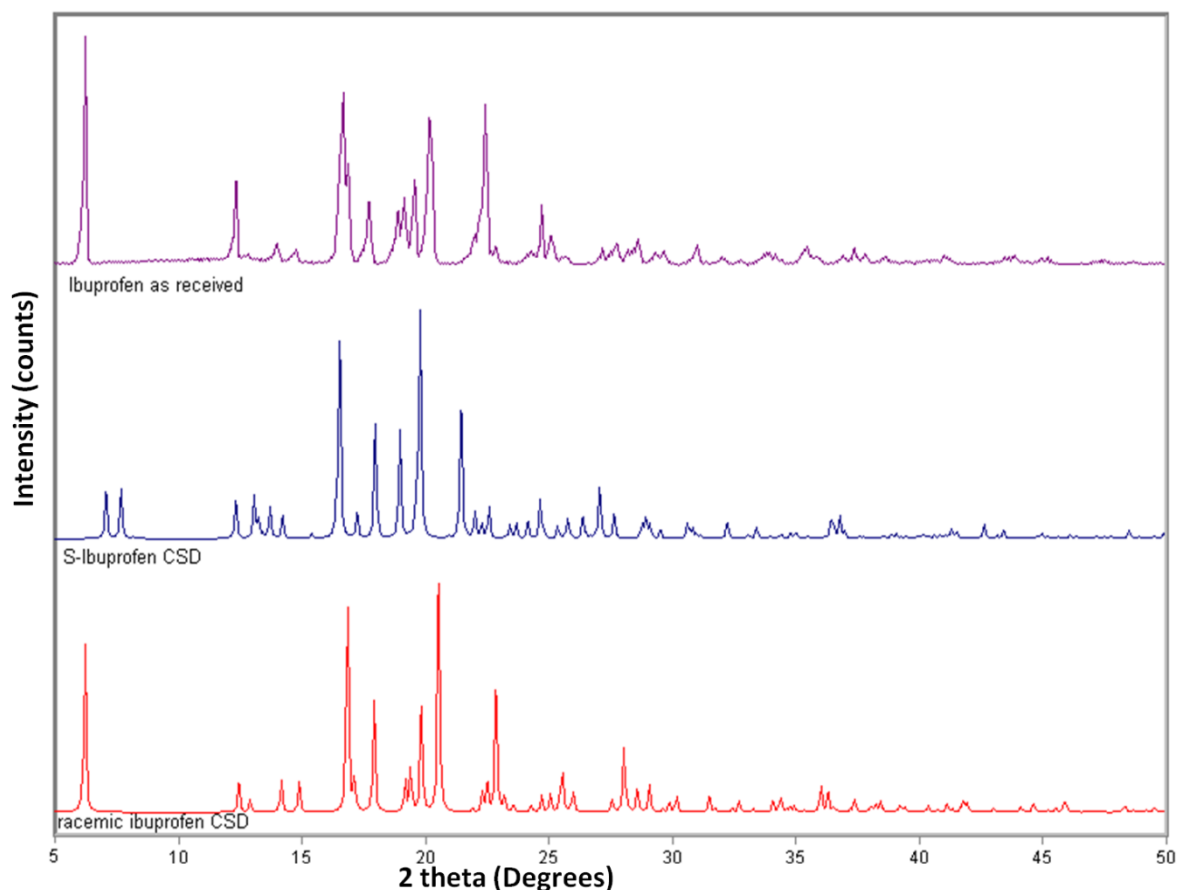


Figure 3.11. A representative powder X-ray diffraction pattern of unprocessed ibuprofen (top), standard diffraction pattern obtained from CSD for ibuprofen S (middle), and standard ibuprofen racemate (CSD) pattern (bottom).

### 3.2.3.3 FT-IR transmission

In order to detect any changes in the energy of the functional groups of ibuprofen that may arise during co-crystal formation, a reference of the unprocessed ibuprofen FT-IR spectrum has to be obtained. Using the method described in section 2.2.3, ibuprofen was analyzed with FT-IR spectroscopy. The spectrum of ibuprofen was plotted in figure 3.12. COOH entity is the major functional group of the molecule. (Jubert et al., 2006) has identified the peak at around  $1700\text{ cm}^{-1}$  and assigned it for C=O and OH vibrations.

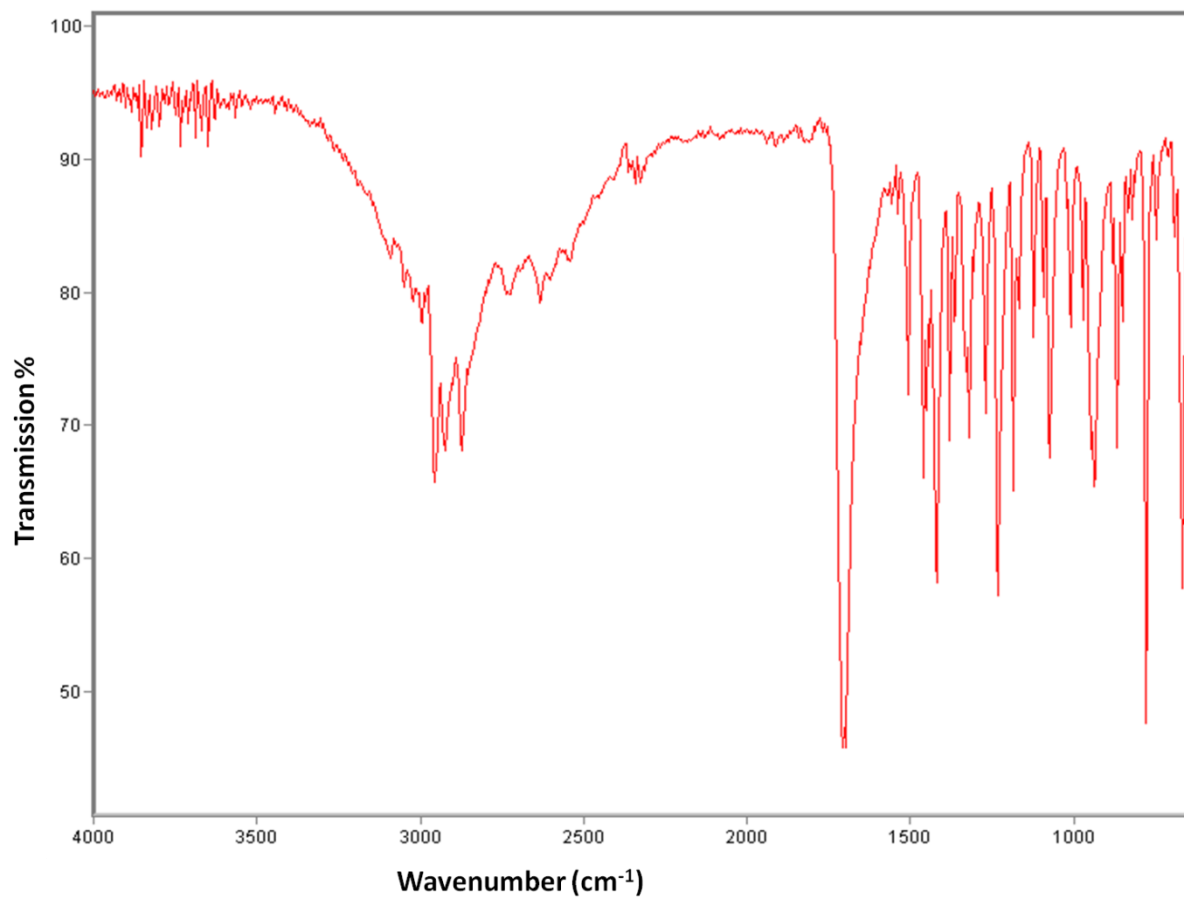


Figure 3.12. A representative FT-IR spectrum of unprocessed ibuprofen.

### 3.2.4 Nicotinamide

Nicotinamide (niacinamide) is an amide of nicotinic acid (figure 3.13). It can be described as a white or whitish

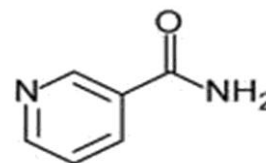


Figure 3.13. Nicotinamide structure

crystalline powder that forms needle-shape crystals from benzene. It has a melting point of 128-131°C and a pKa of 3.3. It is freely soluble in water and alcohol. 1 gram of nicotinamide dissolves in 1 ml of water or 1.5 ml of alcohol.

#### 3.2.4.1 Thermal analysis

##### TGA and DSC

Nicotinamide has four known polymorphs (Hino et al., 2001). Those polymorphs can be differentiated by their thermal behaviour. Thus the thermal behaviour of unprocessed nicotinamide was obtained using TGA and DSC in order to identify its polymorphic type. Nicotinamide was examined using the methods described in section 2.2.1.1 and 2.2.1.2. The weight loss and the DSC profile of nicotinamide were plotted in figure 3.14.

The thermal behaviour of nicotinamide polymorphs reveals different melting points for the polymorphs. The melting point for polymorph I, II, III, and IV as 126°C -128°C, 112°C -117°C, 107°C -111°C, and 101°C -103°C respectively (Akalin and Akyuz, 2006). The TGA profile a weight loss associated with the thermal degradation of unprocessed nicotinamide to begin at around 160°C (figure 3.14). Moreover, the DSC scan shows an endothermic peak at 129.6°C. This peak can be correlated to the melting point of polymorph I.

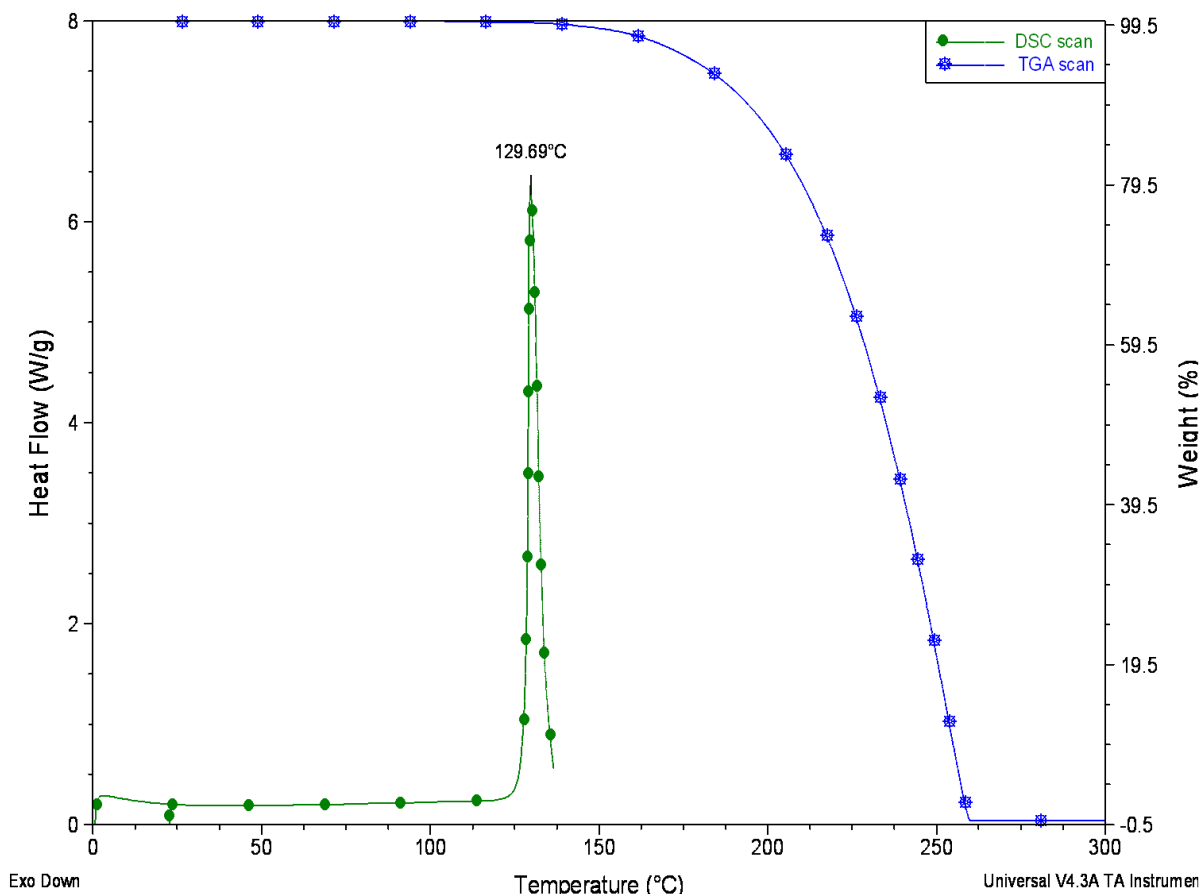


Figure 3.14. Representative TGA and DSC thermal profiles for unprocessed nicotinamide.

### 3.2.4.2 Powder X-ray diffraction

The diffraction pattern of unprocessed nicotinamide was obtained using the method described in section 2.2.2. The results shown in figure 3.15 were comparable to the standard diffraction pattern obtained from CSD library. The measured spectrum will serve as a reference to detect any changes might arise as a result of a polymorphic or co-crystal formation.

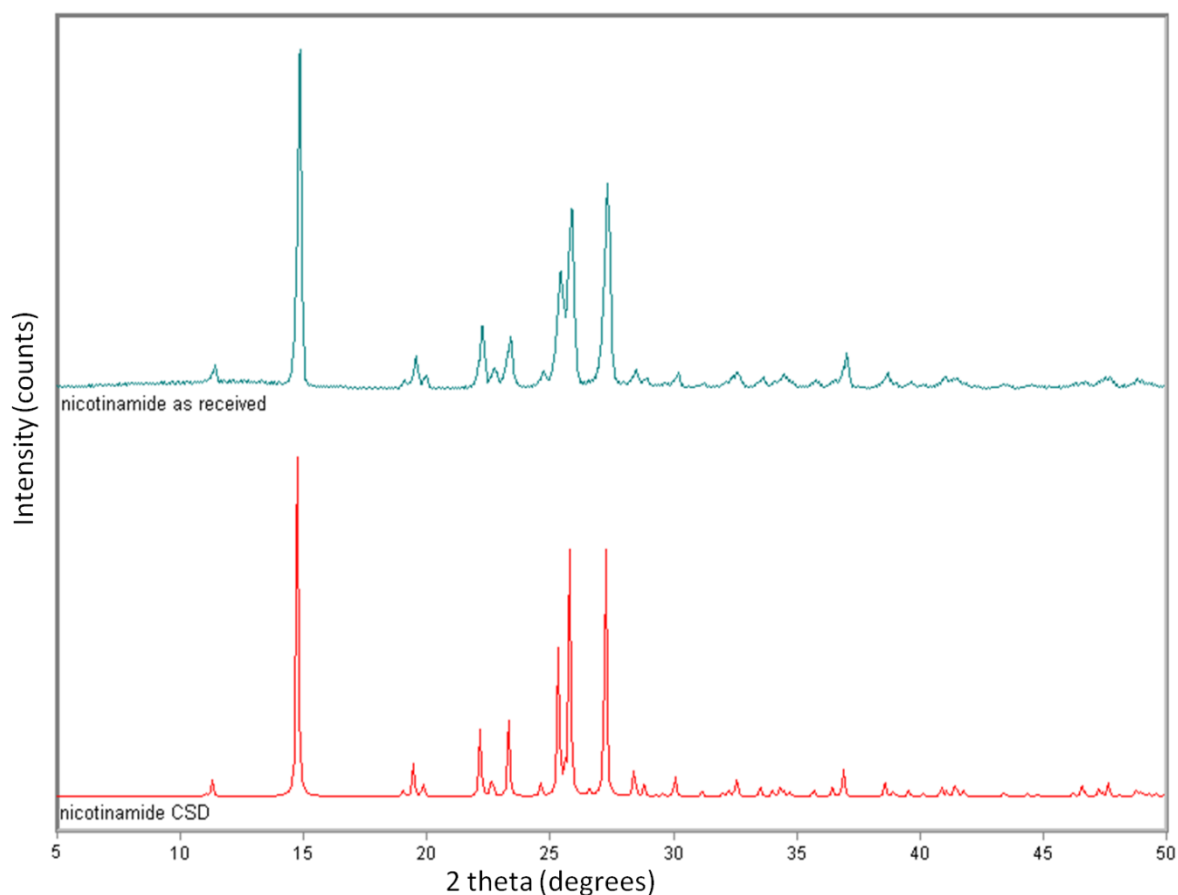


Figure 3.15. A representative powder X-ray diffraction pattern for unprocessed (top) and a standard diffraction pattern of nicotinamide obtained from CSD software (bottom).

### 3.2.4.3 FT-IR transmission

The FT-IR spectrum of unprocessed nicotinamide was obtained using the method described in 2.2.3. To the best of the author's knowledge, there is no available literature comparison between nicotinamide polymorphs FT-IR transmission spectrum. The measured spectrum will serve as a reference to detect any vibrational energy change that might arise due to polymorphic change or co-crystals formation. Figure 3.16 shows a transmission peak at  $3350\text{ cm}^{-1}$ . This peak can be correlated to the  $\text{NH}_2$  vibration (Akalin and Akyuz, 2006). This band is going to be of a particular interest to confirm the formation of nicotinamide-ibuprofen co-crystals.

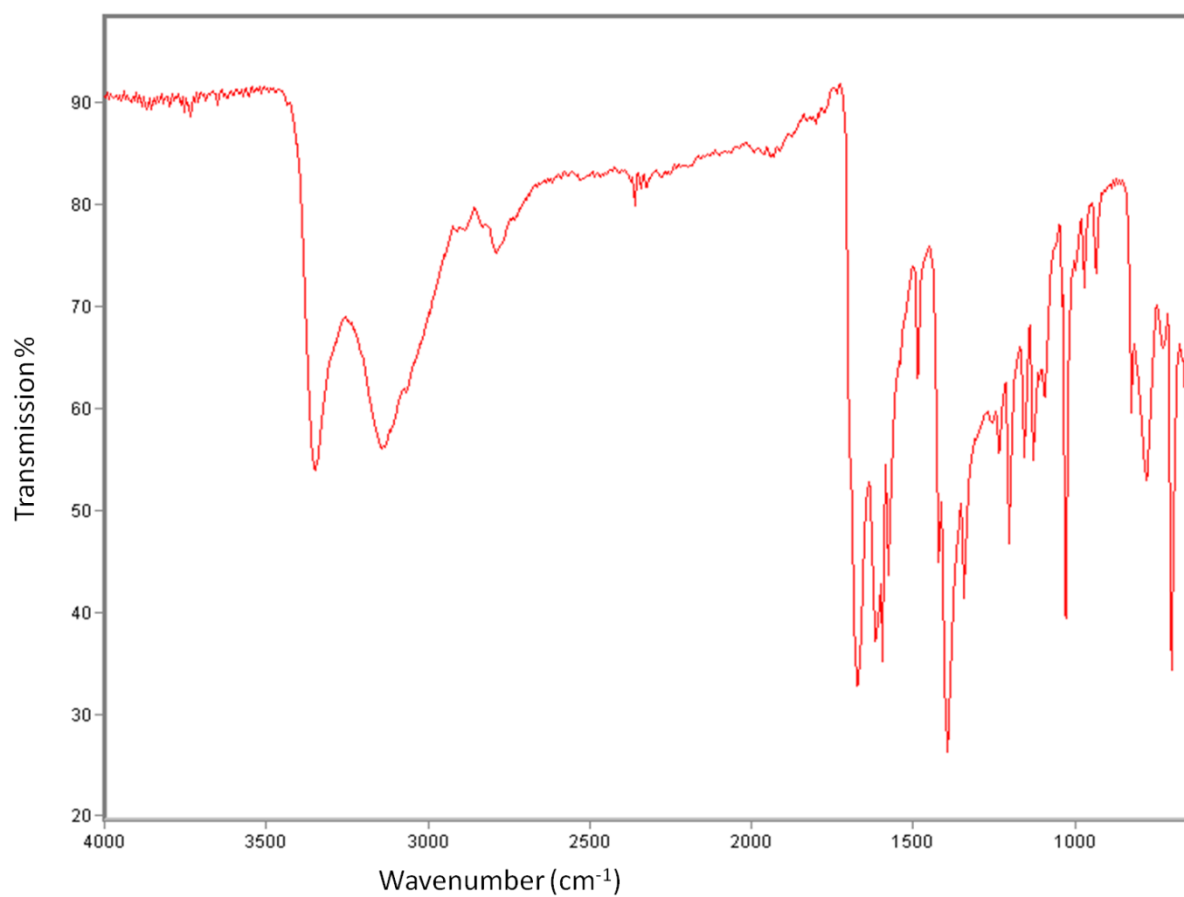


Figure 3.16. A representative FT-IR spectrum for unprocessed nicotinamide.



### 3.2.5 Naproxen

Naproxen or 2S-2-(6-methoxynaphthalen-2-yl) propanoic acid is a non steroidal anti-inflammatory

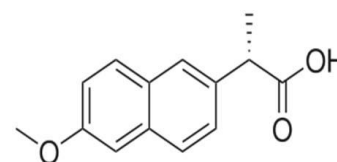


Figure 3.17. Naproxen structure.

drug (figure 3.17). It has analgesic and anti-pyretic activity as well. It is a white or whitish crystalline powder. It forms crystals when recrystallized using acetone-hexane. It melts at 154-158°C. Naproxen is considered to be practically insoluble in water. However, it dissolves in methanol, ethanol, and chloroform.

#### 3.2.5.1 Thermal analysis

##### TGA and DSC

Naproxen has four polymorphs. These polymorphs differ in their thermal profile. The melting point of polymorph I, II, III, IV is 156°C, 76°C, 140°C, and 148°C respectively (Song and Sohn, 2011). The thermal profile of unprocessed naproxen was measured using the methods described in section 2.2.1.1 for TGA and section 2.2.1.2 for DSC. The TGA scan reveals a weight loss associated with the degradation of naproxen begins at around 170°C (figure 3.18). An endothermic peak at 156°C is observed in the DSC scan. This peak can be correlated to the melting of naproxen polymorph I as mentioned above (Song and Sohn, 2011).

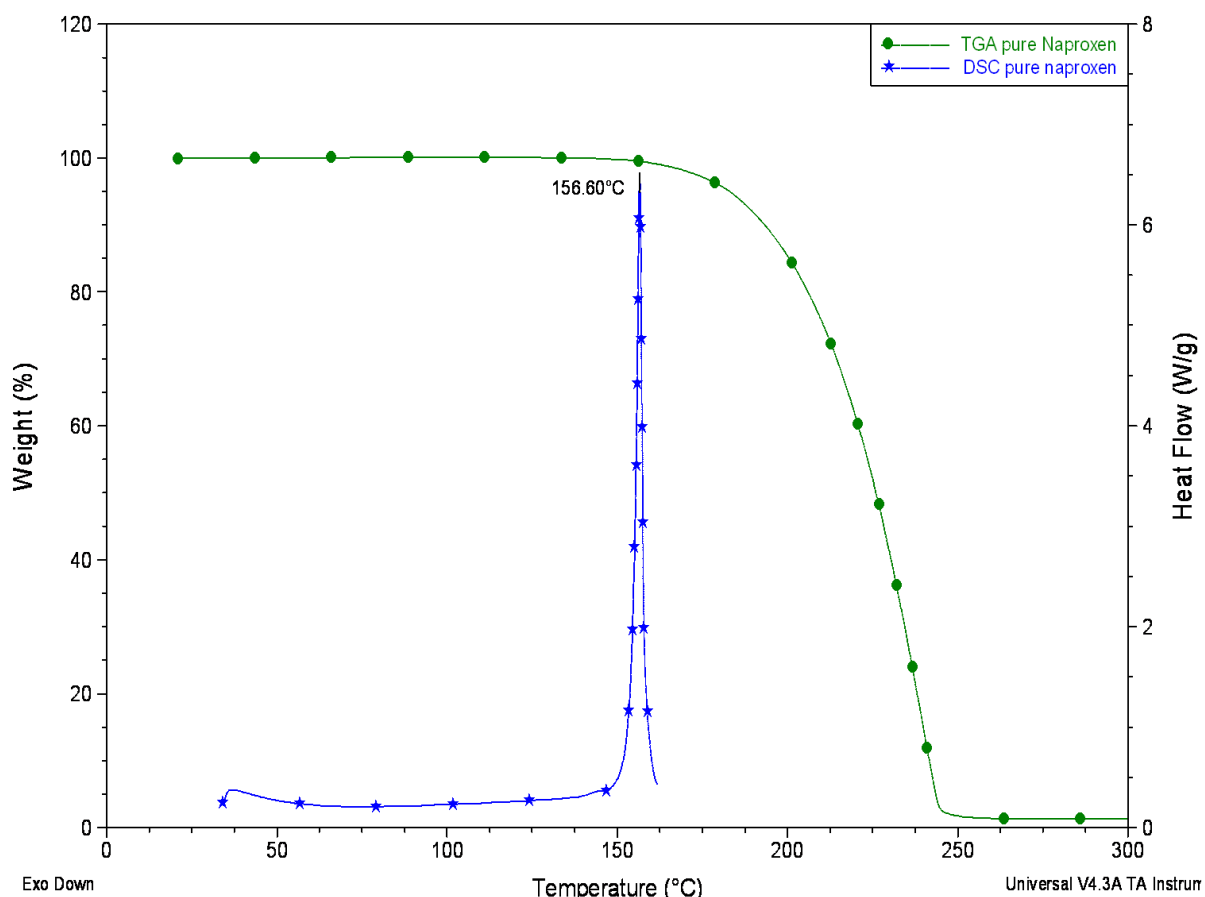


Figure 3.18. Representative TGA and DSC thermal profiles for unprocessed naproxen.

### 3.2.5.2 X-Ray

The x-ray diffraction pattern of naproxen was obtained using the method described in section 2.2.2. The CSD database offers one diffraction pattern for naproxen. The diffraction patterns of naproxen polymorphs are available (Song and Sohn, 2011). The polymorphs I, III, and IV have a peak at  $6^\circ$ . However, polymorph I has two additional peaks at  $11^\circ$  and  $12^\circ$ . The measured diffraction of the unprocessed naproxen shows peaks at  $6^\circ$ ,  $12^\circ$ , and  $13^\circ$  (figure 3.19). The difference in the peak positioning can be related to the use of a powder XRD instead of a single crystal XRD. This result indicates that the unprocessed naproxen as well as the diffraction pattern provided by the CSD software is form I naproxen.

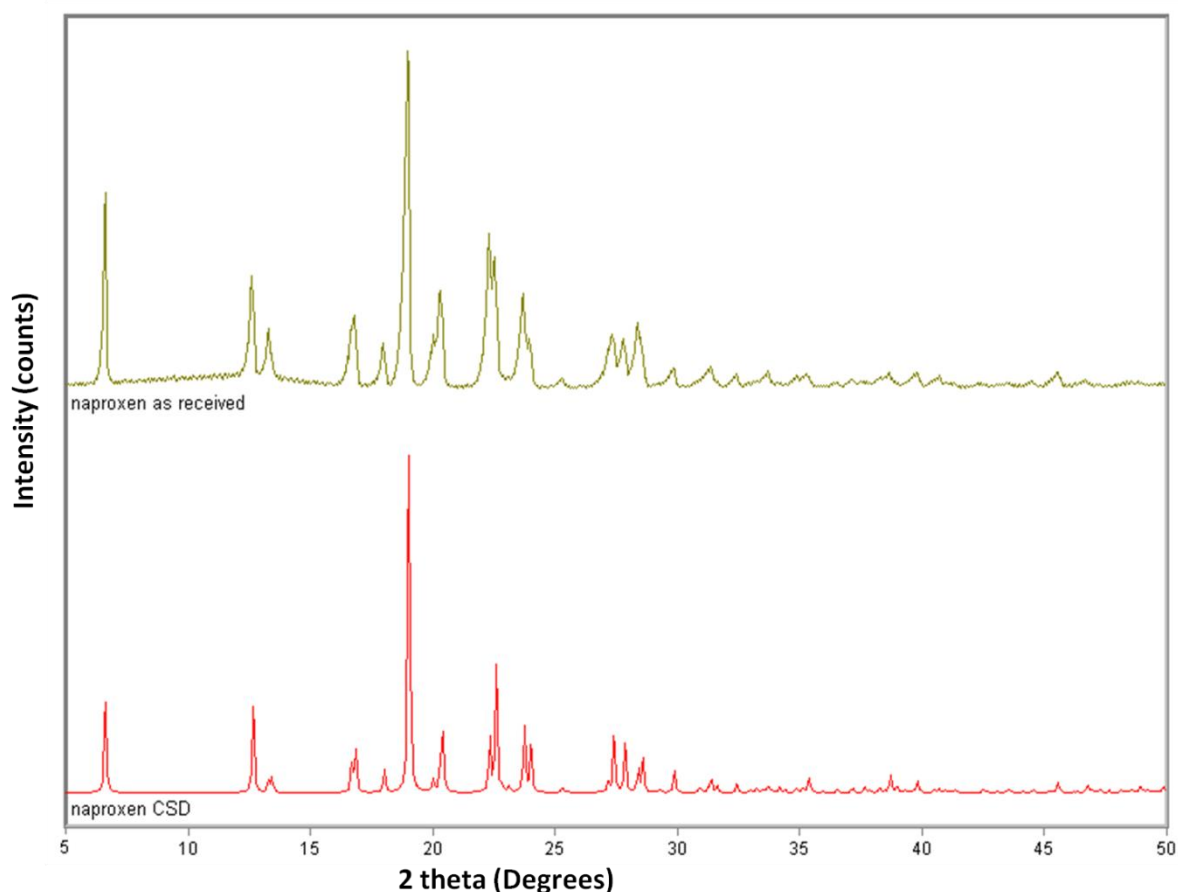


Figure 3.19. A representative powder X-ray diffraction pattern for unprocessed (top) and standard diffraction pattern from CSD library for naproxen (bottom).

### 3.2.5.3 FT-IR transmission

Unprocessed naproxen was analysed with the FT-IR using the method described in section 2.2.3 (figure 3.20). The scan of unprocessed naproxen will be used as a reference for comparison to detect any change in the vibrational behaviour of the bonds in the compound after processing. The full assignment of naproxen bond can be obtained from (Jubert et al., 2006).

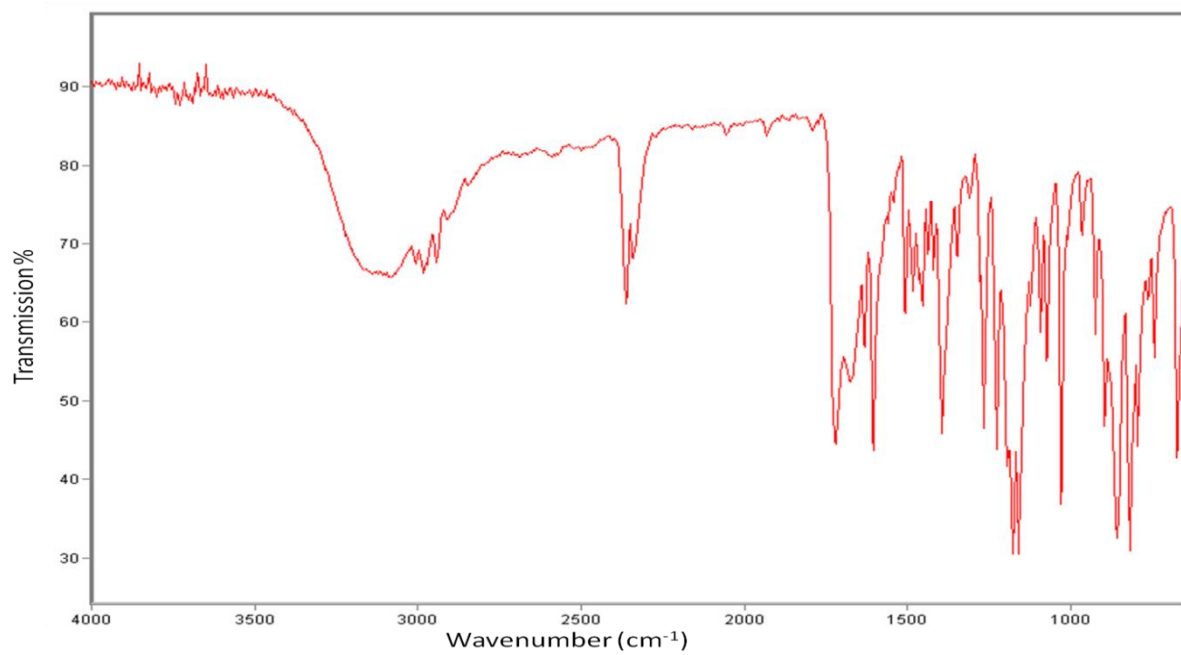


Figure 3.20. A representative FT-IR spectrum for unprocessed naproxen.

### 3.2.6 Flurbiprofen

Flurbiprofen is a white or whitish crystalline powder. It is a non-steroidal anti-inflammatory drug (figure

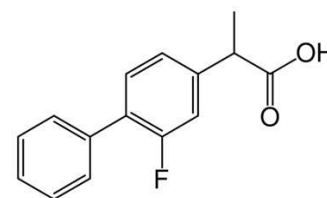


Figure 3.21. Flurbiprofen structure.

3.21). It is considered as practically insoluble in water. However, it is freely soluble in ethanol and methylene chloride. It has a melting point of 114-117°C with a molecular weight of 244.26 g/mol.

#### 3.2.6.1 Thermal analysis

##### TGA and DSC

Flurbiprofen has two polymorphs, each of which has a different thermal behaviour. The melting point of polymorph I and II using a heating rate of 10°C/min is 112.8°±0.2°C and 94°±0.2°C respectively (Lacoulonche et al., 1997). In this study, the unprocessed flurbiprofen thermal profile was obtained using the methods described in section 2.2.1.1 and 2.2.1.2. The thermal profile obtained (figure 3.22) shows a weight loss resulted from the thermal degradation of unprocessed flurbiprofen begins at 155°C. DSC scan of flurbiprofen reveals an endothermic peak at 114.8°C. This indicates that the unprocessed flurbiprofen is form I polymorph. A duplicate scan of pure flurbiprofen is provided in Appendix All.4.

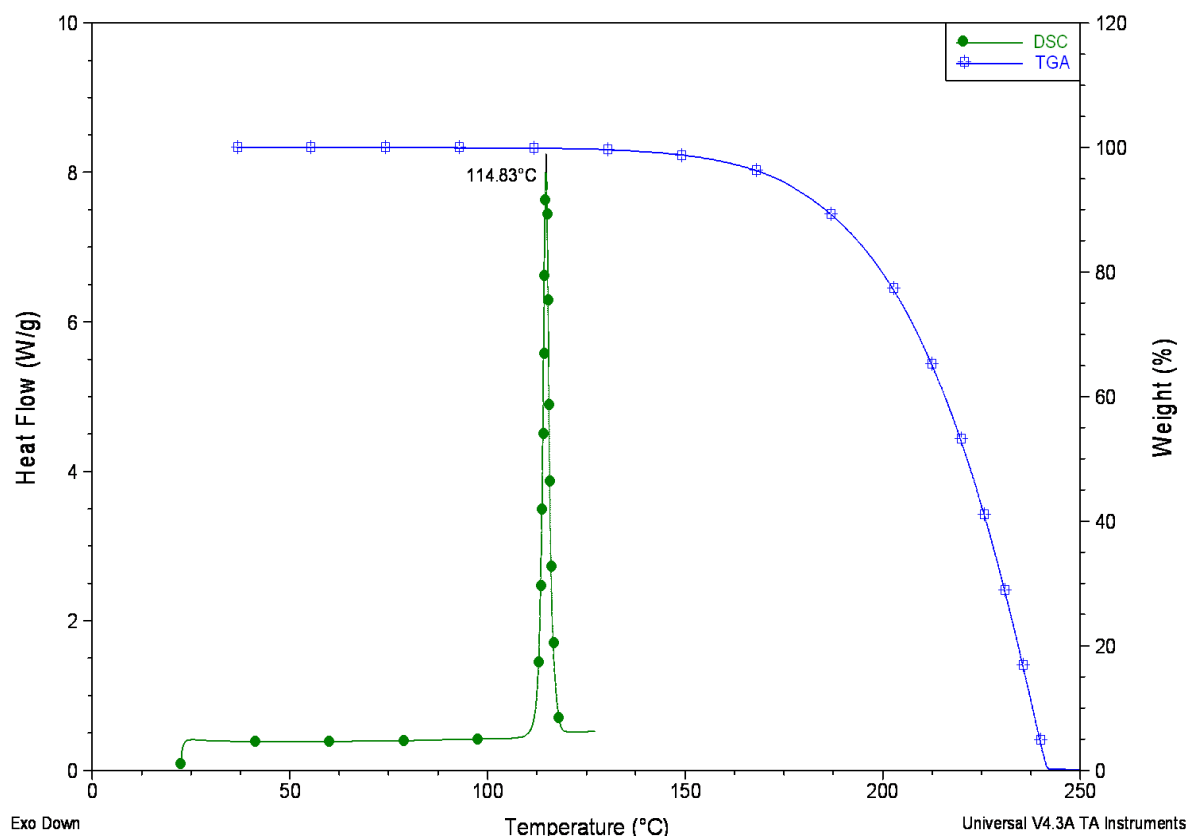


Figure 3.22. Representative TGA and DSC thermal profiles for unprocessed flurbiprofen.

### 3.2.6.2 X-ray

The diffraction pattern of polymorph I flurbiprofen characterized by two peaks at  $3.6^\circ$  and  $5.5^\circ$  while polymorph II has one peak at  $4.6^\circ$  (Lacoulonche et al., 1997). CSD library was found to contain one diffraction pattern for flurbiprofen without specifying the type of polymorph used. A sample of unprocessed flurbiprofen was analyzed with powder XRD using the method described in section 3.2.2. The diffraction pattern was found to contain a high noise/signal ratio preventing the identification of the polymorph (figure 3.23). This was caused by some cracks on the sample holder. Thus the diffraction pattern obtained from the unprocessed flurbiprofen was used as a template for comparison to detect any changes may occur to flurbiprofen.

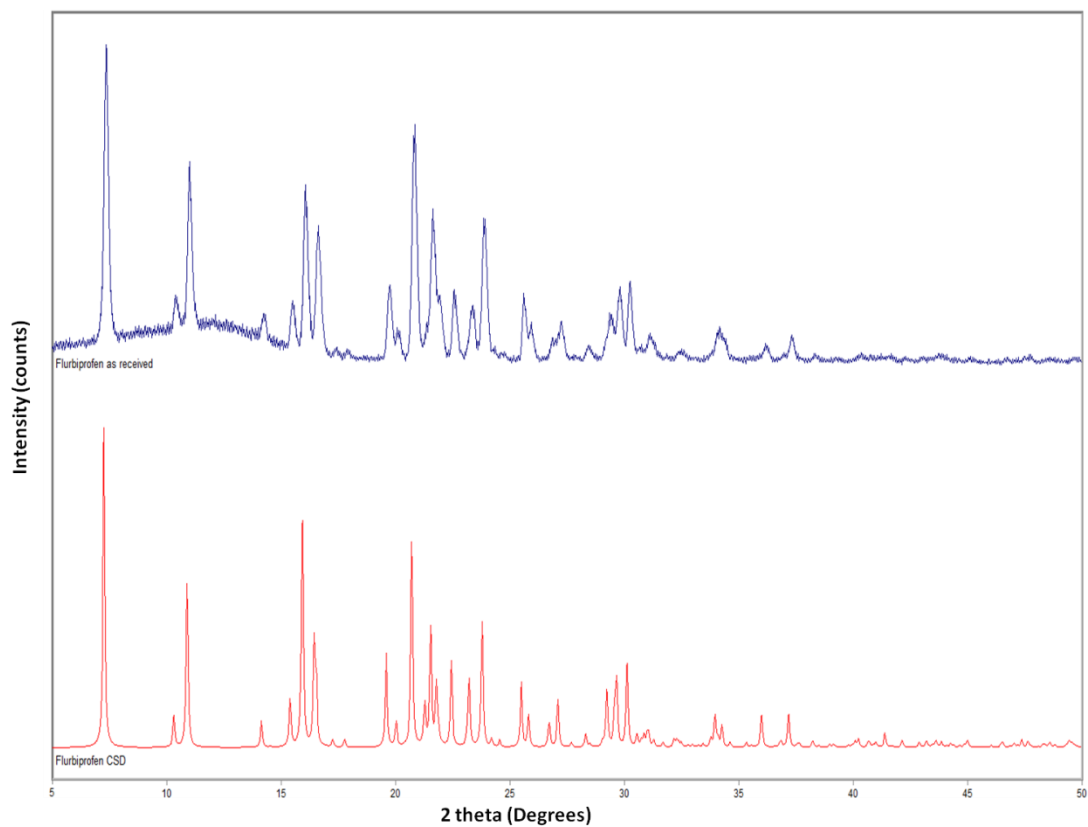


Figure 3.23. A representative powder X-ray diffraction pattern for unprocessed flurbiprofen (top) versus diffraction pattern obtained from CSD library (bottom).

### **3.2.7 HPMCAS**

Hydroxypropyl methyl cellulose or hypromellose acetate succinate is a cellulosic enteric coating agent. It is manufactured by Shin-Etsu.

It is used in aqueous coatings. Tri ethyl citrate is a recommended plasticiser (Shin-Etsu, 2005).

#### **3.2.7.1 Thermal analysis**

##### **TGA and DSC**

HPMCAS is known to be a hygroscopic polymer. In order to estimate the amount of absorbed moisture, the thermal profile for HPMCAS was obtained using the method described in section 2.2.1.1 and 2.2.1.2. The TGA profile (figure 3.24) indicates that the polymer has lost 2% of its weight at 100°C. This loss is believed to be due to the evaporation of residual moisture. The DSC profile shows a glass transition step with a value of 123.13°C calculated with TA software compared to a Tg literature value of around  $122 \pm 0.8^\circ\text{C}$  (Kablitz et al., 2006). A duplicate scan of pure HPMCAS is shown in the Appendix AII.5.



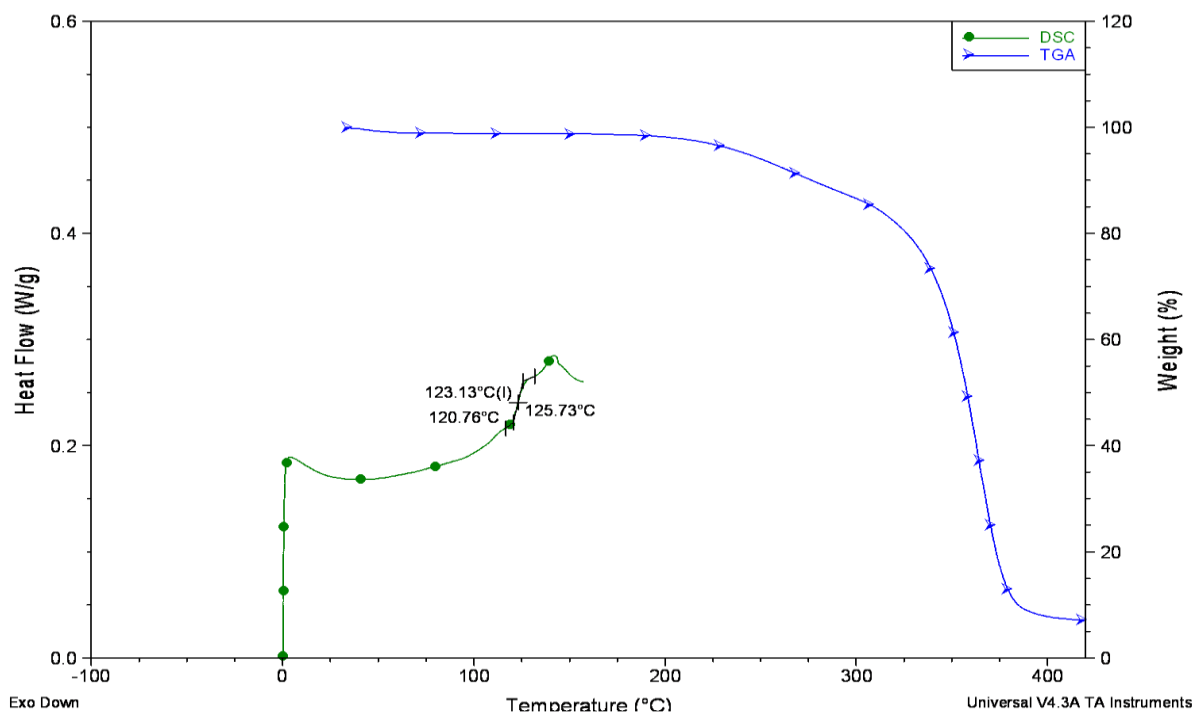


Figure 3.24. Representative TGA and DSC thermal profiles for unprocessed HPMCAS powder.

### 3.2.7.2 Powder X-ray diffraction

The diffraction pattern of HPMCAS was obtained using the method described in section 2.2.2. The diffraction pattern in figure 3.25 reveals a very high noise/signal ratio, in addition to the appearance of two wide peaks. This diffraction pattern is a typical diffraction pattern for amorphous materials. This suggests that the polymer is predominantly amorphous which conforms with the reported literature (Shin-Etsu, 2005).

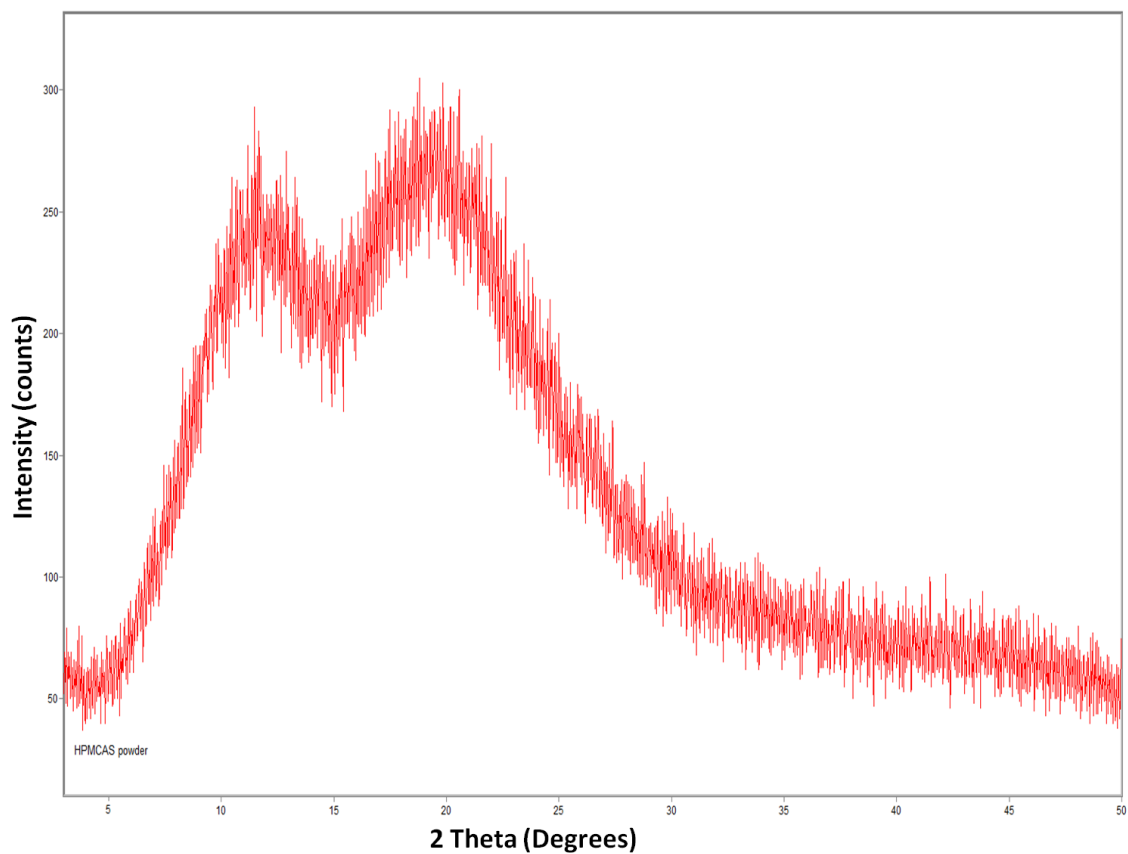


Figure 3.25. A representative powder x-ray diffraction pattern for unprocessed HPMCAS powder.

### 3.2.7.3 FT-IR transmission

The FT-IR transmission spectrum of HPMCAS was obtained using the method described in section 2.2.3. The FT-IR spectrum for unprocessed HPMCAS can be used as a reference to detect any vibrational energy changes might arise during processing (figure 3.26).

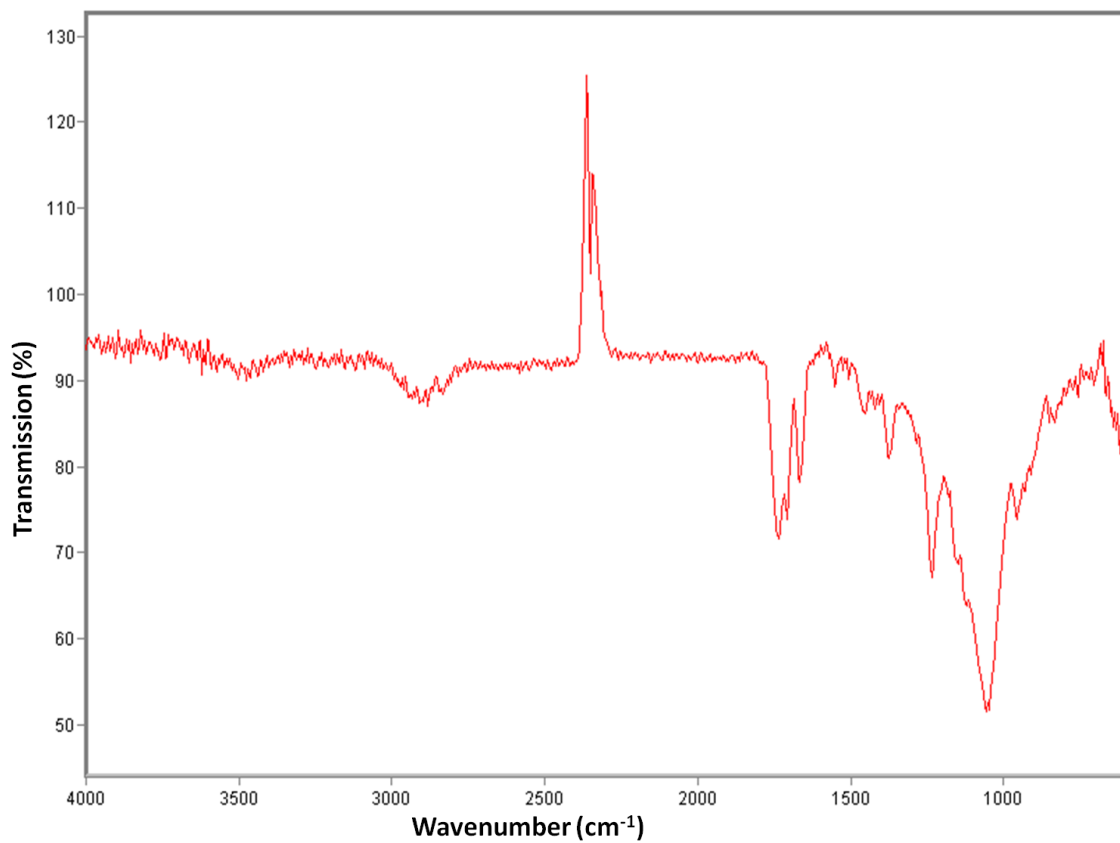


Figure 3.26. A representative FT-IR spectrum for unprocessed HPMCAS powder.

### **3.3 Recrystallization experiments**

The unprocessed materials were studied in section 3.1 in order to identify their thermal, crystallographic, and their spectroscopic characteristics. This section studied the effect of solvent on the raw materials (after a recrystallization with various solvent systems). The comparison of the data obtained from the analysis of the recrystallized materials should provide a clear evidence about the effect of solvent systems on the physicochemical properties of the unprocessed drugs.

#### **3.3.1 Caffeine recrystallization**

The analysis of the unprocessed caffeine section 3.1.1 revealed that caffeine is in the form of polymorph I. The crystal structure and the vibrational features were identified. The study of the solvent effect on unprocessed caffeine was performed by re-crystallizing caffeine using the method described in section 2.3.1 and analyzing the resultant compound.

##### **3.3.1.1 Recrystallization using acetone/chloroform 3:2 v/v**

In order to form a drug-containing film, a suitable solvent was needed to dissolve the polymer (HPMCAS). Acetone is considered as a good solvent for the polymer. However, it is considered as a polar solvent. Therefore, it might disrupt the co-crystals loaded into the polymeric film and prevent their components from re-forming co-crystals again. Chloroform on the other hand, is a good solvent for caffeine, malonic acid, ibuprofen and nicotinamide but not for HPMCAS. Therefore a few attempts were carried out to investigate the best mixing ratio of both solvents. Consequently, the result revealed that the best

ratio is 3:2 v/v acetone/chloroform. Care was taken over the exothermic solvent mixing reaction.

The recrystallization process of caffeine from acetone acetone/chloroform was performed using the method described in section 2.3.1. The physicochemical properties of the final drug after drying was identified and compared to that of unprocessed caffeine.

Recrystallized caffeine was scanned using TGA, DSC, X-ray, and FT-IR.

### **3.3.1.1.1 Thermal analysis**

#### **TGA and DSC**

Recrystallized caffeine was scanned using TGA and DSC in order to detect any change in the thermal behaviour of caffeine, and to identify the existence of any residual solvent. Tzero™ hermetic pans were used for DSC analysis in order to minimize the sublimation and consequently any instrument damage.

Recrystallized caffeine was analyzed using the method described in section 2.2.1.1 and 2.2.1.2. The TGA profile reveals that caffeine lost about 3% of its weight at 35°C of the weight loss continues to around 80°C (figure 3.27). This 3% is expected to be due to the evaporation of the residual solvent. Another sharp onset of weight loss for caffeine appears to begin at about 160°C. The DSC profile reveals 4 endothermic peaks at 79°C, 139°C, 179°C, and 235°C. The peak at 79°C is a strong intensity narrow peak, untypical of a solvent evaporation peak. the literature revealed that this peak is related to the peritectic decomposition process of the hydrate(Griesser and Burger, 1995 , Bothe and Cammenga, 1980). Hence the weight loss in the TGA profile below

80°C may be explained by the evaporation of water molecules. The second endothermic peak at 140°C in the DSC profile is found to be linked to the phase transformation of caffeine from polymorph I into polymorph II (Manduva et al., 2008). It is noticeable from figure 3.27 that the peak at 179°C has a wide base. This peak is linked in the literature to the sublimation temperature of caffeine (Bothe and Cammenga, 1980). The last peak is at the melting range of caffeine thus it can be correlated to the melting of recrystallized caffeine.

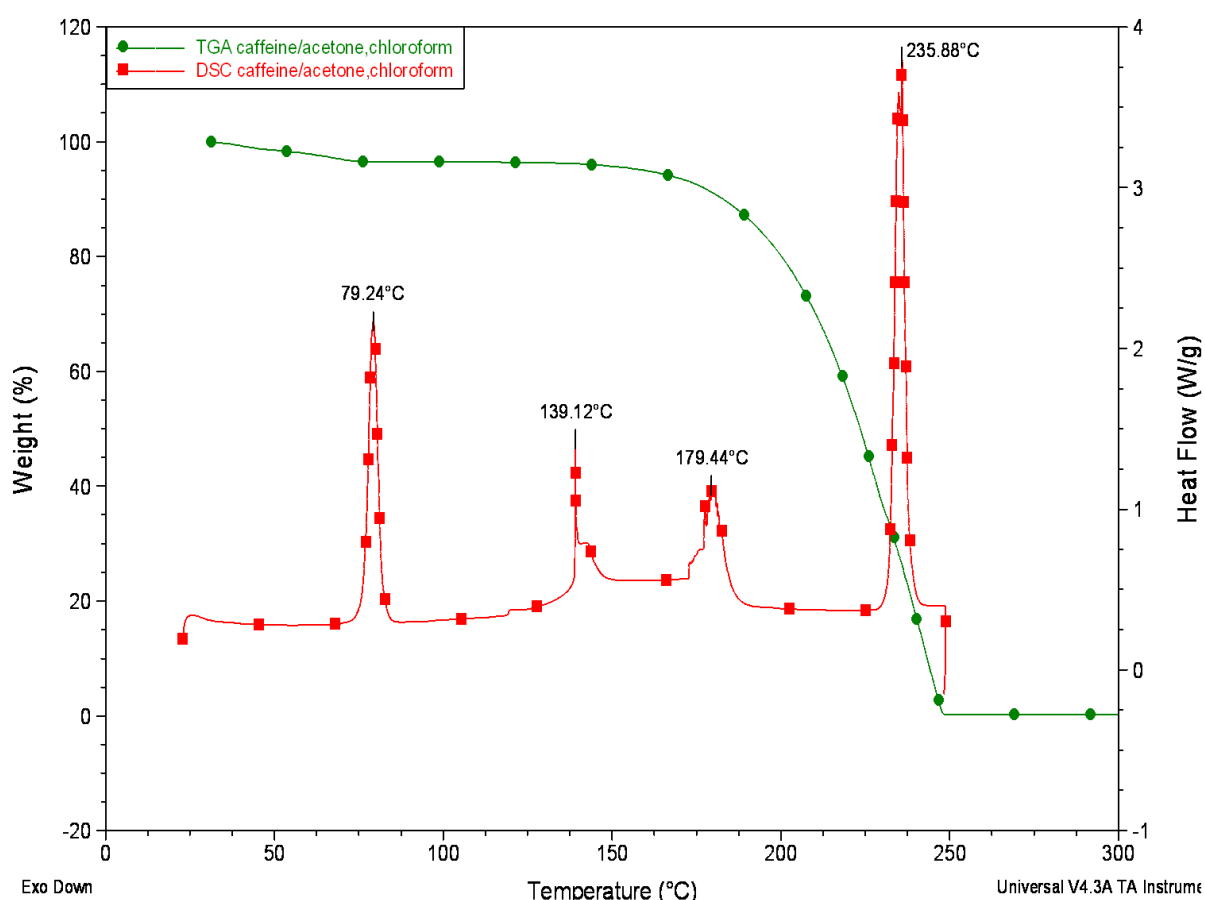


Figure 3.27. Representative TGA and DSC thermal profiles for recrystallized caffeine from acetone/chloroform.

In order to identify the solvent effect on the caffeine physicochemical properties, DSC thermal profile of recrystallized and unprocessed caffeine were plotted in figure 3.28. It is noticeable that caffeine sublimation is shifted from 158°C in the thermal profile in unprocessed caffeine to 179°C in the thermal profile of the

recrystallized one. The melting point of unprocessed caffeine is shifted from 237°C to 235°C. This shift is thought to be related to the water effect in the hydrated form.

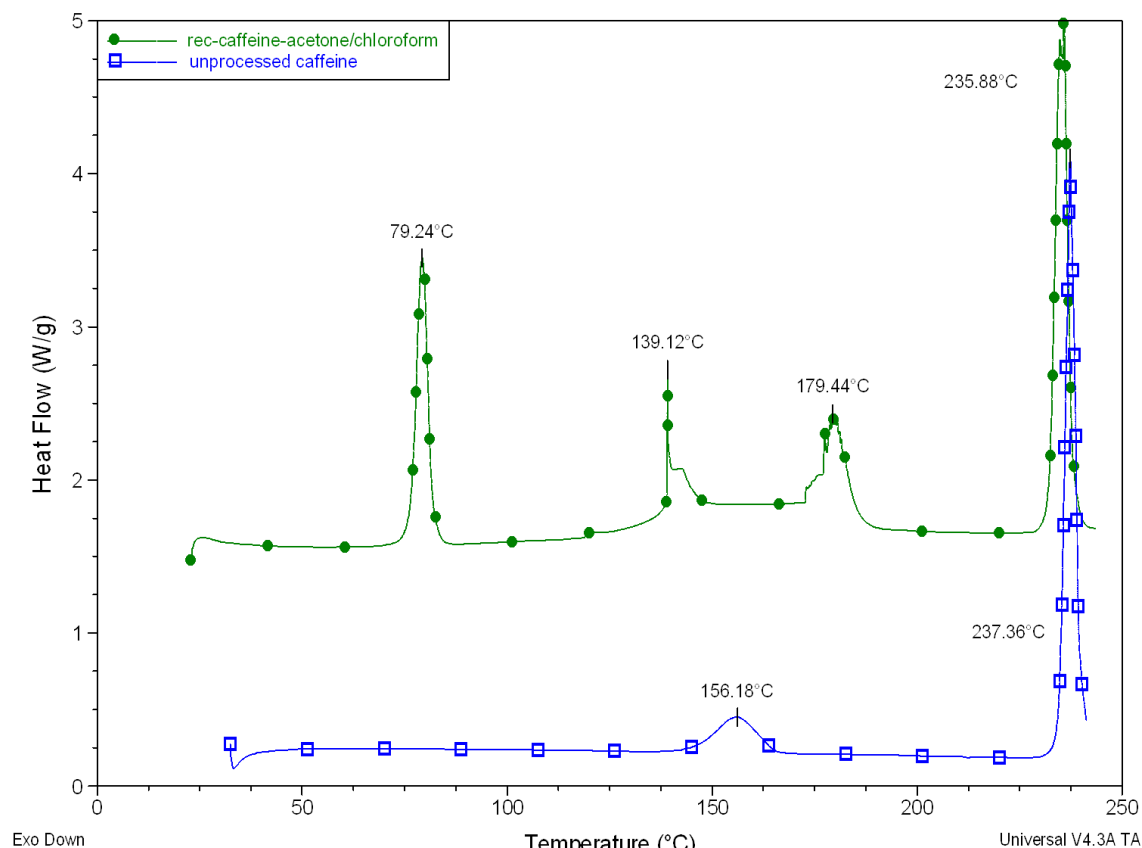


Figure 3.28. A representative DSC thermal profile of recrystallized (green) and unprocessed (blue) caffeine.

As a conclusion, the recrystallization of caffeine from acetone/chloroform solvent system resulted in the conversion of anhydrous caffeine form II into monohydrated caffeine.

### 3.3.1.2 Powder X-ray diffraction

The diffraction pattern of recrystallized caffeine was obtained using the method described in section 2.2.2. The diffraction pattern of the recrystallized caffeine was compared to the diffraction pattern of the unprocessed caffeine and anhydrous and hydrated caffeine obtained from the CSD library (figure 3.29).

The diffraction pattern of recrystallized caffeine reveals a diffraction peak at 6°. This peak is not observed in the diffraction of hydrated or anhydrous caffeine (CSD). To the best of knowledge this peak could not be correlated neither to the polymorphism nor to the hydration of caffeine. However, it might be related to the sampling process. The diffraction pattern of recrystallized caffeine reveals peaks at 8°, 11°, 12°, and 13°. These peaks are correlated to the diffraction pattern of monohydrated caffeine.

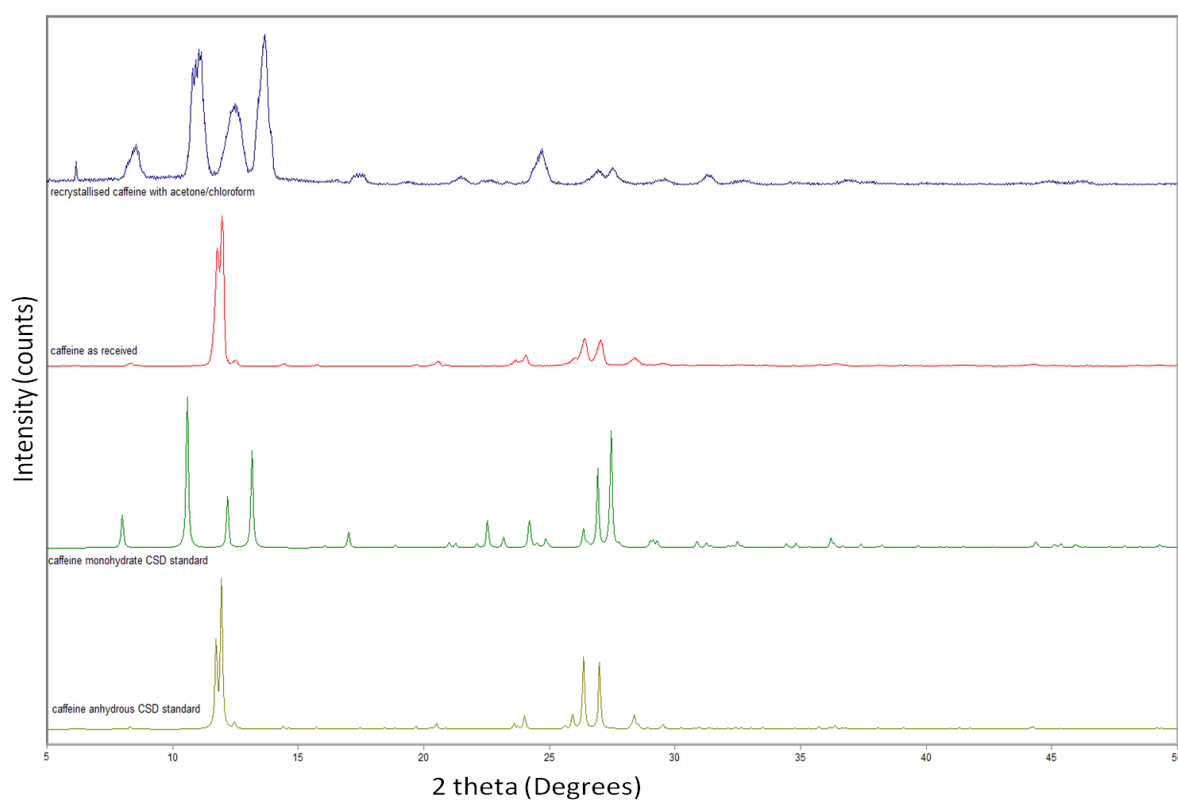


Figure 3.29. A representative powder X-ray diffraction pattern of recrystallized caffeine (top-blue), caffeine as received (second from top-red), caffeine monohydrate CSD (third from top-green), and anhydrous caffeine CSD (bottom-yellow).

Consequently, both thermal profile and the x-ray diffraction pattern confirm the conversion of anhydrous caffeine form II polymorph to monohydrated caffeine.



### **3.3.2 Recrystallization with ethanol/water 4:1 w/w**

Caffeine was recrystallized from ethanol/water using the method described in section 2.3.1. The product was characterized and compared to the physicochemical properties of unprocessed caffeine.

#### **3.3.2.1 Thermal analysis**

##### **TGA and DSC**

Thermal behaviour of recrystallized caffeine was obtained using the method described in section 2.2.1.1 and 2.2.1.2. The thermal behaviour of recrystallized caffeine was plotted in figure 3.30. The TGA profile shows a weight loss of 3% beginning at 35°C and ending at 75°C. This behaviour is similar to the TGA thermal behaviour of recrystallized caffeine section 3.2.1.1.1. The loss is expected to be correlated to the slow evaporation of residual solvent or water evaporation. DSC profile reveals four endothermic peaks at 78°C, 138°C, 192°C and 236°C. Similarly to the DSC analysis of the recrystallized caffeine in section 3.2.1.1.1, those peaks can be correlated to: the peritectic decomposition process of the hydrate (78°C), the phase transformation temperature of caffeine from polymorph I into polymorph II (138°C), the sublimation temperature of caffeine (192°C), and the melting point of caffeine (236°C).

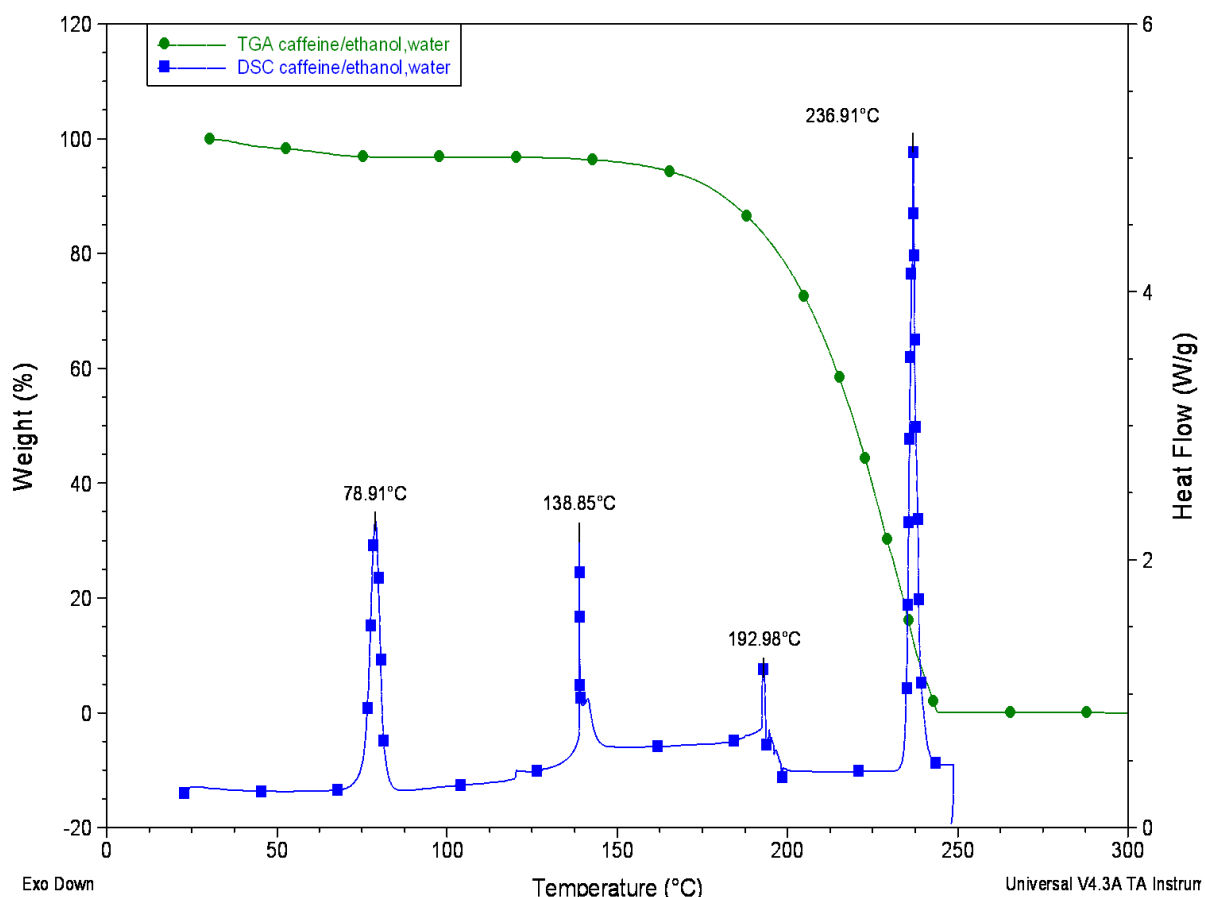


Figure 3.30. Representative TGA and DSC thermal profiles for recrystallized caffeine from ethanol/water.

The same comparison used in section 3.2.1.1.1 is applicable in this section, i.e. This concluded that recrystallization of caffeine from ethanol/water has resulted in the conversion of anhydrous caffeine form II into monohydrated caffeine.

### 3.3.2.2 Powder X-ray diffraction

The diffraction pattern of recrystallized caffeine was obtained using the method described in section 2.2.2. The diffraction pattern of recrystallized caffeine was plotted and compared to the diffraction pattern of unprocessed caffeine and standard diffraction patterns for anhydrous (form II) and monohydrated caffeine (figure 3.31). Similarly to section 3.2.2, the diffraction pattern of recrystallised caffeine revealed four characteristic peaks at 8°, 11°, 12°, and 13°. These peaks can be correlated to monohydrated caffeine diffraction pattern. Thus

caffeine was converted by re-crystallization from anhydrous form II into a monohydrated form. This conclusion conforms with the conclusion obtained in section 3.2.2.1.

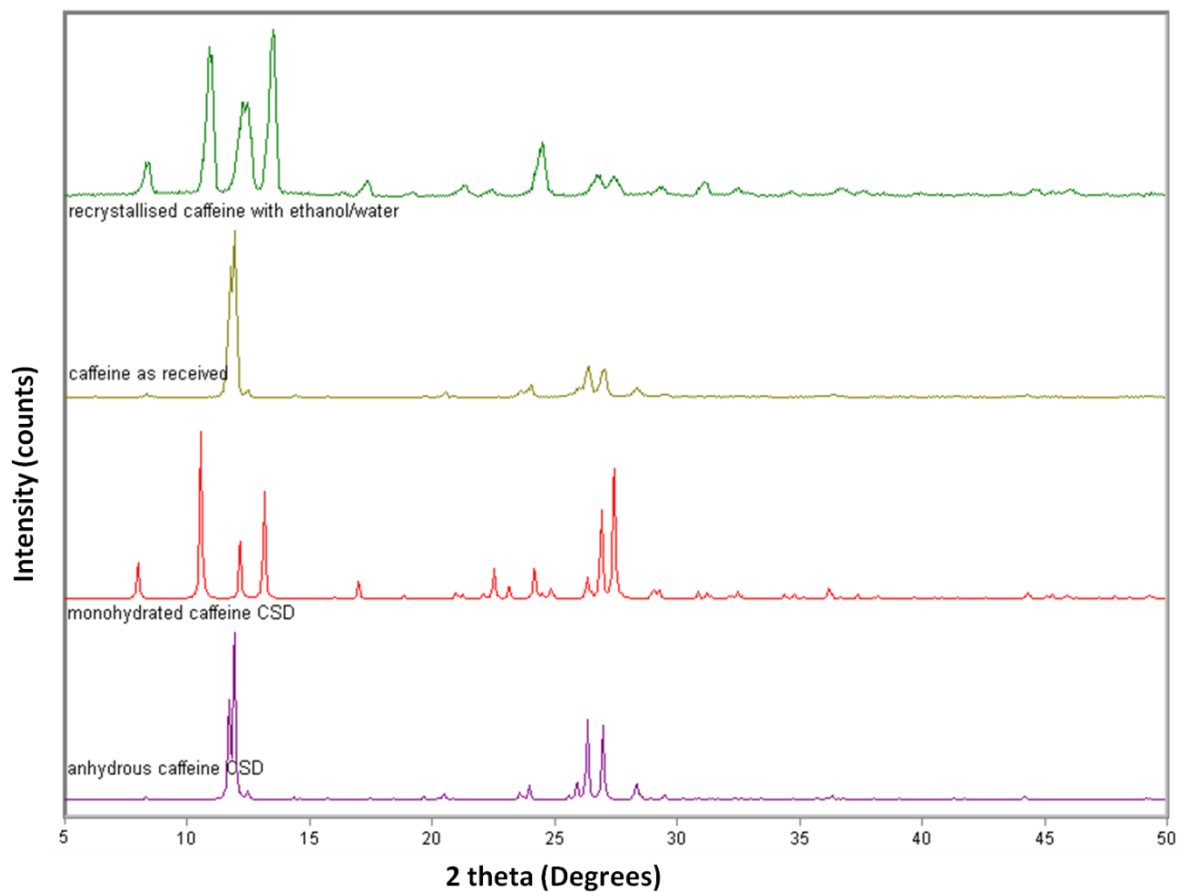


Figure 3.31. A representative powder x-ray diffraction pattern for anhydrous caffeine CSD standard (bottom-purple), monohydrate caffeine CSD standard (second from bottom-red), caffeine as received (third from bottom-yellow), and recrystallized caffeine with ethanol/water (top-green).

### 3.3.3 Recrystallization of caffeine using acetonitrile

Caffeine was recrystallized from acetonitrile using the method described in section 2.3.1. The physicochemical properties of the resultant product were obtained from analysis with TGA, DSC, and X-ray.

#### 3.3.3.1 Thermal analysis

##### TGA & DSC

The thermal profile of recrystallized caffeine was obtained using the method described in section 2.2.1.1 and 2.2.1.2. TGA and DSC thermal profiles were plotted in figure 3.32. TGA profile in figure 3.32 reveals that the weight loss associated with the degradation of caffeine begins at 140°C with no weight loss step at around 35°C such as those observed in section 3.2.1.1.1 and 3.2.2.1. On the other hand, DSC scan reveals the same 4 peaks observed in section 3.2.1.1.1 and 3.2.2.1, i.e. the recrystallization of caffeine with acetonitrile resulted in the formation of caffeine monohydrate.

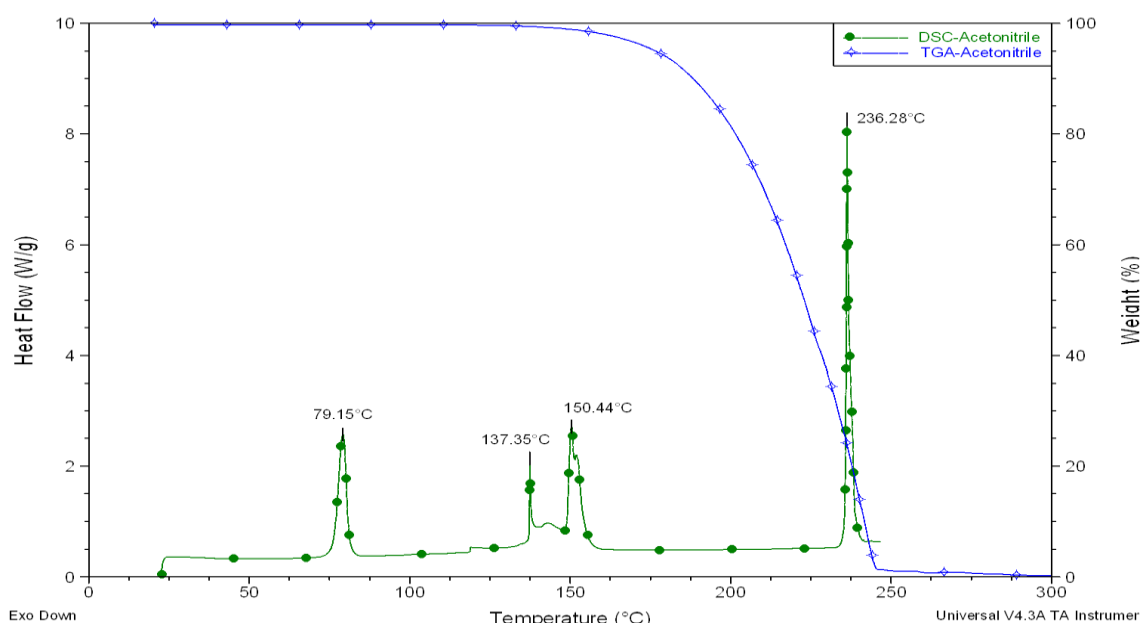


Figure 3.32. A representative TGA and DSC thermal profile for recrystallized caffeine form acetonitrile.

### 3.3.3.2 Powder X-ray scan diffraction

The diffraction pattern of recrystallized caffeine was obtained using the method described in section 2.2.2. The diffraction pattern was compared to the patterns of unprocessed anhydrous and monohydrated caffeine in figure 3.33. The diffraction pattern of the recrystallized caffeine reveals peaks at 8°, 10°, 11°, and 12°. This is similar to the diffraction pattern observed in section 3.1.2.2 and 3.2.2.2. Those peaks can be observed in the diffraction pattern of monohydrated caffeine. Thus the caffeine recrystallized from acetonitrile can be considered as monohydrated caffeine as well. This result conforms with the result obtained from the thermal analysis in section 3.2.3.1.

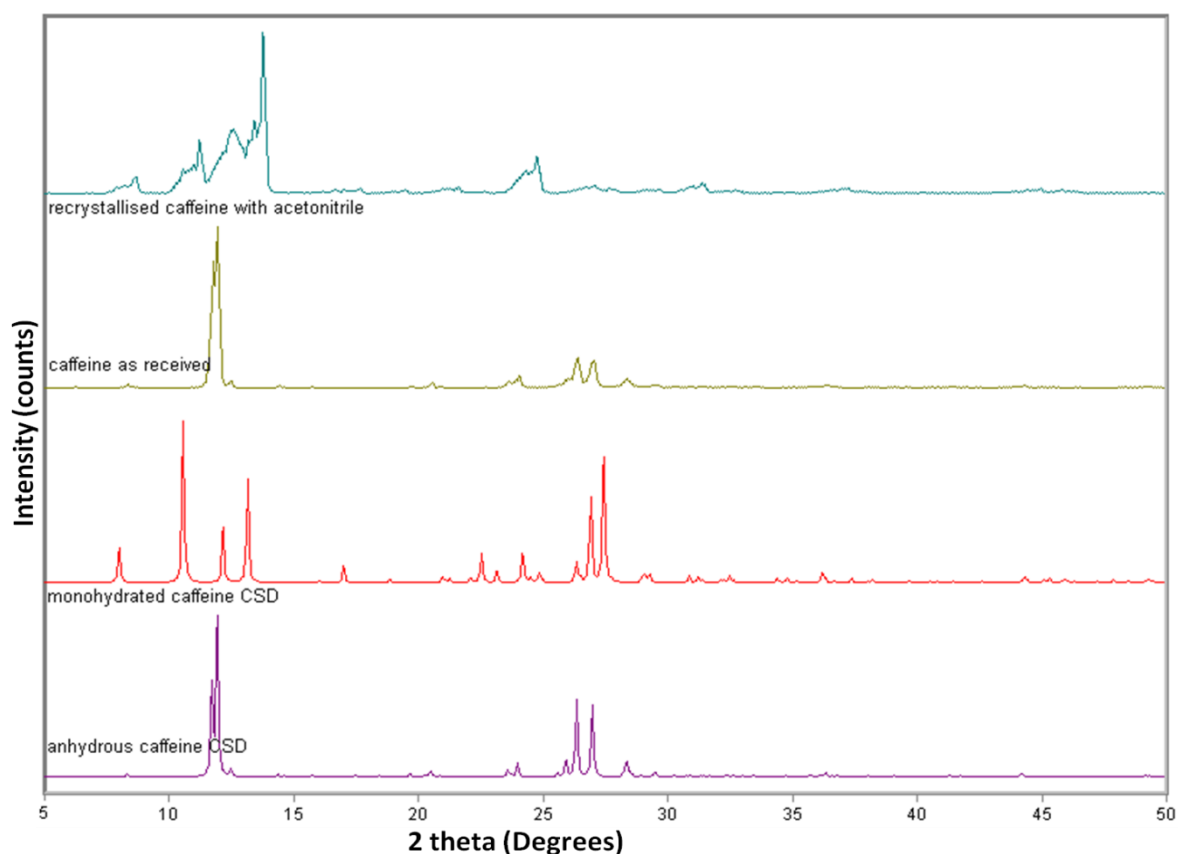


Figure 3.33. Representative powder x-ray diffraction pattern for a standard anhydrous caffeine CSD (bottom purple), a standard monohydrate caffeine CSD (second from bottom-red), caffeine as received (third from bottom- yellow), and caffeine recrystallized from acetonitrile (top-bluish green).

Caffeine recrystallized with acetone/chloroform, ethanol/water, and acetonitrile is found to convert into the monohydrated form. This may be explained in the recrystallization process using ethanol/water as the caffeine comes into a contact with water molecules. However, it is unusual in the case of acetonitrile or acetone/chloroform. Caffeine most likely must have interacted with atmospheric moisture during the evaporation of the solvents to form the monohydrated caffeine form.

### **3.3.2 Recrystallization of malonic acid**

Malonic acid was recrystallized from acetone/chloroform, ethanol/water, and acetonitrile using the method described in section 2.3.1. Physicochemical properties of recrystallized malonic acid were obtained from analysis with TGA, DSC, and XRD.

#### **3.3.2.1. Thermal analysis**

##### **TGA and DSC**

The thermal profiles of recrystallized malonic acid from acetone/chloroform were obtained using the methods described in section 2.2.1.1 and 2.2.1.2. The results of the thermal analyses were plotted in figure 3.34. The TGA profile reveals that a weight loss resulted from the thermal degradation of malonic acid begins at 140°C in a similar manner to the unprocessed malonic acid degradation profile. The DSC thermal profile reveals two endothermic peaks at 90°C and 134°C. The first be can be correlated to the phase transition temperature of malonic acid (Bougeard et al., 1988). However, a shift was observed for the solid phase transition temperature from 85°C in the unprocessed malonic acid to 90°C in the recrystallized form.

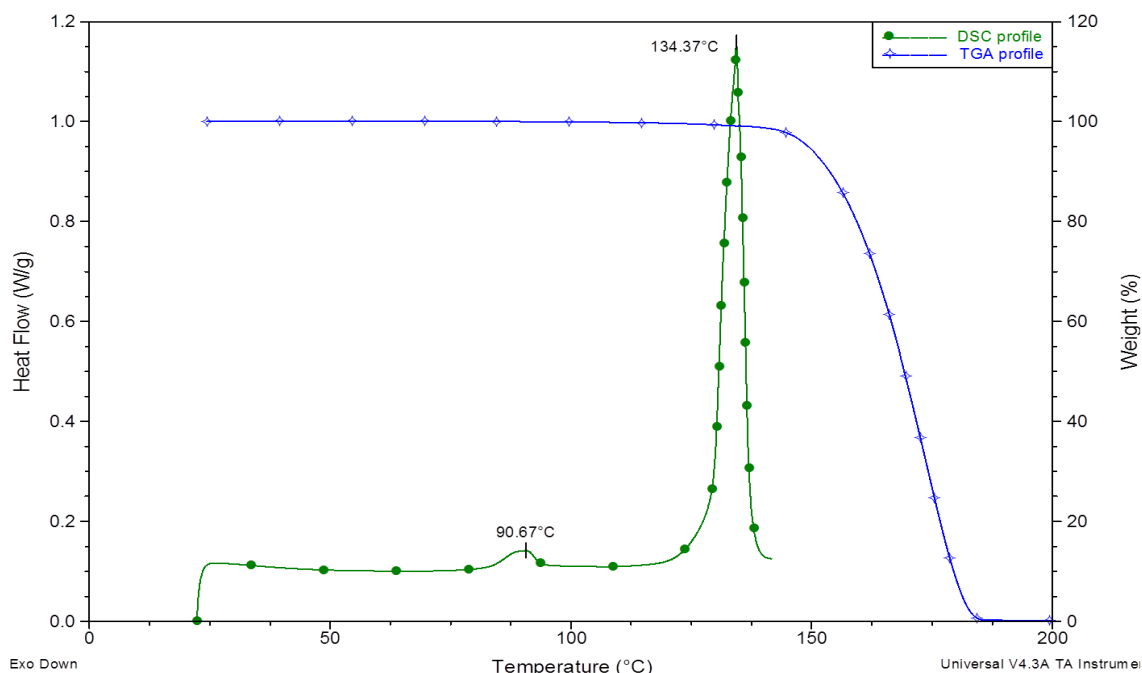


Figure 3.34. A representative TGA and DSC thermal profile for recrystallized malonic acid from acetone/chloroform.

The thermal profiles for malonic acid recrystallized with acetonitrile and ethanol/water were obtained using the methods described in section 2.2.1.1 and 2.2.1.2 the data are given in figure All.7. The thermal profiles for both solvent systems reveal similarity to the thermal profile of recrystallized malonic acid with acetone/chloroform. Hence, the recrystallization of malonic acid from acetone/chloroform, ethanol/water, and acetonitrile shifted the solid phase transition peak. However, it did not change the melting point of malonic acid.

### 3.3.2.2 Powder X-ray diffraction

The diffraction pattern of recrystallized malonic acid was obtained using the method described in section 2.2.2. The collected pattern is shown with the diffraction pattern of malonic acid recrystallized from ethanol/water, recrystallized from acetonitrile, and the unprocessed batch in figure 3.35. Two characteristic diffraction peaks at  $17^\circ$  and  $18^\circ$  are observed in the diffraction patterns of malonic acid recrystallized from ethanol/water, recrystallized from



acetonitrile, or unprocessed. However, the diffraction pattern of recrystallized malonic acid from acetone/chloroform reveals one peak at 17° and a very low intensity peak at 18°. The difference between the diffraction patterns in figure 3.35 can be correlated to the use of a smaller quantity of sample for recrystallized malonic acid with acetone/chloroform, ethanol/water, and acetonitrile.

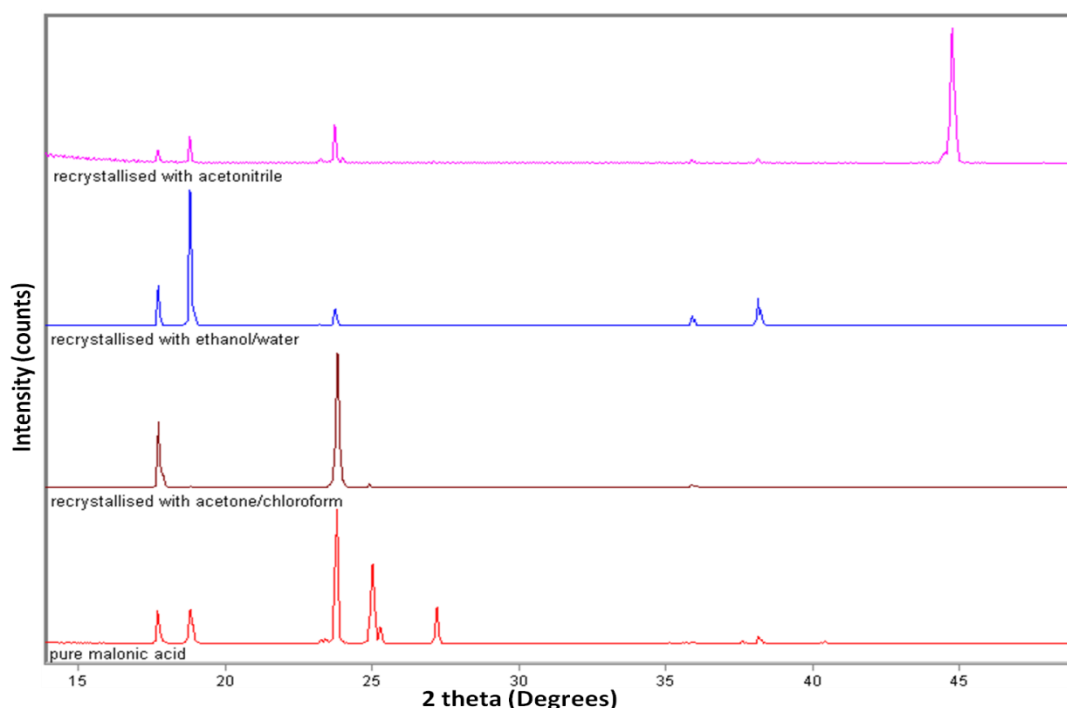


Figure 3.35. Representative powder x-ray diffraction pattern for unprocessed malonic acid (bottom-red), malonic acid recrystallized from acetone/chloroform (second from bottom-dark red), recrystallized from ethanol/water (third from bottom-blue), and recrystallized from acetonitrile (top-pink).

Therefore, it can be concluded that all the solvent systems resulted in the same polymorphic form.

### 3.4 Summary and conclusion

The raw materials were characterized in order to identify their physicochemical properties. In addition to that, the solvent systems effect was studied as well by re-crystallizing these drugs.

The characterization of the unprocessed materials revealed that caffeine is a form II anhydrous caffeine, malonic acid is a form  $\alpha$ , ibuprofen is a racemic mixture, and nicotinamide and naproxen are form I. On the other hand, the morphology of flurbiprofen was hard to identify.

Thermal DSC profile of malonic acid showed a small solid phase transition endotherm from polymorph  $\beta$  to polymorph  $\alpha$ .

The solvent systems were observed to have no effect on the raw materials except in the case of caffeine. Recrystallizing caffeine using the aforementioned solvent systems resulted in the conversion of anhydrous caffeine into a monohydrated one. It was observed as well that the thermal DSC scan of caffeine the appearance of a solid phase transition peak that confirms the presence of polymorph I. This indicates the conversion of some caffeine from polymorph II to polymorph I. The TGA thermal profile for caffeine showed a 3% weight loss except in the case of acetonitrile. This weight loss was correlated to the evaporation of the residual moisture.

## **Chapter 4**

### **Preparation of co-crystals and their characterization**

## 4.1 Introduction

Drug-excipients interaction can impact the bioavailability and stability of the API. The study of such interactions requires a knowledge of the properties and the behaviour of the compounds involved. The interaction of a system composed of a co-crystalline drug and a polymorphic vehicle can be understood by individual components and their behaviour in the preparation media. Chapter 3 has brought to the light the properties of the APIs and other co-crystal formers. It also provided the information needed to understand about the behaviour of those materials in the preparation media of the final dosage form (co-crystals containing films).

This chapter focuses on the process of co-crystal formation and their physicochemical properties. It also studies the possibility of producing the co-crystals using different media in order to provide wider options to select from for the film loading process.

Two co-crystal systems will be studied: caffeine-malonic acid and ( $\pm$ ) ibuprofen (*RS*)-nicotinamide. A novel third system was discovered during the progress of the project. Thus, malonic acid-nicotinamide co-crystal formation is studied in this chapter and its physicochemical properties presented.

## **4.2 Co-crystallization of caffeine and malonic acid**

Caffeine-malonic acid co-crystals were prepared using the method described in section 2.3.2. In addition to the use of chloroform/methanol 30:1 v/v as a co-crystallization solvent (Trask et al., 2005), the possibility of growing caffeine-malonic acid co-crystals from other solvent systems was investigated. The use of acetone/chloroform 3:2 v/v, ethanol/water 4:1 w/w, and acetonitrile as a co-crystallization solvent is investigated in this chapter. The properties of any successfully formed co-crystalline system will be characterized in order to have a better understanding of the formation process.

### **4.2.1 Co-crystal analysis**

Caffeine-malonic acid co-crystals were prepared using the method described in section 2.3.2 using chloroform/methanol, acetone/chloroform, ethanol/water, and acetonitrile as preparation media. The physicochemical properties of the co-crystals were characterized using techniques presented in the previous chapter.

#### **4.2.1.1 Thermal analysis**

##### **4.2.1.1.1 TGA analysis**

Thermal profiles of caffeine-malonic acid co-crystals from the aforementioned solvent systems were obtained using the method described in section 2.2.1.1. The obtained profiles were compared to the thermal profiles of unprocessed caffeine and malonic acid (figure 4.1). The TGA profile reveals a two event for the co-crystals. The first stage commences at around 140°C and the second one commences at around 170°C. Comparing the degradation steps to the

thermal degradation profile obtained for caffeine and malonic acid reveals that the degradation step at 140°C can be correlated to the degradation of malonic in the co-crystals. The second degradation step can be correlated to caffeine degradation. However, there is a noticeable difference between the thermal degradation profiles of co-crystals prepared from different solvents in a similar manner to the profiles of recrystallized caffeine in section 3.1.1.1.

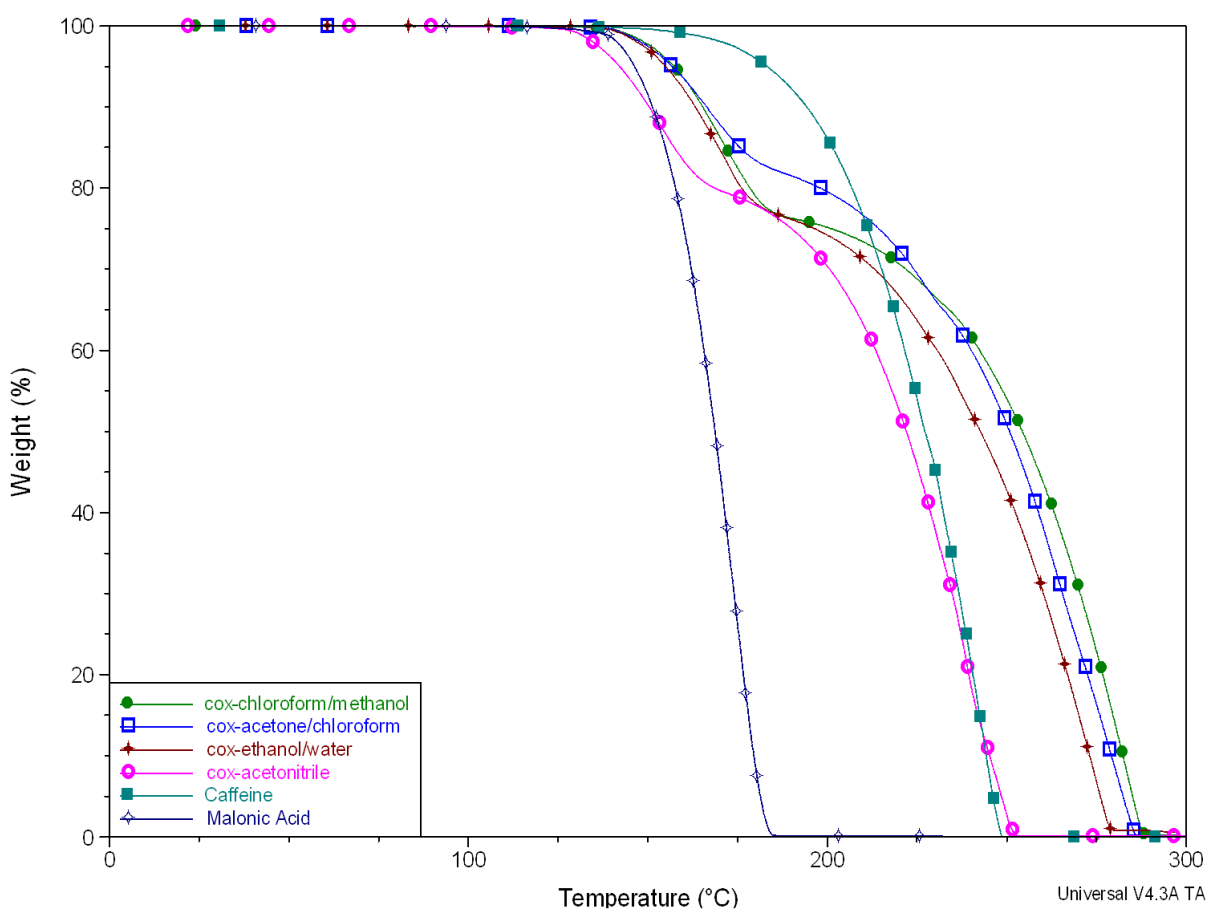


Figure 4.1. A representative TGA thermal profile for caffeine-malonic acid co-crystals prepared from chloroform/methanol (green), acetone/chloroform (blue), ethanol/water (red), and acetonitrile (pink) in comparison to unprocessed caffeine (teal) and malonic acid (navy blue).

#### 4.2.2.1.2 DSC analysis

Caffeine-malonic acid co-crystals were examined using the method described in section 2.2.1.2. for the purpose of comparison we will consider the two largest endotherms obtained (figure 4.2). The first set is observed at around 133°-

135°C. These peaks are similar to the melting peak of malonic acid. The second major peak occur around 234°C- 237°C except for that co-crystals prepared using acetone/chloroform where it was found at 230°C. This set of peaks can be correlated to the melting peak of unprocessed caffeine. The shift in the melting peak in the later case may result from the existence of some impurities. A third set of common peaks with a wider base are observed at 168°C-171°C. This set is similar to the peaks found for recrystallized caffeine in section 3.2.1.1, 3.2.2.1, and 3.2.3.1. These peaks were identified earlier as caffeine sublimation peaks. The shifting of this peak in co-crystals prepared from acetone/chloroform to 200°C might be related to the existence of polymorph II of caffeine (Griesser et al., 1999 , Emel'yanenko and Verevkin, 2008). Figure 4.2 also shows weak intensity wide peaks around 85°C-98°C. These peaks can be correlated to the solid transition phase of malonic acid.

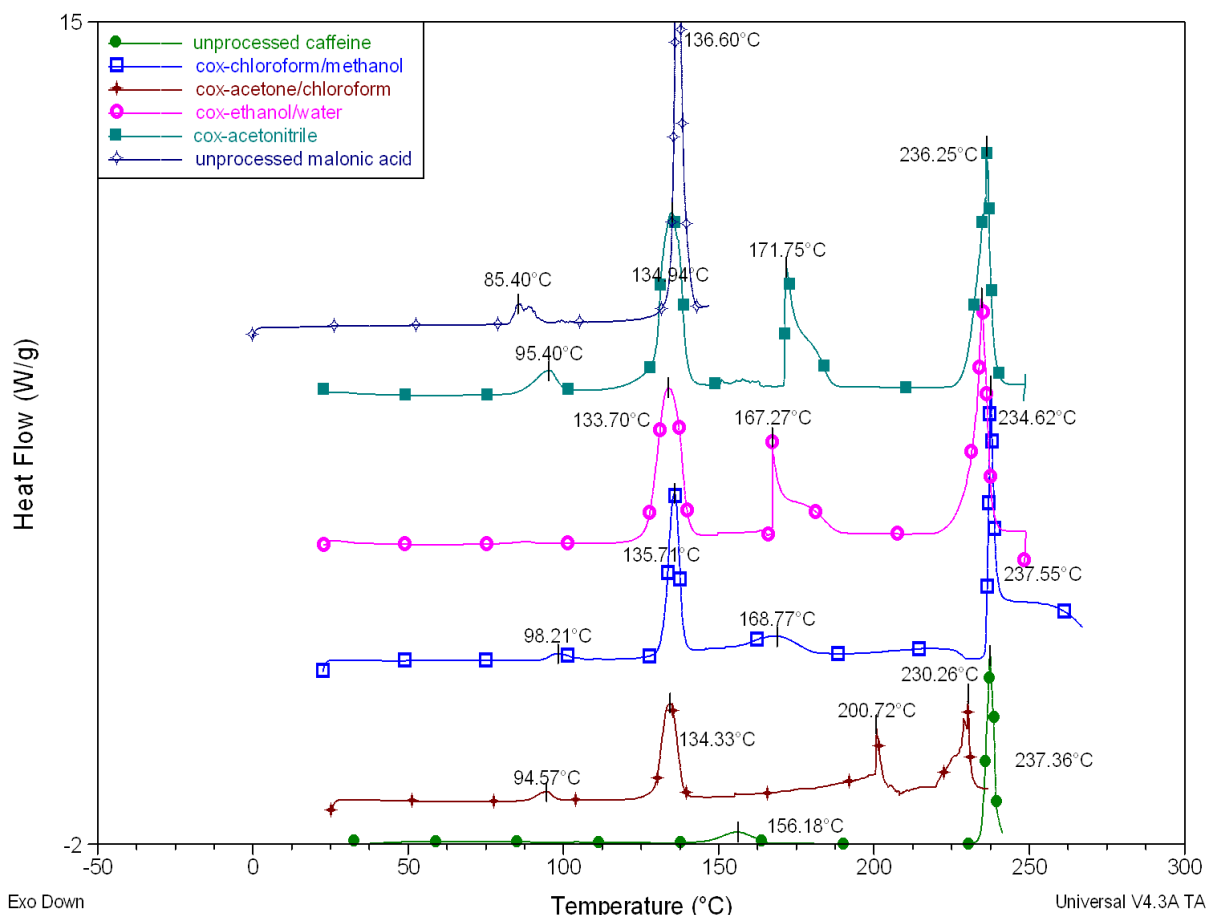


Figure 4.2. A representative DSC thermal profile for unprocessed caffeine (green), unprocessed malonic acid (navy blue), co-crystals prepared from chloroform/methanol (blue), acetone/chloroform (red), ethanol/water (pink), and acetonitrile (teal).

Thermal analysis for caffeine-malonic acid co-crystals reveals a similar pattern to the unprocessed material thermal profile. The absence of new peaks and the existence of the raw materials melting peaks indicate that neither co-crystals nor eutectic mixture were formed.

#### 4.2.1.2 Powder X-ray diffraction

The diffraction patterns of co-crystals prepared with various solvent systems were obtained using the method described in section 2.2.2. The collected diffraction patterns were compared to unprocessed anhydrous caffeine, unprocessed malonic acid, caffeine monohydrate (CSD), and caffeine-malonic acid co-crystals (CSD) diffraction patterns (figure 4.3). The last two diffraction



patterns were obtained from CSD library. The diffraction patterns of all the co-crystals show reference peaks at 16.4°, 22.4°, 25°, and 28°. These peaks are the reference peaks for caffeine-malonic acid co-crystals (Ibrahim et al., 2010). These peaks can also be observed in the diffraction pattern (CSD).

Consequently, the powder x-ray data confirms the formation of co-crystals from all solvent systems. However, co-crystals prepared using acetonitrile showed two extra peaks at 12° and 13.4°. These extra peaks can be observed in the diffraction pattern of caffeine monohydrate. Hence, it can be stated that the product from co-crystallizing caffeine and malonic acid using acetonitrile is a combination of the co-crystal and caffeine monohydrate.

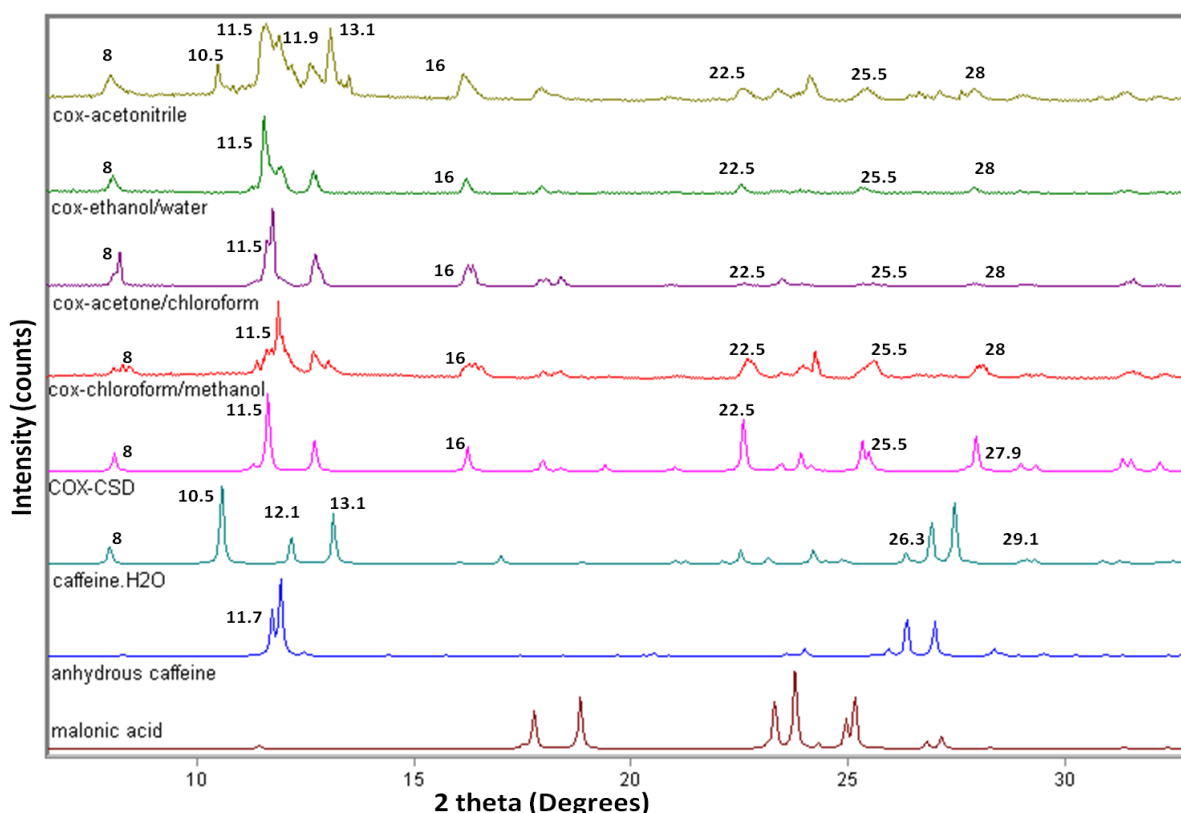


Figure 4.3. A representative powder x-ray diffraction pattern for co-crystals prepared with: acetonitrile (top), ethanol/water (second from top), acetone/chloroform (third from top), chloroform methanol (forth from top), standard co-crystals diffraction (fourth from bottom), standard anhydrous caffeine diffraction (third from bottom), standard monohydrated caffeine diffraction (second from bottom), and standard malonic acid diffraction (bottom).

#### 4.2.1.3 FT-IR transmission

Co-crystals were examined using the method described in section 2.2.3. The collected spectra revealed shift in the following peaks:  $1692\text{ cm}^{-1}$  peak to  $1699\text{ cm}^{-1}$ ,  $1168\text{ cm}^{-1}$  to  $1178\text{ cm}^{-1}$ ,  $962\text{ cm}^{-1}$  to  $957\text{ cm}^{-1}$ ,  $920\text{ cm}^{-1}$  to  $904\text{ cm}^{-1}$ . (Figure 4.4) The first peak is assigned for the vibration energy of C=N, NH bond. This shift indicates the presence of a hydrogen bond. On the other hand, malonic acid has two mirror-image carboxylic acid groups. Thus there are few peaks that assign for the C=O, OH bond vibration energy (Bougeard et al., 1988). Nevertheless, the observed shifted peaks are some of the peaks that assign for these bonds energy. Therefore, the shift can be considered as a result for the hydrogen bond that formed between caffeine and malonic acid. Consequently, it confirms the successful formation of co-crystals using all the aforementioned solvents.

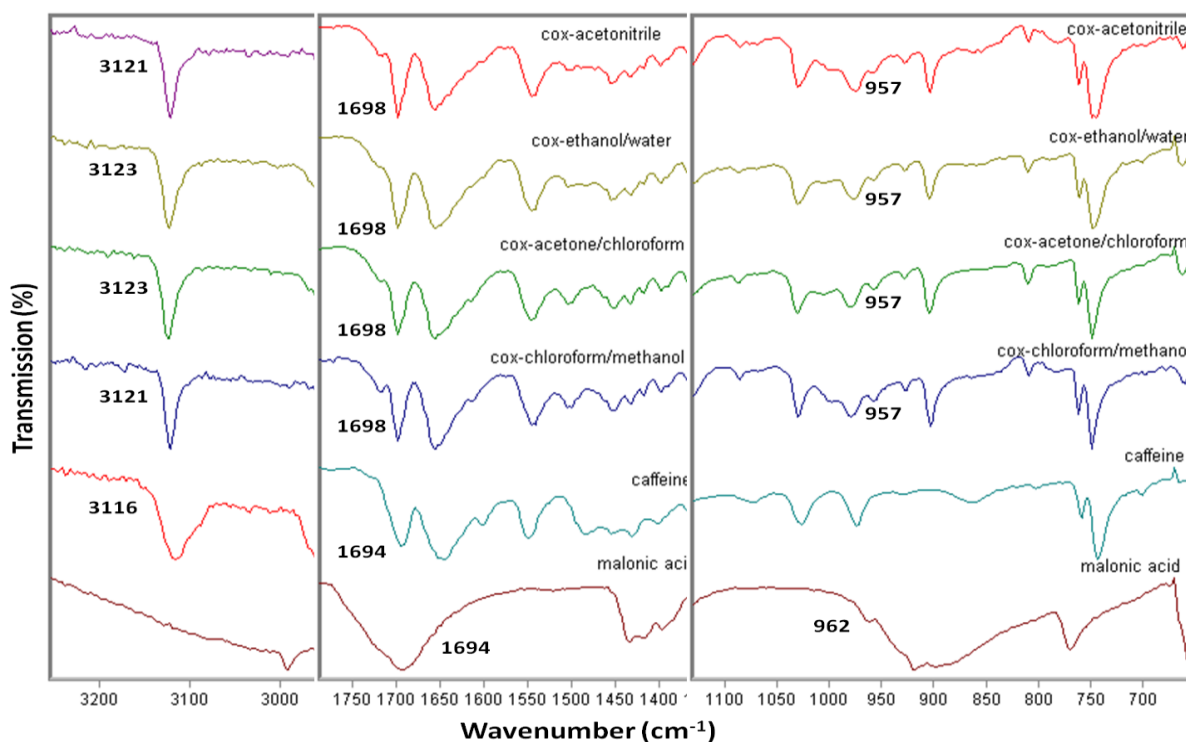


Figure 4.4. A representative FT-IR spectrum for malonic acid (bottom), caffeine (second from bottom), co-crystals prepared with: chloroform/methanol (third from bottom), acetone/chloroform (fourth from bottom), ethanol/water (second from top), and acetonitrile (top).

### **4.3 Co-crystallization of ibuprofen and nicotinamide**

Ibuprofen-nicotinamide co-crystals are one of the two co-crystals to be loaded into a polymeric film. The main difference between this system and the other is the solubility of the co-crystal components. While both caffeine and malonic acid are considered as water soluble drugs, ibuprofen, unlike nicotinamide, is considered to be a sparingly soluble one. This difference can create a challenge in the film loading process. In order to get a clear image about the physicochemical properties of the system, ibuprofen-nicotinamide co-crystals will be prepared and characterized using the aforementioned methods.

Ibuprofen-nicotinamide co-crystals were prepared with acetonitrile using the method described in section 2.3.2. the result of their characterization is presented below.

#### **4.3.1 Thermal analysis**

##### **TGA & DSC**

The DSC and TGA thermal profiles of ibuprofen-nicotinamide co-crystals were obtained using the methods described in sections 2.2.1.1 and 2.2.1.2. The data obtained were compared to the thermal profiles of unprocessed ibuprofen and nicotinamide (figure 4.5). The TGA thermal profile reveals that this co-crystal has a one step thermal degradation in contrast to the two step thermal degradation of caffeine-malonic acid (section 4.2.1.1.1). The degradation of the co-crystal starts after the degradation of ibuprofen and before the degradation of nicotinamide. On the other hand, the DSC profile shows an endothermic peak at 94°C. This peak was investigated and it appeared to be related to the melting of the co-crystalline system (Friscic and Jones, 2007). Another low-intensity

peak was observed on the DSC profile. This peak is observed at 71°C. This peak is consistent with the melting of the residual ibuprofen.

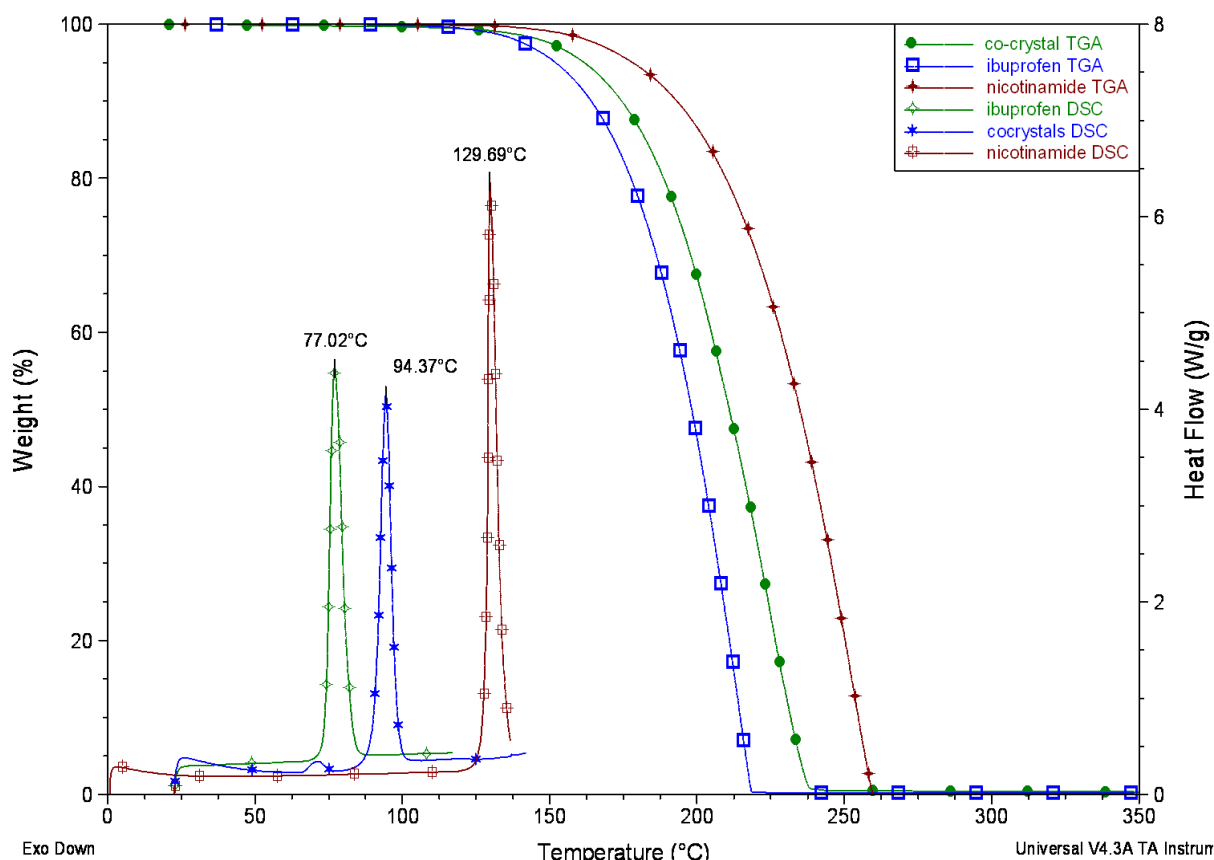


Figure 4.5. A representative TGA and DSC thermal profiles for unprocessed ibuprofen, unprocessed nicotinamide, and co-crystals of ibuprofen-nicotinamide.

### 4.3.2 Powder X-ray diffraction

The powder x-ray diffraction pattern for the co-crystal was collected using the method described in section 2.2.2. The collected pattern was compared to a standard diffraction pattern obtained from the CSD library in addition to the unprocessed components (figure 4.6). The X-ray diffraction pattern of the co-crystals reveals three diffraction peaks at 9°, 16°, and 21°. The same peaks can be observed in the standard diffraction pattern. In addition, the same peaks are not observed in the diffraction pattern of the individual unprocessed ibuprofen

and nicotinamide. This indicates that ibuprofen-nicotinamide co-crystals were successfully formed.

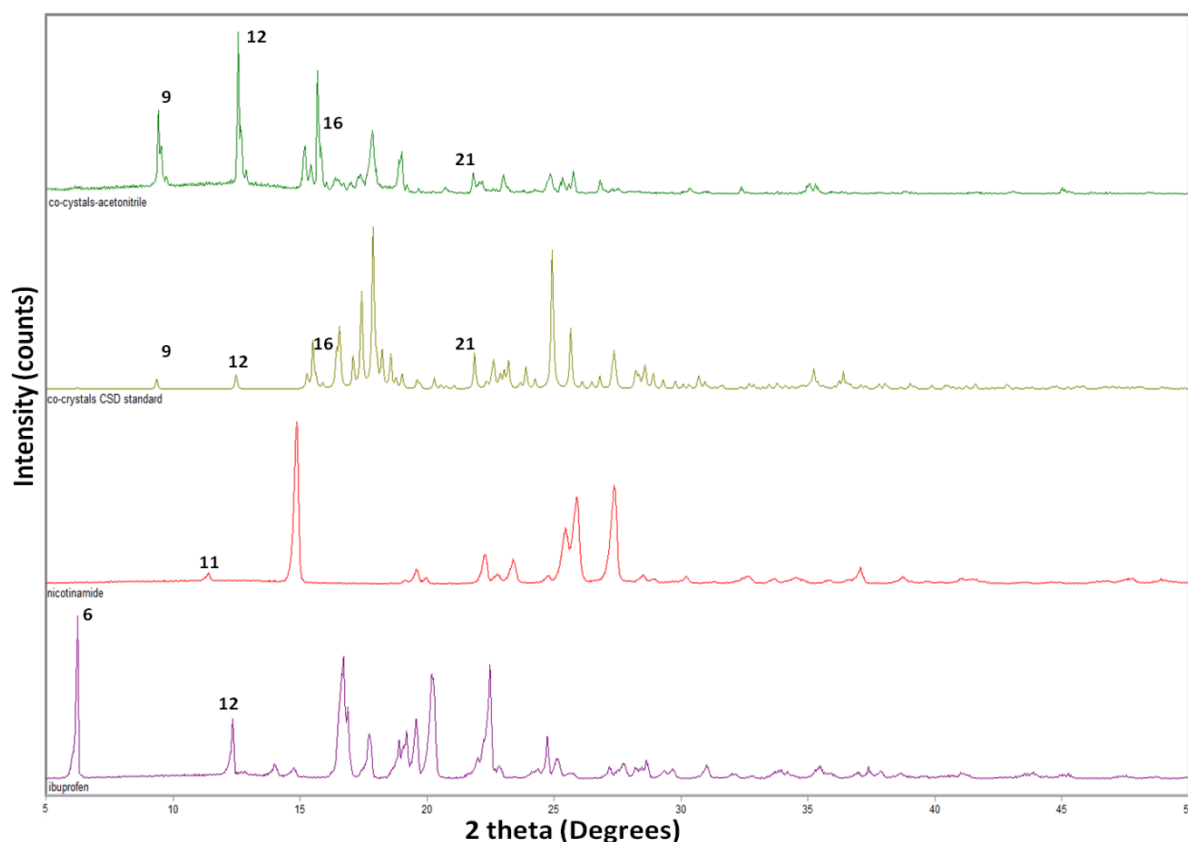


Figure 4.6. Representative powder x-ray diffraction patterns for ibuprofen (purple), nicotinamide (red), ibuprofen, co-crystals standard diffraction pattern obtained from CSD library (yellow), and co-crystals (green).

### 4.3.3 FT-IR transmission

The FT-IR spectrum for the ibuprofen-nicotinamide co-crystal was obtained using the method described in section 2.2.3. The collected spectrum was compared to the FT-IR spectrum for unprocessed ibuprofen and nicotinamide (figure 4.7). The co-crystals spectrum reveals two major peaks shifts from  $3154\text{ cm}^{-1}$  in the unprocessed nicotinamide spectrum and  $1704\text{ cm}^{-1}$  in the unprocessed ibuprofen spectrum to  $3175\text{ cm}^{-1}$  and  $1698\text{ cm}^{-1}$  in the co-crystal spectrum respectively. The first peak shift is assigned in the literature for C=N, NH bond vibrational energy. The second peak is assigned for C=O, OH bond

vibrational energy. Both peak shifts are consistent with the formation of a hydrogen bond formed between the NH group in nicotinamide and C=O group in ibuprofen.

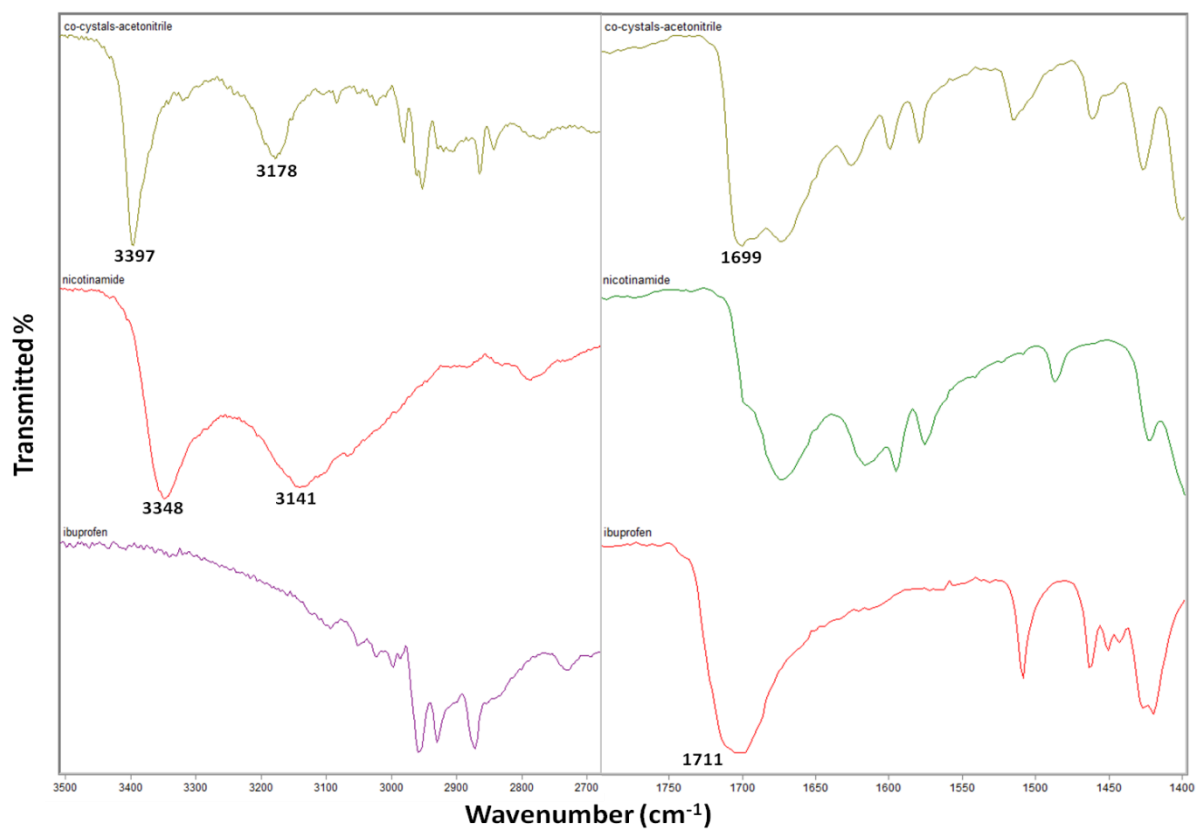


Figure 4.7. Representative FT-IR spectrum for unprocessed ibuprofen (bottom), unprocessed nicotinamide (middle), and co-crystals of ibuprofen and nicotinamide (top).

## **4.4 Co-crystallization of nicotinamide and malonic acid**

Nicotinamide-malonic acid co-crystals were produced during the progress of the study. In order to have a deeper insight for general co-crystal-excipient interaction (chapter 8), their properties are studied in this chapter. Nicotinamide-malonic acid co-crystals were not known until very recently (VOGURI, Sep 2010b). Hence there was an interest for studying this system. Nicotinamide-malonic acid co-crystals were co-crystallized from acetonitrile using the method described in section 2.3.2. Then the co-crystals were characterized using a set of analytical instruments.

### **4.4.1 Thermal analysis**

#### **TGA & DSC**

The TGA and DSC thermal profiles of nicotinamide-malonic acid co-crystals were obtained using the methods described in sections 2.2.1.1 and 2.2.1.2. The TGA profile shows a two step loss of weight for co-crystals prepared in both solvents (figure 4.8). The first step of weight loss commences at around 114°C and the second starts around 160°C. The first step is expected to be associated with its malonic acid component. This is consistent with the observed fact that about 50% weight loss resulted from the first degradation step (malonic acid MW is 104g/mol and nicotinamide 122 g/mol and the co-crystals has a 1:1 stoichiometric ratio).

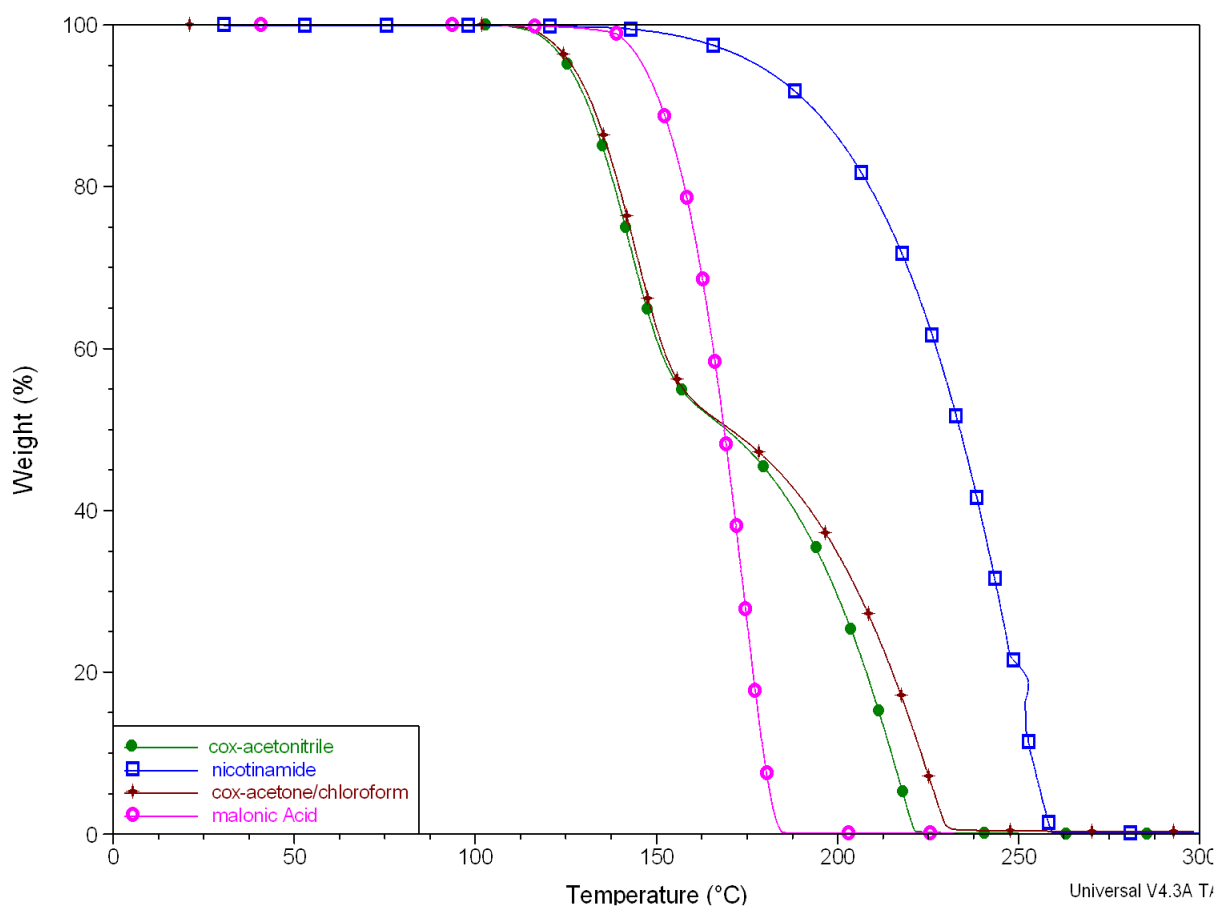


Figure 4.8. Representative TGA thermal profiles for unprocessed malonic acid (pink), unprocessed nicotinamide (blue), co-crystals prepared using acetone/chloroform (red), and co-crystals prepared using acetonitrile (green).

On the other hand, DSC thermal profiles in figure 4.9 reveals the presence of a single endothermic peak at 109°C-110°C and the disappearance of the nicotinamide and malonic acid melting peaks. This indicates the formation of a co-crystalline system of nicotinamide and malonic acid.



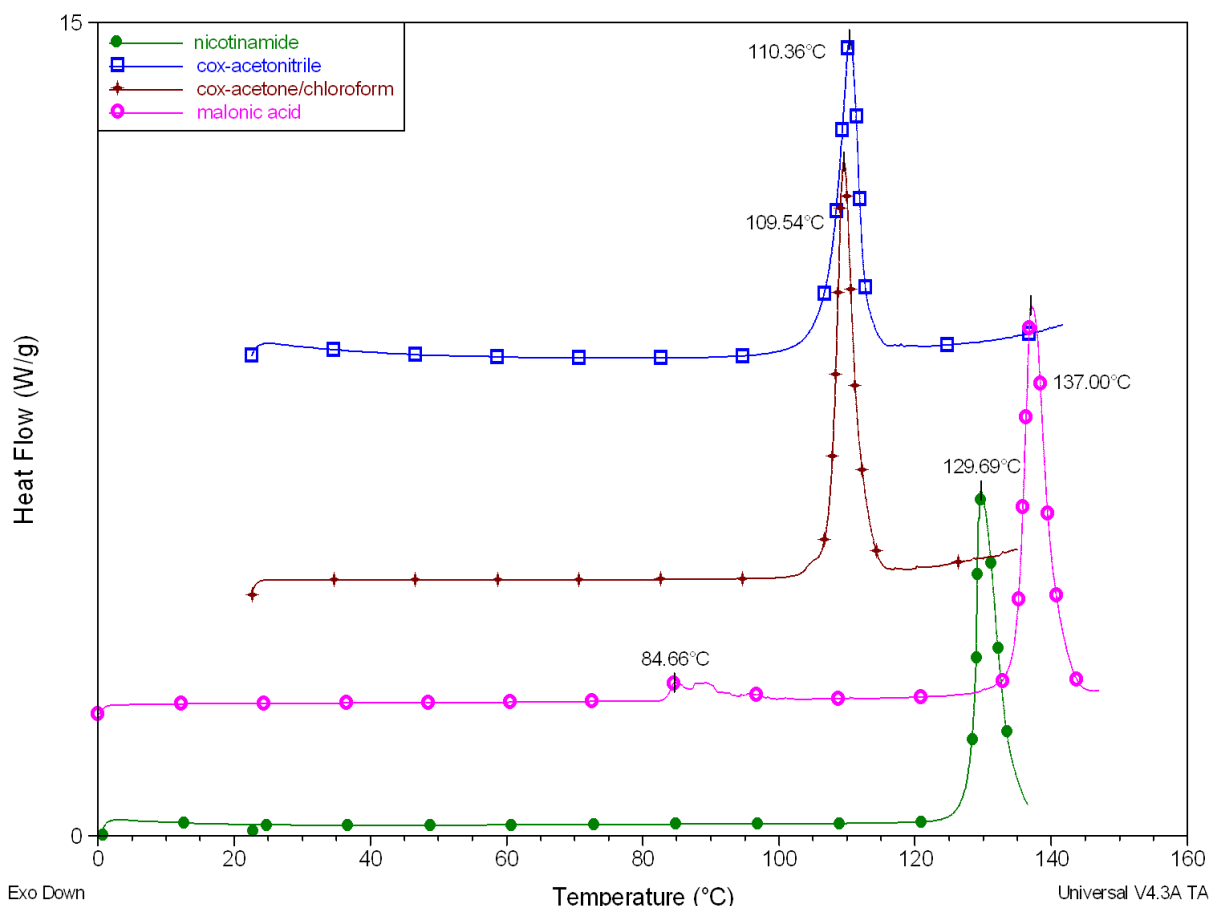


Figure 4.9. Representative DSC thermal profiles for unprocessed nicotinamide green, unprocessed malonic acid (pink), nicotinamide-malonic acid co-crystals prepared using acetone/chloroform (red), and co-crystals prepared using acetonitrile (blue).

#### 4.4.2 Powder X-ray diffraction

The powder x-ray diffraction patterns for co-crystals prepared with both solvents were collected using the method described in section 2.2.2. They were compared to the diffraction pattern of the raw materials (figure 4.10). The diffraction pattern for co-crystals prepared with both solvent systems revealed the presence of three new peaks at 9°, 21°, and 22°. The presence of these peaks indicates the formation of a new crystalline structure (co-crystal). Since this co-crystal system was only recently discovered, no reference pattern was included

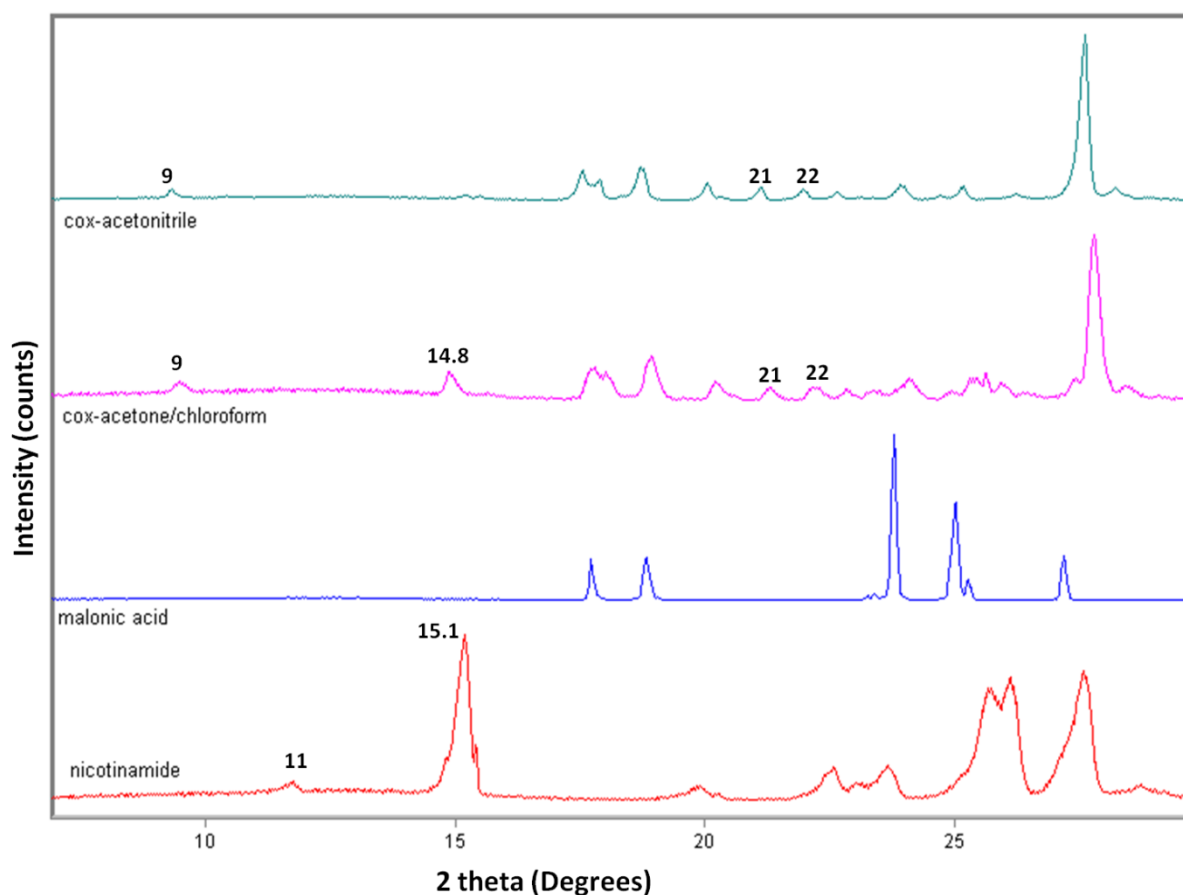


Figure 4.10. Representative powder x-ray diffraction patterns for unprocessed nicotinamide (bottom-red), unprocessed malonic acid (second from bottom- blue), co-crystals prepared using acetone/chloroform (second from top-pink), and co-crystals prepared using acetonitrile (top-teal).

#### 4.4.3 FT-IR transmission

The FT-IR spectrum for the nicotinamide-malonic acid co-crystal was obtained using the method described in section 2.2.3. The spectrum was obtained in order to be used as a reference for comparison between ibuprofen-nicotinamide and nicotinamide-malonic acid co-crystals. Figure 4.11 shows a peak shift was detected in FT-IR transmission pattern from  $3366\text{ cm}^{-1}$  in unprocessed nicotinamide spectrum to  $3374\text{ cm}^{-1}$  and  $3379\text{ cm}^{-1}$  in the co-crystal prepared with acetone/chloroform and acetonitrile respectively. Additional shifts in two other peaks at  $1397$  and  $770\text{ cm}^{-1}$  in unprocessed malonic acid spectrum shifted to  $1392\text{ cm}^{-1}$  and  $764\text{ cm}^{-1}$  in both co-crystal spectra respectively. These

peaks were previously assigned for C=N, NH vibration in nicotinamide (3374  $\text{cm}^{-1}$ ) (Akalin and Akyuz, 2006 , Hino and Ford, 2001) and C=O, OH (1397 and 770  $\text{cm}^{-1}$ ) (Bougeard et al., 1988). The shifts indicate that a hydrogen bond has formed between the nicotinamide nitrogen atom (NH) and malonic acid oxygen atom (C=O).

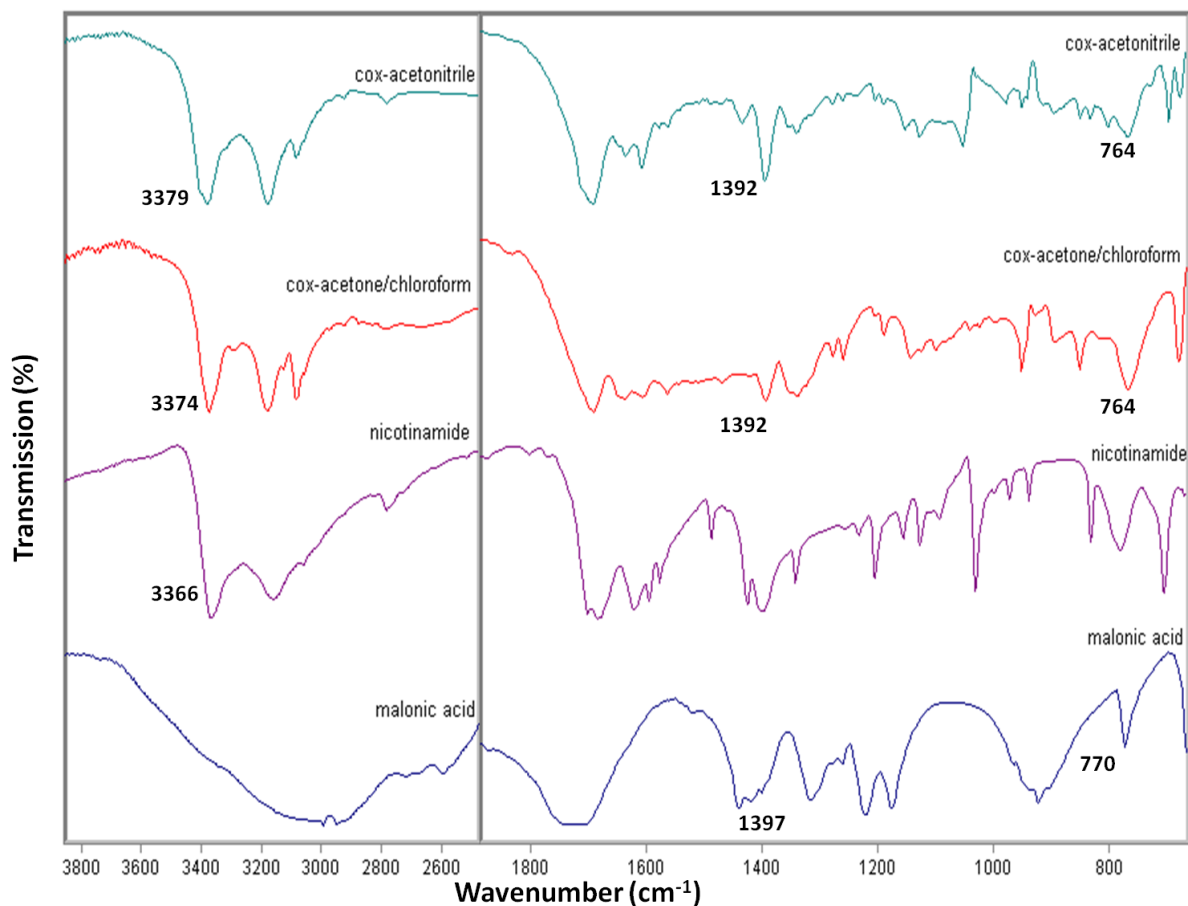


Figure 4.11. Representative FT-IR spectra for unprocessed malonic acid (bottom-blue), unprocessed nicotinamide (second from bottom-purple), co-crystals prepared using acetone/chloroform, (second from top-red), and co-crystals prepared using acetonitrile (top-teal).

## 4.5 Summary and Conclusions

Caffeine-malonic acid co-crystals were prepared using chloroform/methanol as previously mentioned in the literature (Trask et al., 2005). In addition, the co-crystal was prepared using three other solvent systems in order to study the effect of formation of caffeine-malonic acid co-crystals with a suitable solvent for co-crystals containing film preparation. These solvents were:

acetone/chloroform, ethanol/water, acetonitrile. The analysis of the resultant co-crystals prepared with the solvents showed that co-crystal purity was high from acetone/chloroform and ethanol/water. However, when co-crystals prepared with acetonitrile were analyzed, the product of the preparation process showed the presence of some caffeine monohydrate in addition to co-crystals.

An ibuprofen-nicotinamide co-crystal was successfully prepared as previously described in the literature (Berry et al., 2008). Its physicochemical properties were characterized using DSC, X-ray, and FT-IR. The results indicated the co-crystals formation.

A third system was studied as well. Nicotinamide-malonic acid co-crystals were prepared using acetone/chloroform and acetonitrile with a stoichiometric ratio of 1:1 mol/mol. Their physicochemical properties were characterized using thermal analysis: TGA and DSC, Crystallographic analysis: x-ray diffraction, and vibrational analysis: FT-IR spectroscopy.

Other workers (VOGURI, sep 2010a), have recently identified that nicotinamide and malonic acid can form a co-crystal. Thus the previous results indicating co-crystals formation are consistent with this work.

This chapter has identified methods of preparing co-crystals that are suitable for use with solvent systems that potentially could allow co-crystals to be cast in polymeric films.

## **Chapter 5**

### **Solvent effect on the HPMCAS properties and TEC- HPMCAS interaction**

## 5.1 Introduction

Studying the relationship between a co-crystal active compound and a polymeric vehicle or any other excipients requires at least a basic understanding of the behaviour of the unprocessed materials first. This is considered an important process in order to obtain a reference point for comparison. The starting materials of this project and their relationship with the preparation media of the final dosage form were thoroughly studied in chapter 3. Since the final intended dosage form contains a co-crystal rather than a single crystalline drug, investigation of such systems requires a study of the co-crystals prior to loading into the polymer (chapter 4). A third aspect of the project is to study the interaction between each individual component of the co-crystals with the polymeric vehicle. Moreover, the solvent system might have an impact on the drug-polymer interaction. Therefore, this chapter also investigates the effect of potential solvent systems on the polymer physical properties.

## 5.2 Solubility parameters of the raw materials

Solubility parameters were calculated as a potential prediction of the drug behaviour in the polymeric vehicle. They were calculated using Hildebrand equation.

$$\delta = \sqrt{\frac{\Delta H_v - RT}{V_m}} \quad (\text{equation 5.1(Hildebrand and Scott, 1950)})$$

Where  $\Delta H_v$  is the heat of vaporization, R is the gas constant, T temperature, and  $V_m$  molar volume.

Some drugs such as malonic acid have the ability to form a dimer. Such formation will affect the value for the cohesive energy and consequently it will change the solubility parameter value. A correction factor can be introduced to the equation to optimize the parameter value for materials possessing this property. However, the effect of dimerization on the solubility parameter value can be considered small compared to the original value (Barton, 1991). Hence the normal equation was used in the calculation (Table 5.1).

compound	solubility parameter (MPa <sup>1/2</sup> )	Pka
ibuprofen	19.5	4.4
naproxen	21.9	4.2
malonic acid	22.47	2.83-5.69
HPMCAS	24	
flurbiprofen	24.45	4.2
caffeine	26.52	0.5-1.5
nicotinamide	27.52	3.6
TEC	24.78	

Table 5.1. The solubility parameters of the compounds used in the study with their pKa values.

The solubility parameters for solvents were calculated based on the equation 5.1 then the parameters of the solvent mixtures were calculated using the equation provided by (Burke, 1984). The values obtained are detailed in table 5.2.

Solvent	Solubility parameter (MPa <sup>1/2</sup> )
chloroform	19
acetone	20.2
acetonitrile	24.42
ethanol	26
water	47.9
ethanol/water	30.54
acetone/chloroform	19.78

Table 5.2. Calculated Solubility Parameters SP MPa<sup>1/2</sup> of the solvent and solvent combinations used in this study.



## **5.3 The effect of solvent on polymer physical properties**

### **(plasticity)**

Polymers are composed of repeated small units called monomers. These monomers are linked together to form chains of various lengths. In amorphous polymers, the chains are entangled together in a non-organised state. When the polymer is dissolved into a solvent these chains disentangle and chain movement increases as they separate from each other. However, when the solvent starts to evaporate, the free volume between the chains diminish and the chains start to interact with each other and entangle again. The conformation of the chain entanglements might depend on the interaction between the polymer chains and between the chains and the solvent. A residual amount of solvent can still have an impact on the chain dynamics. Solvent molecules will interpose between adjacent chains and weaken the interaction between those chains thus producing a “plasticizing effect”. Furthermore, this effect can be quantified by measurement of the glass transition temperature ( $T_g$ ) of the polymer.

As defined in section 1.9, the measurement of the  $T_g$  will reflect the impact of the solvent on the arrangement of the polymer chains.

## **5.4 Thermal analysis**

Plain HPMCAS films were prepared using acetone/chloroform, ethanol/water, and acetonitrile following the method described in section 2.3.3. The  $T_g$  values of these films revealed a shift from the  $T_g$  value reported in the literature (Kablitz et al., 2006) (figure 5.1).

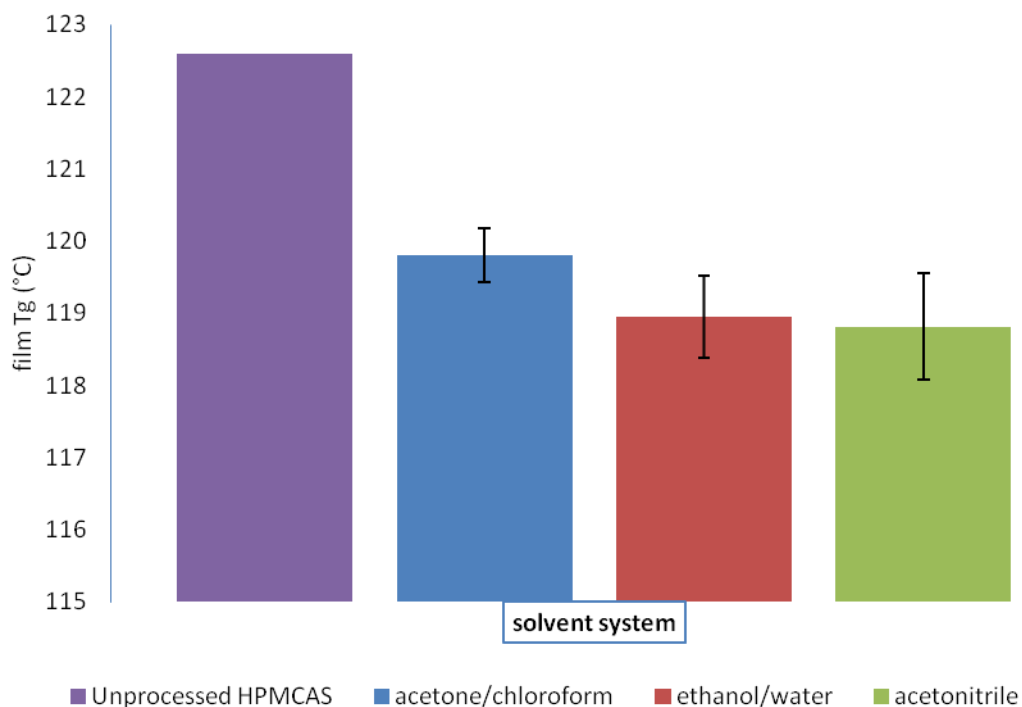


Figure 5.1. A comparison of films Tg values for unprocessed polymer (Kablitz et al., 2006) (purple), films prepared using: acetone/chloroform (blue), ethanol/water (red), and acetonitrile (green). DSC thermal profiles are provided in figures All 10, All 11, and All 12.

The effect of the solvent on the interaction between the polymeric chains appears clearly in figure 5.1. Acetone/chloroform appears to have the lowest effect on the polymeric vehicle. This can be concluded from the higher Tg value (for the polymeric film prepared using acetone/chloroform compared to films prepared with the other two solvents). Nevertheless, the Tg value of the film prepared with acetone/chloroform is lower than the Tg value of the unprocessed polymer. On the other hand, films prepared using acetonitrile or ethanol/water revealed a close Tg values. This result raises the concern about the effect of the solvent system on the loading of the co-crystals into the polymeric film. The polarity and the cohesive energy for the system were believed to have an effect. Therefore, the solubility parameters of these solvents were measured in order to provide an indication for their cohesiveness.

From the data presented in table 5.1 the solubility parameter calculated for acetonitrile is close to the SP value of the polymer (24 MPa<sup>1/2</sup>). This similarity

may explain the preference of the acetonitrile molecule to interact with the polymer in a stronger manner compared to the interaction between the other two solvents and the polymer. This interaction may have interfered with the folding process of the polymeric chains. Hence, the T<sub>g</sub> value of the film prepared with acetonitrile is lower than the T<sub>g</sub> of the film prepared with acetone/chloroform. This explanation cannot be extended however on films prepared by ethanol/water.

Ethanol/water has a SP value that is further away from the SP value of the polymer than acetone/chloroform or acetonitrile. This behaviour might be explained by the fact that water and ethanol have a strong polarity. This polarity can trigger the bonding between the solvent mixture and the polymer. Hence, the effect of that solvent on the HPMCAS cannot be evaluated using the simple SP rule. A more detailed SP that takes into account the polarity and hydrogen bond formations might be needed to give a more accurate representation for this solvent system.

In order to expose the effect of the solvent system on the possible interaction between a drug and the polymer, the interaction between the polymer and a plasticizer using a different solvent was monitored.

## **5.5 Solvent effect on the plasticizer-polymer interaction**

Tri-ethyl citrate (TEC) is a well known plasticizer that is used in pharmaceutical formulations. It is an ester of citric acid. Films containing various concentrations of TEC were prepared using acetone/chloroform, ethanol/water, or acetonitrile. T<sub>g</sub> determination of films prepared using the method described in section 2.3.3 of these films uncover the question raised by the previous section. The results

are presented in figure 5.2. Depending on the concentration of TEC, T<sub>g</sub> is statistically unaffected by the nature of the solvent. However at some of the levels of TEC employed, the effect of the preparation solvent on the T<sub>g</sub> obtained is statistically significant.

It is worthy of mention that the standard error of the measurements was high for certain samples as was the case for films containing 13% (w/w) TEC prepared using acetonitrile. Films prepared with acetonitrile showed a similar or slightly lower T<sub>g</sub> values to those prepared with ethanol/water. On the other hand, films prepared using acetone/chloroform produced the lowest T<sub>g</sub> values for films containing 4-9% (w/w) and but the T<sub>g</sub> obtained was higher than the T<sub>g</sub> of films prepared with the other two solvents when the TEC concentration was 16.7% w/w. Nevertheless in general, films containing 15% (w/w) TEC and cast from acetone/chloroform resulted in a film with about a 5°C higher T<sub>g</sub> than those prepared using the other two solvents (figure 5.2).

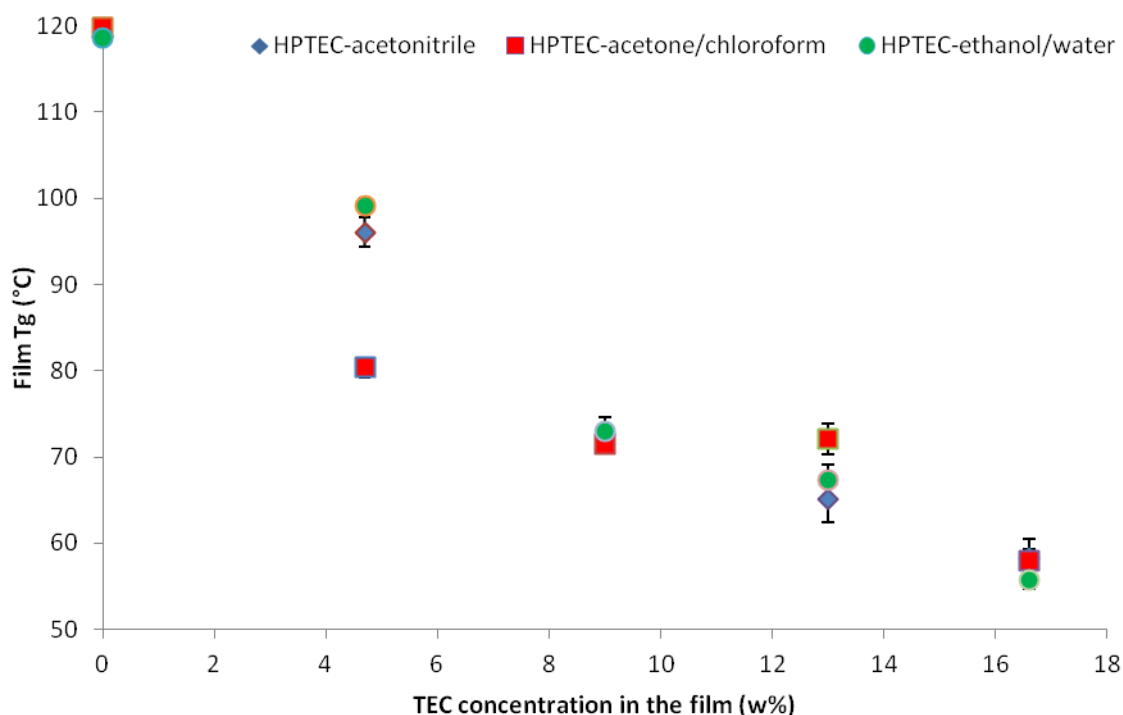


Figure 5.2. Representative T<sub>g</sub> values for polymeric films containing various amounts of TEC prepared using acetone/chloroform (red square), ethanol/water (green circle), and acetonitrile (blue diamond). More details in Appendix All 13-16.

The observed difference in the T<sub>g</sub> values for films prepared with the aforementioned solvents might be explained by the solubility of the plasticizer in each of the previous solvents. When the plasticizer favours to interact with the solvent rather than the polymer, it may result in drawing the plasticizer away from the polymer during the evaporation stage. This will result in concentrating the plasticizer on the upper surface and the sides of the polymer. The strength of such interaction will affect the distribution of the plasticizer in the polymer, i.e. a strong interaction between the drug and the polymer will result in a higher film T<sub>g</sub> value than a weak interaction.

The variation of T<sub>g</sub> values of films prepared using acetonitrile and acetone/chloroform is worthy of comment. To explain the differences in the T<sub>g</sub> values obtained, the solubility parameters of the solvent systems and TEC were compared. The theory we wish to test here is that if the solubility parameter value of the TEC or the polymer is closer to the SP value of the solvent, then either of the two will favour interacting with the solvent more than interacting with each other. On the other hand, if the SP value of TEC and HPMCAS is closer to each other than the SP value of the solvent, the interaction between them will be stronger and consequently the plasticization effect will be greater. TEC has a SP value of 24.78 MPa<sup>1/2</sup>. Acetonitrile is the only solvent with SP value that is closer to the TEC than the polymer. Hence, it is expected that the solvent will interact/dissolve TEC in a strong manner and that the interaction will interfere with the dispersion and the interaction of the TEC with the polymer. Such behaviour would result in high T<sub>g</sub> values being observed with these films. On the other hand, acetone/chloroform has a solubility parameter that is considered far from both polymer and plasticizer. Therefore, theory would be

predicted the film to have a lower Tg values from films prepared using acetone/chloroform. However, films prepared with ethanol/water presents an unusual behaviour. Ethanol/water has SP value of 30.54. This value is remote from the SP values for both the polymer and plasticizer. Thus, it would be expected to observe low Tg values for these films. On the contrary, these films revealed high Tg values. This behaviour might be related to the fact that ethanol and water are quite miscible with each other. They interact in a strong manner that changes their polarity and final SP value. This was observed by Hildebrand and a new method was placed to calculate the SP parameter for liquids that interact in a similar manner (Barton, 1991).

Additionally the SP calculated in this thesis is a hybrid value of the two solvents mixed together and does not reflect differential evaporation of one of the solvents over the other and thus cannot be expected to reflect the complexity in the experimental film production. Furthermore, it is well documented that the amount of the residual solvent in the film can affect the Tg value of that film (Lopez and Mijangos, 1994). However, samples were kept at 100°C for 5 minutes in order to evaporate the residual solvent. Nevertheless, the thermal TGA profile of the previous films were collected and revealed the existence of the 2% weight loss between 30-100°C that can be found in unprocessed HPMCAS and is due to evaporation of the residual moisture (figure A1 7-9).

## 5.6 Summary and conclusion

Plain films casted using acetone/chloroform, ethanol/water, and acetonitrile showed a different  $T_g$  values than the unprocessed HPMCAS. Films prepared using ethanol/water or acetonitrile showed almost the same  $T_g$  values around  $118^\circ\text{C}$ . However, films prepared using acetone/chloroform showed a higher  $T_g$  value of about  $120^\circ\text{C}$ . This difference in the  $T_g$  value was correlated to the effect of solvent on the polymeric chain entanglement. On the other hand, this difference can be explained according to solubility parameter values presented in tables 5.1 and 5.2, the SP value of acetone/chloroform can be considered remote to that of acetonitrile. This reflects the lower affinity for the acetone/chloroform to interact with the polymer chains. Nevertheless, this rule cannot be applied on the calculated SP value of ethanol/water. The aforementioned solvent has a remote SP value to the polymer. However, the  $T_g$  of films casted using that solvent is similar to those prepared using acetonitrile. It is worthy to mention that the equation used to calculate the SP values for solvents and their combination is considered a simple equation and doesn't include the effect of the interactions in the solvent mixtures. Hence, the calculated SP value for ethanol/water might be far away from the true SP value of this solvent.

On the other hand, it was noticed that the use of various solvents in casting films containing the same amount of TEC resulted in the observation of difference in the  $T_g$  values. This difference was linked to the SP values of the solvent systems, HPMCAS, and TEC. A theory was developed after monitoring the behaviour of films prepared with the aforementioned solvents. It states that if the polymer and the plasticizer have a closer SP values to each other than the solvent used, then the solvent effect will be lower than the solvent with a closer

SP value to any of them. In other words, the closeness in the SP values reflects the affinity of the materials to interact with each others. This theory explained the behaviour of films prepared using acetonitrile and acetone/chloroform.

Acetone/chloroform has a remote SP value to the polymer and the plasticizer than acetonitrile. Therefore, the effect of acetone/chloroform on the interaction between HPMCAS and TEC is lower than the effect of acetonitrile. Hence, films prepared using acetone/chloroform showed lower Tg values. However, this theory cannot be applied in the case of films prepared using ethanol/water as they showed almost a similar Tg values to those prepared using acetonitrile.

On the other hand, this phenomenon can be explained by the solubility of the TEC and the polymer in those solvents. The higher the difference in solubility between them, the more phase separation will be. Therefore, it worth to measure the solubility of HPMCAS and TEC in each of the aforementioned solvents in order to clarify the reason for the Tg difference between films prepared with each of them.



## **Chapter 6**

**Preparation and characterisation of HPCMAS films containing  
acidic drugs/species**

## 6.1 Introduction

Understanding the interaction between the polymeric vehicle and the individual components of the co-crystals would be the next step towards understanding the interactions between the co-crystals and the polymer. Studying the unprocessed materials and the effect of the preparation media on their re-crystallization have been investigated in chapters 3 and 4 respectively. Moreover, the findings presented in chapter 5 revealed that the solvent system has a noticeable effect on the interaction between the polymer and a plasticizer. Hence, the study of drug-polymer interaction in this chapter will include the study of the effect of using different solvents on these interactions. Drug-polymer interactions have been well documented in the literature. It has been identified that such interaction might cause a delay of the drug release. However, this property was useful in controlling the release of drug in sustained or controlled release dosage forms (Puttipipatkachorn et al., 2001 , Murdande et al., 2011 , Huang et al., 2008 , Lin et al., 1995 , Feely and Davis, 1988). Moreover, there are few reported cases of drug-HPMCAS interactions (Yamaguchi and Tominaga, 2008 , Dong and Choi, 2008 , Tanno et al., 2004 , Riedel and Leopold, 2005 , Yamaguchi and Tominaga, 2006). These studies revealed the ability of HPMCAS to interact or adhere to the surface of drug crystals, inhibiting their growth and may convert them into amorphous materials. The interaction of HPMCAS with drugs was used in a controlled release drug. Drug-containing films were prepared by the method described in section 2.3.3. In this chapter we consider the interaction of acidic materials with HPMCAS. Namely malonic acid, ibuprofen, naproxen, and flurbiprofen were investigated with the interaction of malonic acid and ibuprofen with the polymer being more

extensively studied. Naproxen and flurbiprofen were used in a limited assessment of a drug substitution theory (where two acidic materials are simultaneously cast in a polymeric film). The other category includes the basic drugs such as caffeine and nicotinamide which will be investigated in a later chapter.

## **6.2 Preparation and characterisation of HPMCAS films containing a single acidic drug/species**

HPMCAS is known to interact with acidic drugs (Dong and Choi, 2008, Tanno et al., 2004, Riedel and Leopold, 2005). However, there are few reported cases of the interaction between basic drugs and HPMCAS (Yamaguchi and Tominaga, 2006, Yamaguchi and Tominaga, 2008).

Films containing acidic drugs were prepared using the method described in section 2.3.3. Malonic acid and ibuprofen interactions with HPMCAS were independently studied thoroughly because of their subsequent use in the incorporation of their co-crystal in the film.

### **6.2.1 Malonic acid**

Various concentrations of malonic acid (1:100-60:100 w/w malonic acid/HPMCAS) were loaded into polymeric films in order to see the effect of malonic acid on the polymer physical properties.

### **6.2.1.1 General analysis**

Films containing low concentrations of malonic acid (1:100-30:100 w/w malonic acid/HPMCAS) were visually similar to a 100% HPMCAS film. On the other hand, the flexibility of the film measured by hand increased with increasing the malonic acid concentrations from 1-30:100 w/w malonic acid/HPMCAS. This increase in flexibility was not accompanied by a change in the film transparency. When the concentration of malonic acid goes above 30:100 w/w malonic acid/HPMCAS, the polymer starts to show some opacity. At that point, the flexibility of the films stopped increasing and became independent on the malonic acid concentration in the film. When the concentration of malonic acid reaches 40:100 w/w, it was hard to detect a T<sub>g</sub> value on the thermal DSC profile (appendix AII 23). Nevertheless, exceeding 40% revealed a lower flexibility in the film and the growth of large malonic acid crystals through all the film. The growth of these crystals might have affected the overall flexibility and made the film brittle.

### **6.2.1.2 Thermal analysis**

#### **TGA and DSC**

The thermal profiles of HPMCAS films containing various concentrations of malonic acid were obtained using the method described in section 2.2.1.1. A 2-6 % weight loss can be observed between 25°-100°C (figure 6.1 and AI 2). A similar weight loss (3%) can be observed with the unprocessed HPMCAS. the extra weight loss can be either correlated to extra moisture trapped in 30:100 and 50:100 w/w malonic acid/HPMCAS films as 60:100 w/w malonic acid/HPMCAS. However, the first heating cycle in the DSC should evaporate

this extra moisture. This loss was linked to the evaporation of the residual solvent and moisture in the sample. The main weight loss of the sample can be divided into two stages. The first commences at about 130°C and involves a weight loss of around 25%. This weight loss can be linked to the thermal degradation of malonic acid in the film as unprocessed malonic acid thermal profile reveals the weight loss caused by the thermal degradation starting at around 140°C. The second commences at 300°C and almost results in a total weight loss. The second step can be correlated to the thermal degradation of the polymer as the weight loss caused by heating the film is similar to that of the unprocessed HPMCAS.

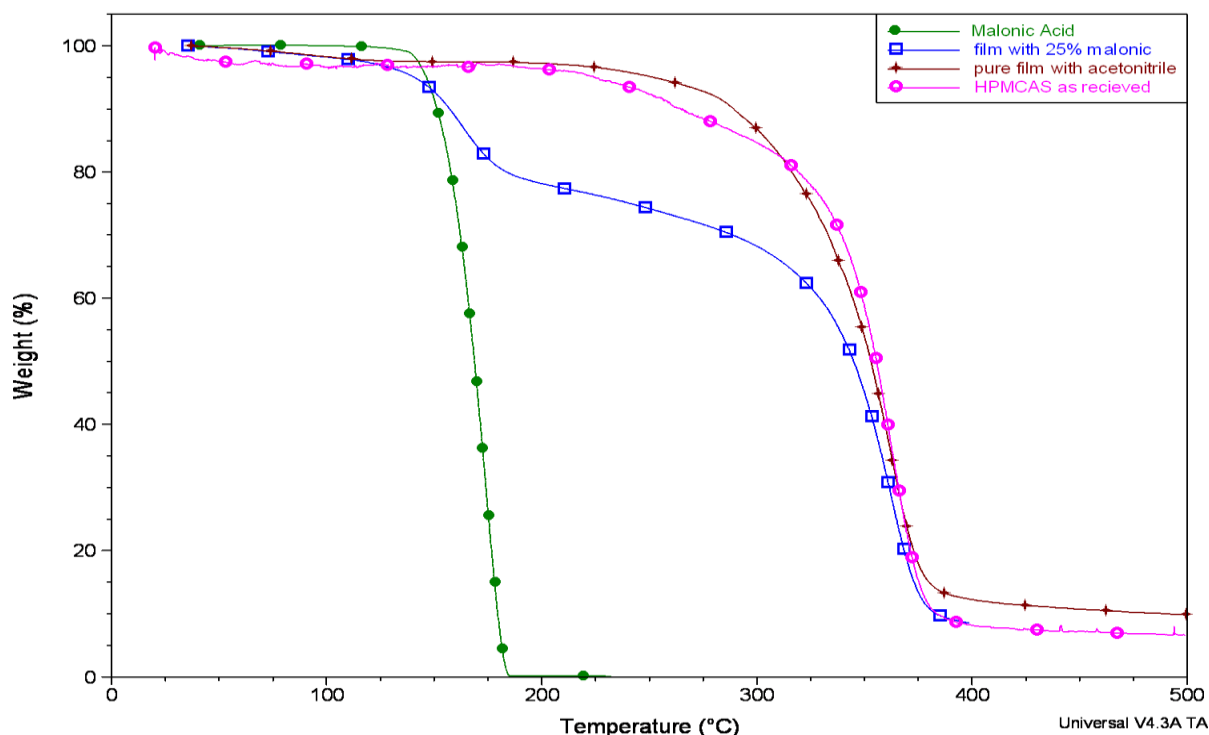


Figure 6.1. Representative TGA thermal profile for unprocessed malonic acid (green), unprocessed HPMCAS (pink), HPMCAS film prepared with acetonitrile (red), and a film containing 25% w/w malonic acid prepared with acetonitrile (blue).

The thermal DSC profiles for the films revealed a shift in the T<sub>g</sub> value of the polymer (appendix A11 24). It can be observed that films prepared using ethanol/water gave the highest T<sub>g</sub> values among other films (figure 6.2)

whereas, in general, films prepared using acetonitrile revealed the lowest T<sub>g</sub> values. Applying the solubility parameter theory shows that the observed results do not conform to the expected behaviour based on the solubility parameter values of solvents, malonic acid and HPMCAS. According to the SP values of the aforementioned materials acetonitrile is expected to more strongly interact with malonic acid as it has a closer SP value to that of malonic acid. Thus it can be anticipated that acetonitrile will act to promote the migration of malonic acid molecules to the surface of the polymeric film when it evaporates. On the other hand, films produced with acetone/chloroform should reveal low T<sub>g</sub> based on their far SP value compared to malonic acid and the polymer. Thus, it can be concluded that the solvent effect on malonic acid-HPMCAS interaction is different from the observed behaviour in section 5.4. However, it is worth mentioning that SP values of solvent systems were calculated without taking the interaction between solvents into consideration. Ethanol and water are known to interact with each other. This interaction will affect the polarity of their mixture. Therefore, the SP values of the solvent systems are not accurate. On the other hand, the previous behaviour could be explained based on the difference of solubility between malonic acid and HPMCAS in the solvent used. Malonic acid is highly soluble in water. However, HPMCAS is considered as a sparingly soluble in it. Thus, malonic acid will prefer to interact with water rather than the polymer. Ethanol/water has a good solubility for malonic acid and the polymer. However, the solubility of malonic acid in that solvent system is expected to be higher than the affinity of malonic acid to HPMCAS. The polarity of ethanol/water plays a role in increasing such interaction. On the other hand, acetonitrile has a weak polarity that doesn't allow for a strong interaction to take

a place, therefore, the effect of acetonitrile on malonic acid-HPMCAS is weaker. Chloroform and acetone are known to have a moderate polarity. Hence, their effect lies between the effect of ethanol/water and acetonitrile (figure 6.2). The solvent effect on the Tg value of polymer was studied for polyvinyl chloride and it was found that solvent type plays a role in the Tg value of that polymer (López and Mijangos, 1994).

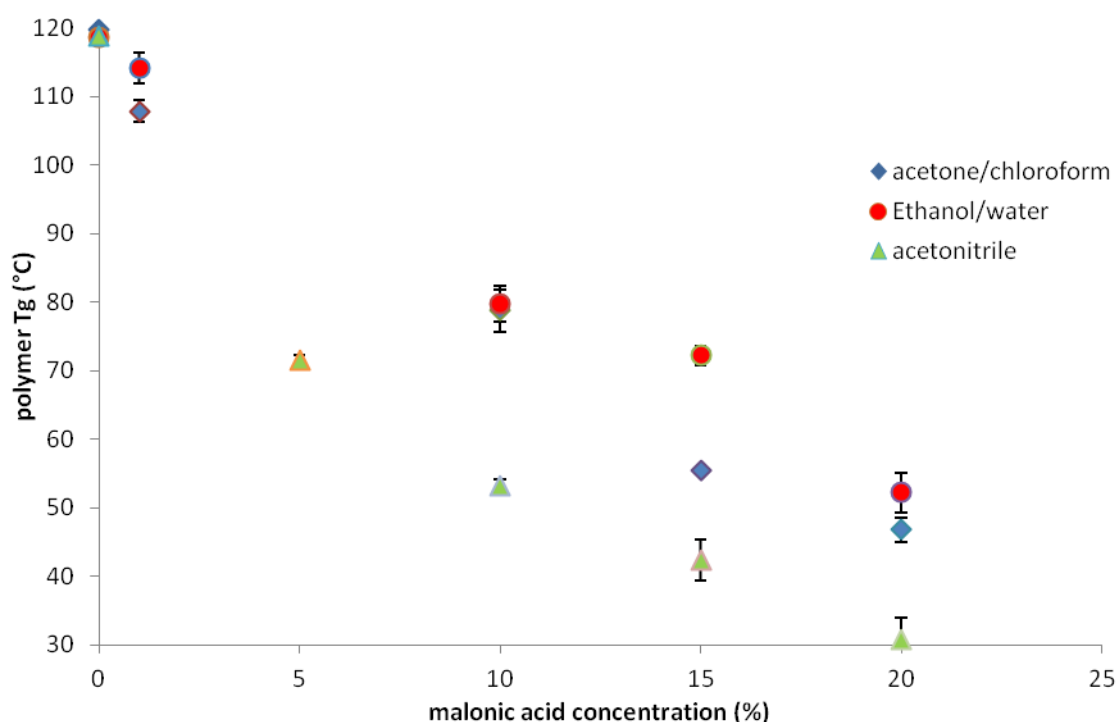


Figure 6.2. Graph to show the relation between the Tg and the percentage weight concentration of malonic acid in HPMCAS films cast from different solvent systems.

### 6.2.1.3 Powder X-ray diffraction

The powder x-ray diffraction patterns for films containing malonic acid were obtained using the method described in section 2.2.2. However, the patterns collected showed a high noise/signal ratio and an amorphous peak. Hence, it was not possible to distinguish the existence of malonic acid diffraction peaks with films containing low concentrations of malonic acid. Films containing 30% malonic acid and higher revealed the existence of some peaks that can be

found in the diffraction pattern of unprocessed malonic acid. A representative for the diffraction pattern is provided in figure AIII 3.

#### 6.2.1.4 FT-IR transmission

The FT-IR spectra obtained for the polymeric films using the method described in section 2.2.3 revealed a low signal/noise ratio (figure 6.3). Additionally, films with a malonic acid concentration below 25:100 w/w malonic acid/HPMCAS produced transmission spectra similar to that of a plain film. However, films containing high concentrations (30% w/w) of malonic acid revealed clear transmission peaks similar to the ones found in the spectrum of unprocessed malonic acid. This indicates that the FT-IR microscope is sensitive enough to detect the presence of malonic acid crystals in films containing 25:100 w/w malonic acid/HPMCAS or less.

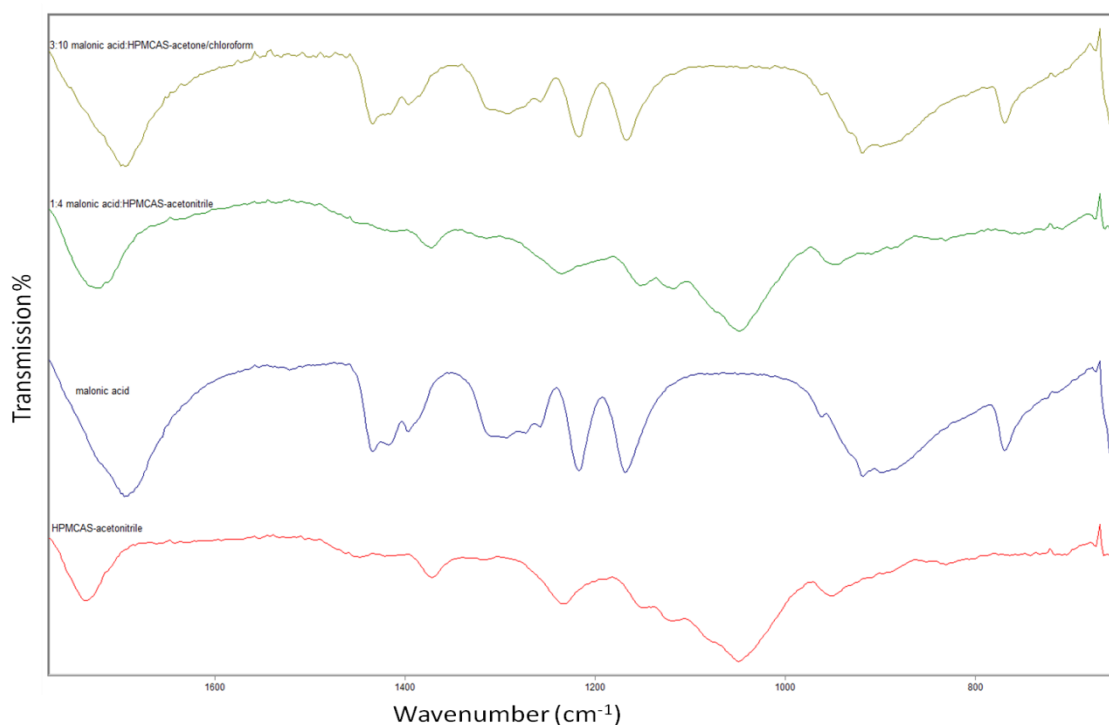


Figure 6.3. Representative FT-IR spectra for HPMCAS film cast using acetonitrile (red), unprocessed malonic acid (blue), a film containing 1:4 w/w malonic acid/HPMCAS (green), and a film containing 3:10 w/w malonic acid/HPMCAS (yellow).



### **6.2.1.5 Hot Stage Microscopy**

Cast films were examined by HSM following the method described in section 2.2.4.2. The events that occurred during the analysis of HPMCAS films containing 40:100 w/w malonic acid/HPMCAS cast using acetone/chloroform. It was noted that the crystals in the film were heavily condensed in a way that blocked the light from passing through. When the heating started, the polymeric matrix started to expand causing a change in the focal length of the observed field. Malonic acid crystals were observed to melt with an onset of around 118°C (figure 6.4). This temperature is low compared to the melting point of the unprocessed malonic acid. However, the dispersion of malonic acid in the polymeric film can cause such a depression in melting point. The depression of melting point of drugs dispersed in the polymer has been observed before in the literature and linked to Flory-Huggins lattice theory (Marsac et al., 2009). The melted malonic acid continued to occupy the cavities in the polymer where the crystals previously used to be. At higher temperatures the liquid malonic acid was observed to diffuse through the polymeric matrix and mix with it forming a homogenous phase. Cooling the sample to room temperature did not induce recrystallization during the time frame of the experiment. Thus it can be concluded that the crystals converted into an amorphous material in the polymeric film.

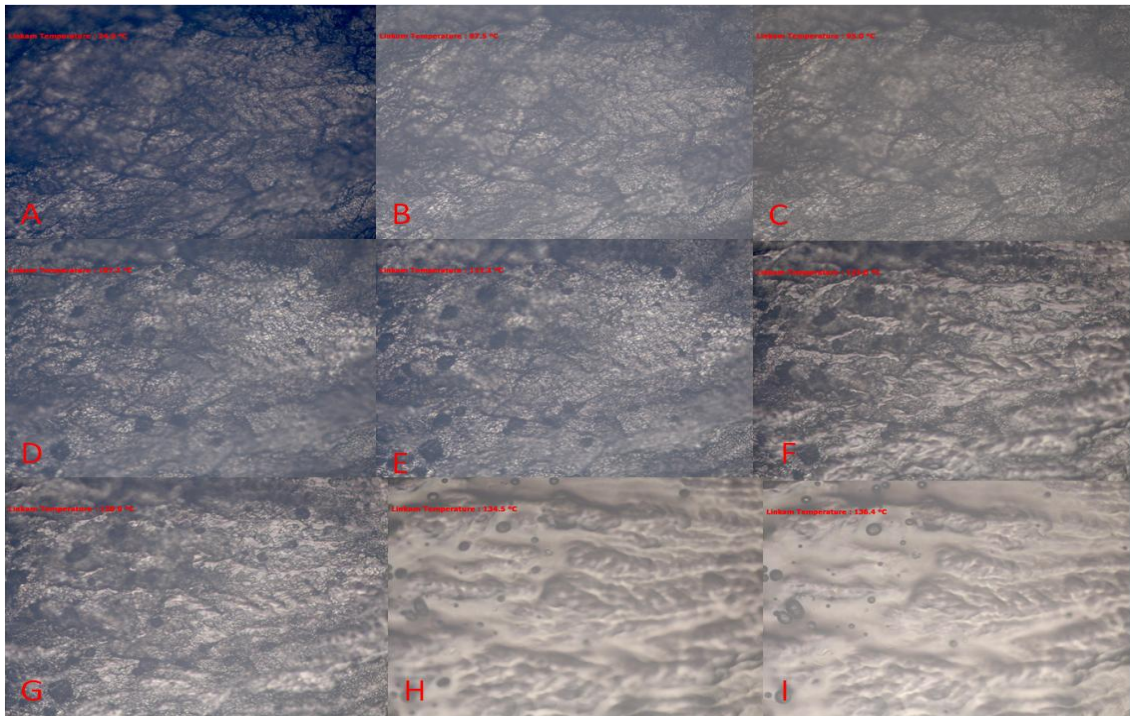


Figure 6.4. Representative HSM images for films 40% w/w malonic acid/HPMCAS at: (A) 24°, (B) 87°, (C) 95°, (D) 107°, (E) 112°, (F) 120°, (G) 124°, (H) 134°, and (I) 136°C all using x10 magnification power.

### 6.2.1.6 SEM

Films containing malonic acid crystals were analyzed using the SEM in order to obtain a good image for the crystal shape. SEM imaging was performed using the method described in section 2.2.4.1. Malonic acid crystals were typically observed to have the length of 30-60 micrometers as exemplified in figure 6.5.

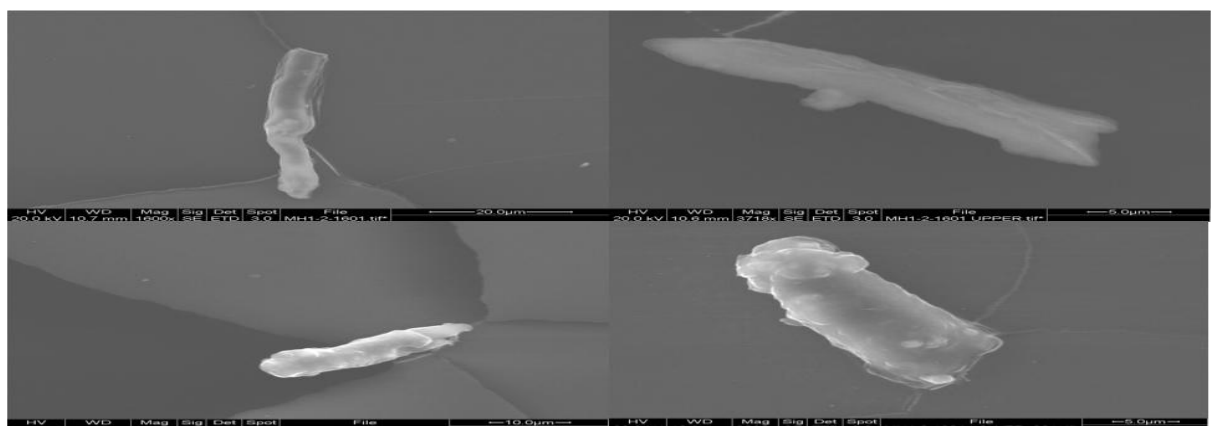


Figure 6.5. Representative SEM images for films containing different concentrations of malonic acid with magnification powers: x1600 (top left), x3180 (top right), x1800 (bottom left), and x3000 (bottom right).

## **6.2.2 Ibuprofen**

Ibuprofen-polymer interaction is well documented in the literature (Kazarian and Martirosyan, 2002 , Nakayama et al., 2009 , Whelan et al., 2002). The polymer inhibits the growth of ibuprofen crystals. It deposits on the active growing surfaces of the crystal inhibiting its growth. In order to characterize the effect of such interaction on the loading process of ibuprofen-nicotinamide co-crystals into the polymeric film, films containing various concentrations of ibuprofen were prepared using the method described in section 2.3.3. Films were prepared using acetone/chloroform and/or acetonitrile as a solvent system.

### **6.2.2.1 Thermal analysis**

#### **6.2.2.1.1 TGA**

In order to characterise the amount of moisture or residual solvent in the prepared films, the thermal profiles for films containing ibuprofen were collected using the method described in section 2.2.1.1. The collected data were compared to the thermal profile for unprocessed ibuprofen and unprocessed HPMCAS (figure 6.6). It can be noticed that the weight loss due to the thermal degradation of the films passes through two steps. The first step commences around 170°C. This step can be correlated to the weight loss resulted from the thermal degradation of ibuprofen in the film as the thermal profile of the unprocessed ibuprofen revealed the same weight loss pattern that commences around 150°C and the observed weight loss at the end of this stage is consistent with the percentage of ibuprofen concentration in the film. The second stage commences around 300°C which can be correlated to the thermal degradation of the polymer as the weight loss at the end of this step is

consistent with the weight loss observed in the thermal profile of the unprocessed polymer. It can be observed that films containing ibuprofen have lost less than 2% weight at 100°C. A similar weight loss can be observed in the thermal profile of unprocessed HPMCAS. thus it is expected to be the result of the evaporation of residual moisture.

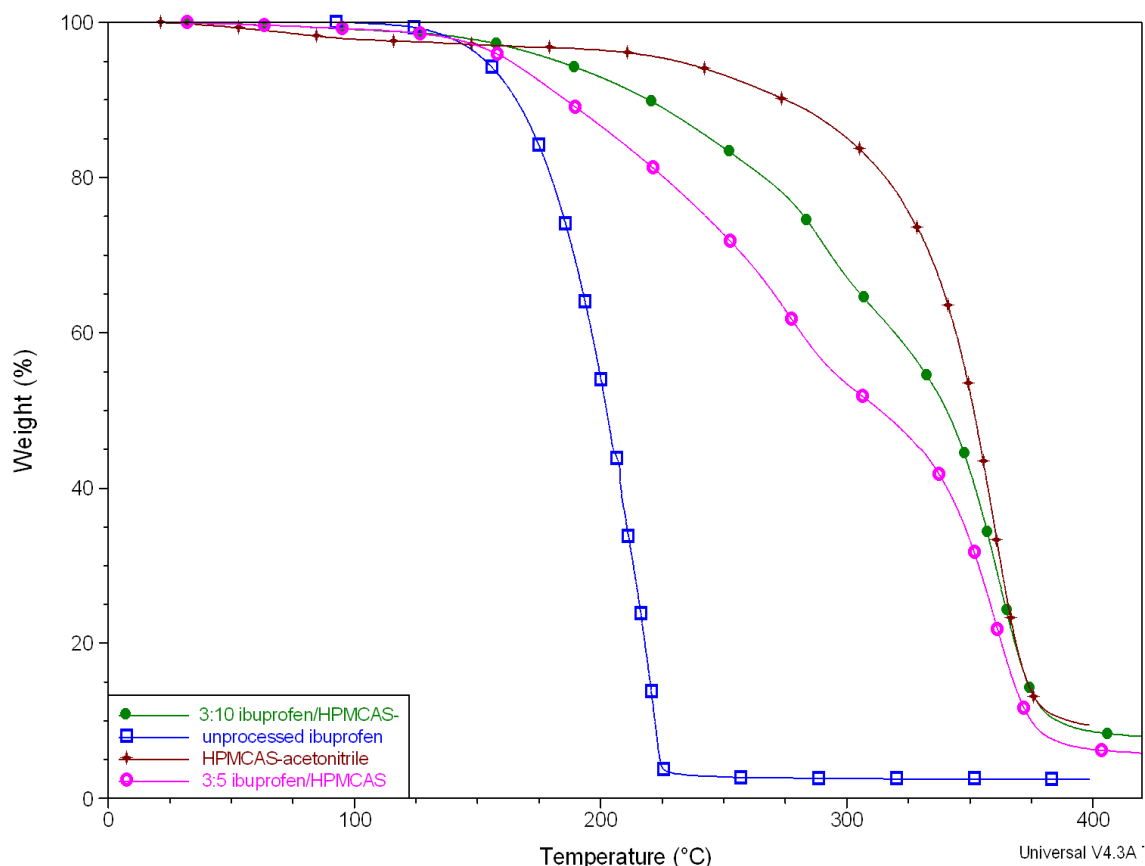


Figure 6.6. Representative TGA thermal profiles for unprocessed ibuprofen (blue), HPMCAS cast from acetonitrile (red), a film containing 3:10 w/w ibuprofen/HPMCAS (green), and a film containing 3:5 w/w ibuprofen/HPMCAS (pink).

### 6.2.2.1.2 DSC

The thermal profiles for films containing various concentrations of ibuprofen were collected using the method described in section 2.2.1.2. The T<sub>g</sub> values were obtained from the thermal data and plotted against the concentration of ibuprofen and compared to the T<sub>g</sub> of films containing various concentrations of malonic acid (section 6.2.1.2.2) in figure 6.7.

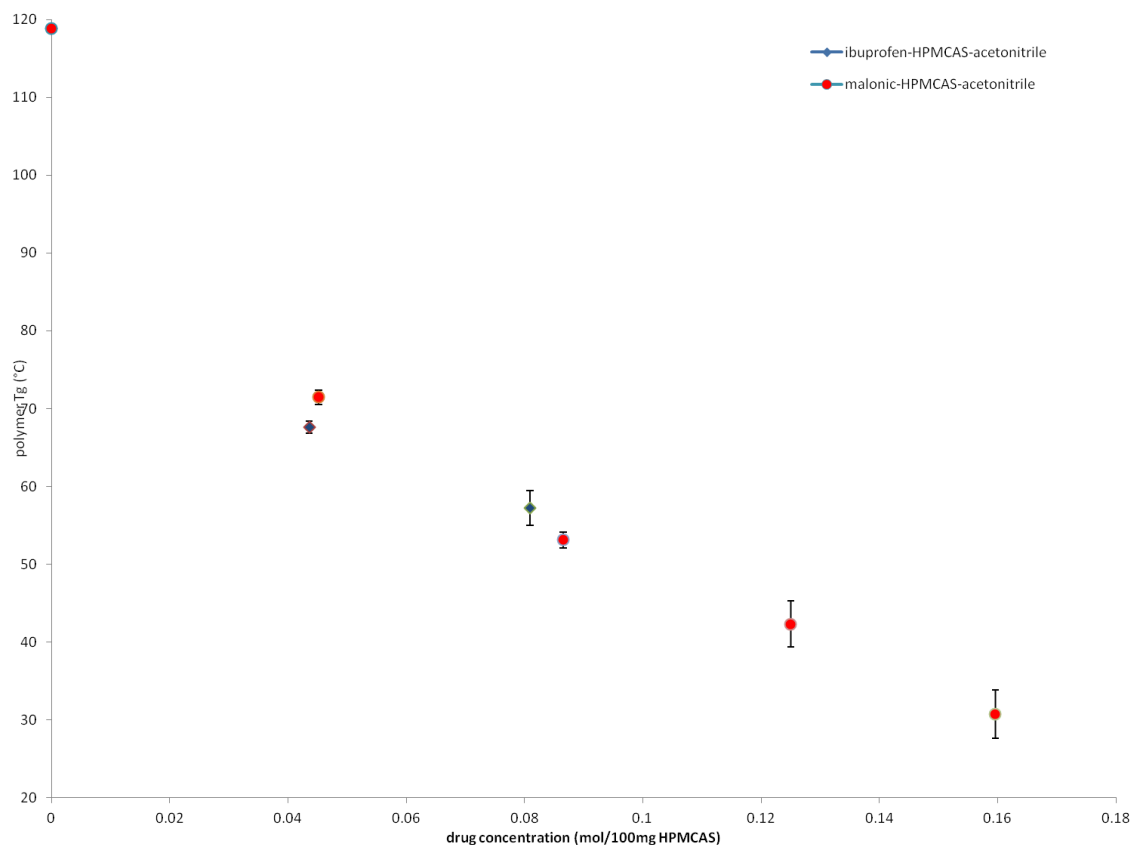


Figure 6.7. A chart of polymer Tg against the concentrations of ibuprofen (blue diamond) and malonic acid (red circle) in polymeric films separately.

It can be noted from figure 6.7 that the malonic acid has plasticized the polymer in almost a similar manner to that produced by using ibuprofen, using the same solvent (acetonitrile).

### 6.2.2.2 Powder X-ray diffraction

The diffraction patterns of films containing ibuprofen were collected using the method described in section 2.2.2. The diffraction pattern of a film containing 60% w/w ibuprofen/HPMCAS displays the appearance of an amorphous peak between 5°-20°. The pattern in figure 6.8 reveals a high noise/signal ratio, yet, there are some clear diffraction peaks that can be observed. The diffraction pattern reveals some peaks at 6°, 12°, 16°, 18°, 19°, 19.8°, 20°, 22°, 25°, and 27° in addition to other peaks (figure 6.8). The above peaks can be observed in

the standard diffraction pattern of ibuprofen RS. Consequently, the ibuprofen isomerism didn't change after loading it into the polymer and the films contained some crystalline ibuprofen.

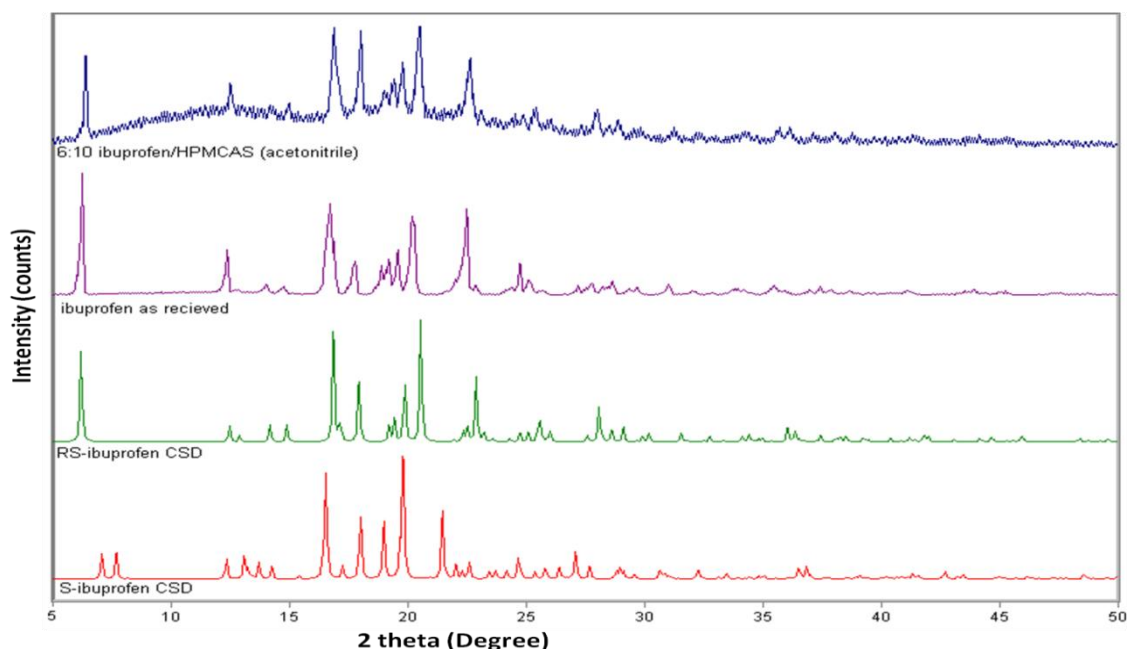


Figure 6.8. Representative powder x-ray diffraction patterns for unprocessed ibuprofen (purple), standard diffraction pattern for S-ibuprofen CSD (red), RS- ibuprofen CSD (green), and a film containing 6:10 w/w ibuprofen/HPMCAS prepared using acetoneitrile (blue).

### 6.2.2.3 FT-IR transmission

FT-IR spectra for films containing ibuprofen were obtained in order to detect any peak shifts in the spectrum resulting from hydrogen bond formation between the polymer and ibuprofen. The spectrum was obtained using the method described in section 2.2.3. The FT-IR spectrum in figure 6.9 revealed a shift in the 1700  $\text{cm}^{-1}$  peak to 1715  $\text{cm}^{-1}$ . In addition to that, it can be noticed that in films containing 5:10 ibuprofen/HPMCAS there are two peaks at 1699 and 1715  $\text{cm}^{-1}$ . This peak was noticed to be assigning for the C=O, OH vibration energy in section 3.1.3.3. However, C=O, OH peaks usually shift to a lower wavenumber when they participate in hydrogen bonding. Hence, this shifting might or might not be related to the formation of a hydrogen bond.

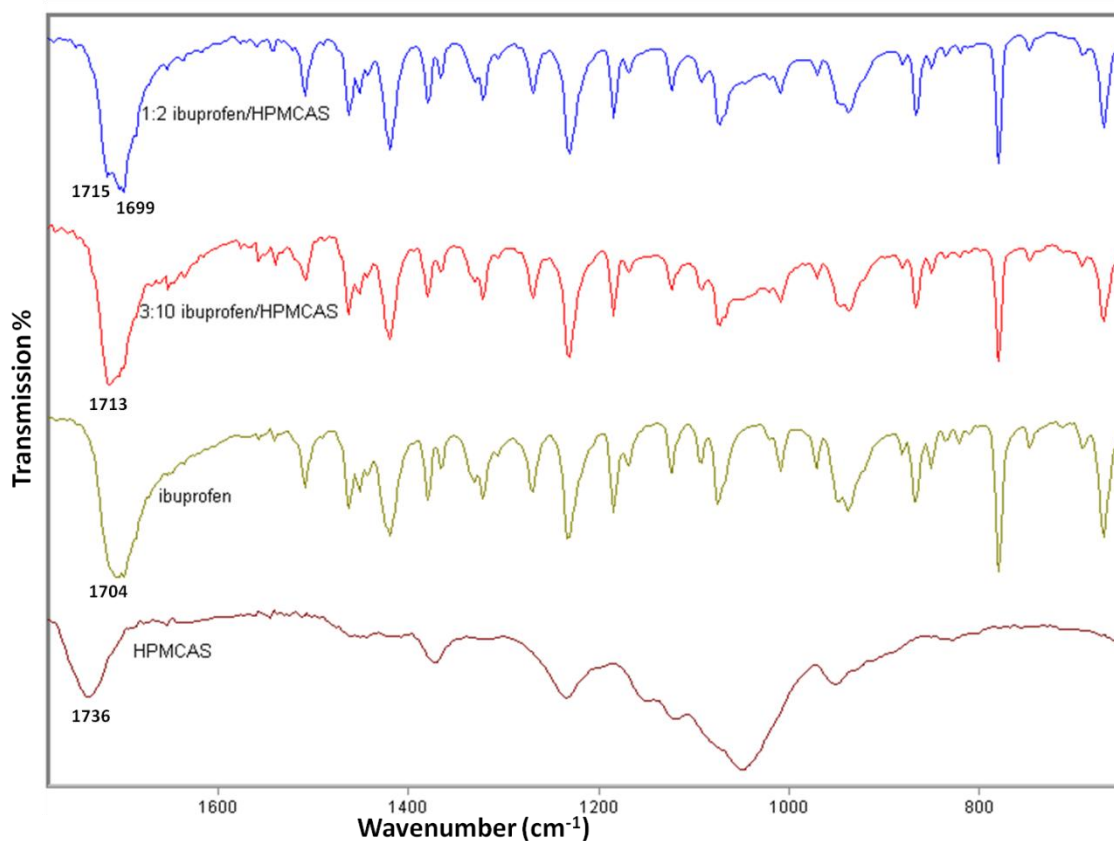


Figure 6.9. Representative FT-IR spectra for unprocessed HPMCAS (dark red), unprocessed ibuprofen RS (yellow), a film containing 3:10 w/w ibuprofen/HPMCAS (light red), and a film containing 1:2 ibuprofen/HPMCAS (blue) both films prepared using acetonitrile.

#### 6.2.2.4 Hot stage microscopy

In order to characterize the behaviour of ibuprofen crystals inside the polymeric film, a sample of a film containing 3:5 w/w ibuprofen:HPMCAS was analyzed using the hot stage microscope following the method described in section 2.2.4.2. The sample was heated to around 95°C (figure 6.10). A magnification power of x10 was used to capture the film images up to 70°C then X20 magnification power was used to get detailed images for the crystals melting. The crystals appeared small using X10 magnification power. This behaviour can be correlated to the ability of the polymer to inhibit the crystal growth of drugs. It can be observed from figure 6.10 that ibuprofen crystals start to melt at around

75°C. The melting of the crystals was noticed to end at around 78°C. Increasing the temperature was noted to causes the polymeric matrix to expand and the liquefied ibuprofen to penetrate into the polymer matrix and form a homogeneous system.

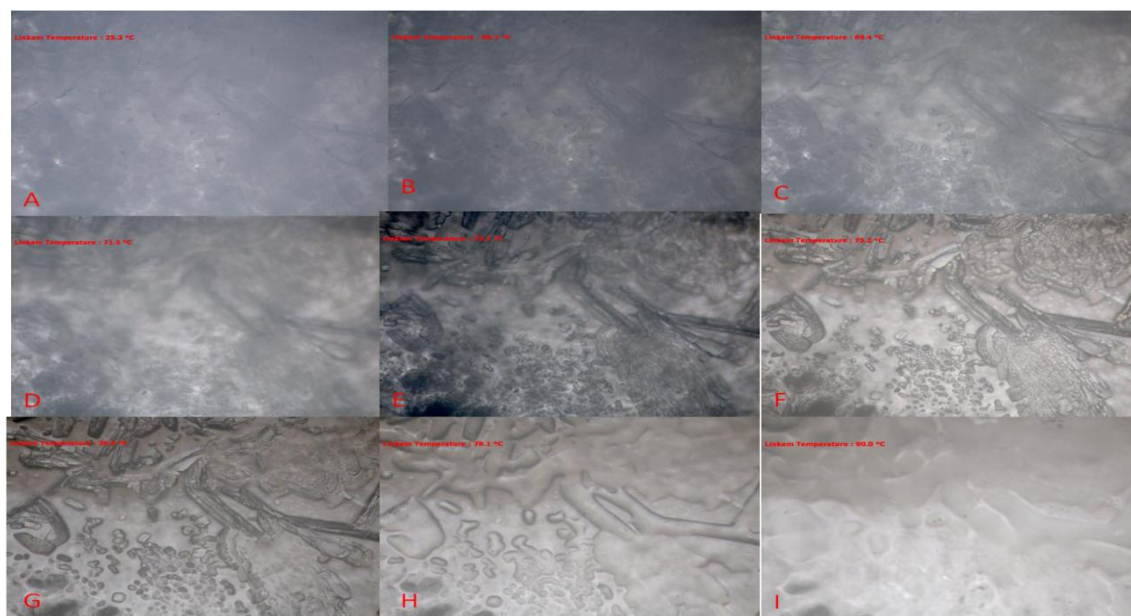


Figure 6.10. A representative HSM scan of a film containing 3:5 w/w ibuprofen/HPMCAS at: (A) 25°, (B) 66°, (C) 69°, (D) 71°, (E) 73°, (F) 75°, (G) 76°C, (H) 78°C, and (I) 90°C. Magnification power is x10 (A) to (D) and x20 from (E) to (I).

Films containing naproxen and flurbiprofen were not extensively studied separately as the two aforementioned drugs were used to investigate a displacement hypothesis only (section 6.3.1.2 and 6.3.3).

## **6.3 Characterisation of films containing two different acidic species/drugs**

### **6.3.1 Films containing malonic acid with ibuprofen**

To this point this thesis has evaluated the behaviour of films cast to contain a single material. It has also evaluated the films prepared from different solvents.



The effect of introducing a second acidic system to the same film is an interesting and novel area to study.

Films containing two acidic species were prepared using the method described in section (2.3.3). In summary, the method involved casting films containing 2:2:10, 3:2:10, 3:3:10, and 3:4:10 w/w/w ibuprofen/malonic acid/HPMCAS. Two solvent systems identified to prepare these films were acetonitrile and acetone/chloroform.

### **6.3.1.1 Thermal analysis**

#### **6.3.1.1.1 TGA**

Thermal profiles for films containing ibuprofen and malonic acid were obtained using the method described in section 2.2.1.1. Collected thermal data of polymeric films containing 3:2:10 and 3:4:10 w/w/w ibuprofen/malonic acid/HPMCAS revealed that the weight loss in their thermal TGA profile can be divided into three steps (Figure 6.11). The first step commences at around 130°C. This step can be easily correlated to the weight loss resulted from the thermal degradation of malonic acid (sections 3.1.2.1 and 3.2.2.1). The second step commences at around 180°C which can be correlated to the weight loss resulted from the thermal degradation of ibuprofen (section 3.1.3.1). The third step commences at around 250°C and it can be correlated to HPMCAS thermal degradation (section 3.1.7.1). It can be noted from figure 6.11 that the film has lost less than 5% of total weight between 30-100°C. This loss was observed in films containing malonic acid (3:10 and 5:10 w/w). This extra percentage might indicate that the solvent has not evaporated completely. Nevertheless, the amount of residual moisture is small to affect the crystallization or the

interaction with the polymer. In addition, malonic acid is considered as a hygroscopic material and that might have caused the increase in the amount of residual moisture. Thus these films might have additional moisture.

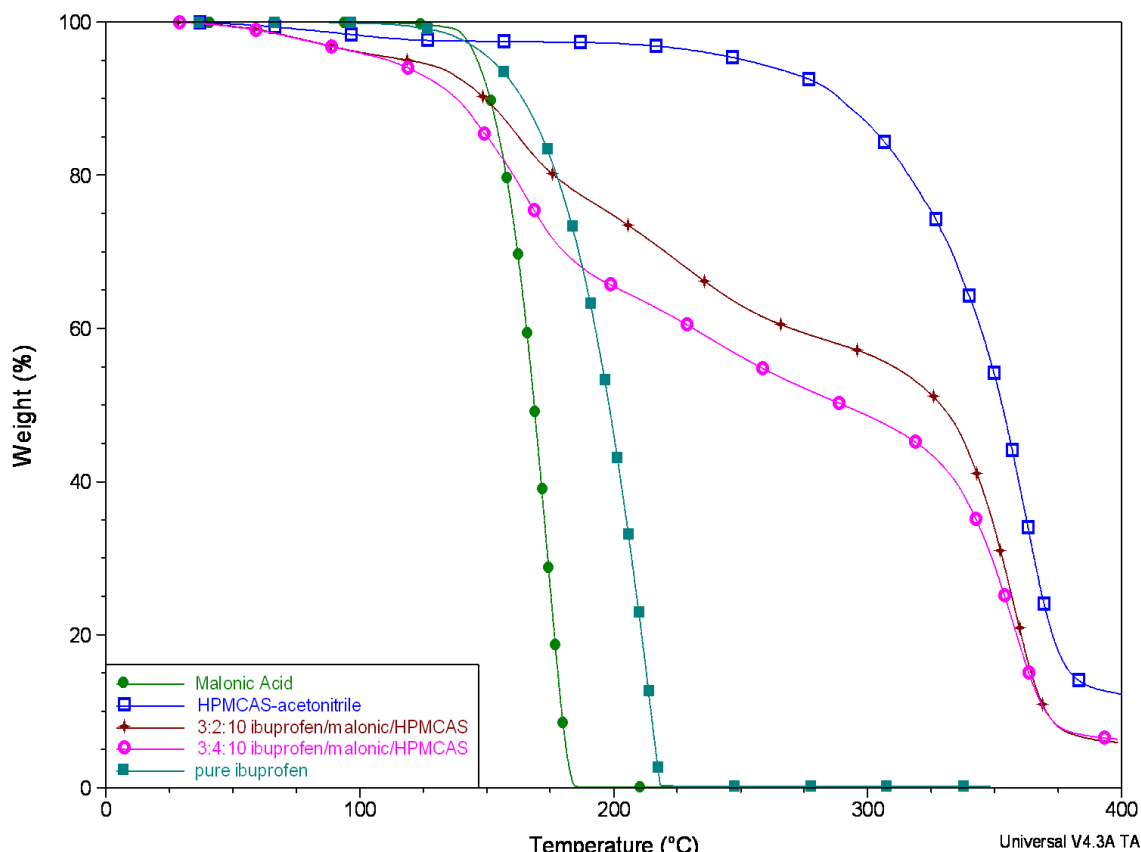


Figure 6.11. Representative TGA thermal profiles for unprocessed ibuprofen (teal), unprocessed malonic acid (green), HPMCAS film prepared with acetonitrile (blue), and films containing 3:2:10 and 3:4:10 w/w/w ibuprofen/malonic acid/HPMCAS (red and pink respectively).

### 6.3.1.1.2 DSC

Thermal profiles for films containing ibuprofen and malonic acid were obtained using the method described in section 2.2.1.2. Collected thermal data revealed the existence of an endothermic peak in the first heating run on the DSC chart as in figure 6.12. This peak appears at 61°C. This peak relates to the melting of ibuprofen crystals in the polymeric film. The reduction in the melting point results from the impurity effect of the polymer on the ibuprofen melting point. In

order to have clear evidence, other films containing malonic acid and a higher concentration of ibuprofen were analyzed. The collected data showed a higher area under the curve for the same peak indicating that this peak is related to a thermal transition for at least a part of the ibuprofen content.

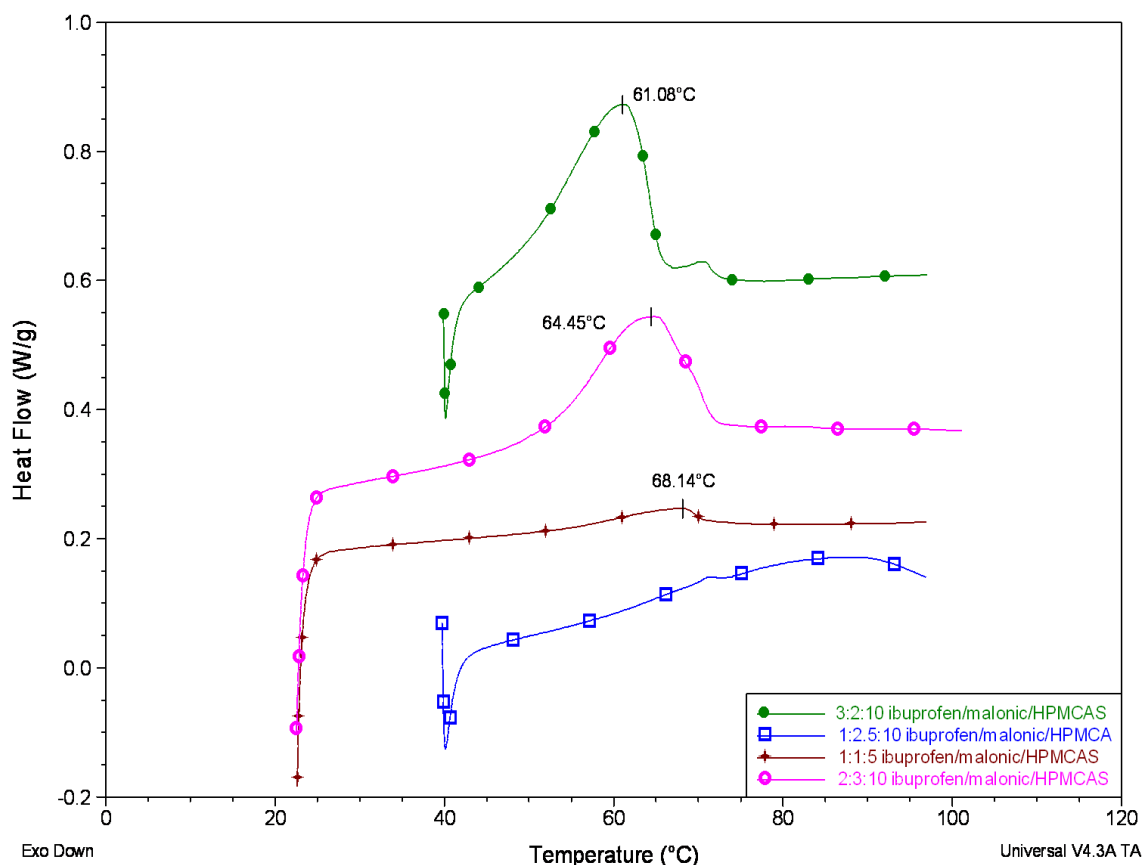


Figure 6.12. DSC scan of films containing 3:2:10 (green), 2:3:10 (pink), 1:2.5:10 (blue), and 1:1:5 (red) ibuprofen/malonic acid/HPMCAS w/w/w.

Cooling the sample and reheating it revealed a flat thermal profile indicating that ibuprofen crystals melted on the first heat and remained amorphous or liquefied in the polymeric film (figure All 19-21).

Interestingly, the thermal profiles showed no other peak at or near the melting point of malonic acid. Malonic acid would therefore be molecularly dispersed in the film and not in a crystalline state.

### 6.3.1.2 powder X-ray diffraction

Powder x-ray diffraction data was collected using the method described in section 2.2.2. The diffraction pattern for films containing 3:4:10, 3:3:10, and 3:2:10 ibuprofen/malonic acid/HPMCAS w/w/w revealed the existence of three characteristic diffraction peaks at 6°, 12°, and 24°. These peaks can be observed in the diffraction pattern of ibuprofen RS. Therefore, it can be concluded that ibuprofen is present in a crystalline state in the film. On the other hand, the absence of any peaks that can be correlated to crystalline malonic acid diffraction pattern was noted. This result conforms to the result obtained in section 6.3.1.1.2. Therefore, it can be concluded that malonic acid was predominantly molecularly dispersed while ibuprofen crystallized in the polymeric film.

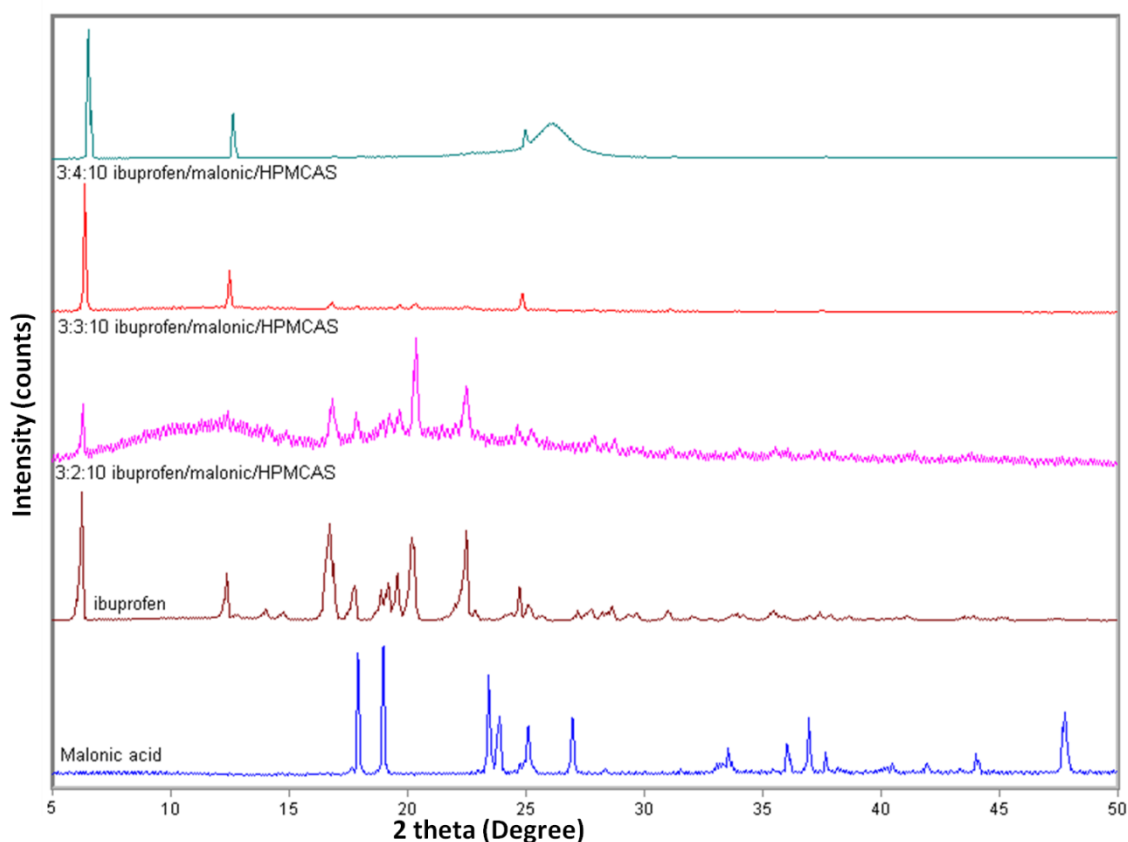


Figure 6.14. Representative powder x-ray diffraction pattern for unprocessed malonic acid (blue), unprocessed ibuprofen RS (red), a film containing 3:4:10 ibuprofen/malonic acid/HPMCAS w/w/w (pink), 3:3:10 (light red), and 3:2:10 (teal).

### 6.3.1.3 FT-IR transmission

The FT-IR spectra for a film containing 3:4:10 w/w/w ibuprofen/malonic acid/HPMCAS were collected using the method described in section 2.2.3. The collected spectrum revealed a similar FT-IR transmission pattern to the unprocessed ibuprofen (figure 6.15). The spectrum revealed a transmission peak at  $1698\text{ cm}^{-1}$ . This peak was previously assigned to C=O, OH vibration energy. There was no obvious shifting for this peak. This might reflect the existence of no bonding between ibuprofen crystals and HPMCAS. On the other hand, the FT-IR could not detect the existence of malonic acid. This might happen due to the small size of malonic acid crystals that hindered the detection by the FT-IR.

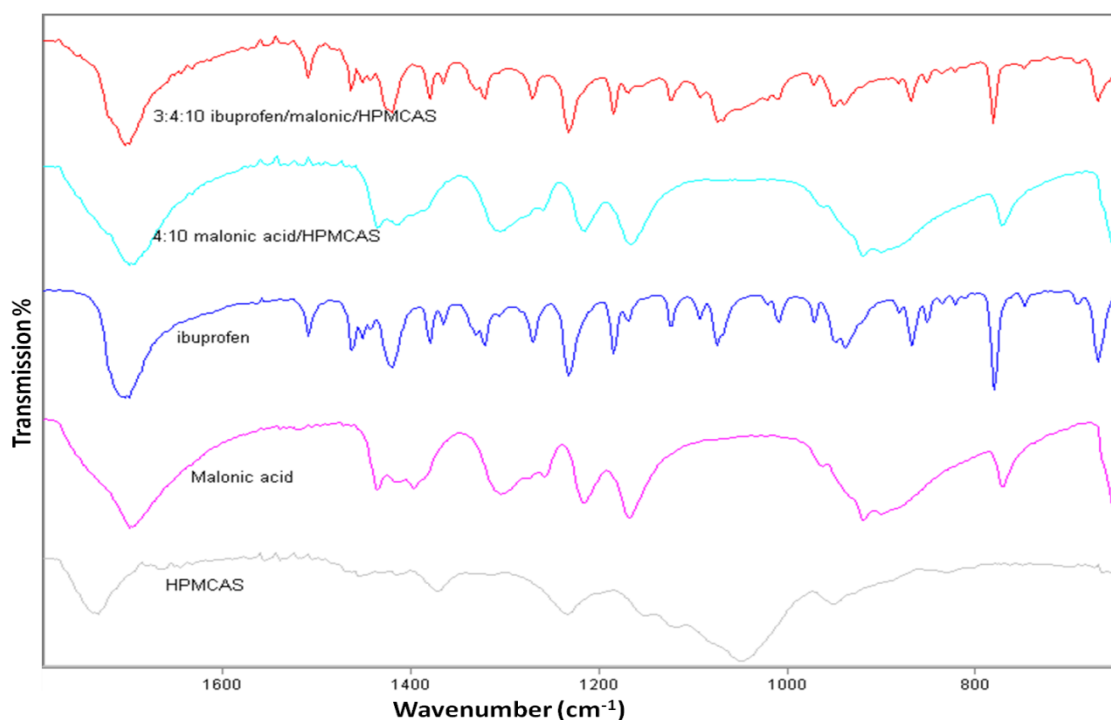


Figure 6.15. Representative FT-IR spectrum for unprocessed HPMCAS (bottom), unprocessed malonic acid (pink), unprocessed ibuprofen (blue), film containing malonic acid (teal), and a film containing 3:4:10 w/w/w ibuprofen/malonic acid/HPMCAS (red).

### 6.3.1.4 Hot Stage Microscopy

Hot stage microscopy was performed in order to have visual evidence that supports the results obtained using DSC. A film containing 3:3:10 w/w/w ibuprofen/malonic acid/HPMCAS was analyzed using the method described in section 2.2.4.2. The film was heated with a heating rate of 2°C/min to 100°C then cooled to room temperature using the same rate (figure 6.16).

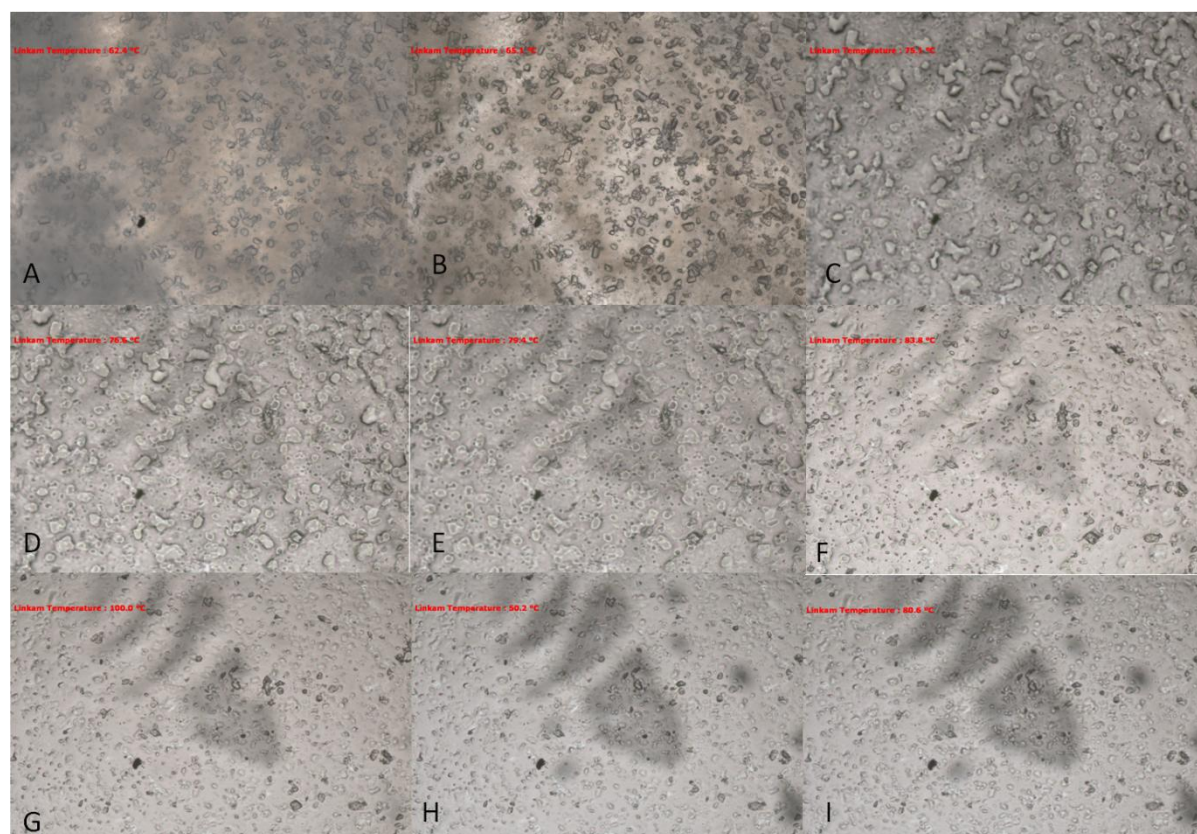


Figure 6.16. Hot Stage Microscope scan of a film containing 3:3:10 w/w/w ibuprofen/malonic acid/HPMCAS prepared with ethanol/water at: (A) 62°C, (B) 65°C, (C) 75°C, (D) 76°C, (E) 79°C, (F) 83°C, (G) 100°C, (H) 50°C, (I) 80°C. Magnification was x10 for all cases.

A large amount of crystals were observed in the film at room temperature.

When commencing heating, the polymeric film expanded. The melting sequence of the crystals started at around 65°C and it lasted until the temperature reached 67°C. After that, the melt was observed to diffuse through the polymeric film and form a homogenous structure. The cooling sequence revealed that re-crystallisation did not occur within the experimental time frame.

The HSM behaviour of the film is consistent with the endothermic peak found in the DSC thermal profile. The crystals observed in the film to melt can be identified as ibuprofen crystals that phase separated from the polymer. Ibuprofen alone in HPMCAS did not crystallise at this concentration.

Only above 60:100 w/w ibuprofen/HPMCAS was this behaviour observed. The finding indicates that the addition of malonic acid lowers the saturation concentration for ibuprofen with HPMCAS. The finding is also consistent with malonic acid having a greater affinity to interact with HPMCAS than ibuprofen.

According to the solubility parameter values of malonic acid, ibuprofen, and HPMCAS obtained from table 5.1 and 5.2. Malonic acid has a closer SP value (22.4) to the polymer (24) than ibuprofen (19). This observation if universally applicable might open the road towards finding a theoretical method for predicting and controlling the interactions between acidic drugs and HPMCAS.

To test the validity of the above finding for other systems, naproxen and flurbiprofen were used to test the applicability of the previous conclusion.

### **6.3.2 Investigation of HPMCAS films containing malonic acid and naproxen**

A film containing 20:20:100 w/w/w naproxen/malonic acid/HPMCAS was prepared using acetonitrile and following the method described in section 2.3.3.

Malonic acid has a solubility parameter (22.47) that is relatively closer to HPMCAS parameter value (24) than naproxen (21.9). Hence, from the SP theory it was expected that malonic acid should dispersed in the polymer

reducing the saturation point for naproxen. Consequently, naproxen crystals should be observed in the polymeric films.

### 6.3.2.1 Thermal analysis

#### 6.3.2.1.1 TGA

TGA thermal profile for the aforementioned film was obtained using the method described in section 2.2.1.1. A weight loss of around 2% was found between 30-100°C (figure 6.17). A similar weight loss was observed in the thermal profile of unprocessed HPMCAS and it was correlated to evaporation of residual moisture.

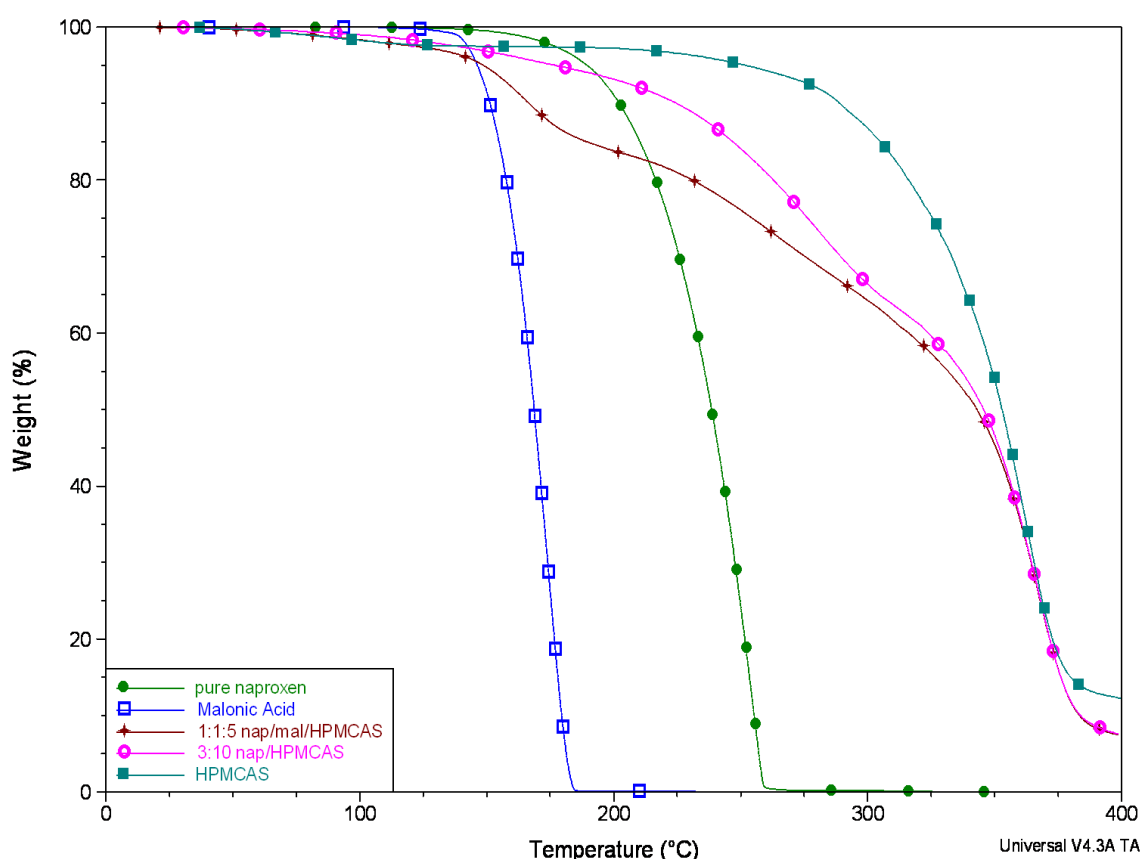


Figure 6.17. Representative TGA thermal profile for unprocessed naproxen (green), unprocessed malonic acid (blue), HPMCAS film (teal), film containing 3:10 w/w naproxen/HPMCAS (pink), and film containing 1:1:5 naproxen/malonic acid/ HPMCAS (red).



### 6.3.2.1.2 DSC

The DSC thermal profiles for films containing naproxen and malonic acid were obtained using the method described in section 2.2.1.2. The collected data reveals an endothermic peak appears in the analysis of films containing 3:10 naproxen/HPMCAS and a film containing 1:1:10 naproxen/malonic acid/HPMCAS. This peak can be observed at 153°C (figure 6.18). Hence, this peak can be correlated to the melting of naproxen crystals in the film. A weak intensity, yet wide endothermic peak can be observed around 100°C. This peak is believed to be related to the evaporation of the residual moisture in the film.

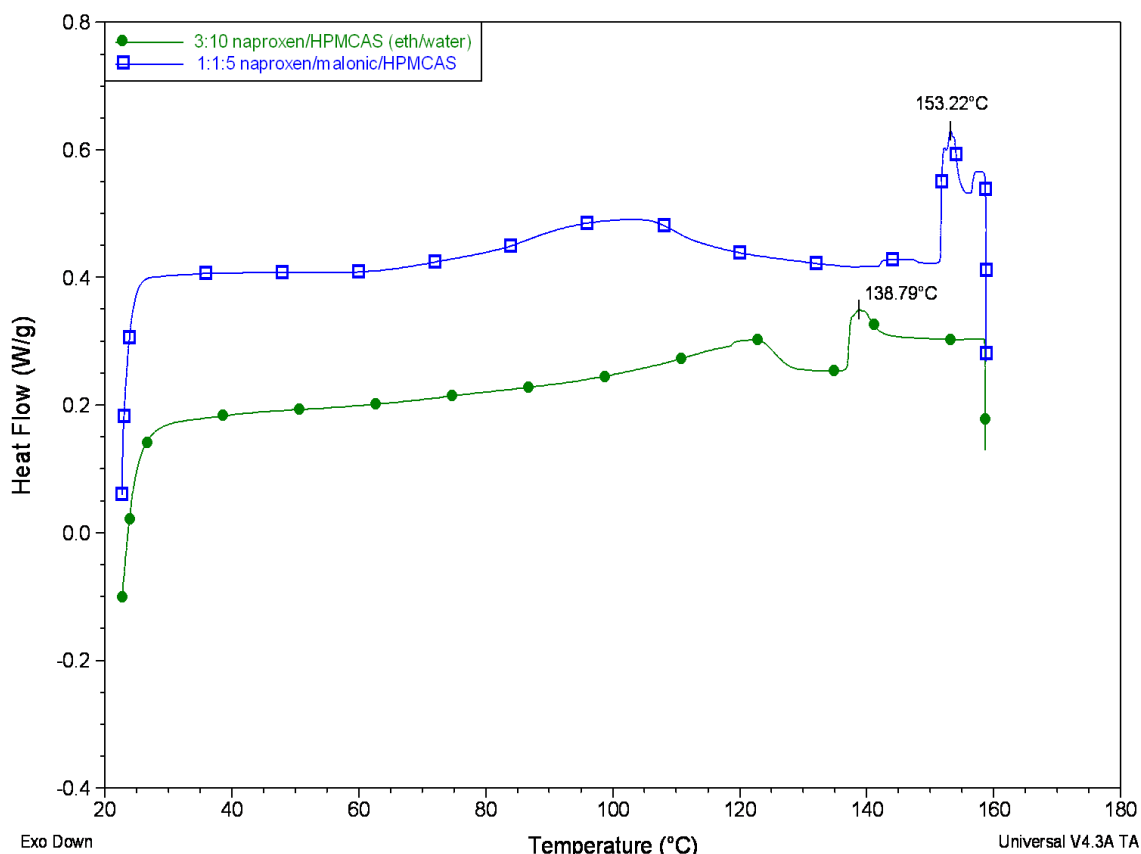


Figure 6.18. Representative DSC thermal profiles for a film containing 3:10 naproxen/HPMCAS prepared with ethanol/water (green) and a film containing 1:1:5 naproxen/malonic acid/HPMCAS prepared with acetone/chloroform (blue).

### 6.3.2.2 Powder X-ray diffraction

The powder x-ray diffraction patterns for films containing 1:1:5 w/w/w naproxen/malonic acid/HPMCAS, 3:10 w/w naproxen/HPMCAS, and 1:5 naproxen/HPMCAS were obtained using the method described in section 2.2.2. The collected diffraction pattern shown in figure 6.19 reveals the existence of a broad amorphous peak around 10°. It can be noticed that the patterns reveals a high noise/signal ratio. However, a number of peaks can be observed in the film diffraction pattern. Those peaks can be found at 16°, 19°, 20°, and 23°. These peaks can be easily observed in the diffraction pattern of unprocessed naproxen. On the other hand, none of the detected peaks can be correlated to the diffraction pattern of malonic acid.

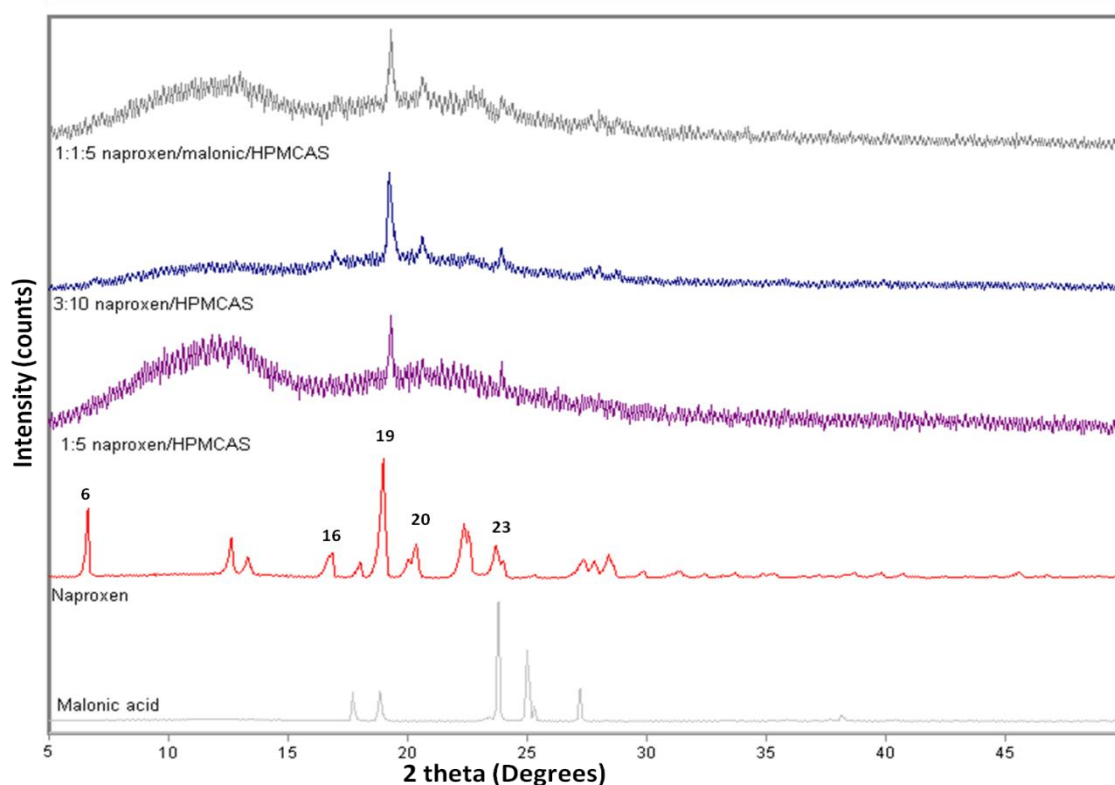


Figure 6.19. X-ray scan of malonic acid, naproxen, a film containing 1:1:5 naproxen/malonic acid/HPMCAS w/w/w, film containing 3:10 naproxen/HPMCAS, and a film containing 1:5 naproxen/HPMCAS. All films were prepared using acetone/chloroform.

### 6.3.2.3 Hot Stage Microscopy

A film containing 20:100 w/w naproxen/HPMCAS was analyzed using hot stage microscopy in order to monitor the behaviour of naproxen crystals. The analysis was performed using the method described in section 2.2.4.2. Figure 6.20 reveals that naproxen crystals started to melt around 126°C.

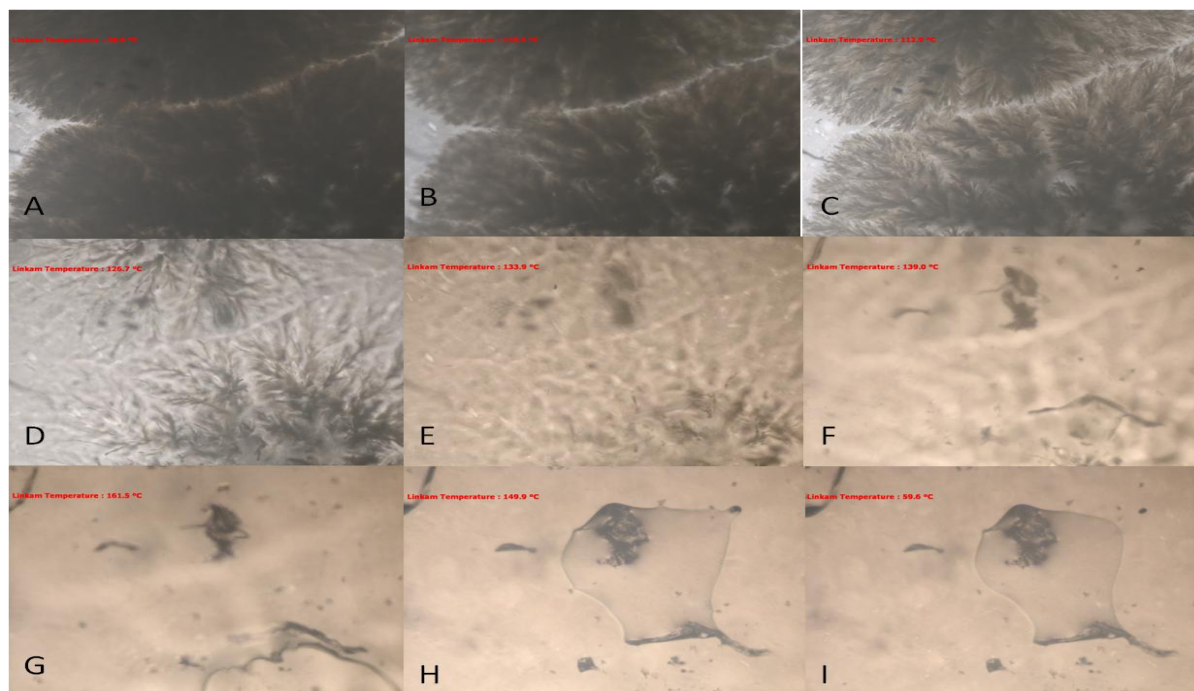


Figure 6.20. A representative Hot Stage Microscope analysis for a film containing 20:100 w/w naproxen/HPMCAS prepared with acetonitrile at: (A) 49°, (B) 110°, (C) 112°, (D) 126°, (E) 133°, (F) 139°, (G) 161°, (H) 150°, (I) 59°C. Magnification power of x10 was used.

In addition, a film containing 20:20:100 w/w/w naproxen/malonic acid/HPMCAS was analyzed by HSM (figure 6.21).

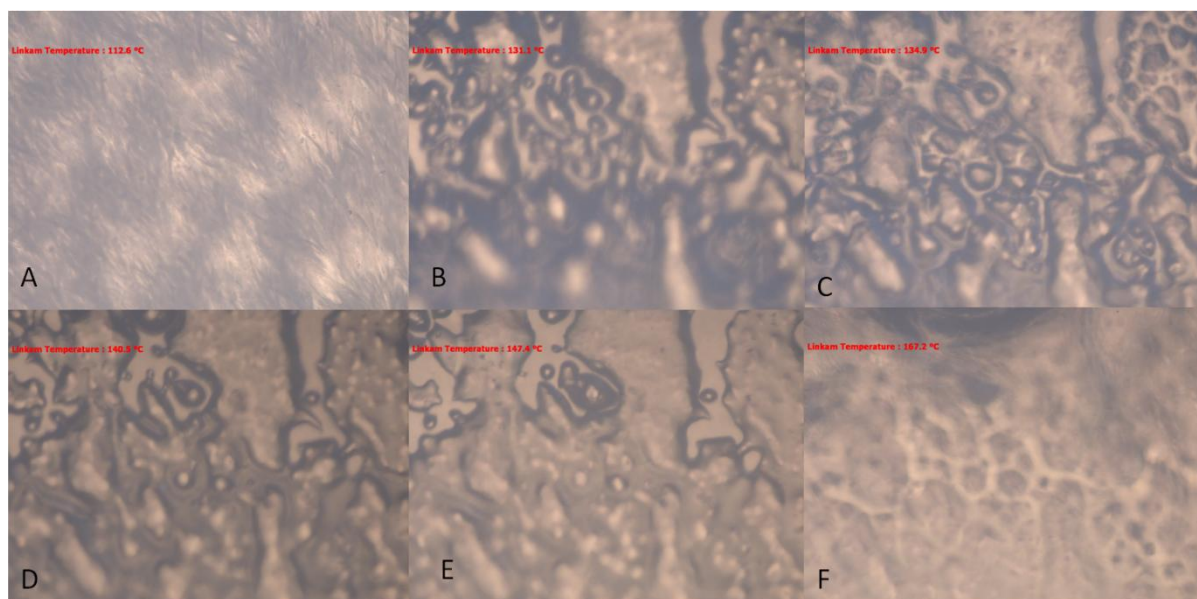


Figure 6.21. A representative Hot Stage Microscope analysis for a film containing 20:20:100 w/w/w naproxen/malonic acid/HPMCAS prepared with acetone/chloroform at: (A) 112°, (B) 131°, (C) 134°, (D) 140°, (E) 147°, (F) 167°. Magnification power of x10 was used.

It was observed that crystals started to melt around 130°C. It was observed that crystals in both films were behaving similarly. Hence, the scan of those films conforms to the results obtained from the DSC scan indicating the existence of naproxen crystals in both films. On the other hand, the characteristic melting of malonic acid crystals could not be detected. Hence, it is expected that malonic acid is once again molecularly dispersed in the polymer and acts to reduce the saturation concentration for naproxen in the polymer.

This result confirms the expected behaviour according to SP theory of malonic acid and naproxen in the polymeric film.

In order to test the applicability of using the solubility parameters to predict the behaviour of two acidic drugs in a polymer, other drug combinations were tested in the next section.

### **6.3.3 Flurbiprofen as a blocker of the acidic drug-polymer interaction**

Flurbiprofen is characterized by having a SP value very close to that of HPMCAS (table 5.1). Hence, according to the previous conclusion and in line with SP theory flurbiprofen should preferably interact with HPMAS reducing the saturation point for the other acidic materials and resulting in their preferential crystallisation. Films containing flurbiprofen and one of the other acids (malonic acid, naproxen, and ibuprofen) were prepared using the method described in section 2.3.3.

Despite the different effect that might arise from adding two acidic drugs to the polymeric matrix, films were analyzed to identify the type of the crystals that might grow inside.

#### **6.3.3.1 General analysis**

Films were prepared using the following concentrations: 800 mg (malonic acid, naproxen, or ibuprofen), 800mg flurbiprofen, and 4000 mg HPMCAS using acetonitrile as the preparation solvent. The visual inspection for films containing malonic acid or naproxen became relatively opaque and the change of their flexibility compared to plain HPMCAS films. However, films containing ibuprofen stayed relatively transparent even when 1200 mg of ibuprofen used instead of 800 mg.

#### **6.3.3.2 Powder X-ray diffraction**

A sample of each film was analyzed using the x-ray diffractometer in order to identify the crystalline material that caused the film opacity. The diffraction data

were obtained using the method described in section 2.2.2. The diffraction patterns obtained from films containing malonic acid and flurbiprofen (figure 6.22) reveals the existence of diffraction peaks at 17, 19, 23.4, 23.9, 25°. These peaks can be observed in the diffraction pattern of unprocessed malonic acid. However, there is a low intensity peak at 21° that matches one found in the diffraction pattern of flurbiprofen. Thus it can be concluded that the majority of flurbiprofen has been molecularly dispersed in the polymer and acts to promote malonic acid crystallization in line with the SP theory being developed in this thesis.

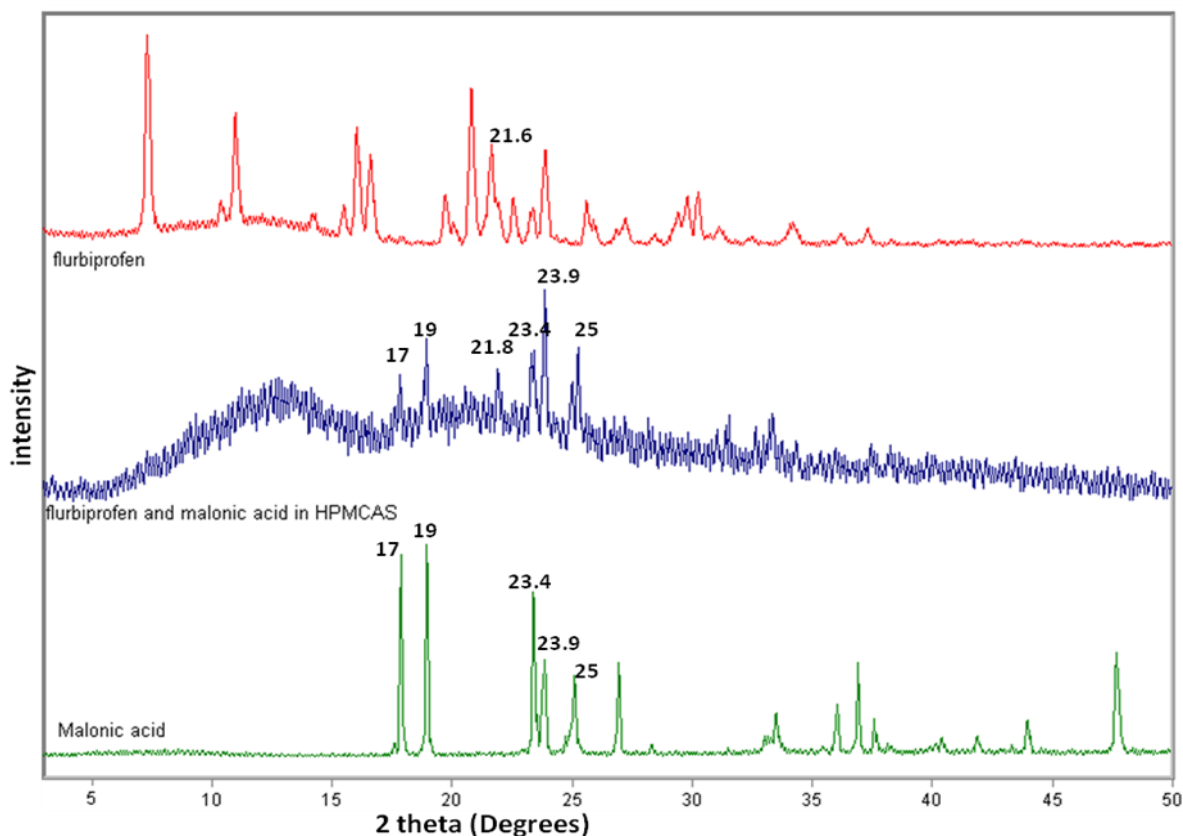


Figure 6.22. Representative powder x-ray diffraction patterns for unprocessed malonic acid (green), unprocessed flurbiprofen (red), and a film containing flurbiprofen and malonic acid (blue).

The diffraction pattern obtained from films containing flurbiprofen and naproxen reveals some peaks at (6°, 12°, 13°, 17°, 19°, 22°, and 24° (2 theta)). These peaks can be easily distinguished in the diffraction pattern of unprocessed

naproxen (figure 6.23). It was difficult to confirm the existence of flurbiprofen crystals in the diffraction pattern, in addition to a high noise/signal ratio. Hence, there may or may not be some flurbiprofen crystals in the films. However, it can be concluded that most of the crystalline phase in the polymeric film can be correlated to naproxen crystals.

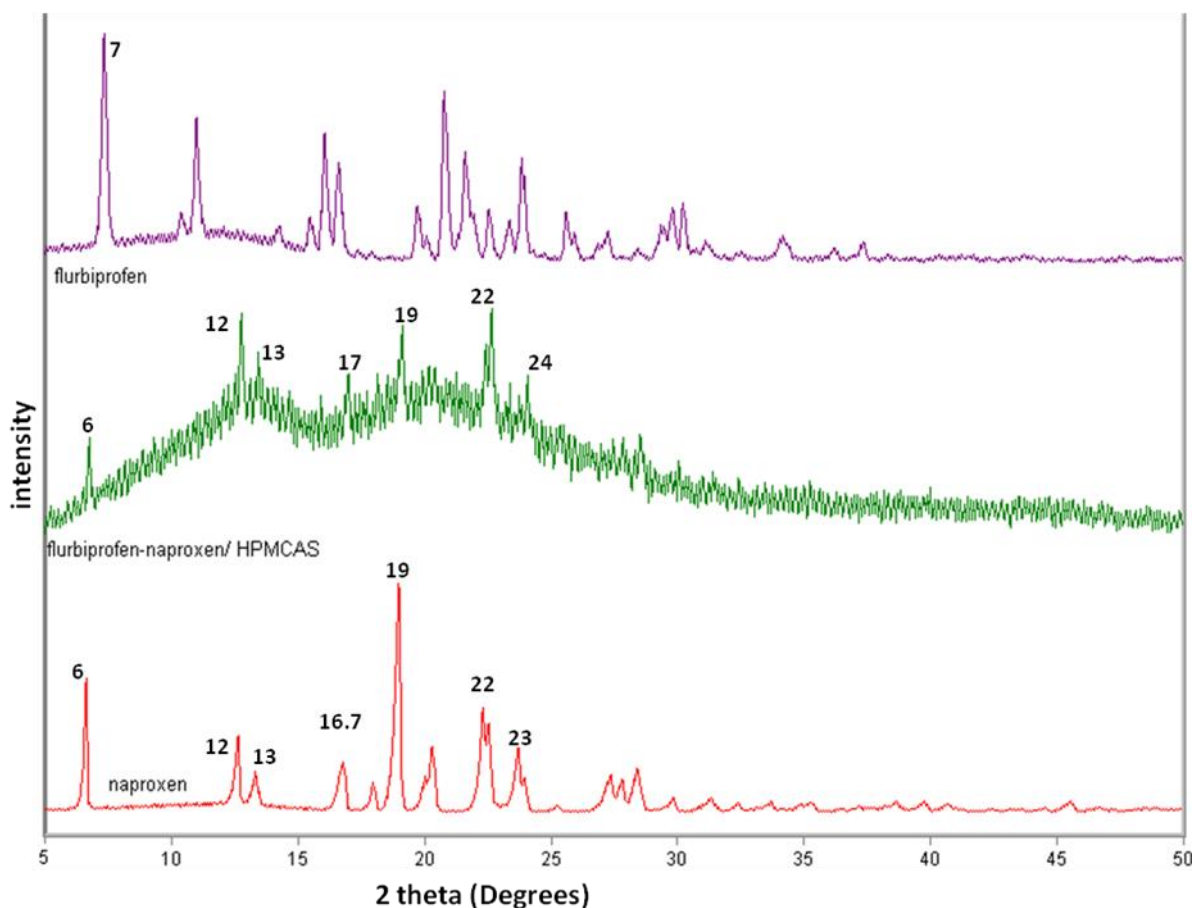


Figure 6.23. Representative powder x-ray diffraction pattern for unprocessed naproxen (red), unprocessed flurbiprofen (purple), and a film containing flurbiprofen and naproxen (green).

Both results obtained from the diffraction patterns of films containing flurbiprofen and either naproxen or malonic acid conform to the previous expectations observed from the solubility parameters of the three materials.

The diffraction pattern of a film containing 20:20:100 w/w/w flurbiprofen/ibuprofen/HPMCAS revealed a low signal/noise ratio. This indicates that the diffractometer couldn't detect the presence of neither flurbiprofen nor

ibuprofen crystals. Hence, the flurbiprofen and ibuprofen might be in the amorphous state or their crystals are too small to be detected by the x-ray.

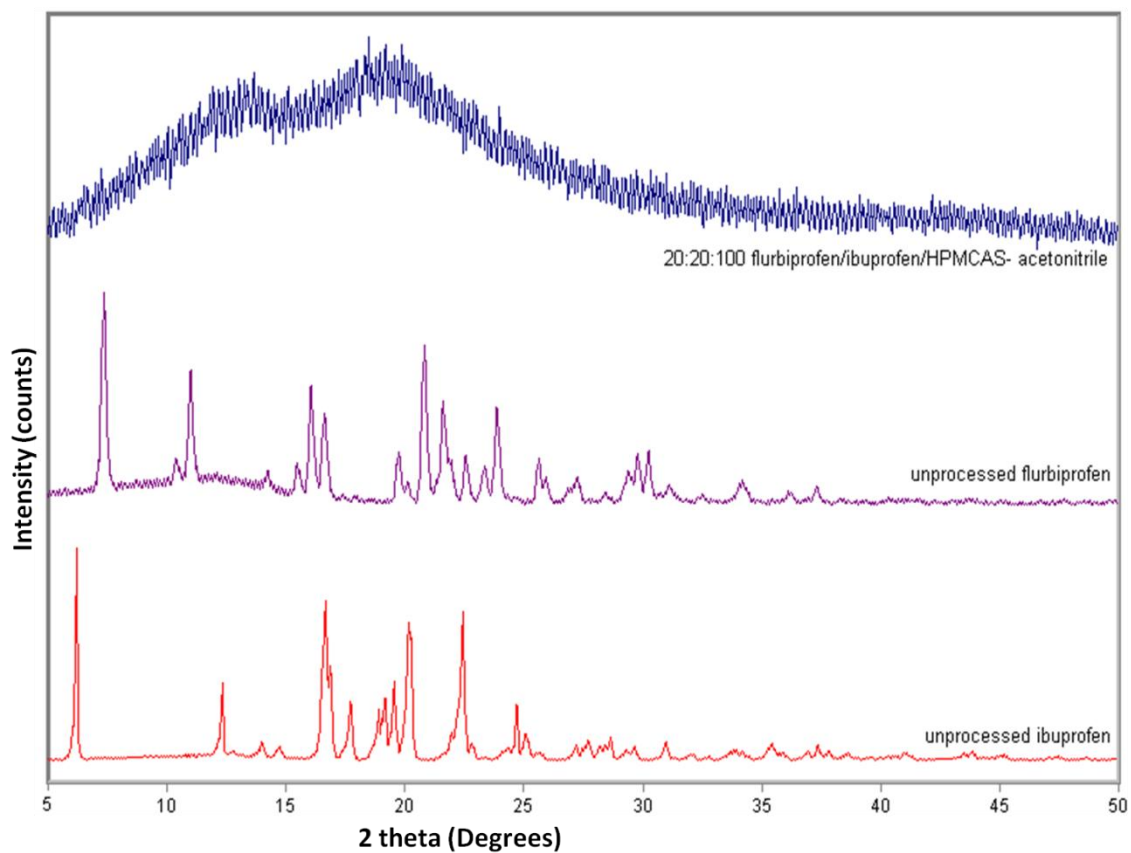


Figure 6.24. Representative powder x-ray diffraction patterns for unprocessed ibuprofen (red), unprocessed flurbiprofen (purple), and a film containing 20:20:100 w/w/w flurbiprofen/ibuprofen/HPMCAS prepared using acetonitrile (blue).



## 6.4 Summary and Conclusion

The acidic materials malonic acid and ibuprofen were found to interact with HPMCAS as shown by a reduction in its T<sub>g</sub> value. Difficulties in signal to noise ratios meant that the exact nature of the malonic acid interaction with the polymer was not identified. It might be a hydrogen bond interaction or Van der Waals interaction. Such interactions for acidic drugs have been observed in the literature (Patrick et al., 1998 , Bharate et al., 2010 , Dong and Choi, 2008 , Konno and Taylor, 2006). Interestingly, the study showed that the nature of the solvent system used to produce the films affected the degree of interaction between malonic acid and HPMCAS. Ethanol/water was found to interfere with this interaction as observed with the high T<sub>g</sub> values of films prepared using ethanol/water in comparison to those prepared using other solvents. This might be due to the interaction between the solvent and malonic acid that competed with malonic acid-HPMCAS interaction. On the other hand, acetonitrile and chloroform has less effect on malonic acid-HPMCAS interaction. The findings were consistent in accordance with the polarity of the solvent used. High polarity solvents (e.g ethanol/water) form a bond with either the acidic component or the polymer and interfere with their interaction. On the other hand, weakly polar solvents did not compete or interfere with acidic drug-HPMCAS interaction.

Increasing the concentration of the acidic species resulted in their saturation of the polymer accompanied by the growth of large crystals as indicated by HSM. The addition of both malonic acid and ibuprofen to the polymer resulted in the growth of large ibuprofen crystals at lower ibuprofen concentrations than were observed without the presence of malonic acid. Similar behaviour was noticed

with films containing malonic acid and naproxen where naproxen crystals were observed in the film. A theory to explain this behaviour was put forward and involved the competition between malonic acid and ibuprofen for interaction with the polymer. The behaviour of two acidic materials in the polymer can be correlated to their SP values. Malonic acid has the closest SP value to that of the polymer. Hence, it can be concluded from the previous experiments that the closer the SP value for the drug to a polymeric vehicle, the more potential for that material to preferably interact with the polymer and thus lower the apparent solubility of the other acidic component in HPMCAS and thus facilitate its apparent earlier onset of crystallisation.

In addition, flurbiprofen was used to prove the aforementioned theory as it has a unique SP value of  $24.45 \text{ MPa}^{1/2}$ . This value is considered to be the closest value to that of HPMCAS than other acidic drugs. The diffraction patterns of films containing flurbiprofen with either malonic acid or naproxen show the presence of malonic acid or naproxen crystals. However, flurbiprofen crystals couldn't be detected. This result conforms to the expected behaviour based on the aforementioned theory considering that both malonic acid and naproxen have a remote SP values from that of HPMCAS in comparison to the SP value of flurbiprofen. However, the diffraction pattern of a film containing flurbiprofen and ibuprofen revealed a low signal/noise ratio with no appearance for any diffraction peaks. This indicates that both flurbiprofen and ibuprofen are in the amorphous state or their crystals were too small to be detected by x-ray diffractometer. The result obtained with the last film doesn't conform to the previous theory. The presence of flurbiprofen might have increased the

solubility of ibuprofen in the polymer. Therefore, further investigations are needed.

## **Chapter 7**

### **Films containing basic drugs and their physicochemical properties**

## **7.1 Introduction**

Acidic drugs interaction with HPMCAS has been studied in chapter 6. This chapter focuses on the interaction between caffeine and nicotinamide with HPMCAS. It also studies the possible effect of the preparation media on that interaction. HPMCAS is reported to interact with some basic drugs such as indomethacin and omeprazole (Bharate et al., 2010 , Stroyer et al., 2006). Therefore it is essential to study the relationship between the basic drugs used in this project with the polymer.

Films containing alkaline drugs were prepared using the method described in section 2.3.3. Various solvent systems were used in order to identify the possible effects of the preparation media on the aforementioned interaction.

## **7.2 Films containing caffeine**

Films containing caffeine were prepared using the method described in section 2.3.3. Three solvent systems were used as film preparation media: acetonitrile, acetone/chloroform, and ethanol/water.

### **7.2.1 General analysis**

Films containing low concentrations of caffeine (up to 3:50 caffeine/HPMCAS w/w) were noted to be transparent and brittle. However, when caffeine concentration increased, the film became more flexible, less brittle and more opaque. It was noted that caffeine crystals started to grow on the external edges of the film initially. Then the growth continued inward with increasing caffeine concentration. Unlike malonic acid, a film containing 2:25 caffeine/HPMCAS w/w was fully opaque whereas a concentration of 3:5 w/w malonic acid/HPMCAS was required to achieve the same outcome.

### **7.2.2 Thermal analysis**

#### **7.2.2.1 TGA**

The TGA thermal profiles for films containing caffeine were obtained using the method described in section 2.2.1.1. It can be observed in figure 7.1 that films containing caffeine lost around 3% of the total weight between 30-100°C. This weight loss was found in the thermal profile of unprocessed HPMCAS and it was considered to be due to the residual moisture in the film. The weight loss accelerated above 110°C as a result of caffeine and HPMCAS degradation. It has to be noted that the degradation of the film containing caffeine starts at

lower temperature than caffeine or HPMCAS alone. This might indicate that the polymer is accelerating the degradation of caffeine.

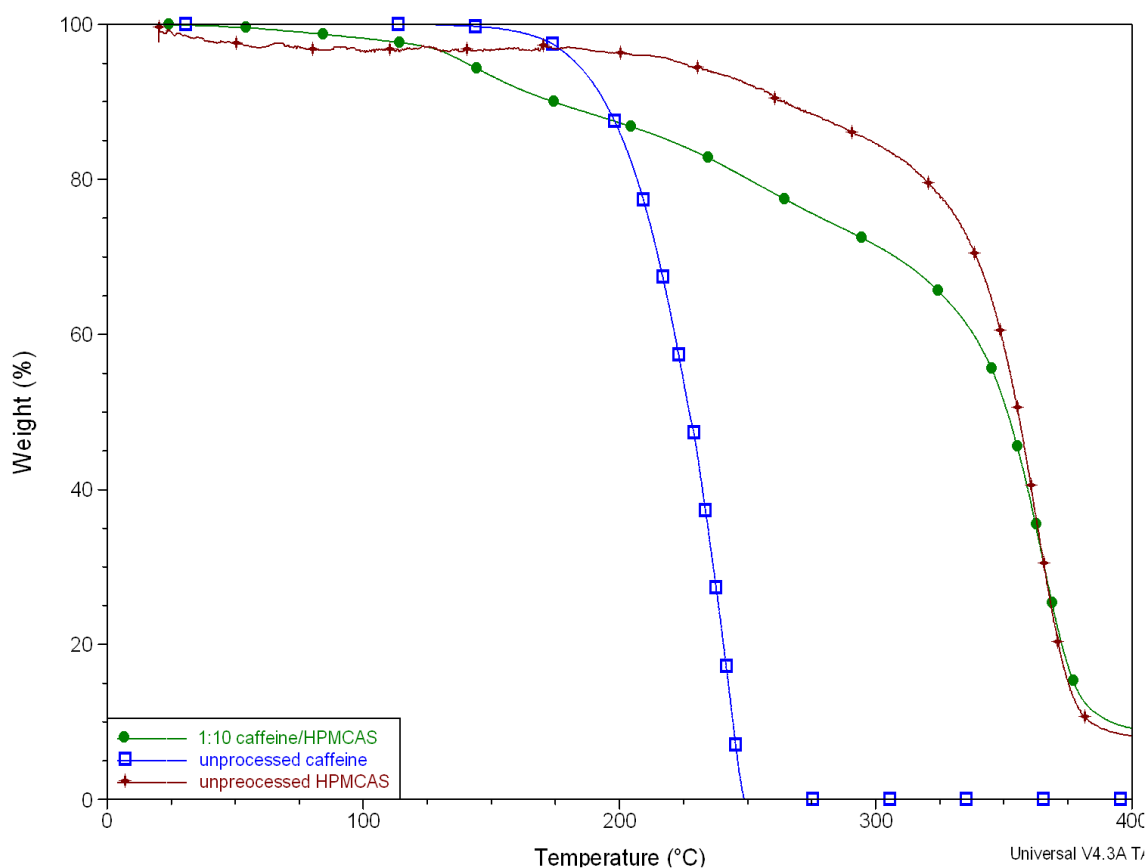


Figure 7.1. Representative TGA thermal profiles for unprocessed caffeine (blue), unprocessed HPMCAS (red), and a film containing 1:10 caffeine/HPMCAS.

### 7.2.2.2 DSC

The DSC thermal profiles for films containing various amounts of caffeine were obtained using the three solvent systems according to the method described in section 2.2.1.2. Thermal data were used to obtain the T<sub>g</sub> values for these films. The T<sub>g</sub> values were plotted against the concentration of caffeine in the film using the aforementioned solvents. Figure 7.2 reveals that films prepared with ethanol/water have the highest T<sub>g</sub> values independent of the caffeine concentration in the film. On the other hand, films prepared with acetone/chloroform shows the lowest values for the T<sub>g</sub>. This behaviour can be

explained by the affinity of the solvent to form a bond with the polymer/drug and consequently interfering with the drug-polymer interaction. In addition to that, the value of the Tg was more or less constant when a concentration of 1:10 w/w caffeine/HPMCAS or more was added to the film. This might indicate that the polymer became saturated with caffeine molecules. Hence any additional caffeine molecules will not affect the Tg or the plasticity of the polymer.

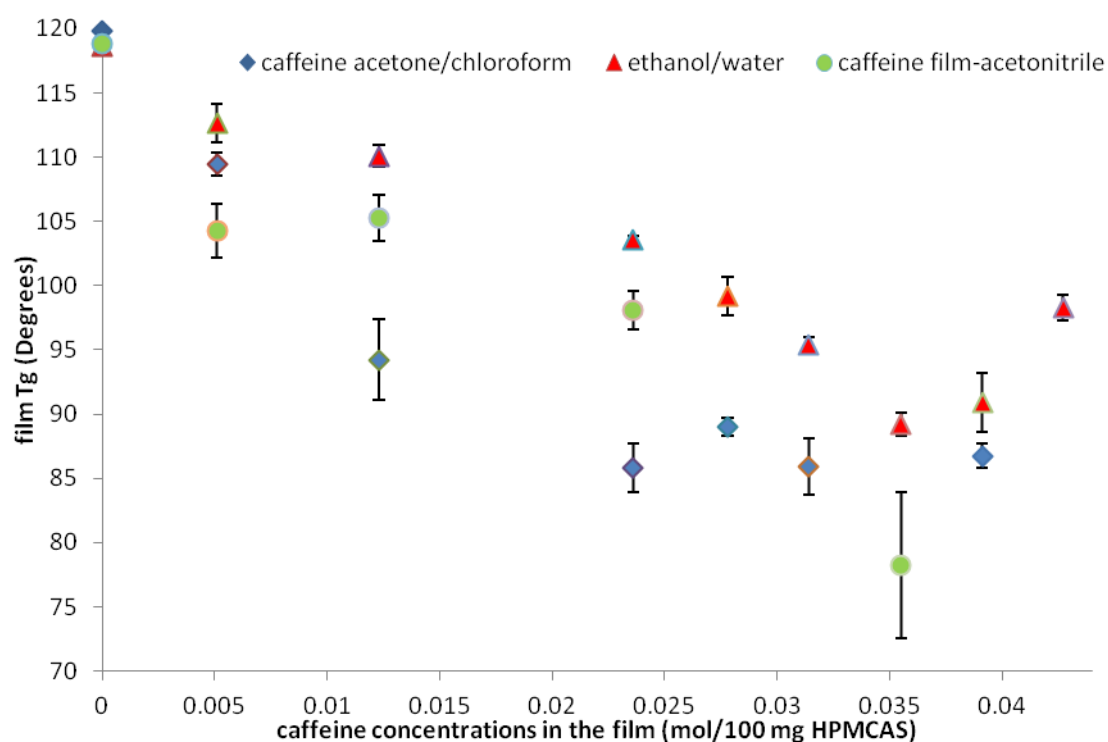


Figure 7.2. Graph to show the relation between the Tg and the percentage weight concentration of caffeine in HPMCAS films cast from different solvent systems

### 7.2.3 Powder X-ray diffraction

The powder x-ray diffraction data were obtained using the method described in section 2.2.2. The diffraction pattern revealed a high noise/signal ratio (figure 7.3). However, it is possible to observe a diffraction peak at 11.9°. This peak can be seen as well in the diffraction pattern of unprocessed caffeine. Hence, it indicates the presence of crystalline caffeine in the film.



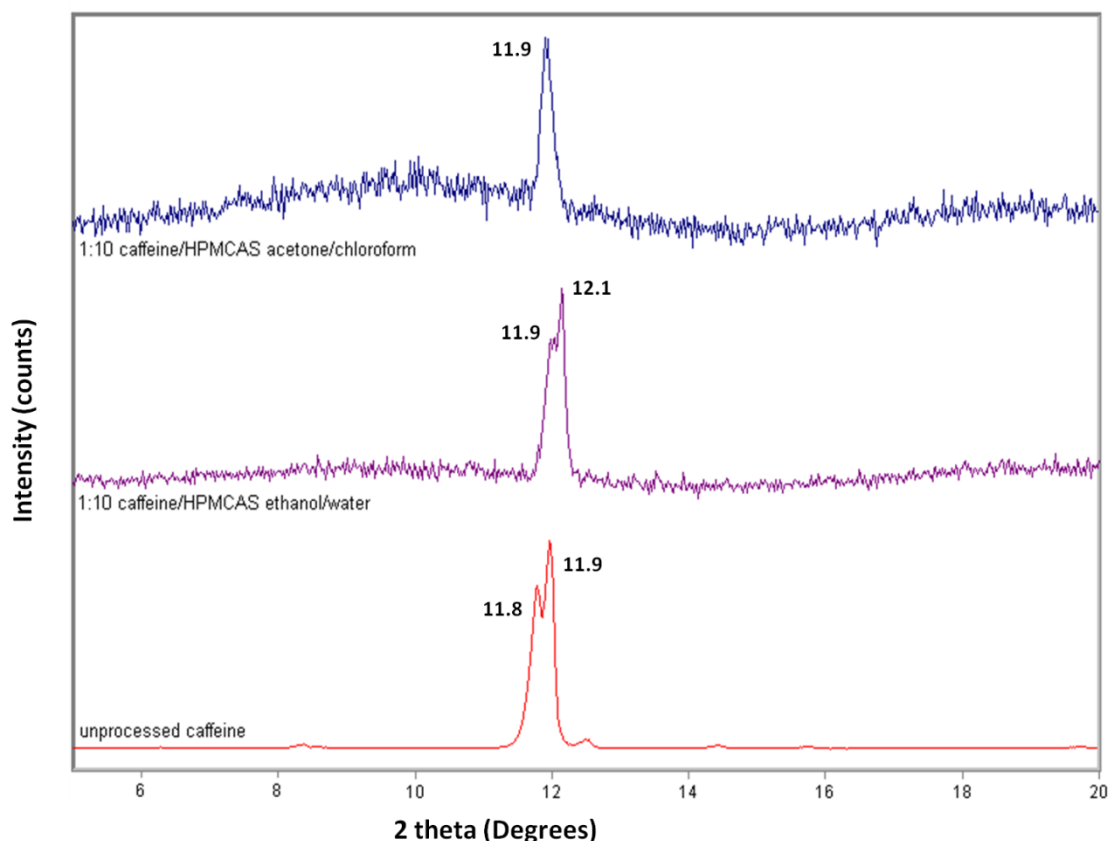


Figure 7.3. Representative powder x-ray diffraction patterns for unprocessed caffeine (red), a film containing 1:10 caffeine/HPMCAS prepared with ethanol/water (purple), and a film containing 1:10 caffeine/HPMCAS prepared with acetone/chloroform (blue).

#### 7.2.4 FT-IR transmission

The FT-IR spectra for films containing 7:100 w/w caffeine/HPMCAS prepared using the aforementioned solvent systems were collected using the method described in section 2.2.3 in order to identify the presence of any potential interaction between caffeine and HPMCAS. The FT-IR spectra for films containing various amounts of caffeine revealed a shift in the  $1692\text{ cm}^{-1}$  peak. This peak was assigned to C=N, NH vibrational energy (section 3.1.1.3). It can be noticed that this peak has shifted to around  $1704\text{-}1709\text{ cm}^{-1}$ . This indicates that the NH group is participating in the bond between caffeine and HPMCAS through a hydrogen bond.

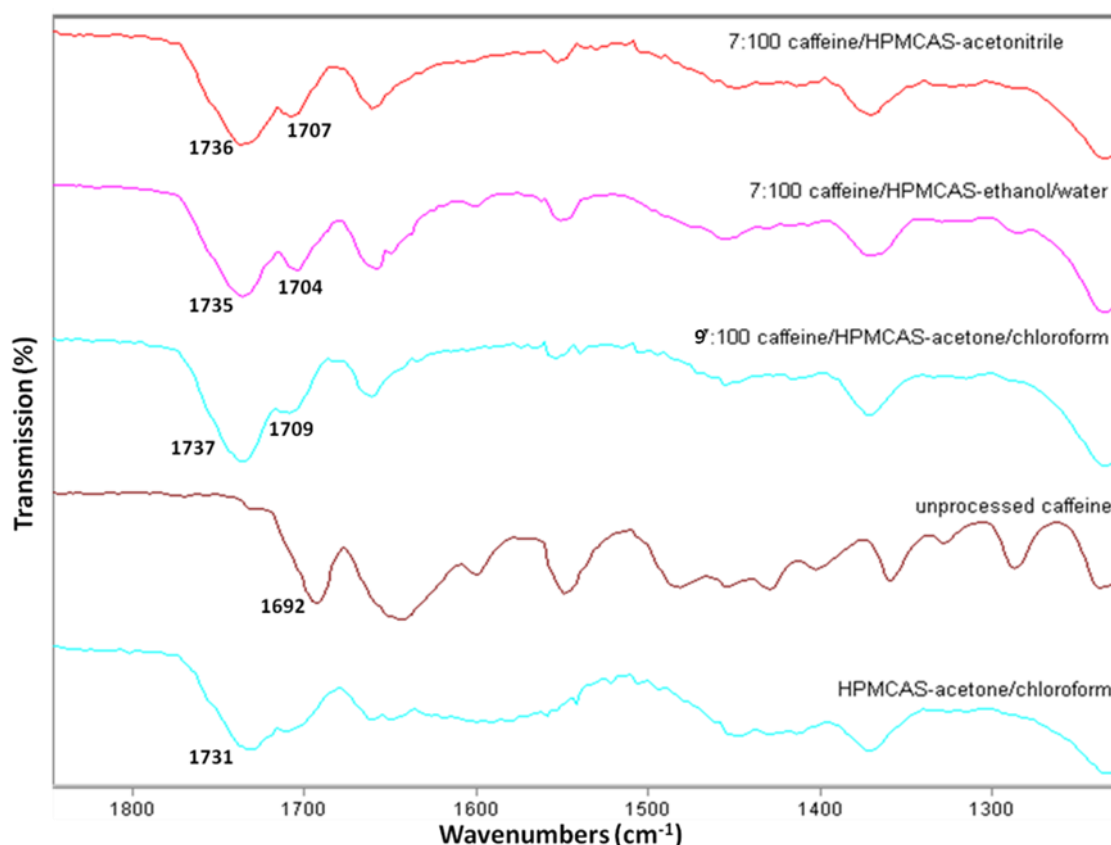


Figure 7.4. representative FT-IR spectra for unprocessed HPMCAS (teal), unprocessed caffeine (red), film containing 9:100 w/w caffeine/HPMCAS prepared using acetone/chloroform (teal), film containing 7:100 w/w caffeine prepared with ethanol/water (pink), and a film containing 1:10 w/w caffeine prepared with acetonitrile (red).

### 7.2.5 SEM

Films containing malonic acid crystals were analyzed using the SEM in order to obtain a good image for the crystal shape. SEM imaging was performed using the method described in section 2.2.4.1. The collected data revealed that crystals had a diameter of around 50 micrometer (figure 7.5). Some small particles appeared to cluster around the crystals. These particles might be some carbon dust resulting from the carbon coating of the sample that was needed due to the high electrostatic charge of the films. On the other hand, those particles might be HPMCAS particles that are adhering to the edges of the caffeine crystals.

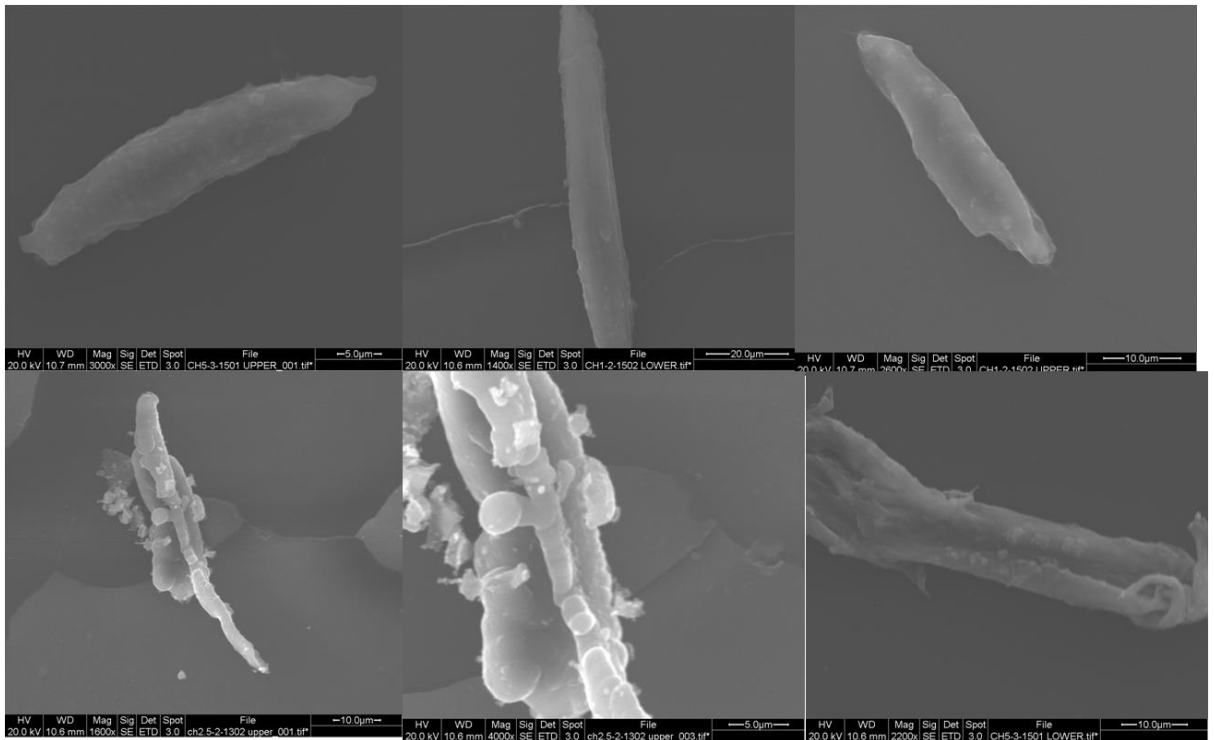


Figure 7.5. SEM scan of films containing 1:100 w/w caffeine/HPMCAS with magnification powers of X3000 (top left), X1400 (top middle), X2600 (top right), X1600 (bottom left), X4000 (bottom middle), and X2200 (bottom right).

## **7.3 Films containing nicotinamide**

Nicotinamide was planned to be used as a co-crystal former with ibuprofen. A possible nicotinamide-HPMCAS interaction was studied by analyzing films containing various amount of nicotinamide. These films were prepared using the method described in section 2.3.3.

### **7.3.1 Thermal analysis**

#### **7.3.1.1 TGA analysis**

The TGA thermal profile for a film containing 1:5 nicotinamide/HPMCAS was collected using the method described in section 2.2.1.1. The data obtained in the profile reveal a weight loss of about 2% between 30-100°C. A similar weight loss was observed in the thermal profile of unprocessed HPMCAS and was correlated to the evaporation of the residual moisture in the film (figure 7.6). It is noted that the weight loss in the film containing nicotinamide starts earlier than the degradation of the unprocessed polymer or the API. This might indicate that the interaction between the two components is accelerating the degradation of the nicotinamide.

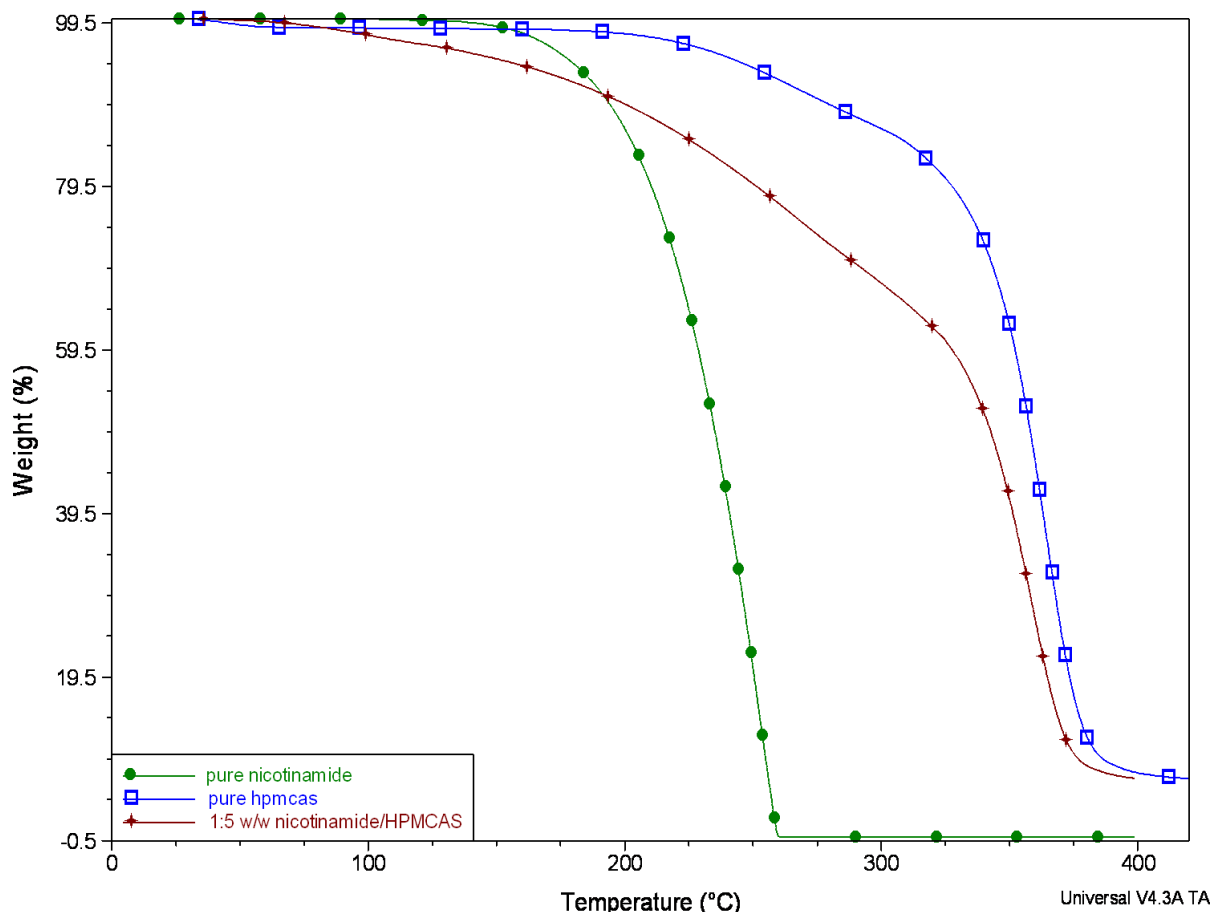


Figure 7.6. Representative TGA thermal profiles for unprocessed nicotineamide (green), unprocessed HPMCAS (blue), and a film containing 1:5 w/w nicotineamide/HPMCAS prepared with acetonitrile (red).

### 7.3.1.2 DSC analysis

The DSC thermal profiles for films containing various amount of nicotineamide were obtained using the method described in section 2.2.1.2. The collected data were used to calculate the T<sub>g</sub> values for these films. Then the T<sub>g</sub> values were plotted against nicotineamide concentration in films (figure 7.7). It can be noticed from figure 7.7 that the T<sub>g</sub> values decrease as the concentration of nicotineamide increase. However when the nicotineamide concentration exceeds 15:100 w/w in the film, the change in the T<sub>g</sub> values becomes minimal. The plateau effect might be related to a saturation point of nicotineamide in the film.

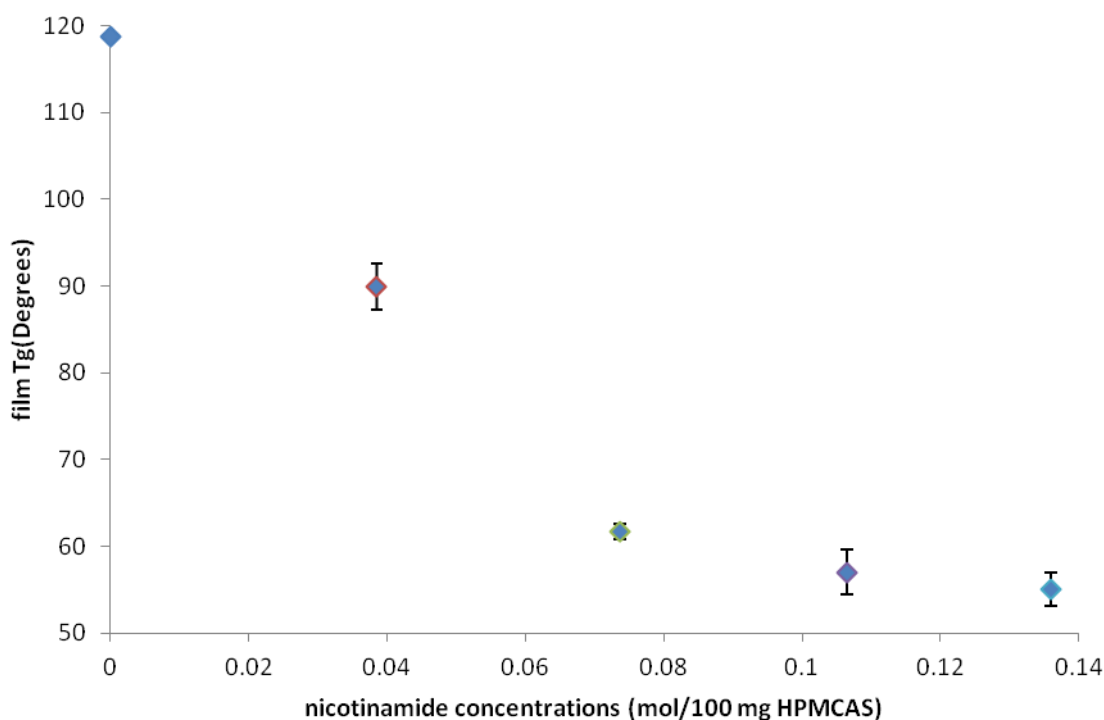


Figure 7.7. A representative plot for the polymeric film Tg values against nicotinamide concentrations in these films.

### 7.3.2 FT-IR transmission

The FT-IR spectra of films containing 15:100 and 20:100 w/w nicotinamide/HPMCAS of nicotinamide were collected following the method described in section 2.2.3. It can be noticed in figure 7.8 the presence of a peak shift from  $3348\text{ cm}^{-1}$  in nicotinamide to around  $3358\text{ cm}^{-1}$  in films containing nicotinamide. This peak was assigned for the C=N, NH vibrational energy in nicotinamide (section 3.1.4.3). Consequently, it can be concluded that nicotinamide NH group is participating in hydrogen bonding with HPMCAS.

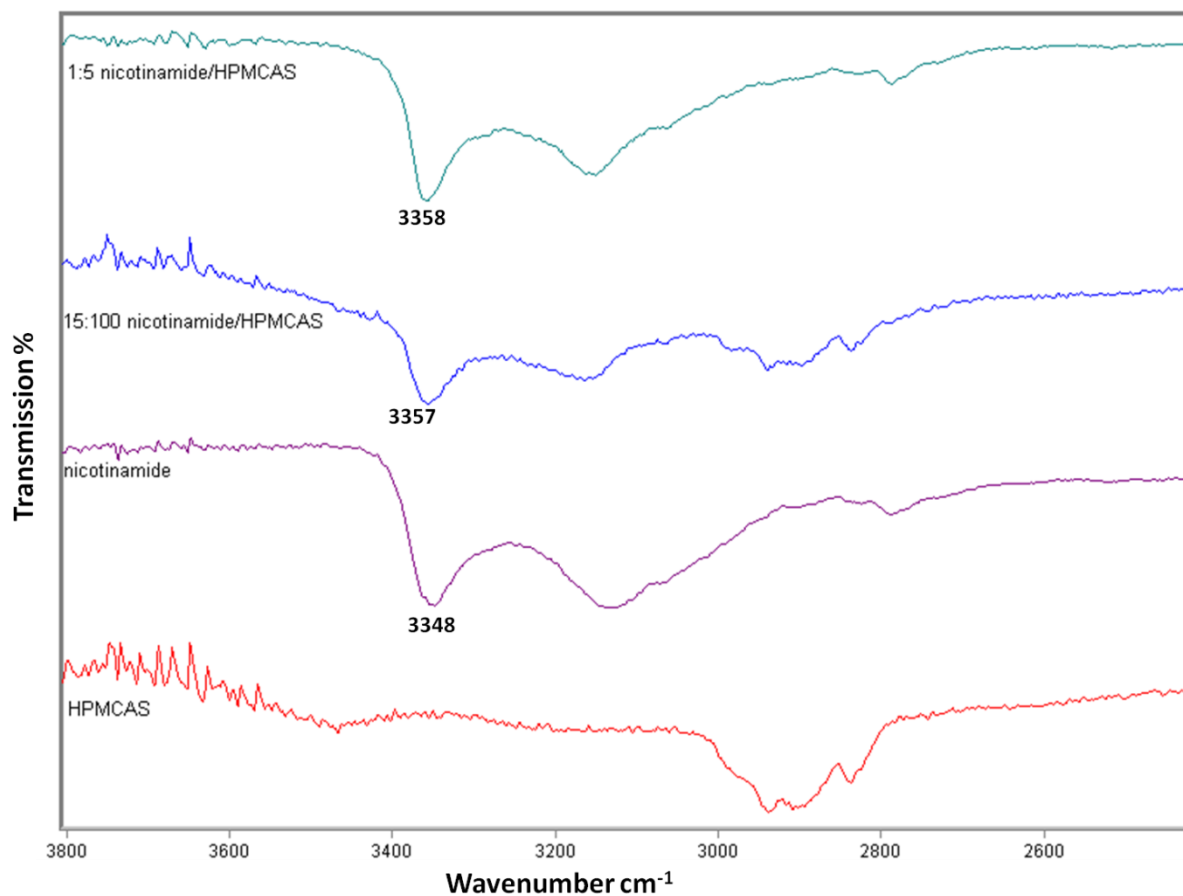


Figure 7.8. Representative FT-IR spectra for unprocessed HPMCAS (red), unprocessed nicotinamide (purple), film containing 15:100 w/w nicotinamide/HPMCAS (blue), and film containing 1:5 w/w nicotinamide/HPMCAS (teal).

## **7.4 Characterisation of films prepared containing one acidic and one basic species/drug**

In chapter 6, it was found that adding two acidic drugs to the film resulted in one being “salted out” by the other. However, in this chapter, it was decided to investigate the effect of including two drugs in the polymer, one is acidic and one is basic. . The acidic compound used here is malonic acid and the basic counterparts are caffeine and nicotinamide. The films were prepared using the method described in section 2.3.3.

Caffeine and malonic acid are known to form a co-crystalline system (section 4.2). This system might be affected by the interaction of either one or both of them with the polymer. Solubility parameter data were employed in order to predict the behaviour of those drugs inside the polymeric film. it can be noticed by looking to table 5.1 and 5.2 that both caffeine and malonic acid have SP values that are closer to that of HPMCAS than each other. Therefore, theoretically, malonic acid and caffeine will preferably interact with the polymer rather than interacting with each other. Similar behaviour is expected between nicotinamide and malonic acid.

### **7.4.1 Films containing caffeine and malonic acid**

In order to monitor the interaction affinity of caffeine and malonic acid, both materials were added to the film using the same stoichiometric ratio required for their co-crystal formation.



### **7.4.1.1 Thermal analysis**

#### **TGA & DSC**

Thermal profiles for films containing various concentrations of caffeine and malonic acid were obtained using the methods described in sections 2.2.1.1 and 2.2.1.2. The TGA thermal profile reveals a weight loss of 2% between 30-100°C. A similar weight loss was found in the thermal profile of unprocessed HPMCAS and was correlated to the evaporation of the residual moisture. On the other hand, DSC thermal profiles were used to calculate the T<sub>g</sub> values for these films (table 7.1). The T<sub>g</sub> values of films prepared with acetone/chloroform appeared to be higher than those prepared using ethanol/water independent of the caffeine and malonic acid concentrations. On the other hand, the T<sub>g</sub> of the films containing mixture of caffeine and malonic acid revealed T<sub>g</sub> values in between the T<sub>g</sub> values of the films containing caffeine alone or malonic acid alone previously discussed in sections 7.2.2 and 6.2.1.2.

The T<sub>g</sub> values of the previous films are less than it would be expected to be for films containing mixtures of caffeine and malonic acid behaviour of the T<sub>g</sub> can be explained by the presence of an interaction between some molecules of caffeine and malonic acid. Hence, the effect on the T<sub>g</sub> is not linear or additive.

Films prepared by acetone/chloroform		Average Tg value (°C)	Standard deviation
Malonic acid concentration (w%)	Caffeine concentration (W%)		
0	0	119.79	0.3748
1.4	4.8	82.097	2.1093
2.6	9.2	74.815	1.5452
5.3	16.8	64.438	2.2596
Films prepared by ethanol/water		Average Tg value	Standard deviation
Malonic acid concentration	Caffeine concentration		
0	0	118.63	0.5769
0.2	0.8	114.92	2.0141
1.3	5	92.997	2.0740
2.6	9.2	88.477	1.2050
5.2	16.8	73.863	0.8680

Table 7.1. Tg values for HPMCAS films containing various concentrations of caffeine and malonic acid prepared by acetone/chloroform and ethanol/water.

#### 7.4.1.2 Powder X-ray diffraction

Powder x-ray diffraction patterns for films containing both caffeine and malonic acid were obtained using the method described in section 2.2.2. The diffraction patterns (figure 7.9) revealed a high noise/signal ratio, probably due to the high amorphous content of the film. However, a peak was observed at 11°. This peak was found to exist in unprocessed caffeine diffraction pattern. On the other hand, a co-crystal formation peak at 8° was not observed. This indicates that caffeine and malonic acid might have not formed a co-crystalline system in the polymer or that their co-crystal concentration was below the detection limit.

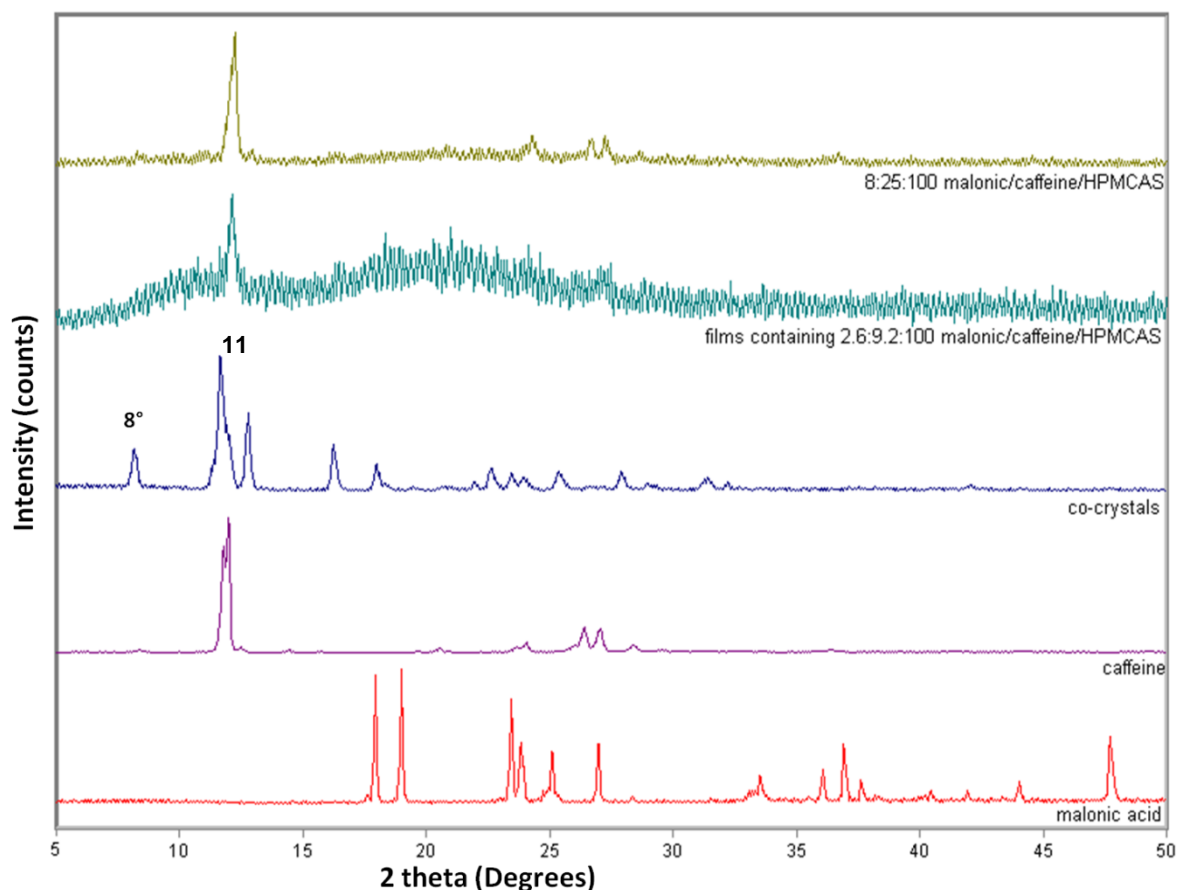


Figure 7.10. A representative powder x-ray diffraction patterns for unprocessed malonic acid (red), unprocessed caffeine (purple), co-crystals of both (blue), a film containing 2:9:100 malonic acid/caffeine/HPMCAS (teal), and a film containing 8:25:100 malonic acid/caffeine/HPMCAS (yellow). The last three were prepared using ethanol/water.

#### 7.4.1.3 FT-IR transmission

The FT-IR transmission spectrum for a film containing 10:3:100 w/w/w caffeine/malonic acid/HPMCAS was obtained following the method described in section 2.2.3. The collected spectrum reveals a shift in  $1692\text{ cm}^{-1}$  peak in caffeine to  $1705\text{ cm}^{-1}$  in the film containing the mixture (figure 7.10). This shift is similar to that observed in films containing caffeine alone. This indicates that at least some of the caffeine in these films is not forming a bond with malonic acid.

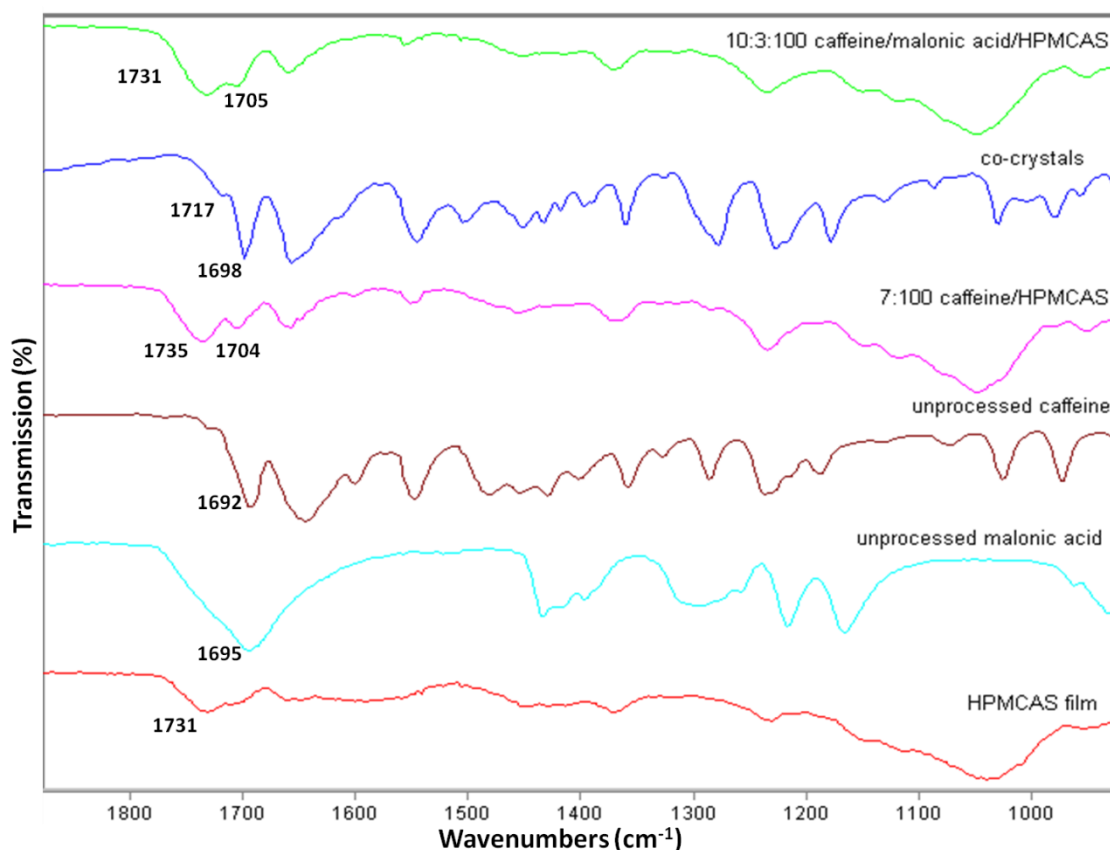


Figure 7.10. Representative FT-IR spectra for plain HPMCAS film (red), unprocessed caffeine (teal), unprocessed malonic acid (dark red), co-crystals prepared using acetone/chloroform (blue), film containing 7:100 w/w caffeine/HPMCAS (pink), and film containing 10:3:100 caffeine/malonic acid/HPMCAS (green).

It can be concluded that caffeine and malonic acid have interacted with the polymer and plasticized it. However, there is a possibility that some particles might have formed co-crystals as the observed  $T_g$  values of the film were lowered than expected for films containing caffeine malonic acid mixture.

Nevertheless, the thermal profile of the co-crystals appeared in section 4.2.2.1.2 to be hard to measure. Hence, it cannot be used as an identification tool.

#### 7.4.1.4 Hot stage microscopy

A film containing 1.4:4.8:100 w/w/w malonic acid/caffeine/HPMCAS was examined by HSM following the method described in section 2.2.4.2. The

crystals inside the polymer revealed a thin and long shape. It can be noticed that the crystals spread through all the layers of the film (figure 7.12).

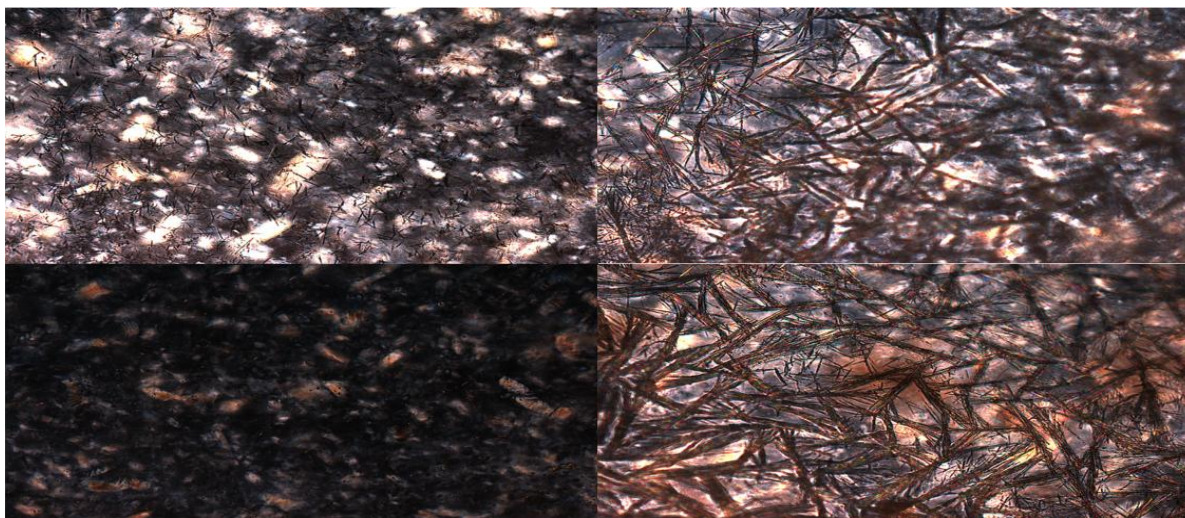


Figure 7.12. A representative HSM imaging for a film containing 1.4:4.8:100 w/w/w malonic acid/caffeine/HPMCAS with different magnification power: X10 (top and bottom left), X20 (top right), and X50 (bottom right).

In summary: loading malonic acid and caffeine in the film resulted in their interaction with the polymer. This result conforms to the expected behaviour of both drugs obtained from their SP values. However, there was a possibility of growing the co-crystals after they reach their saturation concentration.

Therefore, films containing 8:15:100, 8:20:100, and 8:25:100 w/w/w caffeine/malonic acid/HPMCAS were prepared. Acetonitrile was used as a solvent system. Films were analyzed using the X-ray diffractometer following the method described in section 2.2.2 (figure 7.13). The diffraction patterns revealed the presence of diffraction peaks at  $16^\circ$  for all the films. The film containing 8:25:100 w/w/w caffeine/malonic acid/HPMCAS revealed the presence of two other significant peaks at  $22.8^\circ$  and  $25.6^\circ$ . These peaks collectively are considered as the characteristic peaks for caffeine-malonic acid co-crystals. On the other hand, films prepared with acetonitrile showed the

conversion of anhydrous caffeine into caffeine monohydrate. However, the x-ray diffraction pattern did not detect caffeine monohydrate in the film.

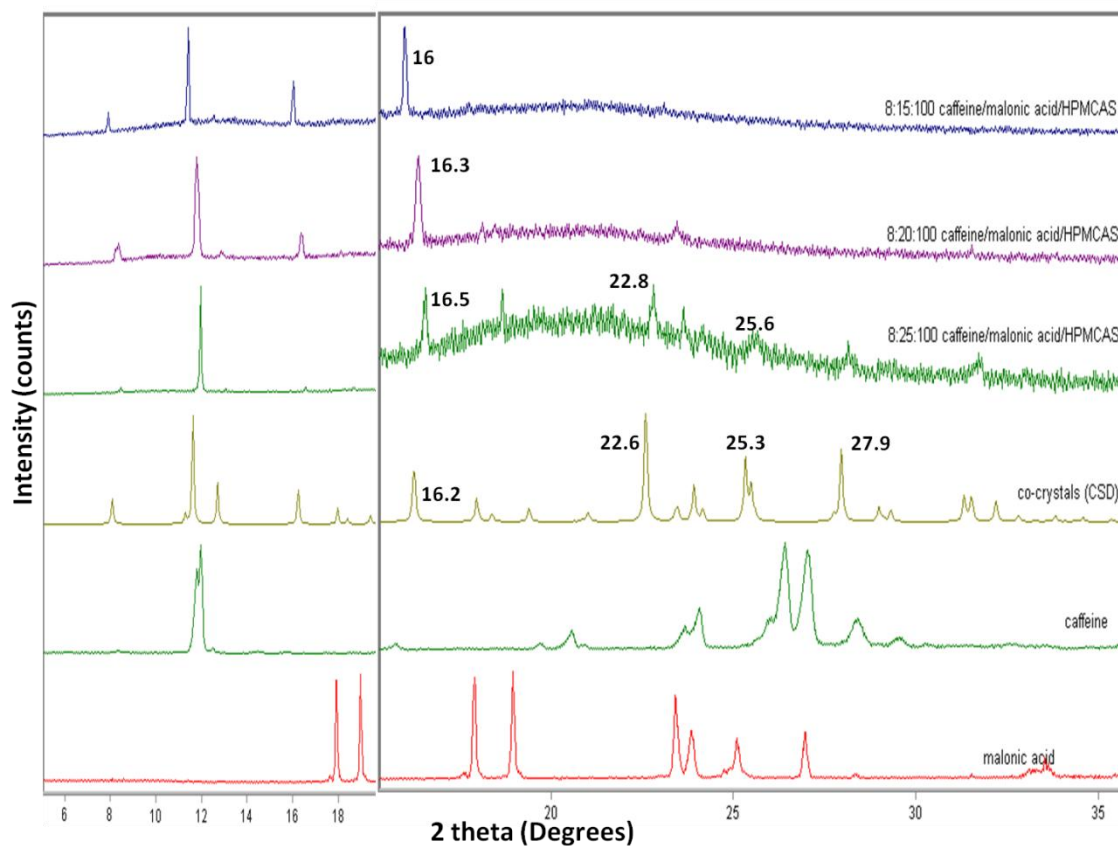


Figure 7.13. Representative powder x-ray diffraction patterns for unprocessed malonic acid (red), unprocessed caffeine (green), co-crystal (CSD) (yellow), 8:25:100 (green), 8:20:100 (purple), and 8:15:100 w/w/w caffeine/malonic acid/HPMCAS (blue).

## 7.4.2 Films containing nicotinamide and malonic acid

Films containing malonic acid and nicotinamide were prepared using the method described in section 2.3.3. Films were analyzed in order to identify the molecular interactions that occurred within the film.

### 7.4.2.1 Thermal analysis

#### 7.4.2.1.1 TGA

The thermal profiles for films containing nicotinamide and malonic acid were obtained using the method described in section 2.2.1.1. The data collected reveals a 2% weight loss between 30-100°C. A similar weight loss was also observed in the thermal profile of unprocessed HPMCAS and was correlated to the evaporation of residual moisture (figure 7.13).

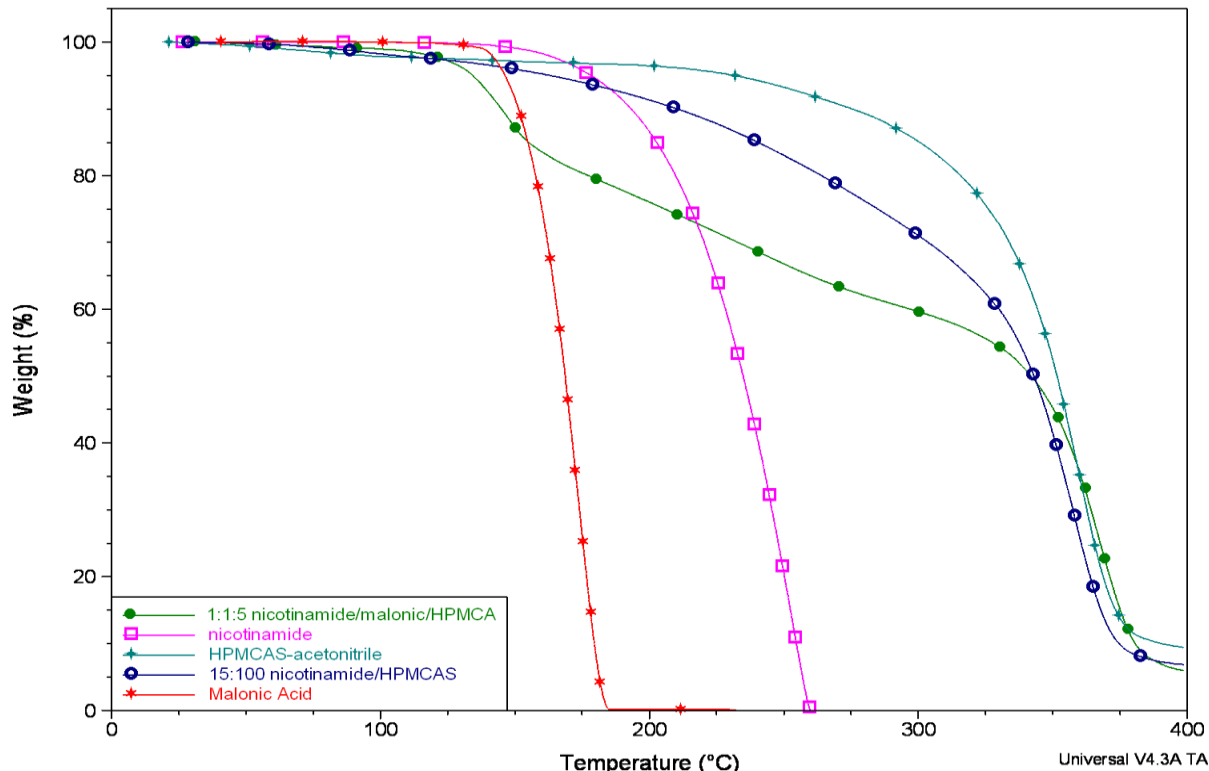


Figure 7.13. Representative TGA thermal profiles for unprocessed malonic acid (red), unprocessed nicotinamide (pink), HPMCAS film (teal), a film containing 15:100 w/w nicotinamide/HPMCAS (blue), and a film containing 1:1:5 nicotinamide/malonic acid/HPMCAS (green).

### 7.4.2.1.2 DSC analysis

Thermal profiles for films containing nicotinamide and malonic acid were collected using the DSC following the method described in section 2.2.1.2. The collected data reveals the existence of a strong intensity peak at 109°C (figure 7.14). This peak might be related to the melting of either malonic acid or nicotinamide crystals inside the polymer. On the other hand, a new system might have formed inside the film and this endothermic peak is the melting peak for that system. Another small peak can be noticed at 92°C. This peak might be an indication for the presence of some impurities.

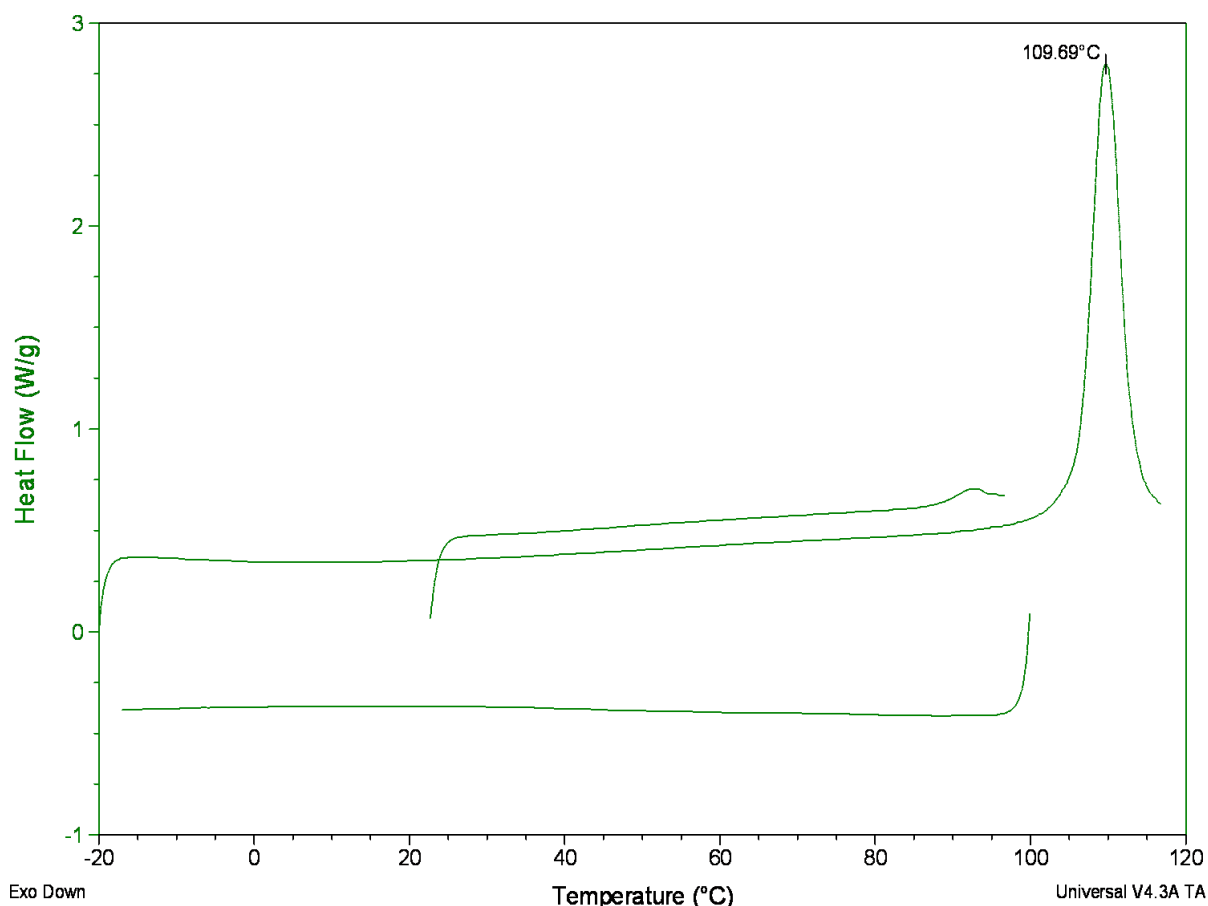


Figure 7.14. A representative thermal DSC profile for a film containing 1:1:5 w/w/w nicotinamide/malonic acid/HPMCAS and prepared with acetone/chloroform.



### 7.4.2.2 Powder X-ray diffraction

The powder diffraction patterns for films containing malonic acid and nicotinamide were obtained using the method described in section 2.2.2. The diffraction pattern reveals the existence of new peaks at 21° and 28° (figure 7.15). These two peaks have no matching in the diffraction pattern of unprocessed nicotinamide or malonic acid diffraction pattern. However, these peaks were observed in the diffraction pattern of malonic acid-nicotinamide co-crystals (section 4.4.2). Consequently, it can be concluded that part of the two drugs may have formed a co-crystalline system inside the polymeric film.

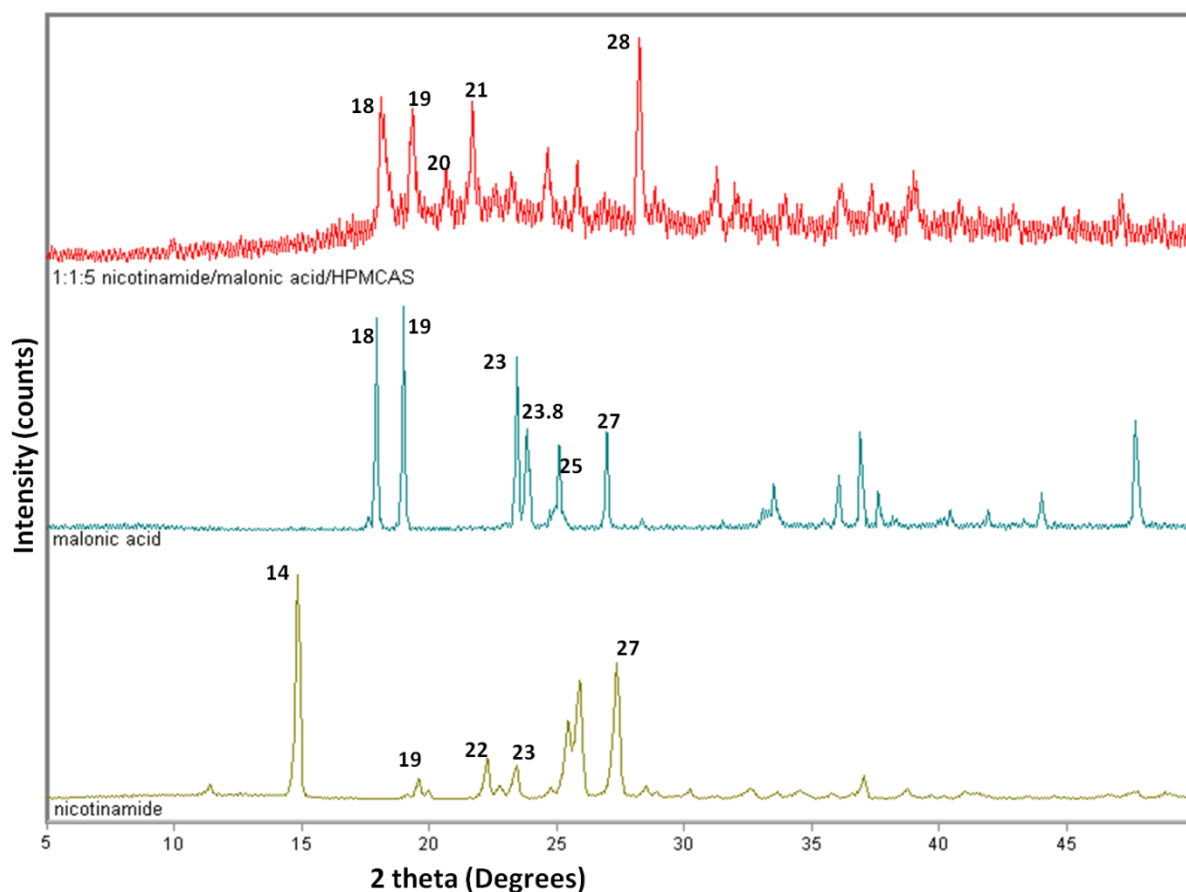


Figure 7.15. Representative powder x-ray diffraction patterns for unprocessed nicotinamide (yellow), unprocessed malonic acid (blue), and a film containing 1:1:5 w/w/w nicotinamide/malonic acid/HPMCAS (red).

### 7.4.2.3 FT-IR transmission

The FT-IR spectra for films containing malonic acid and nicotinamide were obtained using the method described in section 2.2.3. The resulting spectrum reveals a shift in the  $3354\text{ cm}^{-1}$  peak to  $3372\text{ cm}^{-1}$  (figure 7.16). This peak was previously assigned to the C=N, NH vibration in nicotinamide (section 4.4.3). The shift indicates the participation of this group in a bond between nicotinamide and either HPMCAS or malonic acid. However, the x-ray diffraction pattern showed the existence of new peaks that were observed with the diffraction pattern of nicotinamide-malonic acid co-crystals. In addition the similarity of this shift with the FT-IR shift in the co-crystals spectrum. Hence, the shift might be another indication for the formation of nicotinamide-malonic acid co-crystals in the film.

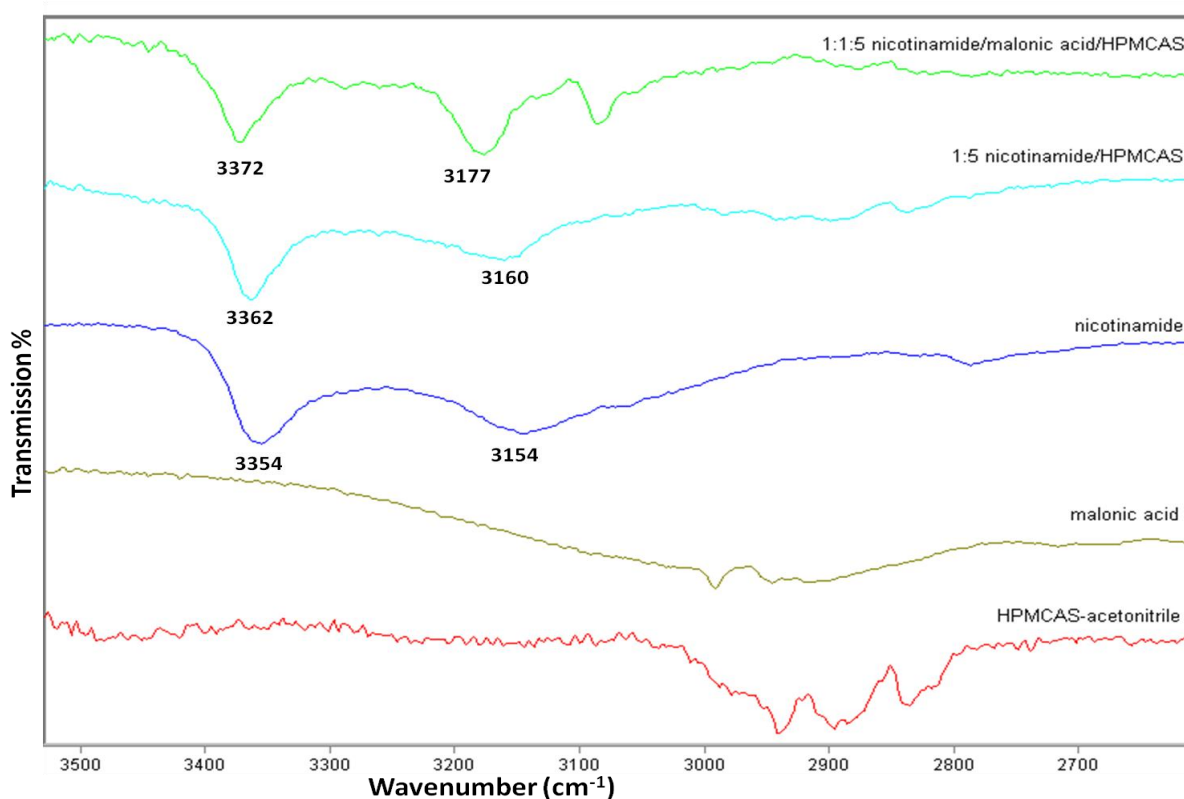


Figure 7.16. Representative FT-IR spectra for a plain HPMCAS film (red), unprocessed malonic acid (yellow), unprocessed nicotinamide (blue), a film containing 1:5 nicotinamide/HPMCAS (teal), and a film containing 1:1:5 w/w/w nicotinamide/malonic acid/HPMCAS (green).

## 7.5 Summary and conclusion

Basic drugs interacted with HPMCAS affecting its plasticity. However, unlike the case for acidic additives, a relatively small amount of caffeine or nicotinamide amount was enough to saturate the polymer. In addition a slightly lower effect on the Tg reduction was observed in comparison to acidic drugs. This can be demonstrated by comparing the effect of each of malonic acid, caffeine, and nicotinamide on the Tg of the polymer (figure 7.17). It can be seen that caffeine has affected the Tg to almost a similar manner like nicotinamide. However, a smaller amount of caffeine was enough to produce the saturation concentration.

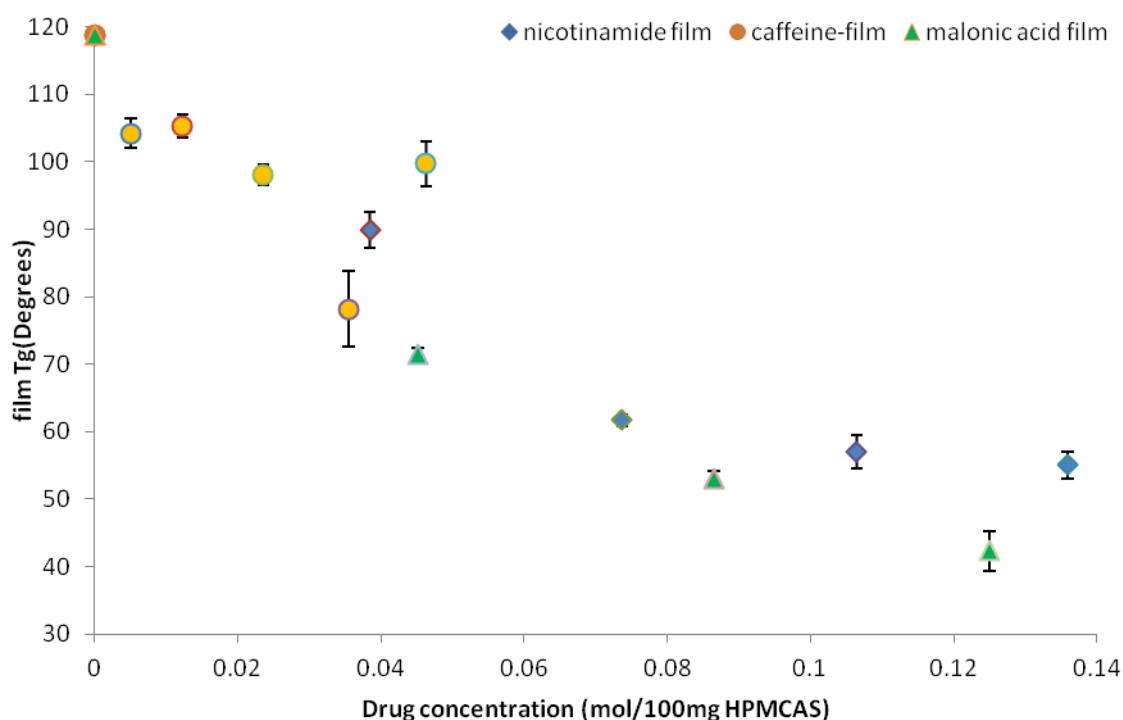


Figure 7.17. A comparison between the Tg values of films containing: caffeine, nicotinamide, or malonic acid against the concentrations of these drugs in the film.

FT-IR spectra for films containing caffeine or nicotinamide revealed a shift in the peak assigned for the C=N, NH vibration in both of the compounds. This indicates that each of them is formed a hydrogen bond with the polymeric matrix.

When films containing caffeine were prepared using various solvent systems, it was noticed that the high polarity solvent system (ethanol/water) interfered with the drug-polymer interaction. On the other hand, the low polarity solvent (acetonitrile) had less effect on that interaction and resulted in a low T<sub>g</sub> values expected.

Malonic acid was used to study the effect of loading an acidic and a basic drug into the polymeric film. Despite that solubility parameter values provided in table 5.1 indicated that malonic acid and nicotinamide or caffeine would theoretically favour to interact with the polymer rather than interacting with each other, malonic acid managed to form a bond with caffeine and nicotinamide forming a co-crystalline system during the loading of the two materials (malonic acid-nicotinamide and/or malonic acid- caffeine) into a polymeric film. However, a smaller amount of malonic acid was needed to interact with nicotinamide than that needed to interact with caffeine. The excess amount in the second case appeared to be needed to saturate the polymer first and bring the interaction favour toward caffeine. This result doesn't conform to the proposed theory of interaction affinity prediction based on the closeness of the solubility parameter values of the drugs and the polymer. This difference can be explained by the affinity factor between the acidic and basic compounds to interact which has not been taken into consideration in the proposed theory.

It can be concluded from the previous observation that increasing the concentration of the acidic part of the co-crystal system can be considered as a technique to grow co-crystals in a polymeric carrier of HPMCAS. this technique proved itself in the case of caffeine-malonic acid co-crystals in HPMCAS film. however, this technique cannot be considered as a general rule as it may

resulted in the use of an excess amount of the drug over its therapeutic level as in the case of ibuprofen-nicotinamide were ibuprofen is the acidic part of the drug.

## **Chapter 8**

**Manufacture and stability of co-crystals in a polymeric carrier**

## 8.1 Introduction

This chapter examines the loading process of co-crystals (caffeine-malonic acid and ibuprofen-nicotinamide) into a polymeric vehicle (HPMCAS). It will also investigate the factors that affect this process and study the dissolution release and stability of the co-crystals in the film.

Caffeine-malonic acid co-crystals can be grown in the polymeric film by using an excess above their saturation concentrations. Therefore, the excess amount of the acidic moiety of the co-crystals was used in chapter 7 to saturate the polymer for the acidic drug. This in turn has allowed the growth of free crystals in the film that have the ability to interact with the basic moiety and form a co-crystal (as in caffeine-malonic acid co-crystal formation in chapter 7). However, the increase in the acidic moiety may not always be possible for the rest of co-crystalline systems, e.g. Ibuprofen-nicotinamide co-crystals are one of the examples where the API is the acidic moiety. Increasing the ibuprofen concentration to reach the saturation concentration may not be possible as it will result in overdosing.

Therefore, it was necessary to find a method that can preserve the concentrations around their acceptable therapeutic concentrations.

The possibility of loading the co-crystals without increasing the acidic moiety concentration was investigated. Therefore, the co-crystals of caffeine-malonic acid and ibuprofen-nicotinamide were prepared and then dispersed in a HPMCAS solution.

The solvent effect on the loading process and on co-crystal integrity was evaluated through the use of different solvents for the loading process.

It was revealed in chapter 7 that the HPMC-AS film has a higher affinity to interact with the acidic moiety of the co-crystal, therefore the approach of using another acidic drug with a closer SP to that of the polymer was investigated to verify if it can reduce the saturation concentration of the co-crystal acidic moiety and therefore protect the co-crystal integrity.

Two co-crystal systems were studied, caffeine-malonic acid and ibuprofen-nicotinamide.

## **8.2 HPMCAS films containing co-crystals of caffeine and malonic acid**

Films designed to contain 500 mg caffeine-malonic acid co-crystal in 4000 mg HPMCAS were prepared using the method described in section 2.3.4. Two solvent systems were used for the loading process: acetonitrile and acetone/chloroform. The resulting films were analyzed in order to confirm co-crystal integrity.

### **8.2.1 Thermal analysis**

#### **TGA & DSC**

Films containing 500 mg of caffeine-malonic acid co-crystals prepared and cast using acetonitrile or acetone/chloroform were analysed using TGA and DSC to obtain their thermal profiles. The moisture content of the film was similar to the moisture content of unprocessed HPMCAS (section 3.1.7.1) around 2% between 30-100°C (Appendix AI 10).



The thermal DSC profile for films containing co-crystals didn't reveal any of the melting peaks observed in the thermal profile of caffeine-malonic acid co-crystals (figure 4.1 and 4.2). In addition to that, the T<sub>g</sub> values of films containing co-crystals prepared using acetone/chloroform was difficult to measure. However, the two measureable T<sub>g</sub> values (91.52° and 35.73°C) are lower than those observed with films prepared using acetonitrile (110.37° and 72.73°C). This may reflect that the type of materials interacting with the polymer is different between the two films. It was noticed that malonic acid (or acidic drugs generally) causes more depression for the T<sub>g</sub> of the polymer than basic ones. Therefore, this might suggest that the amount of free malonic acid in the film prepared using acetone/chloroform is higher than that in a film prepared using acetonitrile (figure 8.1).

Nevertheless, it is unclear if the T<sub>g</sub> shift is the result of the interaction between the co-crystals and the polymer or the caffeine and malonic acid interaction with the polymer. Consequently, detecting T<sub>g</sub> changes to quantify drug interaction with the polymer and compare the effect of using various solvents on such interaction was not practical.

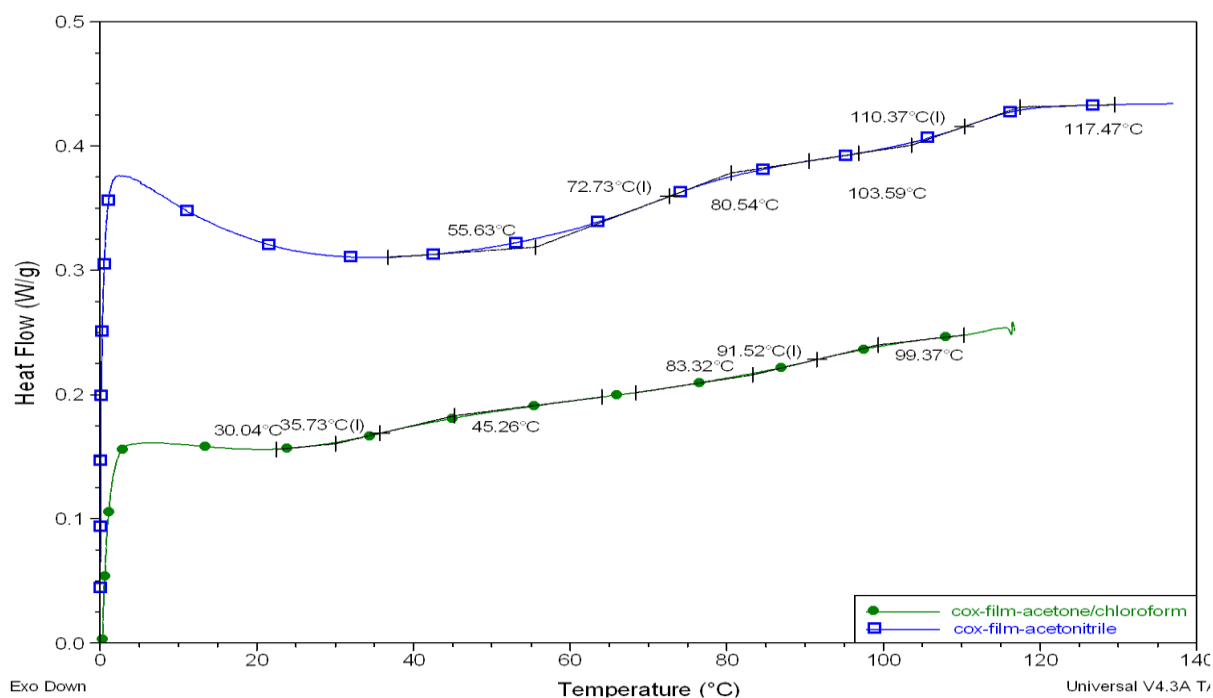


Figure 8.1. Representative thermal DSC profiles for films containing caffeine-malonic acid co-crystals prepared using acetone/chloroform (green) and acetonitrile (blue).

## 8.2.2 Powder X-ray diffraction

The diffraction pattern obtained from a film containing co-crystals prepared using acetonitrile revealed two diffraction peaks at  $12.5^\circ$  and  $27.4^\circ$ . The second diffraction peak can be correlated to the diffraction pattern of caffeine-malonic acid co-crystals (section 4.2.1.2). On the other hand, the diffraction pattern obtained from films prepared using acetone/chloroform revealed a high noise/signal ratio with a weak diffraction peak appeared at  $12^\circ$ . Therefore, it was not possible to confirm conclusively the co-crystals presence in these films (figure 8.2).

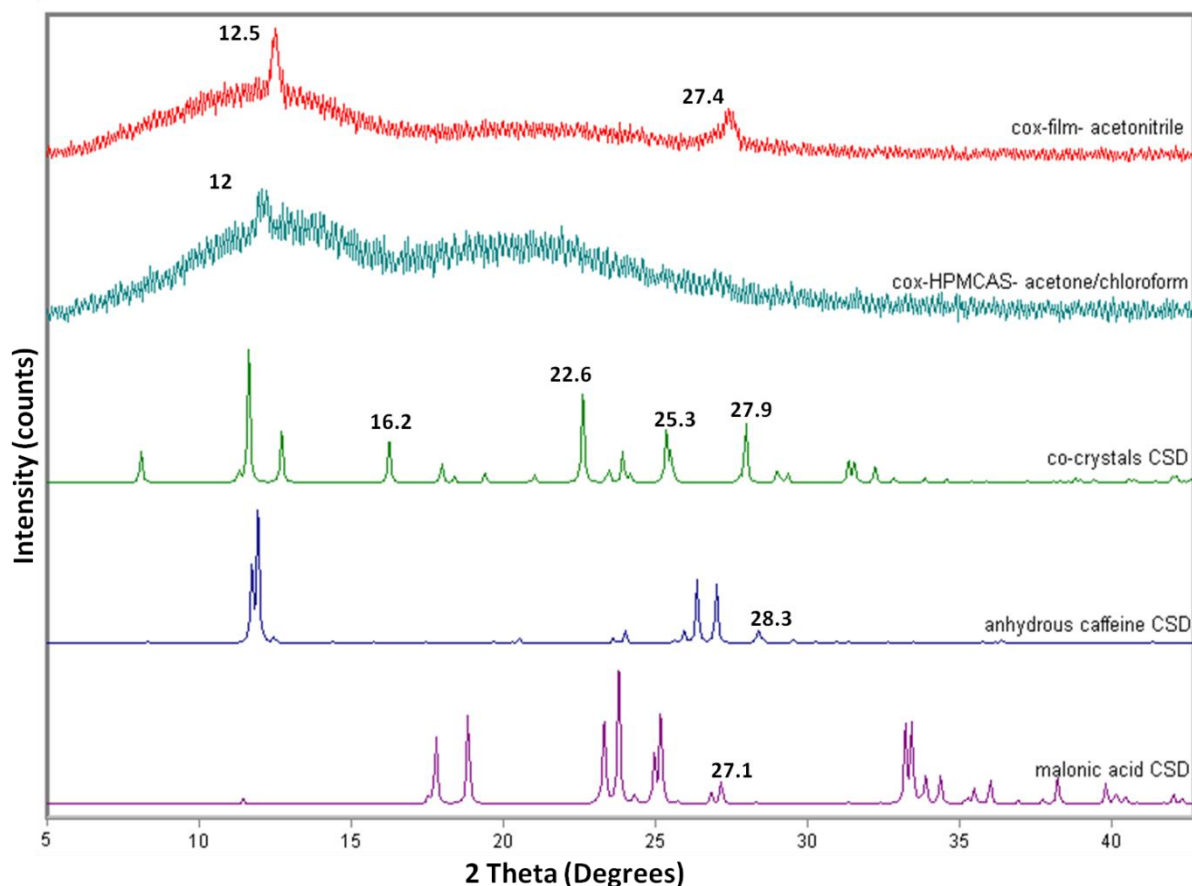


Figure 8.2. Representative x-ray diffraction patterns for unprocessed malonic acid (purple), unprocessed caffeine (blue), co-crystals diffraction pattern obtained from CSD (green), a film containing co-crystals prepared using acetone/chloroform (teal), and a film containing caffeine-malonic acid co-crystals prepared using acetonitrile (red).

### 8.2.2 FT-IR transmission

The collected FT-IR spectra using the method described in section 3.2.3 revealed a shift in caffeine C=N, NH peak from  $1692\text{ cm}^{-1}$  to  $1699\text{ cm}^{-1}$  and  $1705\text{ cm}^{-1}$  in films containing co-crystals prepared with acetonitrile and acetone/chloroform respectively. The shift of C=N, NH peak from  $1692$  to  $1698\text{ cm}^{-1}$  was observed previously in the FT-IR transmission pattern of caffeine-malonic acid co-crystals (section 4.2.1.3). As the degree of shifting reflects the change of the vibrational energy of the system, therefore it can be concluded that the films prepared using acetonitrile reveals the presence of co-crystals. On the other hand, the observed shift in films containing 500 mg co-crystals and

prepared using acetone/chloroform is similar to the shift in films containing caffeine alone. In addition, this shift is higher than the shift resulting from co-crystal formation. Therefore, it can be concluded that a shift of the C=N, NH peak in the analysis of films prepared using acetone/chloroform is an indication of the bond formed between caffeine and HPMCAS which in turns reflect the absence of co-crystals in the scanned spot (figure 8.3). It was difficult to identify the shift in malonic acid C=O, OH representative peaks as the polymer transmission pattern was covering a wide range of the chart and due to the high number of peaks that assign for that particular functional group. Therefore, the vibrational energy in the C=N, NH bond was used as an indicator for the presence of caffeine-HPMCAS or caffeine-malonic acid interaction. It is worth mentioning that films prepared using both solvents showed the presence of both co-crystals and caffeine-HPMCAS interaction. However, it was easier to find co-crystals in films prepared using acetonitrile than those prepared using acetone/chloroform. Nevertheless, since the FT-IR microscopy is a single spot scan therefore it is difficult to quantify the co-crystals/crystals ratio in each film.

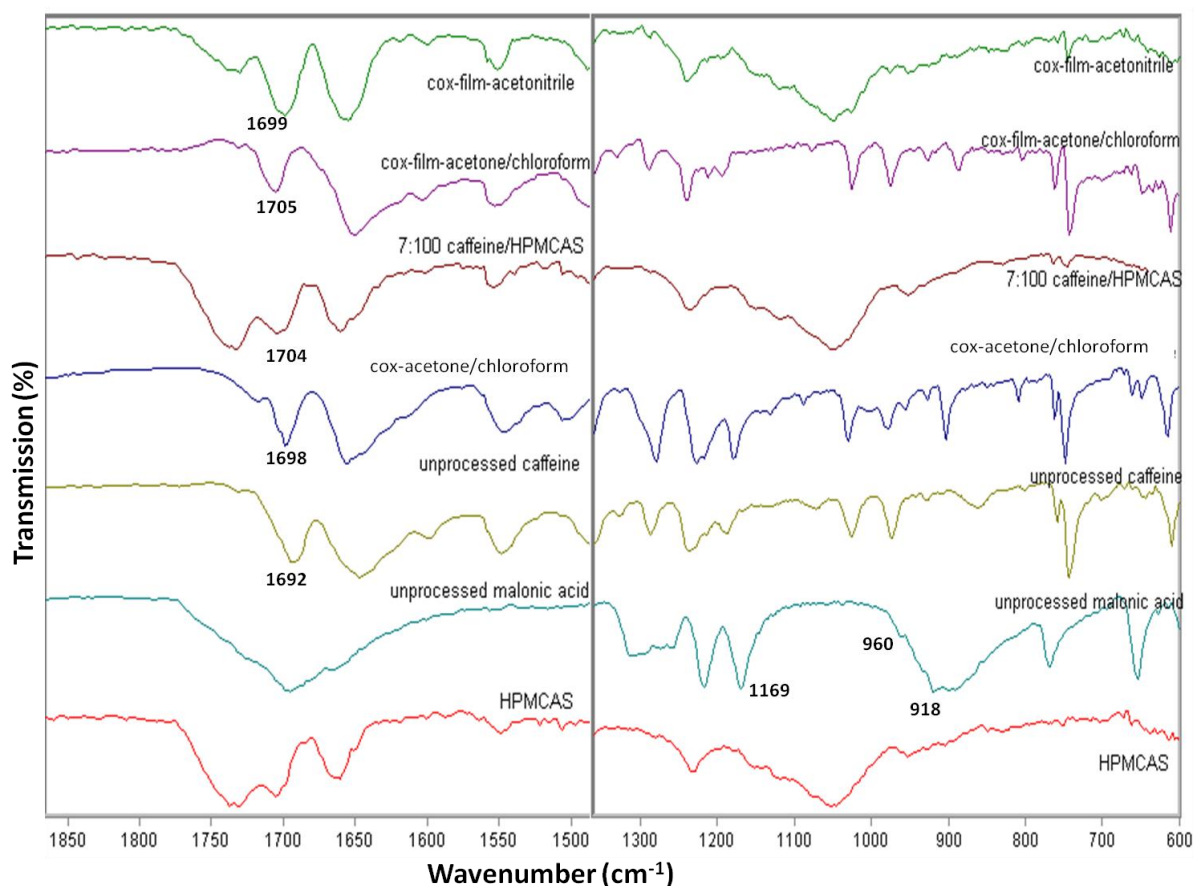


Figure 8.3. Representative FT-IR spectra for unprocessed HPMCAS (red), unprocessed malonic acid (teal), unprocessed caffeine (yellow), a film containing 1:10 caffeine/HPMCAS (blue), co-crystals prepared using acetone/chloroform (brown), film containing co-crystals prepared using acetone/chloroform (purple), and a film containing co-crystals prepared using acetonitrile (green).

It can be concluded that caffeine-malonic acid co-crystals were successfully loaded into the polymer and that some of them stayed intact. A quantitative study for the co-crystals/constituents ratio was difficult to perform; therefore no blocker was used as its effect cannot be measured.

### **8.3 Films containing co-crystals of ibuprofen and nicotinamide**

Films containing 500 mg ibuprofen-nicotinamide co-crystals were prepared using the method described in section 2.3.4. Acetonitrile and acetone/chloroform were used for the loading of these co-crystals in the polymeric film.

#### **8.3.1 Thermal analysis**

##### **TGA and DSC**

The thermal profiles of films containing ibuprofen-nicotinamide co-crystals prepared with acetone/chloroform and/or acetonitrile reveal a weight loss around 2% between 30-100°C which was similarly observed in the thermal profile of unprocessed HPMCAS. This weight loss was correlated to the evaporation of the residual moisture in the film (Appendix A1 11). A shift of the polymer Tg can be observed as well. From figure 8.4, the Tg values were 53° and 41°C for films prepared using acetonitrile and acetone/chloroform respectively. Comparing these values to the values observed in films containing ibuprofen and nicotinamide separately reveals that the observed Tg shift in films loaded with ibuprofen-nicotinamide co-crystals might be due to the plasticizing effect produced by the effect of the constituents on the polymer. Hence, free ibuprofen and nicotinamide were detected (figure 8.4). On the other hand, this change in Tg value might be the result of co-crystals interaction with the polymer.

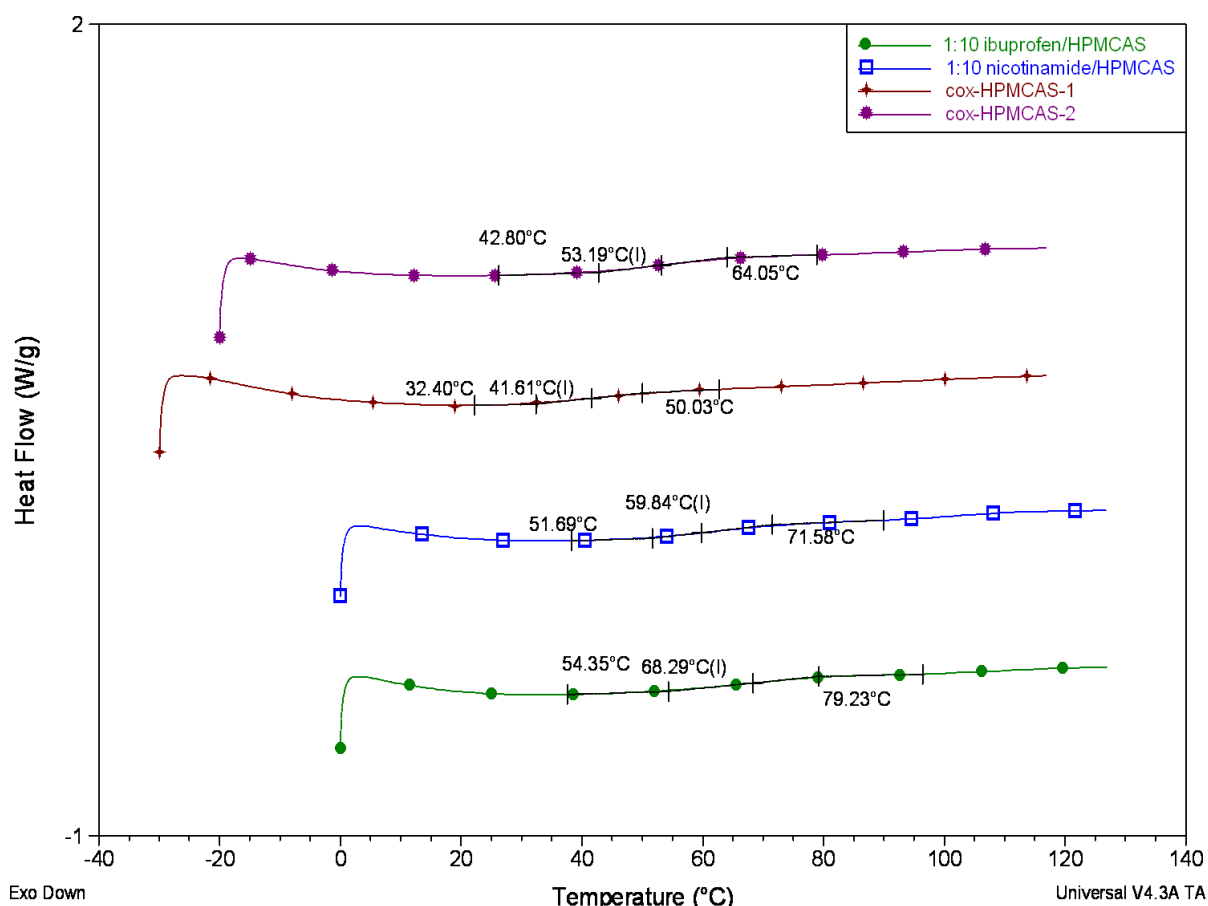


Figure 8.4. Representative DSC thermal profiles for a film containing 1:10 w/w ibuprofen/HPMCAS (green), 1:10 w/w nicotinamide/HPMCAS (blue), a film containing co-crystals prepared with acetone chloroform (1) (red), and acetonitrile (2) (purple).

### 8.3.2 powder X-ray diffraction

The diffraction pattern obtained from films containing ibuprofen-nicotinamide co-crystals prepared using acetonitrile revealed the existence of three peaks at 3°, 16°, and 17°. The presence of these peaks is confirmatory of the presence of co-crystal inside the polymer. On the other hand, the diffraction pattern of the film prepared using acetone/chloroform failed to provide any diffraction peak due to the low signal/noise ratio due to the domination of the amorphous peaks related to the polymeric matrix (figure 8.5).

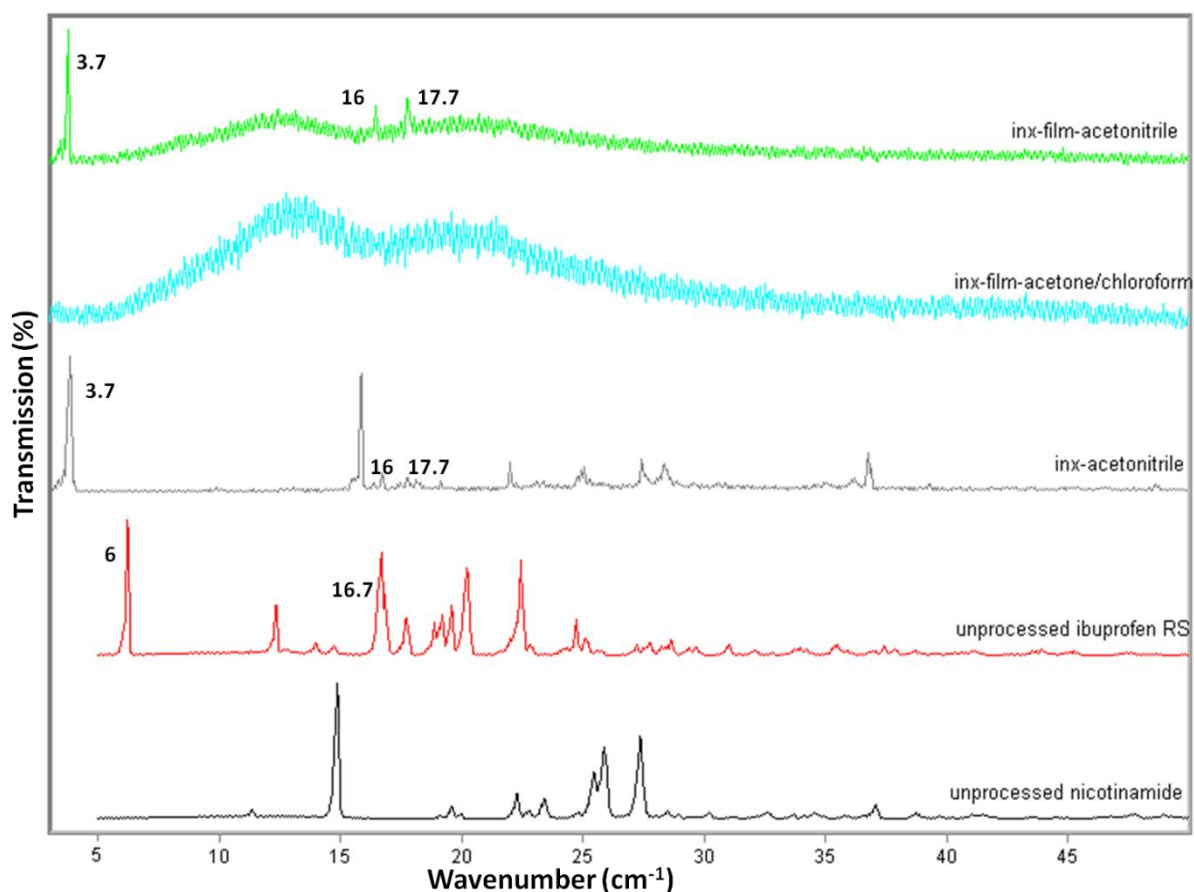


Figure 8.5. representative powder x-ray diffraction pattern for unprocessed nicotinamide (black), unprocessed ibuprofen (red), co-crystals (silver), a film containing co-crystals prepared using acetone/chloroform (teal), and a film containing co-crystals prepared using acetonitrile (green).

This result doesn't prove or disprove the existence of ibuprofen-nicotinamide co-crystals in films prepared using acetone/chloroform. Therefore, FT-IR microscopy was used to provide supporting evidence for identifying the type of crystal in the film.

### 8.3.3 FT-IR transmission

Analysis of the data in figure 8.6 revealed that it was difficult to detect the shift in films containing ibuprofen-nicotinamide co-crystals. This is due to the nature of the polymer that has wide range of interfering vibrations.



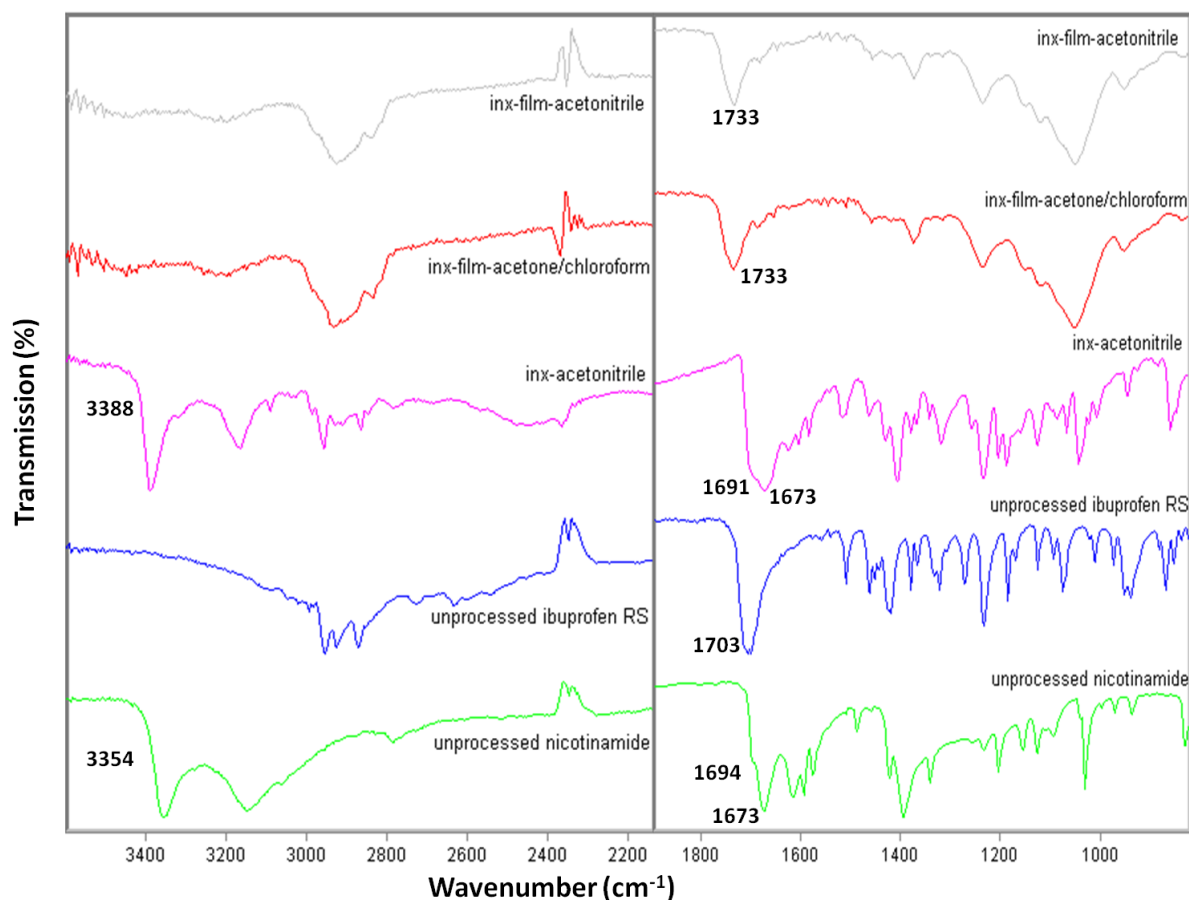


Figure 8.6. Representative FT-IR spectra for, unprocessed ibuprofen RS (green), unprocessed nicotinamide (blue), co-crystals (pink), a film containing co-crystals prepared using acetone/chloroform (red), and a film containing co-crystals prepared using acetonitrile (silver).

The results collected from the DSC, X-ray, and FT-IR indicate the presence of some ibuprofen-nicotinamide co-crystals in the film prepared using acetonitrile, contrary to films prepared using acetone/chloroform. However, the co-crystal percentage appeared to be lower than that that the DSC can detect. The FT-IR data revealed no shifting in the analyzed spots. Hence, it can be concluded that free nicotinamide and ibuprofen are present in the film. Thermal analysis of both films revealed the presence of an interaction between the drug, crystalline/co-crystalline, and the polymeric matrix. This interaction caused the depression noticed in the  $T_g$  value of the polymer.

HPMCAS is known to have a preferential interaction with acidic drugs. Hence, in order to prevent such an interaction from affecting the integrity of the loaded co-crystals, a second acid was selected based on the observations in sections 6.3 and 6.4 in order to reduce the saturation concentration for ibuprofen and consequently reduce the affinity of HPMCAS to interacting with ibuprofen. Malonic acid was selected as it has a SP value that is closer to HPMCAS SP value than that of ibuprofen and HPMCAS. Since malonic acid SP value is closer to that of the polymer rather than nicotinamide SP value, there should theoretically be no or little interaction between malonic acid and nicotinamide.

#### **8.4 The use of a blocking agent for ibuprofen-HPMCAS interaction**

Malonic acid was noticed to reduce the saturation point of ibuprofen by competing with it on the interaction with the polymer as in section 6.3.1.

Therefore, malonic acid is used in this experiment to reduce the affinity of ibuprofen to interact with the polymer. This might preserve more co-crystals during the loading process. As it was mentioned earlier, there is some affinity between nicotinamide and malonic acid to interact and form co-crystals.

However, based on the affinity rule derived from the SP values, malonic acid should preferably interact with HPMCAS more than nicotinamide. Hence, if no excess amount of malonic acid were used, the right environment for loading the co-crystals should be achieved.

Films were prepared using the method described in section 2.3.4. Various concentrations of malonic acid were tested to find an optimum amount of 800 mg/4000 mg HPMCAS to use with all films.

#### **8.4.1 General analysis**

Visual inspection of these films revealed an increase in opacity of the polymeric matrix compared to films containing the same concentration of co-crystals only. In addition, small white crystals were noticed dispersing in the polymeric films.

#### **8.4.2 Thermal analysis**

##### **TGA & DSC**

Thermal profiles for films containing ibuprofen-nicotinamide co-crystals with a blocking agent (malonic acid) prepared using acetone/chloroform and acetonitrile revealed about 2% weight loss between 30-100°C. A similar weight loss was observed in the thermal profile for unprocessed HPMCAS and was correlated to the evaporation of the residual moisture in the film. In addition to that, these profiles main difference from the thermal profile of films containing no blocking agent is the degradation step that around 140°C. This step can be correlated to the degradation of malonic acid (Appendix AI 11). On the other hand, the T<sub>g</sub> values of these films were difficult to measure. However, two interesting peaks were detected in the thermal profile of films prepared using acetonitrile. Those peaks were found at 92°C and 104°C (figure 8.7). These peaks can be correlated to the melting peaks of ibuprofen-nicotinamide co-crystals (93°C) and malonic acid-nicotinamide co-crystals (110°C). The endothermic peak at 92°C was noticed in the first heating run in the DSC thermal profile. This peak disappeared from the second heating run. It can be noticed that heat melted the co-crystals and the polymeric matrix prevented their reformation on cooling. This can be observed in the disappearance of the co-crystals peak from the second heating run. However, the second peak is not

close to the melting point of the individual components of the melted co-crystals. It is rather close to the melting point of malonic acid-nicotinamide melting point. Hence, this may indicate the presence of malonic acid-nicotinamide co-crystals in the film. Since the last co-crystal system was not added to the film, this means that malonic acid has substituted ibuprofen in the co-crystal and took its place (similar to substitution reaction in salts). This substitution was predicted according to the solubility parameter values of the three compounds. However, malonic acid was expected to interact preferentially with the polymer.

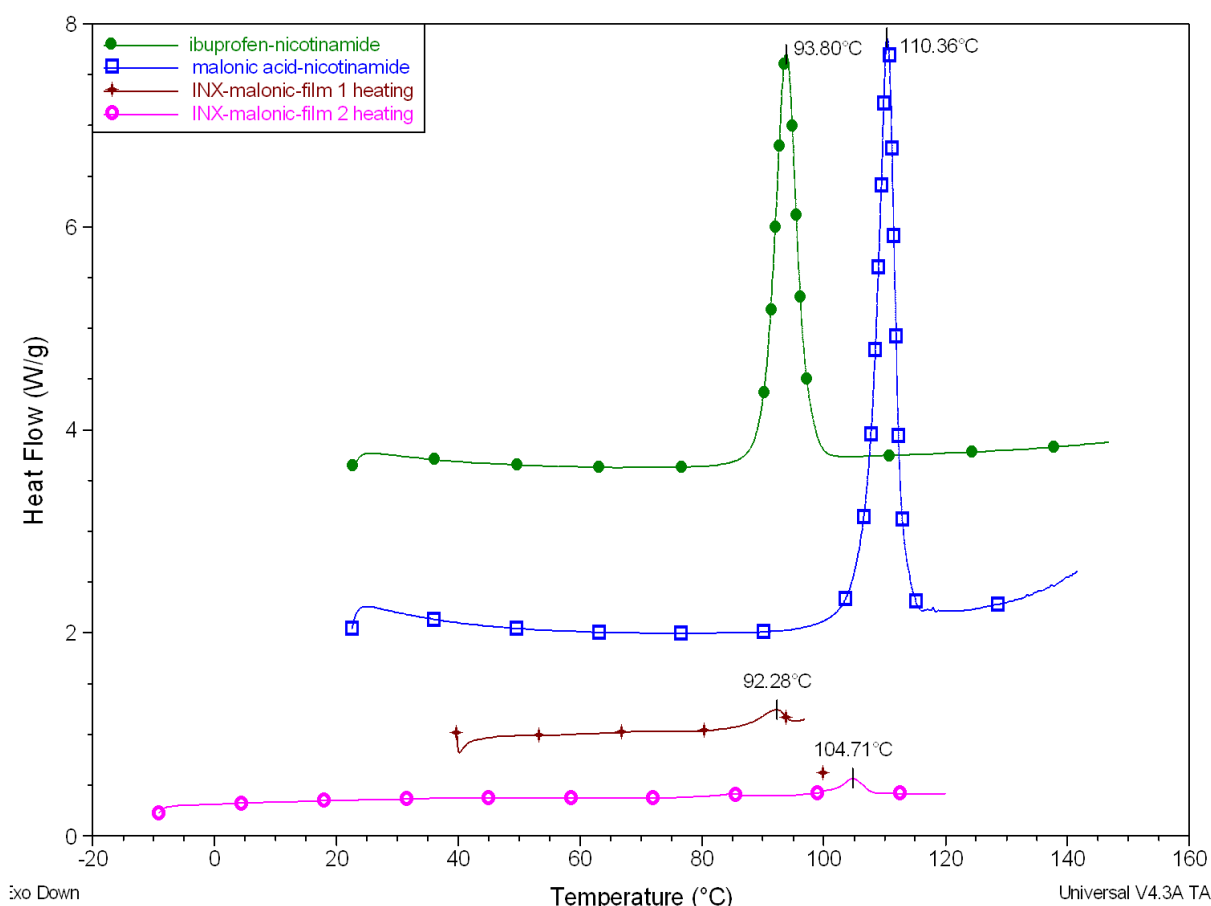


Figure 8.7. Representative DSC thermal profiles for ibuprofen-nicotinamide co-crystals (green), malonic acid-nicotinamide co-crystals (blue), the first heating run of a film containing co-crystals and malonic acid prepared with acetonitrile (brown), and the second heating step for the same film (pink).

### 8.4.3 Powder X-ray diffraction

The X-ray diffraction pattern reveals the existence of 3 peaks diffraction at 6°, 19° and 28° (figure 8.8) These peaks can be observed in the diffraction pattern of unprocessed ibuprofen (6°) and nicotinamide-malonic acid co-crystals (19° and 28°). Therefore, according to the thermal and the X-ray analysis, it can be said that the film contains ibuprofen-nicotinamide co-crystals, malonic acid-nicotinamide co-crystals, ibuprofen, and malonic acid crystals.

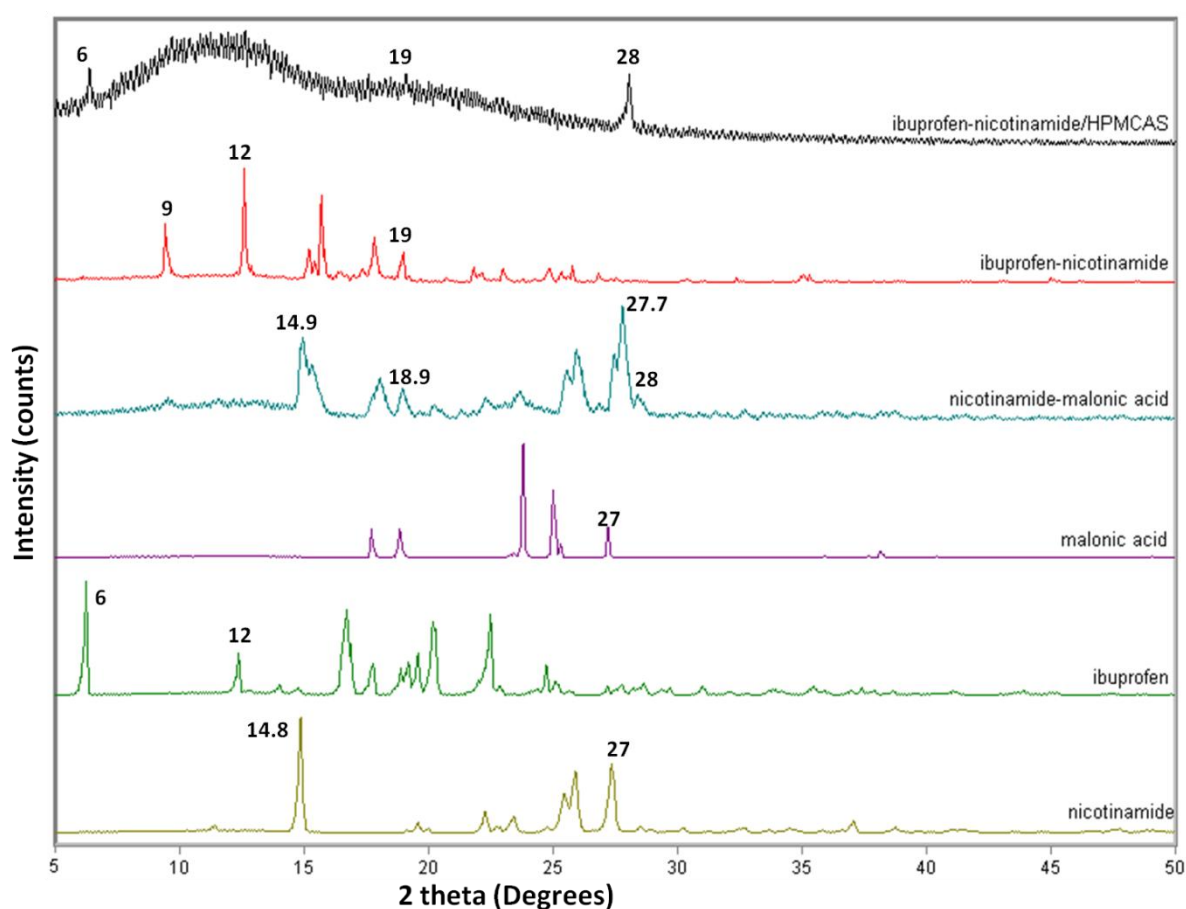


Figure 8.8. Representative powder x-ray diffraction pattern for unprocessed nicotinamide (yellow), unprocessed ibuprofen (green), unprocessed malonic acid (purple), nicotinamide-malonic acid co-crystals (teal), ibuprofen-nicotinamide co-crystals (red), and film containing ibuprofen-nicotinamide co-crystals with malonic acid (black).

### 8.4.4 FT-IR transmission

The FT-IR spectrum was used in order to probe the interactions that exist in the polymeric film. The FT-IR spectrum revealed a peak shift at 3354 to 3371  $\text{cm}^{-1}$ .

This peak was correlated to the C=N, NH vibrational energy in nicotinamide. There was no observed shift in the 1698 cm<sup>-1</sup> in ibuprofen that assign for C=O, OH bond. In addition to that, there was a peak observed at in scan shows that the nicotinamide peak at 1686cm<sup>-1</sup> (figure 8.9). This peak can be observed in malonic acid-nicotinamide co-crystals. This peak was found to assign for C=O, C-O vibrational energy in malonic acid. Hence, the FT-IR analysis reveals the existence of nicotinamide-malonic acid co-crystals in films loaded with ibuprofen-nicotinamide co-crystals in addition to malonic acid as well.

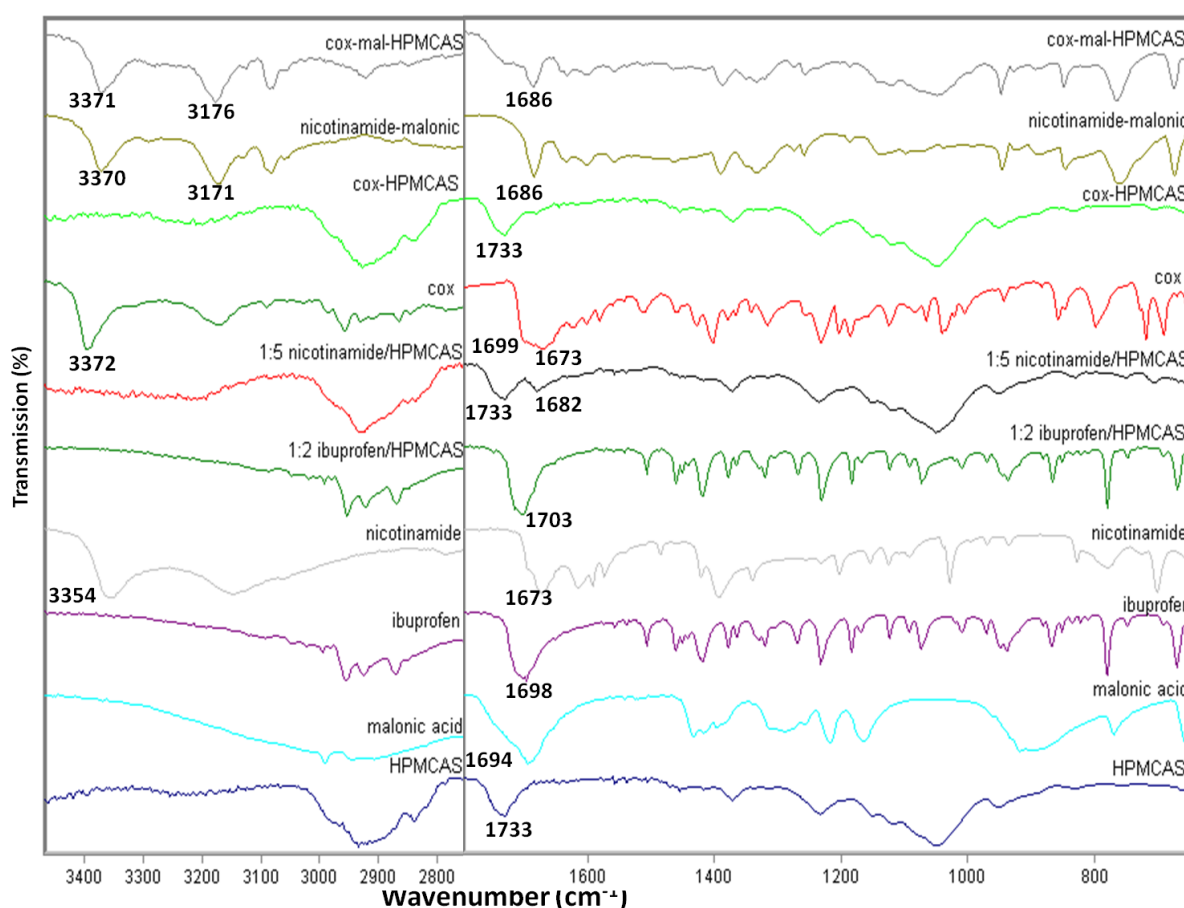


Figure 8.9. Representative FT-IR spectra for unprocessed HPMCAS (blue), unprocessed malonic acid (teal), unprocessed ibuprofen RS (purple), unprocessed nicotinamide (silver), 1:2 ibuprofen/HPMCAS (green), 1:5 nicotinamide/HPMCAS (black), ibuprofen-nicotinamide co-crystals (red), film containing ibuprofen-nicotinamide co-crystals (light green), malonic acid-nicotinamide co-crystals (yellow), and film containing ibuprofen-nicotinamide co-crystals with malonic acid (white). Films were prepared using acetonitrile.

The analysis of films containing ibuprofen-nicotinamide co-crystals and malonic acid revealed the existence of a free ibuprofen and malonic acid in addition to a

mixture of two co-crystalline systems: ibuprofen-nicotinamide and malonic acid-nicotinamide. Therefore, the use of malonic acid to improve the outcome of the loading process of co-crystals into a polymeric film can be described as ineffective in terms that it was not 100 percent efficient in preserving the desired co-crystals. On the other hand, it was not feasible to quantify the percentage of both co-crystalline systems in the film. Therefore, any improvement in the total loading ratio is difficult to measure.

### **8.5 Dissolution test**

Generally co-crystals have a faster dissolution rate than their parent drug (Blagden et al., 2007 , Vishweshwar et al., 2006 , Mirza et al., 2008). However, there is a dearth of information about the release and the dissolution behaviour of co-crystals dispersed in a polymeric carrier. Caffeine and malonic acid can be easily measured with UV spectroscopy as there is no major overlap for their absorption profiles. On the other hand, the UV absorption spectra for ibuprofen, nicotinamide and malonic acid overlap which render the use of UV to measure the release profile very complex. Therefore, the dissolution test was performed only on films containing caffeine-malonic acid co-crystals. The release pattern was obtained following the method described in section 2.2.5. The collected data was then compared to the dissolution rate of a film containing a similar caffeine concentration to that used in films containing co-crystals (1:10 w/w caffeine/HPMCAS). The experiment was repeated twice in order to reduce the effect of experimental error. Even though that the average dissolution rate of films containing caffeine alone is greater than that of films containing co-crystalline caffeine (figure 8.10), the standard error for the experiment was high

and thus prevented any significance from being assigned or real comparison from taking place (Appendix AVI 1-3).

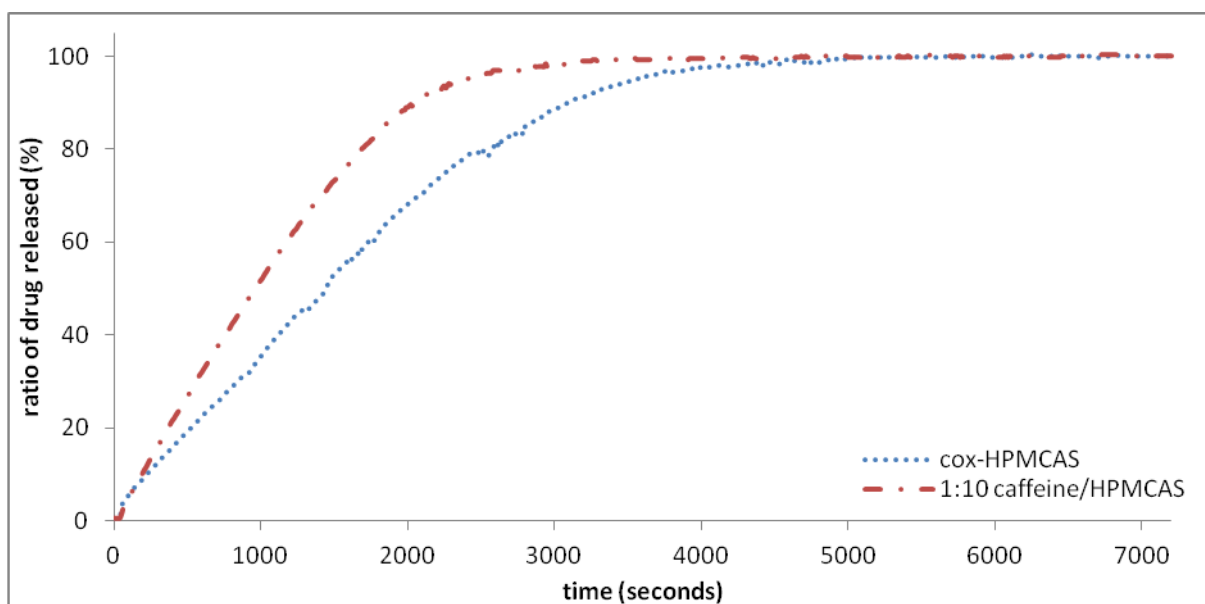


Figure 8.10. Comparison of the dissolution rate of caffeine from a film containing 1:10 caffeine/HPMCAS w/w, and a film containing equivalent amount of caffeine as co-crystals. Error bars removed for clarity and can be found at Appendix AVI 1-3.

Given the above constraints, the graph (Fig. 8.10) shows that the dissolution of caffeine from the polymer is higher than the dissolution of it when formulated as a co-crystal and loaded into the polymeric film.

#### 8.4.6 Stability study

The stability of caffeine-malonic acid co-crystals against high humidity and temperature was measured in order to monitor the effect of the film coating (dispersion of co-crystals in the polymeric film) on caffeine resistance to hydration.

The stability test was performed on films containing caffeine-malonic acid co-crystals only due to the abundance of caffeine-malonic acid co-crystals in



comparison to ibuprofen-nicotinamide co-crystals in films containing either. In addition, it is easier to detect the presence of caffeine-malonic acid co-crystals in comparison to ibuprofen-nicotinamide co-crystals using FT-IR microscopy.

Although the ICH guidelines suggest the use of 40°C and 75% relative humidity for 6 months (Guideline, 2003), the parameters were chosen as 45°C and 95% relative humidity as the available time was 3 months. However, the sample didn't reveal any difference after the end of the third month. Therefore, the samples were kept for additional 4 months.

Caffeine-malonic acid co-crystals was reported in the literature to have a good stability for hydration more than caffeine alone (Trask et al., 2005). HPMCAS is known to be a hygroscopic material. Therefore, dispersing caffeine-malonic acid co-crystals in HPMCAS film will bring the co-crystals in contact with the moisture.

HPMCAS films containing 500 mg of caffeine-malonic acid co-crystals were divided into small pieces and analyzed with FT-IR to ensure the presence of the co-crystals and to obtain a reference for future comparison. Samples were stored in a closed oven with a relative humidity (RH) of 95% and temperature of 45°C.

Caffeine-malonic acid co-crystals revealed a good stability against relative humidity of 75% for 7 weeks. However, when the RH was increased to 98%, the co-crystals was stable for the first week and the FT-IR analysis showed the disappearance of their transmission profile after 7 weeks (Schultheiss and Newman, 2009). On the other hand, another study in the literature revealed that

the co-crystals disappeared after one day of storing them at 98% RH at room temperature (Trask et al., 2005).

The available stability study oven was limited to 95% RH, Therefore the study was performed on 95% and a temperature of 45°C to provide an extra challenge for the co-crystals dispersed in the HPMCAS film.

The samples were removed periodically and analyzed using the FT-IR microscopy to monitor the presence of caffeine-malonic acid co-crystals. The analysis revealed that samples stored for 8 weeks containing intact co-crystals (Appendix AVII 1-23). Afterward the analysis revealed the disappearance of the co-crystals transmission profile and the appearance of caffeine or caffeine-HPMCAS transmission profile. Therefore, it can be concluded that dispersing caffeine-malonic acid co-crystals in a film of HPMCAS increased the stability of those co-crystals against 95% RH and 45°C temperature.

## 8.5 Summary and conclusions

Loading caffeine-malonic acid co-crystals was successful using acetonitrile and acetone/chloroform. However, the percentage of intact co-crystals was observed to be higher with the first solvent.

On the other hand, loading ibuprofen-nicotinamide co-crystals into HPMCAS films revealed the presence of a very small number of intact co-crystals that couldn't be detected by the DSC and were only detectable by x-ray.

When malonic acid was used as a blocking agent to reduce the ibuprofen saturation concentration, it was noticed that some ibuprofen-nicotinamide co-crystals were detected by the DSC in addition to the detection of malonic acid-nicotinamide co-crystals as well.

### **A- Caffeine-malonic acid co-crystals in HPMCAS film:**

Caffeine-malonic acid co-crystals were loaded into a polymeric vehicle using two solvent systems: acetonitrile and acetone/chloroform. Although acetonitrile was found to aid formation of caffeine monohydrate (chapter 3 and 4), the FT-IR results in this chapter showed no sign of caffeine monohydrate. The quantitative comparison between films containing caffeine-malonic acid co-crystals prepared using acetonitrile or acetone/chloroform was difficult through thermal analysis (DSC) as the T<sub>g</sub> values for films prepared using acetone/chloroform were difficult to be measured. However, the calculated T<sub>g</sub> values for films prepared using acetone/chloroform is lower than that prepared using acetonitrile (91.52° and 35.73°C for films prepared using acetone/chloroform compared to 110.37° and 72.73°C observed for films prepared using acetonitrile). Since malonic acid and caffeine in their free state can interact better with the polymer and

consequently reduce the Tg more. The amount of free drugs is inversely related to the amount of the intact co-crystals. Therefore, it can be concluded that the amount of free drug in the film prepared using acetone/chloroform containing less amount of co-crystals than the one prepared using acetonitrile.

#### **B- Ibuprofen-nicotinamide co-crystals in HPMCAS film:**

The second part of this chapter focused on the loading of ibuprofen-nicotinamide co-crystals into a polymeric film in the presence of malonic acid. The DSC thermal profile shows the presence of two endothermic peaks at 92°C and 104°C. These peaks are expected to be the melting peaks of ibuprofen-nicotinamide co-crystals (92°C) and malonic acid-nicotinamide (110°C) respectively. The X-ray diffraction pattern of films containing ibuprofen-nicotinamide co-crystals revealed the presence of nicotinamide-malonic acid co-crystals in the film. Therefore, it can be stated that films loaded with ibuprofen-nicotinamide co-crystals and malonic acid as a blocking agent revealed the presence of: ibuprofen-nicotinamide co-crystals, malonic acid-nicotinamide co-crystals, ibuprofen, nicotinamide, and a possible malonic acid-HPMCAS and ibuprofen-HPMCAS.

#### **C- Ibuprofen-nicotinamide co-crystals in HPMCAS film using malonic acid as a blocker:**

Malonic acid was used in order to protect the co-crystals of ibuprofen-nicotinamide from interacting with the polymer. Malonic acid was chosen based on its SP value which is closer to that of the polymer than either ibuprofen or nicotinamide to the polymer SP value.

Malonic acid was not used in excess in order not to affect the co-crystals as well. Nevertheless, the analysis of these films showed the presence of malonic acid-nicotinamide co-crystals.

The quantification of co-crystals was not feasible, thus it was difficult to quantify the effect of using the malonic acid on the loading of the co-crystals.

#### **D- Dissolution test of caffeine-malonic acid co-crystals in HPMCAS film**

The dissolution test of films containing caffeine-malonic acid co-crystals revealed a lower dissolution rate than films containing the same amount of caffeine alone. However, the standard error of the release profile was high. Thus the actual superiority for films containing caffeine alone is not fully confirmed.

#### **E- Stability test of caffeine-malonic acid co-crystals in HPMCAS film**

The ability of HPMC-AS as a protective film to enhancing the stability of caffeine-malonic acid co-crystal against high RH and temperature was measured through a stability test for films containing co-crystals over 7 months. The test revealed that co-crystals disappeared after 8 weeks of storage. This is considered to be higher than the documented stability test for caffeine-malonic acid co-crystals alone in the literature where the co-crystals stayed stable for 1 day or less (Trask et al., 2005 , Schultheiss and Newman, 2009). Therefore, it

can be concluded that the polymer enhanced the stability of caffeine-malonic acid co-crystals against high RH and temperature.

## **Chapter 9**

### **Summary, conclusions, and future work**

## Summary and conclusion

This thesis has investigated whether co-crystals can be formed within a polymer film (HPMC-AS) and has used a range of techniques to characterise their solid-state form. The dissolution and stability properties of the co-crystal in the film systems have also been investigated. The aim of the thesis was novel and the literature contains only one limited study of the behaviour of co-crystals formed and dispersed in a polymeric carrier, namely nicotinamide-carbamazepine dispersed in polyvinyl pyrrolidone (Good et al., 2011). The study in this thesis is much more extensive and highlights the difficulty of producing co-crystals within films.

To outline the structure of this thesis:

The first step was analyzing the raw materials to identify their properties. This step revealed that the anhydrous caffeine used in this study was obtained as polymorph I. On the other hand, malonic acid was shown to contain a mixture of two polymorphs in the received batch:  $\alpha$  and  $\beta$ .

Ibuprofen was characterised in its received state and was found to be its racemic mixture. Nicotinamide was found to be in its polymorph I form.

The effect of the recrystallization solvent systems to be used in casting films on the initial starting materials was evaluated in chapter 3. The aim was to observe the effect of the preparation media (solvent systems) on the physicochemical properties of each of the raw materials. Three solvent systems were used: acetone/chloroform 3:2 v/v, ethanol/water 4:1 w/w, and acetonitrile.

Ethanol/water was included in particular to dissolve the polymer as was advised by the manufacturer. . Acetonitrile was used because of its known capability to



form ibuprofen-nicotinamide co-crystals (Berry et al., 2008). A third solvent system was identified after preliminary experimental work. This system consisted of acetone/chloroform 3:2 v/v. Re-crystallization of the raw materials with the aforementioned solvent systems revealed no change in the solid state form of any of the raw materials properties except in the case of caffeine. Re-crystallizing caffeine revealed the formation of caffeine monohydrate as evidenced by thermal and X-ray methods.

The third step in this study was studying the formation and properties of the selected co-crystals using a solvent evaporation method (the co-crystals evaluated would be later incorporated into the polymeric film) and the effect of various solvent systems on their properties. It was noticed that caffeine-malonic acid co-crystals were successfully produced using all the solvent systems. However, use of acetonitrile revealed the formation of a mixture of a co-crystal and residual caffeine monohydrate in the final product of the co-crystallization experiment. A new co-crystal system was discovered during the study. It is a co-crystalline system of nicotinamide and malonic acid 1:1 mol/mol. This system was found to be easily formed with acetonitrile and acetone/chloroform using the solvent evaporation method for preparation. Very recently in comparison, solution mediated and drop grinding was used in the literature to prepare 1:1 nicotinamide/malonic acid co-crystals using ethanol or methanol as a solvent system (Voguri, 2010).

The next area for investigation was to study the interaction of each of the raw materials with the polymeric film. The interaction was found to be related to the solvent system used in the loading process. High polarity solvents were noticed to interfere with the interaction more significantly than low polarity solvents. For

example, malonic acid was found to have a higher affinity to the polymer and lowered its T<sub>g</sub> value by a greater extent than basic additives with the same molar ratio in the film.

Loading two acidic additives simultaneously to the polymer was found to affect the interaction of those materials with the polymer. It was found that compound A (e.g. flurbiprofen) interacts more favourably with the polymer than compound B (e.g. malonic acid and naproxen), saturating it and competitively inhibiting interaction. The evidence for this was provided by the X-ray, FT-IR, and DSC analysis of the polymeric films that shows the existence of B crystals in the presence of A in the film at a lower concentration than films containing B alone. Additionally the disappearance of A crystals from the analysis data confirms their conversion into the amorphous form. This in turn reflects the interaction between the polymer and compound A that lead to saturating the polymer and reducing the saturation concentration for compound B.

In a novel way the thesis explored the use of solubility parameters as a predictive tool for the incorporation of co-crystals into films. The behaviour could be predicted from use of calculated solubility parameter values of acidic additives. The solubility parameters theory was developed mainly to predict the miscibility of liquids. However, the theory was expanded to include the miscibility of solid compounds. However, it is worth mentioning that this theory cannot be applied for negative deviations from Raoult's law solutions or compounds, in other words, it doesn't take the polarity of the molecules into account. This was noticed when a mixture of acidic and basic compounds was dispersed in the polymeric film. It was also noticed with the formation theory prediction of the co-crystals alone (Mohammad et al., 2011). The theory

developed and refined in this project suggested that an acidic drug with a closer SP value to the polymer will dominate the interaction process and prevent the majority of the other material from interacting with the polymer. This was investigated using flurbiprofen as a drug with a closer SP value to the polymer one than other acidic drugs (malonic acid, naproxen, and ibuprofen). The experiment revealed that naproxen and malonic acid mixtures with flurbiprofen in the polymeric film behaved according to the postulated theory. However, when ibuprofen was added to a film containing flurbiprofen both drugs dissolved in the film. The concentration was increased in order to reach the saturation point of ibuprofen. Nevertheless, the films remained clear. It is not clear if the presence of flurbiprofen enhanced the solubility of ibuprofen in the film. . The way SP is calculated may have contributed to the theory not being generally applicable for the acidic systems.

The SP theory was found to be not applicable for basic additives when mixed with acidic drugs in the polymeric film. This might be considered as one of limitations to the previous theory. However, it was noticed that adding malonic acid to films containing nicotinamide resulted in the formation of nicotinamide-malonic acid co-crystals. These co-crystals were identified by analysis with powder X-ray diffractometry and FT-IR spectroscopy. It is difficult to compensate for the interaction between the co-crystal formers.

On the other hand, adding malonic acid to films containing caffeine resulted in the formation of caffeine-malonic acid co-crystals. However, it was noticed that the amount needed of malonic acid to form caffeine-malonic acid co-crystals in the film was higher than that needed to form nicotinamide-malonic acid co-crystals in the film. Thus the use of another additive to block polymer binding

sites and allow the easier formation of co-crystals in films has been demonstrated. Each system needs its own preliminary experiments to titrate the level of additive needed for the blockage.

Adding an excess amount of malonic acid was noted to saturate the polymeric film and allow the rest of malonic acid molecules to interact with the basic molecule to form co-crystals. This method might be not practical when the acidic moiety is the API since using an excess amount might lead to overdosing. Therefore another approach was used to load the co-crystals into the polymeric film. Co-crystals were prepared and loaded to the polymer solution.

Briefly we should consider whether the SP theory developed in this thesis is applicable to other published systems. Carbamazepine-nicotinamide co-crystals have previously been noted to form within the polymeric carrier PVP (Good et al., 2011). From the data presented in the study it is notable that both drugs possess a good affinity to form co-crystals in a polymeric carrier in an easy manner compared to the behaviour noted by the systems in this thesis, with both caffeine-malonic acid and ibuprofen-nicotinamide co-crystal systems in a polymeric film of HPMCAS not readily forming. Applying the theory advanced in this thesis to nicotinamide-carbamazepine co-crystals in PVP revealed the closeness of carbamazepine SP value ( $27 \text{ MPa}^{1/2}$ ) to that of nicotinamide ( $30 \text{ MPa}^{1/2}$ ) over that of PVP ( $21 \text{ MPa}^{1/2}$ ). These values propose the affinity of carbamazepine to interact with nicotinamide and form a co-crystal rather than interacting with PVP. This result provides the evidence for the possible application of the theory developed in this thesis to other polymers other than HPMC-AS.

Considering the effect of the choice of solvent for the materials in this thesis, loading the co-crystals into the polymeric vehicle was noted to be affected by the solvent used in this process. The depression of the T<sub>g</sub> values of films prepared using acetonitrile was noticed to be greater than those prepared using acetone/chloroform for the same concentration of caffeine-malonic acid co-crystals (91.52° and 35.73°C for films prepared using acetone/chloroform and 110.37° and 72.73°C for films prepared using acetonitrile). In addition to the FT-IR transmission profiles collected after analysing different points of films prepared with either solvent systems which revealed a higher percentage of co-crystals existed in films prepared using acetonitrile than those prepared using acetone/chloroform. Nevertheless, the analysis method possessed limitations as it was hard to scan the whole film and in spite of repeating the whole analysis for the raw materials, co-crystals, films containing the raw materials separately, and films containing co-crystals in order to minimize possible error, there still exists the need to find a better quantification method to measure the percentage of the co-crystals in films prepared using each solvent.

On the other hand, films containing ibuprofen-nicotinamide co-crystals in a concentration of around 500 mg per 4000 mg HPMCAS showed no sign of co-crystals or any crystalline form in the film. Because acidic materials showed a higher affinity to polymer than basic compounds, an acidic drug (malonic acid) with a closer SP value to that of HPMC-AS was added in an attempt to reduce the interaction of ibuprofen with the polymer and thus promote its interaction to form co-crystals. The results showed that the final film contained four species; co-crystals, ibuprofen, nicotinamide and even a new co-crystal system (nicotinamide-malonic acid) figure 9.1. This behaviour was linked to the

solubility parameters of the three molecules. The schematic below illustrates the range of the interactions between the three molecules and HPMC-AS.

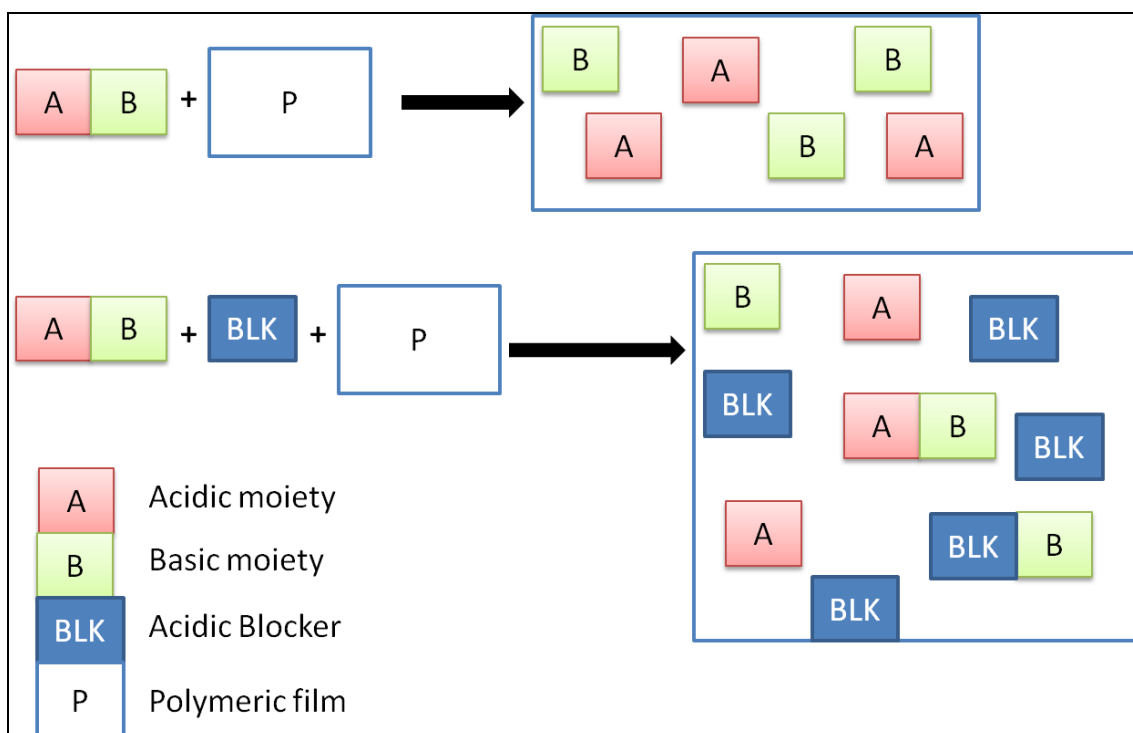


Figure 9.1. Chart representing the behaviour of acidic (A) and basic (B) moiety of co-crystals with and without the use of acidic blocker (BLK) in a polymeric film (P).

Before work on this thesis commenced there was a dearth of information about the behaviour of co-crystals in polymeric carrier. Recently, a report has come into the literature showing that nicotinamide and carbamazepine co-crystals tend to form co-crystals when dispersed in a polymeric carrier of PVP (Good et al., 2011). The formation rate and percentage co-crystal content varied in relation to the molecular weight of the PVP used in the experiment. However, the formation of the co-crystals in the polymer fits the previously mentioned theory.

Whilst the formation of co-crystals may confer an advantage so that higher drug loads can be used, it is also important to understand how the polymer affects drug release. This is studied using a dissolution test. The preliminary

dissolution study suggested that the films containing caffeine alone released caffeine more readily than those containing caffeine containing co-crystals. It is possible that the different micro-environmental pH's controlled the dissolution behaviour. However, the high standard error values prevented too much significance being attached to the data.

An accelerated stability study showed that co-crystals loaded into the polymer were intact for 8 weeks in 45°C and 98% RH in comparison to 8 weeks for co-crystals in 25°C and 75% RH. Therefore, the HPMCAS polymer acts to prolong co-crystal stability for this system.

It can be concluded from the previous results of the project that dispersing caffeine-malonic acid co-crystals in a polymeric carrier was successful in improving their stability while it was not successful in improving their dissolution rate.

### **Future work**

The relationship between two drugs dispersed in a polymeric carrier revealed a link between the acidic drugs solubility parameter values and their competitive interaction with the polymer. On the other hand, the same link was observed with the dispersion of an acidic drug (malonic acid) with basic drugs. However, the behaviour of the dispersed ibuprofen and flurbiprofen in HPMCAS was an exception from the discussed role. Therefore, it is worth to monitor the behaviour of other acidic and basic drugs in other polymers in order to evaluate the new approach for predicting the drugs behaviour. In addition, the proposed

theory can be tested on the behaviour of dispersed basic drugs in polymeric carriers.

Since drug-polymer interaction is one of the techniques to produce small drug crystals, the observed effect of the preparation solvent on the degree of such interaction may result in affecting the properties of the produced crystals. Therefore, the effect of the solvent on the polymer properties and drugs-polymers interaction should be studied.

Using an acidic blocker to minimise the interaction between the acidic moiety of the co-crystals and the film is an interesting approach. However, more investigation is needed to refine the process of selecting this blocking agent. SP has been shown here to have an influence. However it is worth investigating other factors such as the expanded SP proposed by Hansen (Barton, 1991), the capability of forming hydrogen bonding and the polarity of the molecule. This theory needs to be investigated using other polymers and other co-crystal systems. Refining the blocking agent might improve the co-crystal yield inside the polymer and avoid its interaction with the co-crystal formers. Finally, a productive area would be to investigate the effect of a blocking agent that has no affinity to form an interaction with any of the co-crystal components on the loading process of those co-crystals in a polymeric film.



## References

- AAKEROY, C. B. (1999) Hydrogen-bonding in solids - Some strategies and aspects of crystal engineering. In: SEDDON, K. R. and ZAWOROTKO, M. (Eds.) *Crystal Engineering: The Design and Application of Functional Solids*. (Nato Advanced Science Institutes Series, Series C, Mathematical and Physical Sciences) Vol. 539. Dordrecht: Kluwer Academic Publ, pp. 303-324.
- AAKEROY, C. B., et al. (2001) "Total synthesis" supramolecular style: design and hydrogen-bond-directed assembly of ternary supermolecules. *ANGEWANDTE CHEMIE-INTERNATIONAL EDITION IN ENGLISH*, 40 (17), 3240-3242.
- AAKERÖY, C. B. and SALMON, D. J. (2005) Building co-crystals with molecular sense and supramolecular sensibility. *CrystEngComm*, 7 (72), 439-448.
- ABRAMOWITZ, R. and YALKOWSKY, S. H. (1990) Melting Point, Boiling Point, and Symmetry. *Pharmaceutical Research*, 7 (9), 942-947.
- AINOUZ, A., et al. (2009) Modeling and prediction of cocrystal phase diagrams. *International Journal of Pharmaceutics*, 374 (1-2), 82-89.
- AKALIN, E. and AKYUZ, S. (2006) Vibrational analysis of free and hydrogen bonded complexes of nicotinamide and picolinamide. *Vibrational Spectroscopy*, 42 (2), 333-340.
- ALMARSSON, O. and ZAWOROTKO, M. J. (2004) Crystal engineering of the composition of pharmaceutical phases. Do pharmaceutical co-crystals represent a new path to improved medicines? *Chemical Communications*, (17), 1889-1896.
- ALSHAHATEET, S. F., et al. (2004) Co-crystalline hydrogen bonded solids based on the alcohol-carboxylic acid-alcohol supramolecular motif. *CrystEngComm*, 6 (3), 5-10.
- ANDERSON, K. M., et al. (2008) Designing Co-Crystals of Pharmaceutically Relevant Compounds That Crystallize with  $Z' > 1$ . *Crystal Growth & Design*, 9 (2), 1082-1087.
- BARTON, A. F. M. (1991) *CRC handbook of solubility parameters and other cohesion parameters*. CRC.
- BASAVOJU, S., et al. (2008) Indomethacin-saccharin cocrystal: design, synthesis and preliminary pharmaceutical characterization. *Pharmaceutical Research*, 25 (3), 530-541.
- BASHIRI-SHAHROODI, A., et al. (2008) Preparation of a Solid Dispersion by a Dropping Method to Improve the Rate of Dissolution of Meloxicam. *Drug development and industrial pharmacy*, 34 (7), 781-788.
- BERRY, D. J., et al. (2008) Applying hot-stage microscopy to co-crystal screening: A study of nicotinamide with seven active pharmaceutical ingredients. *Crystal Growth and Design*, 8 (5), 1697-1712.

- BERTOLASI, V., et al. (2001) General rules for the packing of hydrogen-bonded crystals as derived from the analysis of squaric acid anions: aminoaromatic nitrogen base co-crystals. *Acta Crystallographica Section B*, 57 (4), 591-598.
- BETHUNE, S. J. (2009). *Thermodynamic and Kinetic Parameters that Explain Crystallization and Solubility of Pharmaceutical Cococrystals*. Doctor of Philosophy. The University of Michigan
- BHARATE, S. S., et al. (2010) Interactions and incompatibilities of pharmaceutical excipients with active pharmaceutical ingredients: a comprehensive review. *Journal of Excipients and Food Chemicals*, 1.
- BIKIARIS, D., et al. (2005) Physicochemical studies on solid dispersions of poorly water-soluble drugs: Evaluation of capabilities and limitations of thermal analysis techniques. *Thermochimica Acta*, 439 (1&2), 58-67.
- BLAGDEN, N., et al. (2007) Crystal engineering of active pharmaceutical ingredients to improve solubility and dissolution rates. *Advanced Drug Delivery Reviews*, 59 (7), 617-630.
- BONDI, A. (1947) On the Solubility of Paraffin-chain Compounds. *The Journal of Physical Chemistry*, 51 (4), 891-903.
- BONDI, A. (1968) *Physical properties of molecular crystals, liquids, and glasses*. Wiley New York.
- BOTHE, H. and CAMMENGA, H. K. (1980) Composition, properties, stability and thermal dehydration of crystalline caffeine hydrate. *Thermochimica Acta*, 40 (1), 29-39.
- BOUGEARD, D., et al. (1988) Vibrational spectra and dynamics of crystalline malonic acid at room temperature. *Spectrochimica Acta Part A: Molecular Spectroscopy*, 44 (12), 1281-1286.
- BRAGA, D., et al. (2007) Making crystals from crystals: A solid-state route to the engineering of crystalline materials, polymorphs, solvates and co-crystals; considerations on the future of crystal engineering. In: *39th Course of the International School of Crystallography on Engineering of Crystalline Materials Properties*. Erice, ITALY: Springer, pp. 131-156.
- BUDAVARI, S. (2006) *The Merck index: an encyclopedia of chemicals, drugs, and biologicals*. Vol. 113. Merck and Co., Inc.
- BURKE, J. (1984) Solubility parameters: theory and application.
- CAIRA, M. R., et al. (1995) Selective formation of hydrogen bonded cococrystals between a sulfonamide and aromatic carboxylic acids in the solid state. *Journal of the Chemical Society, Perkin Transactions 2*, (12), 2213-2216.
- CAIRES, F. J., et al. (2009) Thermal behaviour of malonic acid, sodium malonate and its compounds with some bivalent transition metal ions. *Thermochimica Acta*, 497 (1-2), 35-40.
- CEBALLOS, A., et al. (2005) Influence of formulation and process variables on in vitro release of theophylline from directly-compressed Eudragit matrix tablets. *Il Farmaco*, 60 (1&2), 913-918.

- CHARMAN, S. A. and CHARMAN, W. N. (2003) Oral modified-release delivery systems. *DRUGS AND THE PHARMACEUTICAL SCIENCES*, 126, 1-10.
- CHEMFINDER, C. S. C. (2004) Chemfinder. com database, 2004. Retrieved May–Dec.
- CHIARELLA, R. A., et al. (2007) Making Co-Crystals The Utility of Ternary Phase Diagrams. *Crystal Growth & Design*, 7 (7), 1223-1226.
- CHILDS, S. L. (2008) Novel cocrystallization. Google Patents.
- CHILDS, S. L., et al. (2008) Screening strategies based on solubility and solution composition generate pharmaceutically acceptable cocrystals of carbamazepine. *CrystEngComm*, 10 (7), 856-864.
- CHIOU, W. L. and RIEGELMAN, S. (1969) Preparation and dissolution characteristics of several fast release solid dispersions of griseofulvin. *Journal of Pharmaceutical Sciences*, 58 (12), 1505-1510.
- CHIOU, W. L. and RIEGELMAN, S. (1971) Pharmaceutical applications of solid dispersion systems. *Journal of Pharmaceutical Sciences*, 60 (9), 1281-1302.
- COLIN W, P. (2006) Formulation of poorly water-soluble drugs for oral administration: Physicochemical and physiological issues and the lipid formulation classification system. *European Journal of Pharmaceutical Sciences*, 29 (3&4), 278-287.
- DAMIAN, F., et al. (2000) Physicochemical characterization of solid dispersions of the antiviral agent UC-781 with polyethylene glycol 6000 and Gelucire 44/14. *European Journal of Pharmaceutical Sciences*, 10 (4), 311-322.
- DESAI, J., et al. (2006) Characterization of polymeric dispersions of dimenhydrinate in ethyl cellulose for controlled release. *International Journal of Pharmaceutics*, 308 (1&2), 115-123.
- DONG, Z. and CHOI, D. S. (2008) Hydroxypropyl Methylcellulose Acetate Succinate: Potential Drug–Excipient Incompatibility. *AAPS PharmSciTech*, 9 (3), 991-997.
- DUNKEL, M. Z. (1928) Calculation of intermolecular forces in organic compounds. *Phys Chem*, 138, 42-54.
- EMEL'YANENKO, V. N. and VEREVKIN, S. P. (2008) Thermodynamic properties of caffeine: Reconciliation of available experimental data. *The Journal of Chemical Thermodynamics*, 40 (12), 1661-1665.
- ETTER, M. C. (1990) Encoding and decoding hydrogen-bond patterns of organic compounds. *Accounts of Chemical Research*, 23 (4), 120-126.
- ETTER, M. C. (1991) Hydrogen bonds as design elements in organic chemistry. *The Journal of Physical Chemistry*, 95 (12), 4601-4610.
- ETTER, M. C. and REUTZEL, S. M. (1991) Hydrogen bond directed cocrystallization and molecular recognition properties of acyclic imides. *Journal of the American Chemical Society*, 113 (7), 2586-2598.

- FEELY, L. C. and DAVIS, S. S. (1988) The influence of polymeric excipients on drug release from hydroxypropylmethylcellulose matrices. *International Journal of Pharmaceutics*, 44 (1&#x2013;3), 131-139.
- FISCHER, H. C. and CHAN, W. C. W. (2007) Nanotoxicity: the growing need for in vivo study. *Current Opinion in Biotechnology*, 18 (6), 565-571.
- FRISCIC, T. and JONES, W. (2007) Cocrystal architecture and properties: design and building of chiral and racemic structures by solid–solid reactions. *Faraday Discuss.*, 136, 167-178.
- FRIŠČIĆ, T. and JONES, W. (2010) Benefits of cocrystallisation in pharmaceutical materials science: an update. *Journal of Pharmacy and Pharmacology*, 62 (11), 1547-1559.
- GAGNIERE, E., et al. (2009) Cocrystal Formation in Solution: In Situ Solute Concentration Monitoring of the Two Components and Kinetic Pathways. *Crystal Growth & Design*, 9 (8), 3376-3383.
- GHADERI, R., et al. (1999) Preparation of biodegradable microparticles using solution-enhanced dispersion by supercritical fluids (SEDS). *Pharmaceutical Research*, 16 (5), 676-681.
- GOOD, D., et al. (2011) Dependence of cocrystal formation and thermodynamic stability on moisture sorption by amorphous polymer. *CrystEngComm*, 13 (4), 1181-1189.
- GREENHALGH, D. J., et al. (1999) Solubility parameters as predictors of miscibility in solid dispersions. *Journal of Pharmaceutical Sciences*, 88 (11), 1182-1190.
- GRIESSER, U. J. and BURGER, A. (1995) The effect of water vapor pressure on desolvation kinetics of caffeine 4/5-hydrate\* 1. *International Journal of Pharmaceutics*, 120 (1), 83-93.
- GRIESSER, U. J., et al. (1999) Vapor pressure and heat of sublimation of crystal polymorphs. *Journal of thermal analysis and calorimetry*, 57 (1), 45-60.
- GUIDELINE, I. C. H. H. T. (2003) Stability testing of new drug substances and products. *Recommended for Adoption at Step*, 4.
- HICKEY, M. B., et al. (2007) Performance comparison of a co-crystal of carbamazepine with marketed product. *European journal of pharmaceutics and biopharmaceutics*, 67 (1), 112-119.
- HILDEBRAND, J. H. and SCOTT, R. L. (1950) Solutions of Nonelectrolytes. *Annual Review of Physical Chemistry*, 1 (1), 75-92.
- HINO, T. and FORD, J. L. (2001) Characterization of the hydroxypropylmethylcellulose-nicotinamide binary system. *International Journal of Pharmaceutics*, 219 (1&#x2013;2), 39-49.
- HINO, T., et al. (2001) Assessment of nicotinamide polymorphs by differential scanning calorimetry. *Thermochimica Acta*, 374 (1), 85-92.
- HUANG, J., et al. (2008) Drug-polymer interaction and its significance on the physical stability of nifedipine amorphous dispersion in microparticles of an ammonio methacrylate copolymer and ethylcellulose binary blend. *Journal of Pharmaceutical Sciences*, 97 (1), 251-262.

- HUBERT, S., et al. (2011) Process induced transformations during tablet manufacturing: Phase transition analysis of caffeine using DSC and low frequency micro-Raman spectroscopy. *International Journal of Pharmaceutics*.
- IBRAHIM, A. Y., et al. (2010) Spontaneous crystal growth of co-crystals: the contribution of particle size reduction and convection mixing of the co-formers. *CrystEngComm*.
- JAYASANKAR, A. (2008) Understanding the Mechanisms, Thermodynamics and Kinetics of Cocrystallization to Control Phase Transformations.
- JAYASANKAR, A., et al. (2007) Mechanisms by Which Moisture Generates Cocrystals.
- JAYASANKAR, A., et al. (2006a) Cocrystal Formation during Cogrounding and Storage is Mediated by Amorphous Phase. *Pharmaceutical Research*, 23 (10), 2381-2392.
- JAYASANKAR, A., et al. (2006b) Cocrystal formation during cogrounding and storage is mediated by amorphous phase. *Pharmaceutical Research*, 23 (10), 2381-2392.
- JUBERT, A., et al. (2006) Vibrational and theoretical studies of non-steroidal anti-inflammatory drugs Ibuprofen [2-(4-isobutylphenyl)propionic acid]; Naproxen [6-methoxy-[alpha]-methyl-2-naphthalene acetic acid] and Tolmetin acids [1-methyl-5-(4-methylbenzoyl)-1H-pyrrole-2-acetic acid]. *Journal of Molecular Structure*, 783 (1-3), 34-51.
- KABLITZ, C. D. S. E., et al. (2006) Dry coating in a rotary fluid bed. *European Journal of Pharmaceutical Sciences*, 27 (2â€“3), 212-219.
- KANG, B. K., et al. (2004) Development of self-microemulsifying drug delivery systems (SMEDDS) for oral bioavailability enhancement of simvastatin in beagle dogs. *International Journal of Pharmaceutics*, 274 (1â€“2), 65-73.
- KANIG, J. L. (1964) Properties of fused mannitol in compressed tablets. *Journal of Pharmaceutical Sciences*, 53 (2), 188-192.
- KAZARIAN, S. G. and MARTIROSYAN, G. G. (2002) Spectroscopy of polymer/drug formulations processed with supercritical fluids: in situ ATR-IR and Raman study of impregnation of ibuprofen into PVP. *International Journal of Pharmaceutics*, 232 (1-2), 81-90.
- KISHI, Y. and MATSUOKA, M. (2010) Phenomena and Kinetics of Solid-State Polymorphic Transition of Caffeine. *Crystal Growth & Design*, 10 (7), 2916-2920.
- KONNO, H. and TAYLOR, L. S. (2006) Influence of different polymers on the crystallization tendency of molecularly dispersed amorphous felodipine. *Journal of Pharmaceutical Sciences*, 95 (12), 2692-2705.
- KRISTYÁN, S. and PULAY, P. (1994) Can (semi) local density functional theory account for the London dispersion forces? *Chemical physics letters*, 229 (3), 175-180.

- LACOUILONCHE, F., et al. (1997) An investigation of flurbiprofen polymorphism by thermoanalytical and spectroscopic methods and a study of its interactions with poly-(ethylene glycol) 6000 by differential scanning calorimetry and modelling. *International Journal of Pharmaceutics*, 153 (2), 167-179.
- LEUNER, C. and DRESSMAN, J. (2000) Improving drug solubility for oral delivery using solid dispersions. *European Journal of Pharmaceutics and Biopharmaceutics*, 50 (1), 47-60.
- LEVY, G. (1963) Effect of particle size on dissolution and gastrointestinal absorption rates of pharmaceuticals. *American journal of pharmacy and the sciences supporting public health*, 135, 78.
- LI, Z., et al. (2009) A Practical Solid Form Screen Approach To Identify a Pharmaceutical Glutaric Acid Cocrystal for Development. *Organic Process Research & Development*, 13 (6), 1307-1314.
- LIN, S. Y., et al. (1995) Drug-polymer interaction affecting the mechanical properties, adhesion strength and release kinetics of piroxicam-loaded Eudragit E films plasticized with different plasticizers. *Journal of Controlled Release*, 33 (3), 375-381.
- LLOYD, G. R., et al. (1999) A calorimetric investigation into the interaction between paracetamol and polyethylene glycol 4000 in physical mixes and solid dispersions. *European Journal of Pharmaceutics and Biopharmaceutics*, 48 (1), 59-65.
- LONDON, F. (1937) The general theory of molecular forces. *Trans. Faraday Soc.*, 33 (0), 8b-26.
- LOPEZ, D. and MIJANGOS, C. (1994) Effect of solvent on glass transition temperature in chemically modified polyvinyl chloride (PVC). *Colloid & Polymer Science*, 272 (2), 159-167.
- LÓPEZ, D. and MIJANGOS, C. (1994) Effect of solvent on glass transition temperature in chemically modified polyvinyl chloride (PVC). *Colloid & Polymer Science*, 272 (2), 159-167.
- LU, E., et al. (2008) A rapid thermal method for cocrystal screening. *CrystEngComm*, 10 (6), 665-668.
- MAHANTY, J. and NINHAM, B. W. (1976) *Dispersion forces*. Vol. 5. IMA.
- MAHESHWARI, C., et al. (2009a) Factors that influence the spontaneous formation of pharmaceutical cocrystals by simply mixing solid reactants. *CrystEngComm*, 11 (3), 493-500.
- MAHESHWARI, C., et al. (2009b) Factors that influence the spontaneous formation of pharmaceutical cocrystals by simply mixing solid reactants. *CrystEngComm*, 11 (3), 493-500.
- MANDUVA, R., et al. (2008) Calorimetric and spatial characterization of polymorphic transitions in caffeine using quasi isothermal MTDSC and localized thermomechanical analysis. *Journal of Pharmaceutical Sciences*, 97 (3), 1285-1300.
- MARSAC, P., et al. (2009) Estimation of Drug-Polymer Miscibility and Solubility in Amorphous Solid Dispersions Using Experimentally Determined Interaction Parameters. *Pharmaceutical Research*, 26 (1), 139-151.

- MAYERSOHN, M. and GIBALDI, M. (1966) New method of solid state dispersion for increasing dissolution rates. *Journal of Pharmaceutical Sciences*, 55 (11), 1323-1324.
- MCNAMARA, D., et al. (2006) Use of a Glutaric Acid Cocrystal to Improve Oral Bioavailability of a Low Solubility API. *Pharmaceutical Research*, 23 (8), 1888-1897.
- MIRZA, S., et al. (2008) Co-crystals: An emerging approach to improving properties of pharmaceutical solids. In: *19th Helsinki Drug Research*. Helsinki, FINLAND: Elsevier Science Bv, pp. S16-S17.
- MOHAMMAD, M. A., et al. (2011) Hansen solubility parameter as a tool to predict cocrystal formation. *International Journal of Pharmaceutics*.
- MURDANDE, S. B., et al. (2011) Solubility advantage of amorphous pharmaceuticals, part 3: Is maximum solubility advantage experimentally attainable and sustainable? *Journal of Pharmaceutical Sciences*.
- NAKAYAMA, S., et al. (2009) Structure and properties of ibuprofen-hydroxypropyl methylcellulose nanocomposite gel. *Powder Technology*, In Press, Corrected Proof.
- OGUCHI, T., et al. (2000) Specific complexation of ursodeoxycholic acid with guest compounds induced by co-grinding. *Physical Chemistry Chemical Physics*, 2 (12), 2815-2820.
- PADRELA, L., et al. (2010) Screening for pharmaceutical cocrystals using the supercritical fluid enhanced atomization process. *The Journal of Supercritical Fluids*, 53 (1-3), 156-164.
- PADRELA, L., et al. (2009) Formation of indomethacin-saccharin cocrystals using supercritical fluid technology. *European Journal of Pharmaceutical Sciences*, 38 (1), 9-17.
- PAN, R. N., et al. (2000) Enhancement of dissolution and bioavailability of piroxicam in solid dispersion systems. *Drug development and industrial pharmacy*, 26 (9), 989-994.
- PATEL, T., et al. Enhancement of dissolution of Fenofibrate by Solid dispersion Technique. *Intern J Res Pharm Sci*, 1 (2), 127-132.
- PATRA, B. B. and SAMANTRAY, B. (2011) *Engineering Chemistry I*. Pearson Education India.
- PATRICK, J. J., et al. (1998) Characterization of impurities formed by interaction of duloxetine HCl with enteric polymers hydroxypropyl methylcellulose acetate succinate and hydroxypropyl methylcellulose phthalate. *Journal of Pharmaceutical Sciences*, 87 (1), 81-85.
- PEDIREDDI, V. R., et al. (1996) Creation of crystalline supramolecular arrays: a comparison of co-crystal formation from solution and by solid-state grinding. *Chemical Communications*, (8), 987-988.
- POKHARKAR, V. B., et al. (2006) Development, characterization and stabilization of amorphous form of a low Tg drug. *Powder Technology*, 167 (1), 20-25.
- PORTER III, W. W., et al. (2008) Polymorphism in carbamazepine cocrystals. *Crystal Growth and Design*, 8 (1), 14-16.

- PUTTIPIPATKHACHORN, S., et al. (2001) Drug physical state and drug-polymer interaction on drug release from chitosan matrix films. *Journal of Controlled Release*, 75 (1-2), 143-153.
- REDDY, L. S., et al. (2008) Cocrystals and salts of gabapentin: pH dependent cocrystal stability and solubility. *Crystal Growth and Design*, 9 (1), 378-385.
- REMENAR, J. F., et al. (2003) Crystal engineering of novel cocrystals of a triazole drug with 1, 4-dicarboxylic acids. *J. Am. Chem. Soc*, 125 (28), 8456-8457.
- RIEDEL, A. and LEOPOLD, C. S. (2005) Degradation of omeprazole induced by enteric polymer solutions and aqueous dispersions: HPLC investigations. *Drug development and industrial pharmacy*, 31 (2), 151-160.
- RODIER, E., et al. (2005) A three step supercritical process to improve the dissolution rate of Eflucimibe. *European Journal of Pharmaceutical Sciences*, 26 (2), 184-193.
- RODRÍGUEZ-HORNEDO, N., et al. (2006) Reaction crystallization of pharmaceutical molecular complexes. *Molecular Pharmaceutics*, 3 (3), 362-367.
- SANDER, J. R. G., et al. (2010) Pharmaceutical Nano-Cocrystals: Sonochemical Synthesis by Solvent Selection and Use of a Surfactant. *Angewandte Chemie*, 122 (40), 7442-7446.
- SCHULTHEISS, N. and NEWMAN, A. (2009) Pharmaceutical Cocrystals and Their Physicochemical Properties. *Crystal Growth & Design*, 9 (6), 2950-2967.
- SEKIGUCHI, K., et al. (1964) Studies on absorption of eutectic mixture. ii. absorption of fused conglomerates of chloramphenicol and urea in rabbits. *Chemical & Pharmaceutical Bulletin*, 12, 134.
- SEKIGUCHI KEIJI and OBI NOBORU (1961) Studies on Absorption of Eutectic Mixture. I. A Comparison of the Behavior of Eutectic Mixture of Sulfathiazole and that of Ordinary Sulfathiazole in Man. *Chemical & Pharmaceutical Bulletin*, 9 (11), 866-872.
- SEO, A., et al. (2003) The preparation of agglomerates containing solid dispersions of diazepam by melt agglomeration in a high shear mixer. *International Journal of Pharmaceutics*, 259 (1-2), 161-171.
- SHAN, N., et al. (2002) Mechanochemistry and co-crystal formation: effect of solvent on reaction kinetics. *Chemical Communications*, 2002 (20), 2372-2373.
- SHAN, N. and ZAWOROTKO, M. J. (2008) The role of cocrystals in pharmaceutical science. *Drug Discovery Today*, 13 (9-10), 440-446.
- SHIN-ETSU (2005) *Shin-Etsu AQOAT*.
- SONG, J. S. and SOHN, Y. T. (2011) Crystal forms of naproxen. *Archives of pharmacal research*, 34 (1), 87-90.
- STANTON, M. K., et al. (2009) Drug substance and former structure property relationships in 15 diverse pharmaceutical co-crystals. *Crystal Growth and Design*, 9 (3), 1344-1352.



- STOTT, P. W., et al. (1998) Transdermal delivery from eutectic systems: enhanced permeation of a model drug, ibuprofen. *Journal of Controlled Release*, 50 (1-3), 297-308.
- STROYER, A., et al. (2006) Solid state interactions between the proton pump inhibitor omeprazole and various enteric coating polymers. *Journal of Pharmaceutical Sciences*, 95 (6), 1342-1353.
- TANNO, F., et al. (2004) Evaluation of hypromellose acetate succinate (HPMCAS) as a carrier in solid dispersions. *Drug development and industrial pharmacy*, 30 (1), 9-17.
- TIMKO, R. J. and LORDI, N. G. (1979) Thermal characterization of citric acid solid dispersions with benzoic acid and phenobarbital. *Journal of Pharmaceutical Sciences*, 68 (5), 601-605.
- TRASK, A. V. and JONES, W. (2005a) Crystal engineering of organic cocrystals by the solid-state grinding approach. In: *Organic Solid State Reactions*. (Topics in Current Chemistry) Vol. 254. Berlin: Springer-Verlag Berlin, pp. 41-70.
- TRASK, A. V. and JONES, W. (2005b) Crystal Engineering of Organic Cocrystals by the Solid-State Grinding Approach  
Organic Solid State Reactions. In: TODA, F. (Ed.) (Topics in Current Chemistry) Vol. 254. Springer Berlin / Heidelberg, pp. 131-131.
- TRASK, A. V., et al. (2005) Pharmaceutical cocrystallization: Engineering a remedy for caffeine hydration. *Crystal Growth & Design*, 5 (3), 1013-1021.
- TRASK, A. V., et al. (2006) Physical stability enhancement of theophylline via cocrystallization. *International Journal of Pharmaceutics*, 320 (1-2), 114-123.
- VAN DEN MOOTER, G., et al. (2006) Evaluation of Inutec SP1 as a new carrier in the formulation of solid dispersions for poorly soluble drugs. *International Journal of Pharmaceutics*, 316 (1-2), 1-6.
- VAN DROOGE, D. J., et al. (2006) Characterization of the molecular distribution of drugs in glassy solid dispersions at the nano-meter scale, using differential scanning calorimetry and gravimetric water vapour sorption techniques. *International Journal of Pharmaceutics*, 310 (1-2), 220-229.
- VARIANKAVAL, N., et al. (2006) Preparation and solid-state characterization of nonstoichiometric cocrystals of a phosphodiesterase-IV inhibitor and L-tartaric acid. *Crystal Growth & Design*, 6 (3), 690-700.
- VASCONCELOS, T. and COSTA, P. (2007) Development of a rapid dissolving ibuprofen solid dispersion.
- VASCONCELOS, T. F., et al. (2007) Solid dispersions as strategy to improve oral bioavailability of poor water soluble drugs. *Drug Discovery Today*, 12 (23-24), 1068-1075.
- VERRECK, G., et al. (2005) The effect of pressurized carbon dioxide as a temporary plasticizer and foaming agent on the hot stage extrusion process and extrudate properties of solid dispersions of itraconazole with PVP-VA 64. *European Journal of Pharmaceutical Sciences*, 26 (3-4), 349-358.

- VIPPAGUNTA, S. R., et al. (2007) Factors affecting the formation of eutectic solid dispersions and their dissolution behavior. *Journal of Pharmaceutical Sciences*, 96 (2), 294-304.
- VISHWESHWAR, P., et al. (2006) Pharmaceutical co-crystal. *Journal of Pharmaceutical Sciences*, 95 (3), 499-516.
- VOGURI, R. S. (2010). *Co-crystallisation of  $\alpha,\omega$ -dicarboxylic acids with nicotinamide and isonicotinamide*. MSc. University of Birmingham.
- VOGURI, R. S. (sep 2010a). *Co-crystallisation of  $\alpha,\omega$ -dicarboxylic acids with nicotinamide and isonicotinamide*. MSc. University of Birmingham.
- VOGURI, R. S. (Sep 2010b). *CO-CRYSTALLISATION OF  $\alpha,\omega$ -DICARBOXYLIC ACIDS WITH NICOTINAMIDE AND ISONICOTINAMIDE*. MASTER OF RESEARCH. University of Birmingham.
- WANG, C., et al. (2007) Effect of Drug-Polymer Interaction on Drug Diffusion through Polymeric Membranes. *Journal of Medical and Biological Engineering*, 27 (1), 35.
- WANG, X., et al. (2005) Solid state characteristics of ternary solid dispersions composed of PVP VA64, Myrj 52 and itraconazole. *International Journal of Pharmaceutics*, 303 (1â€“2), 54-61.
- WARD, S. C., et al. (2003) Systematic study into the salt formation of functionalised organic substrates. *School of chemistry, University of Southampton, SO 17BJ, UK School mathematics, University of Southampton, SO 17BJ, UK*.
- WHELAN, M. R., et al. (2002) Simultaneous determination of ibuprofen and hydroxypropylmethylcellulose (HPMC) using HPLC and evaporative light scattering detection. *Journal of Pharmaceutical and Biomedical Analysis*, 30 (4), 1355-1359.
- YAMAGUCHI, H. and TOMINAGA, T. (2006) Fine particles of poorly water-soluble drug having enteric material adsorbed on particle surface. Google Patents.
- YAMAGUCHI, H. and TOMINAGA, T. (2008) Microparticle of hardly-soluble substance having enteric base material adsorbed on the surface of the substance. EP Patent 1,923,051.
- YOSHIHASHI, Y., et al. (2006) Estimation of physical stability of amorphous solid dispersion using differential scanning calorimetry. *Journal of thermal analysis and calorimetry*, 85 (3), 689-692.

## Appendix I (TGA)

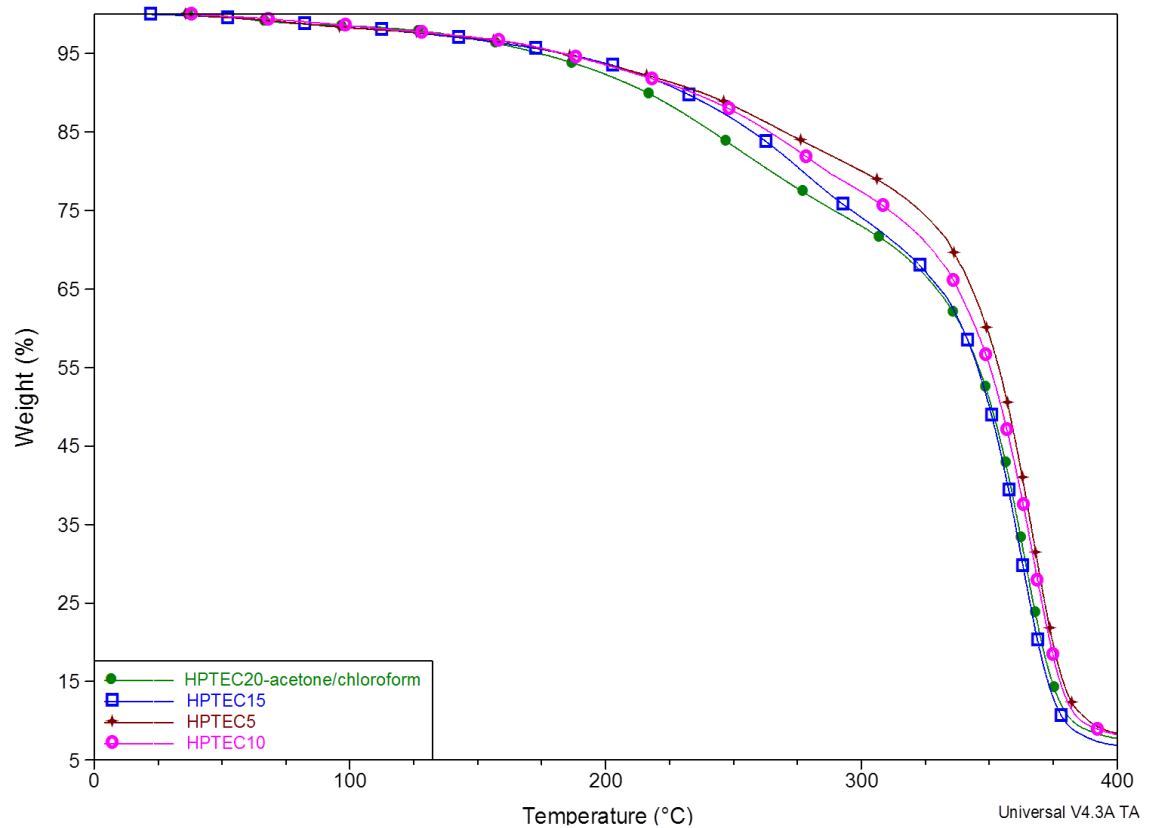


Figure Al.1. TGA scan of HPMCAS films containing TEC prepared with acetone/chloroform.

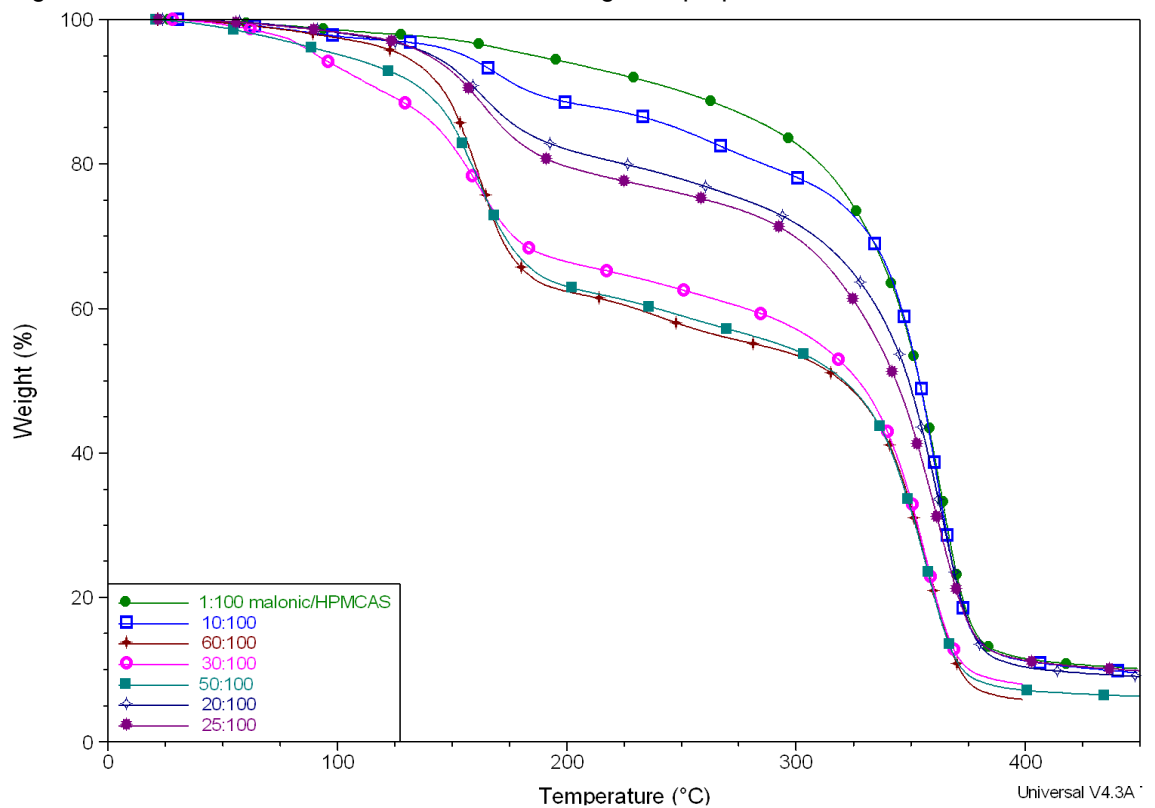


Figure Al.2. TGA scan of HPMCAS films containing 1:100, 10:100, 20:100, 25:100, 30:100, 50:100, and 60:100 w/w malonic acid/HPMCAS.

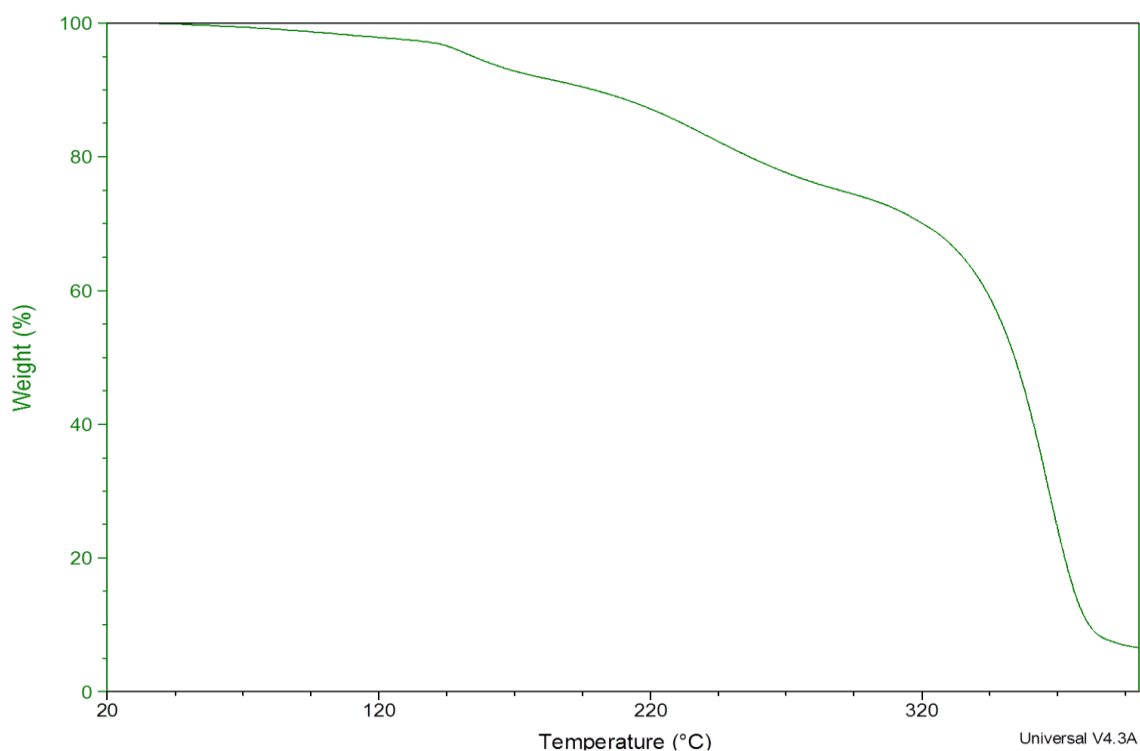


Figure A1.3. A representative TGA thermal profile for a film containing caffeine and malonic acid prepared using acetone/chloroform.

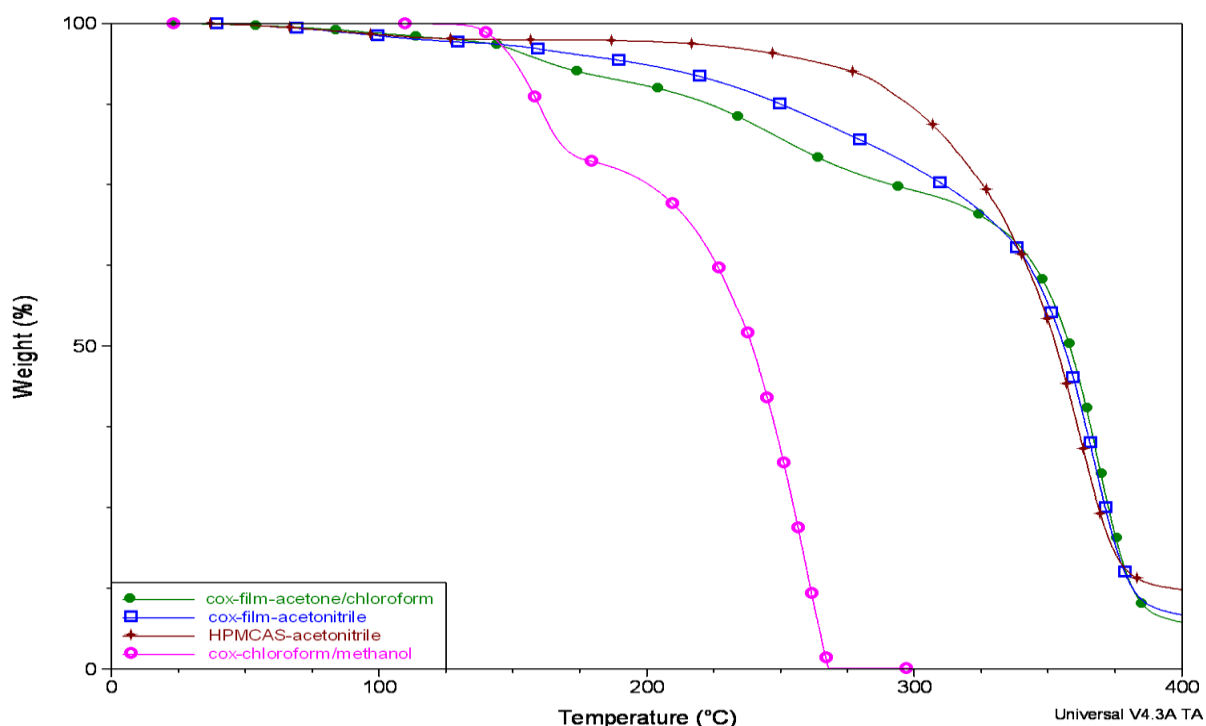


Figure A1.4. Representative TGA thermal profile for co-crystals prepared with chloroform/methanol (pink), HPMCAS film prepared using acetonitrile (red), film containing co-crystals prepared with acetone/chloroform (green), and film containing co-crystals prepared with acetonitrile (blue).

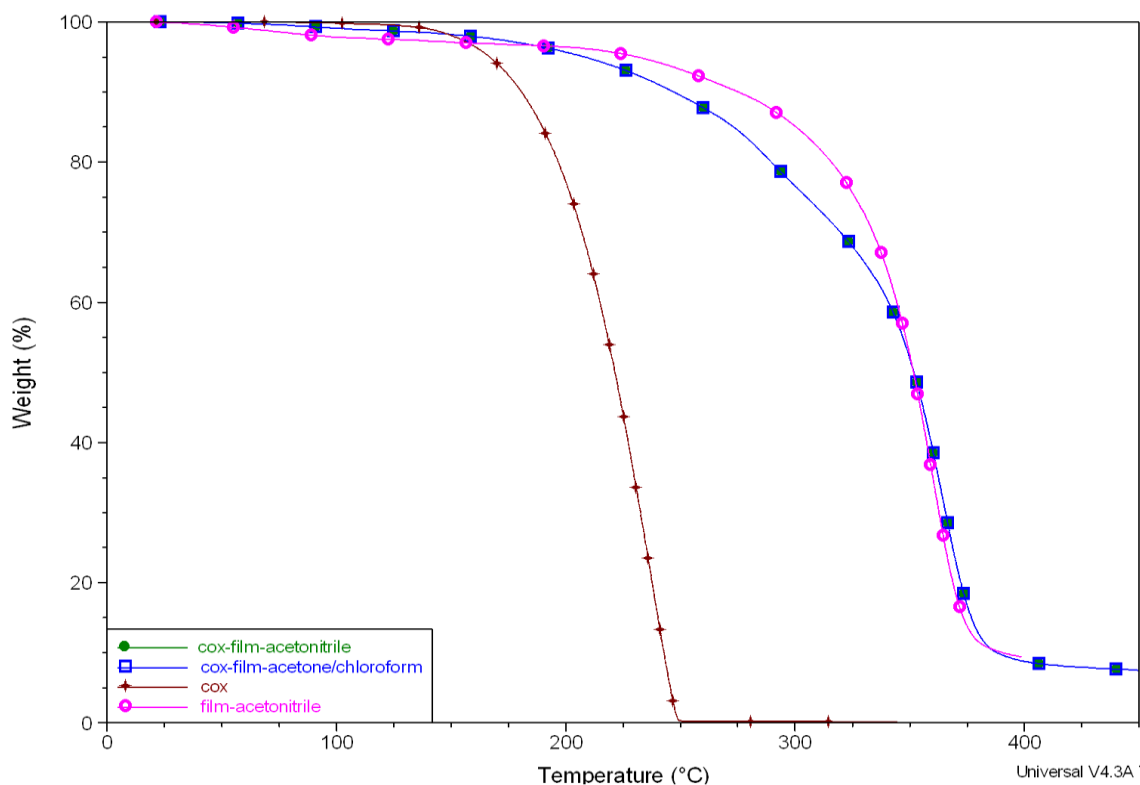


Figure A1.5. Representative TGA thermal profile for plain film (pink), co-crystals of ibuprofen and nicotinamide (red), films containing co-crystals prepared with acetonitrile (green), and a film containing co-crystals prepared with acetone/chloroform (blue).

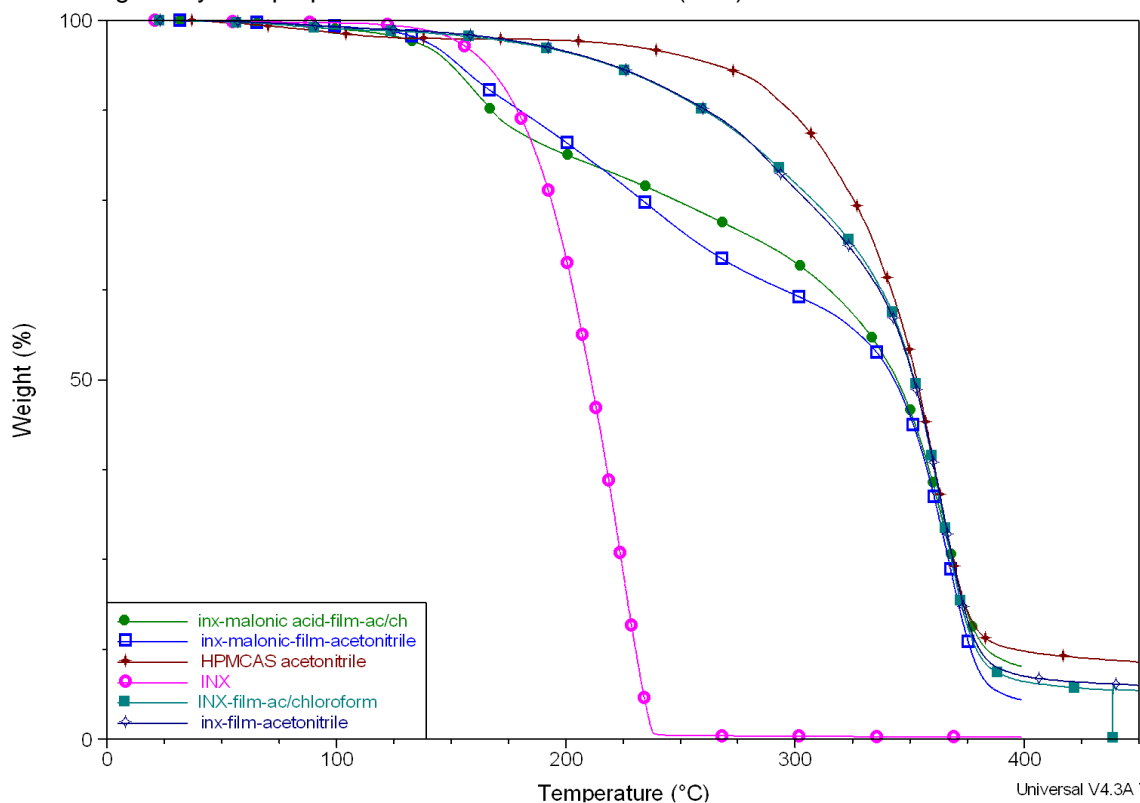


Figure A1.6. Representative thermal analysis for films containing ibuprofen-nicotinamide co-crystals and malonic acid prepared using acetone/chloroform (green) and acetonitrile (blue), films containing co-crystals alone prepared using acetone/chloroform (teal) and acetonitrile (dark blue), and co-crystals of ibuprofen and nicotinamide (pink).

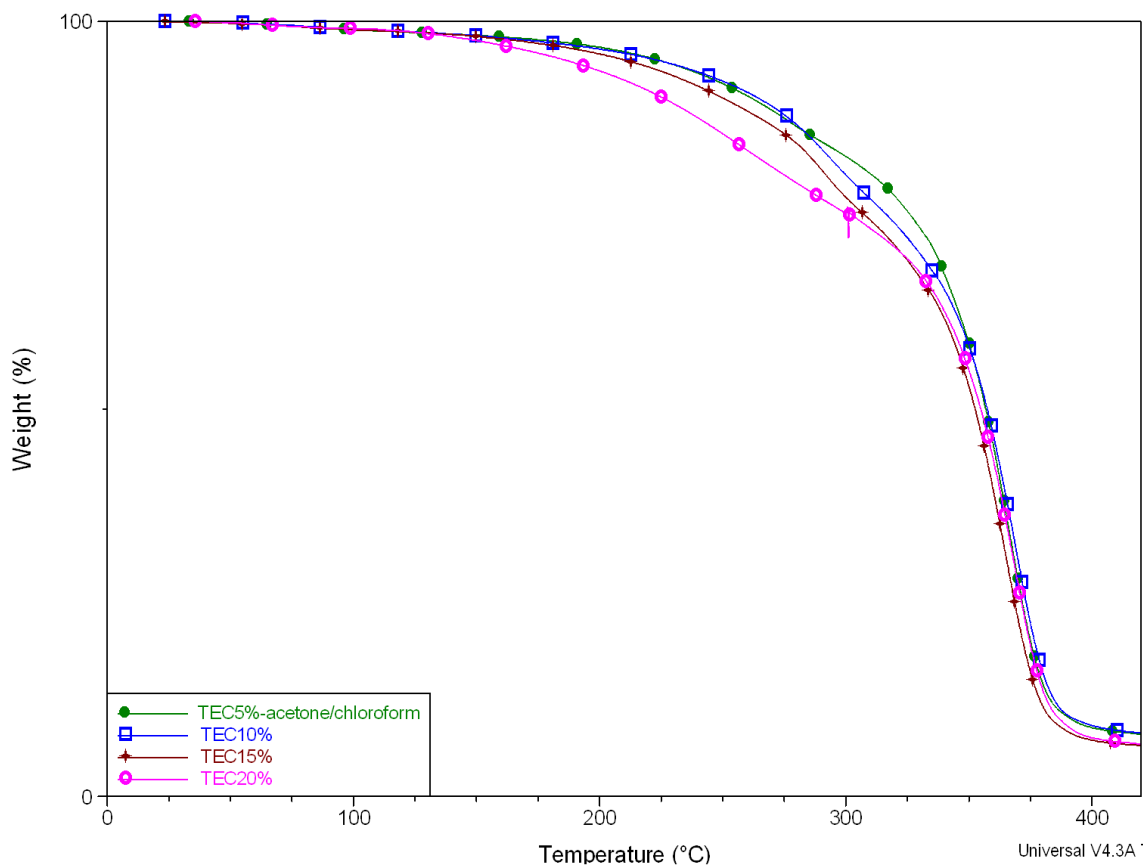


Figure AI.7. Representative TGA thermal profiles for films containing: 5% (green), 10% (blue), 15% (red), and 20% (pink) of TEC.

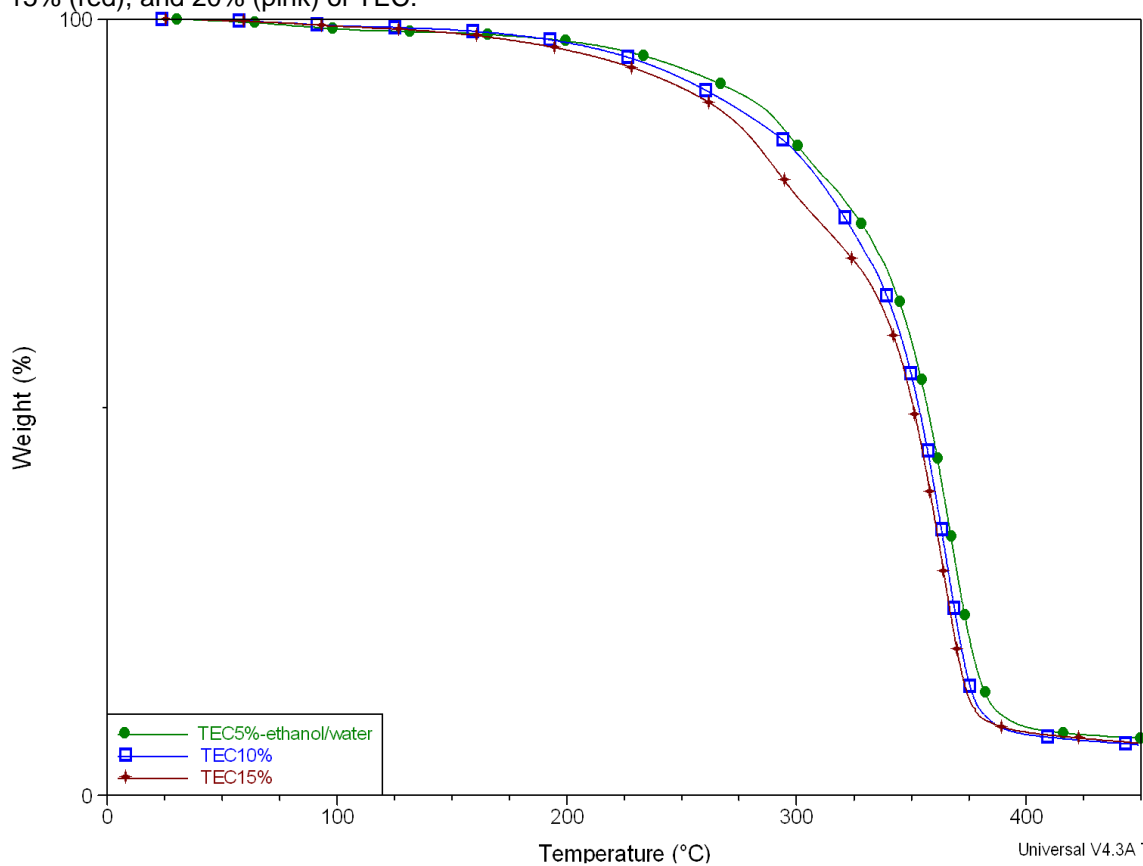


Figure AI.8. Representative TGA thermal profiles for films containing: 5% (green), 10% (blue), and 15% (red) of TEC.

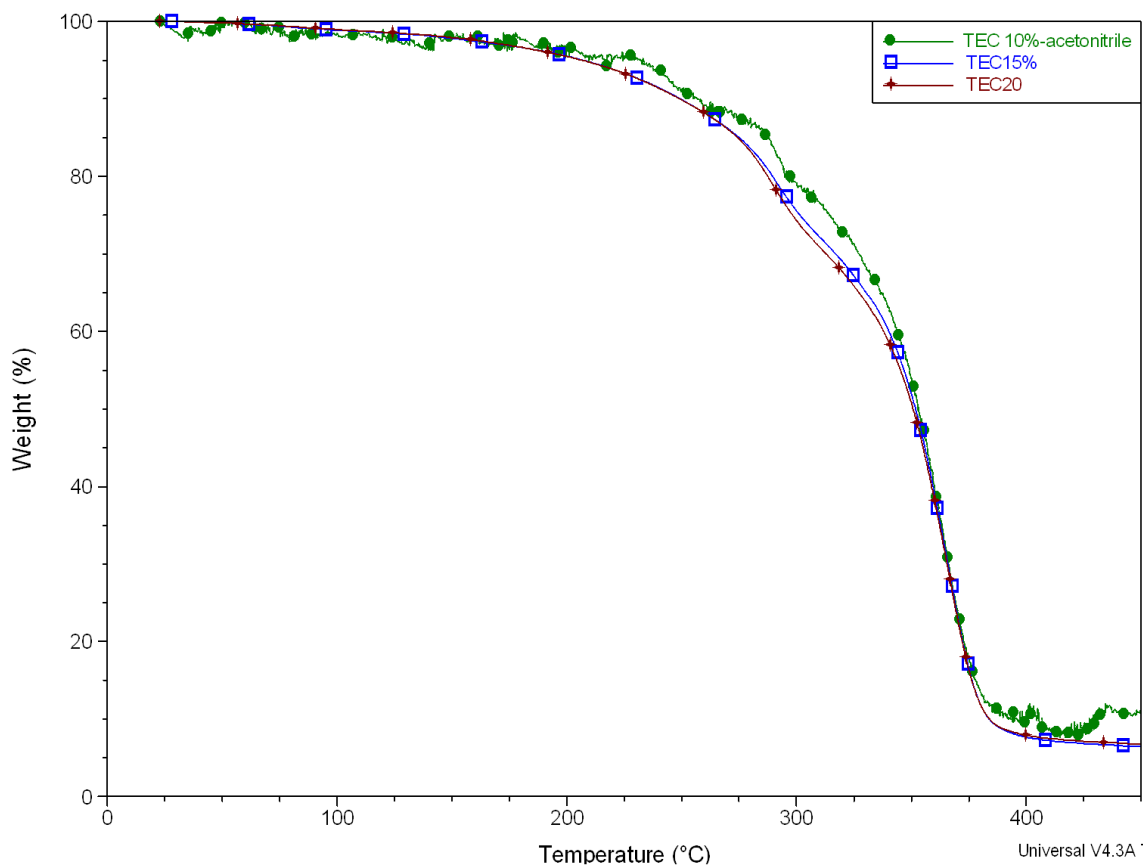


Figure AI.9. Representative TGA thermal profiles for films containing: 10% (green), 15% (blue), and 20% (red) of TEC.

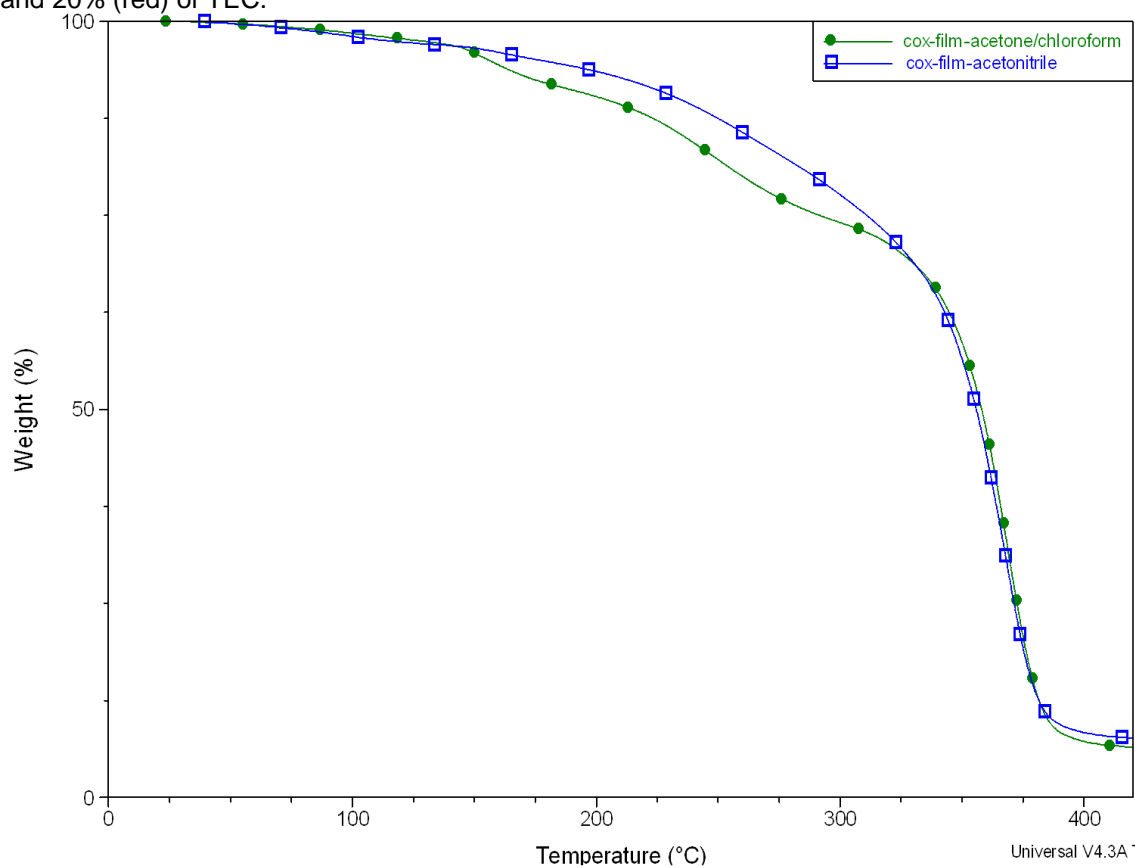


Figure AI. 10. Representative thermal TGA profiles for films containing caffeine-malonic acid co-crystals prepared using acetone/chloroform or acetonitrile.

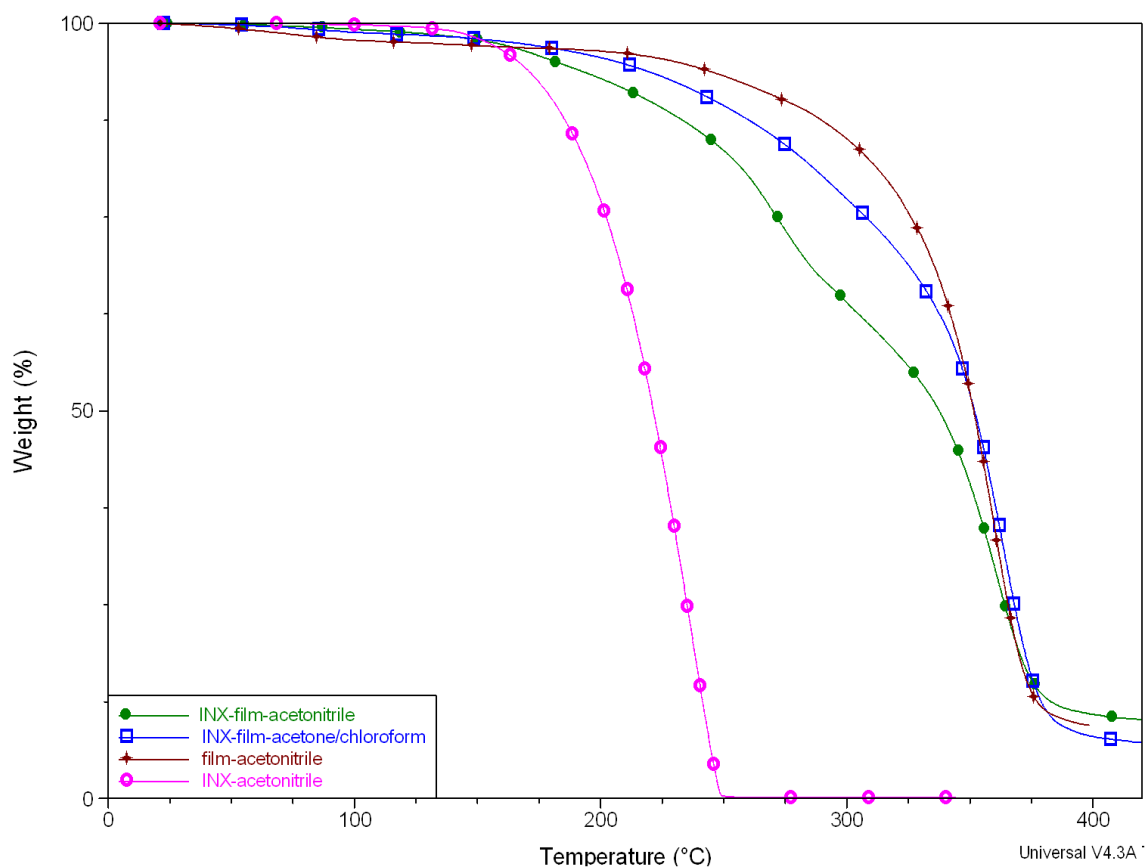


Figure AI. 11. Representative thermal profiles for films containing ibuprofen-nicotinamide co-crystals prepared with either acetonitrile (green) or acetone/chloroform (blue), plain film prepared with acetonitrile (red), and ibuprofen-nicotinamide co-crystals (pink).



## Appendix II (DSC)

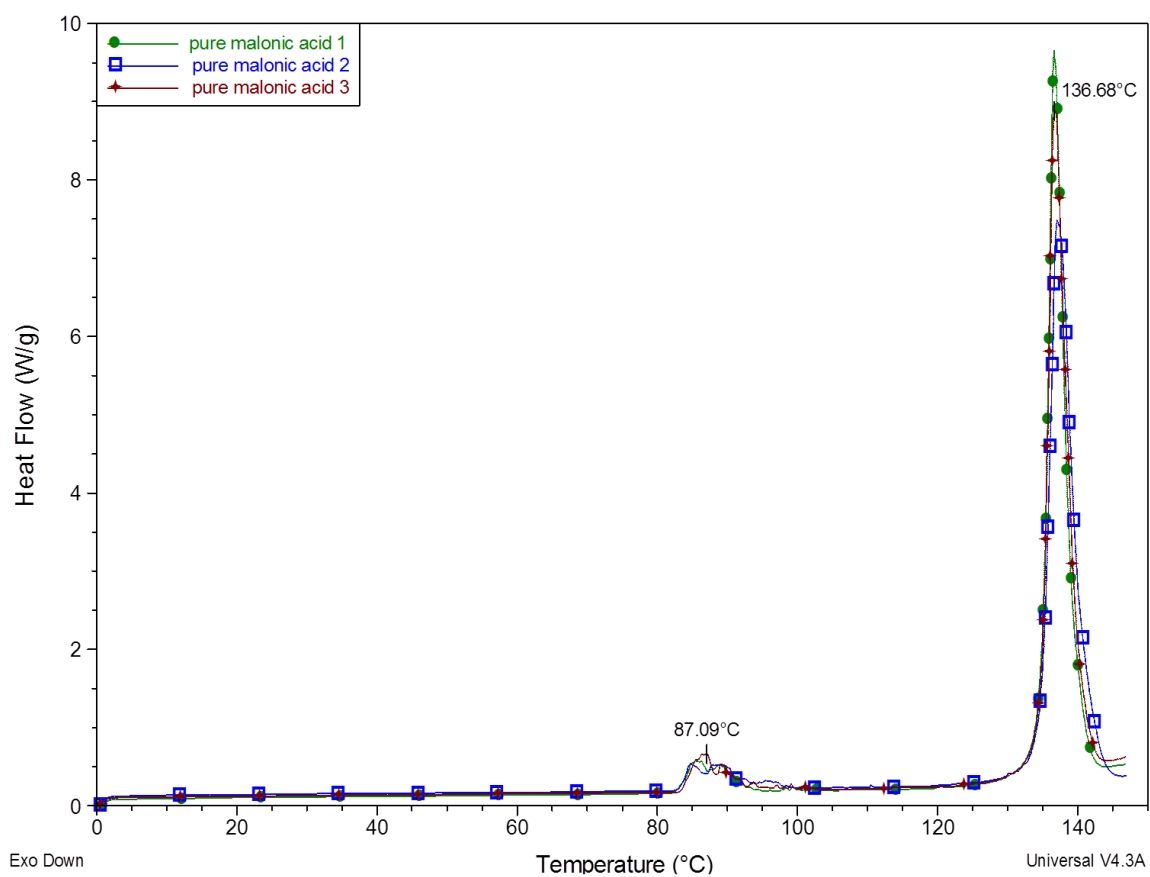


Figure All.1, DSC triplicate scan of pure malonic acid.

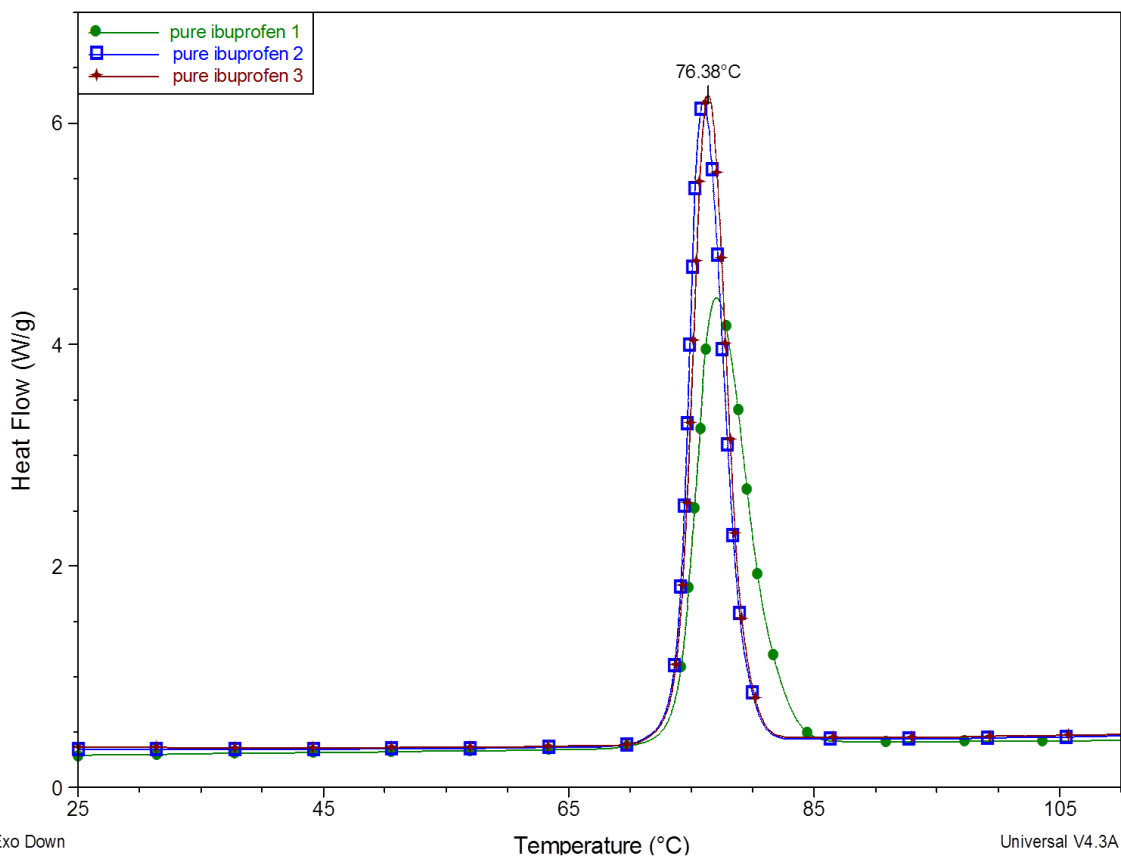


figure All.2. DSC triplicate scan of pure ibuprofen.

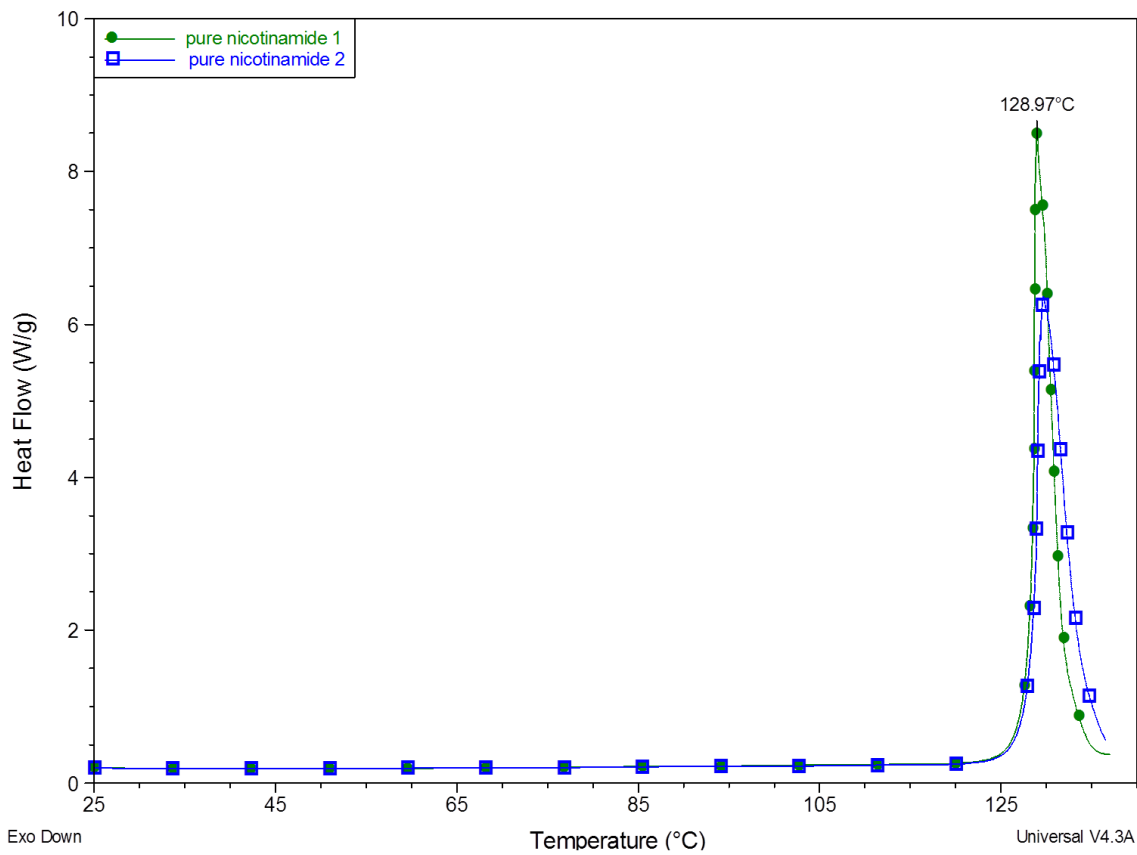


Figure All.3. DSC duplicate scan of pure nicotinamide.

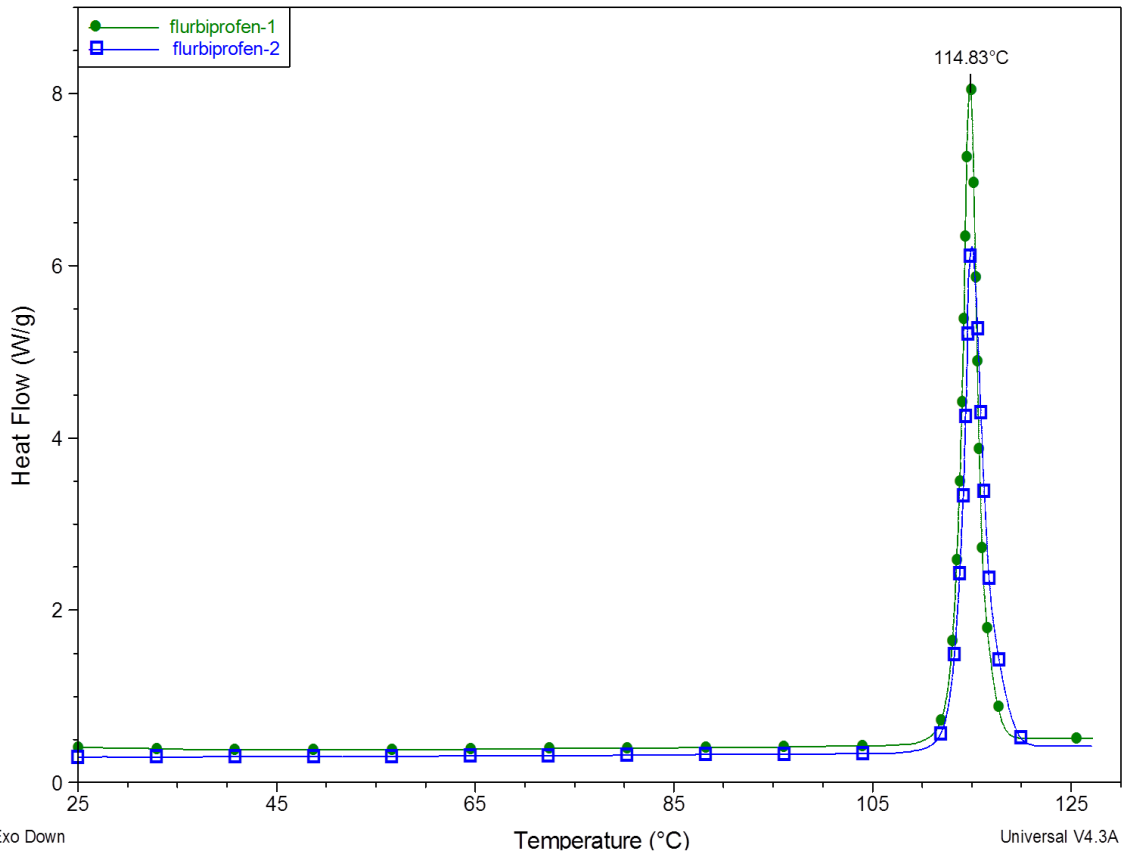


figure AII.4. DSC duplicate scan of pure flurbiprofen.

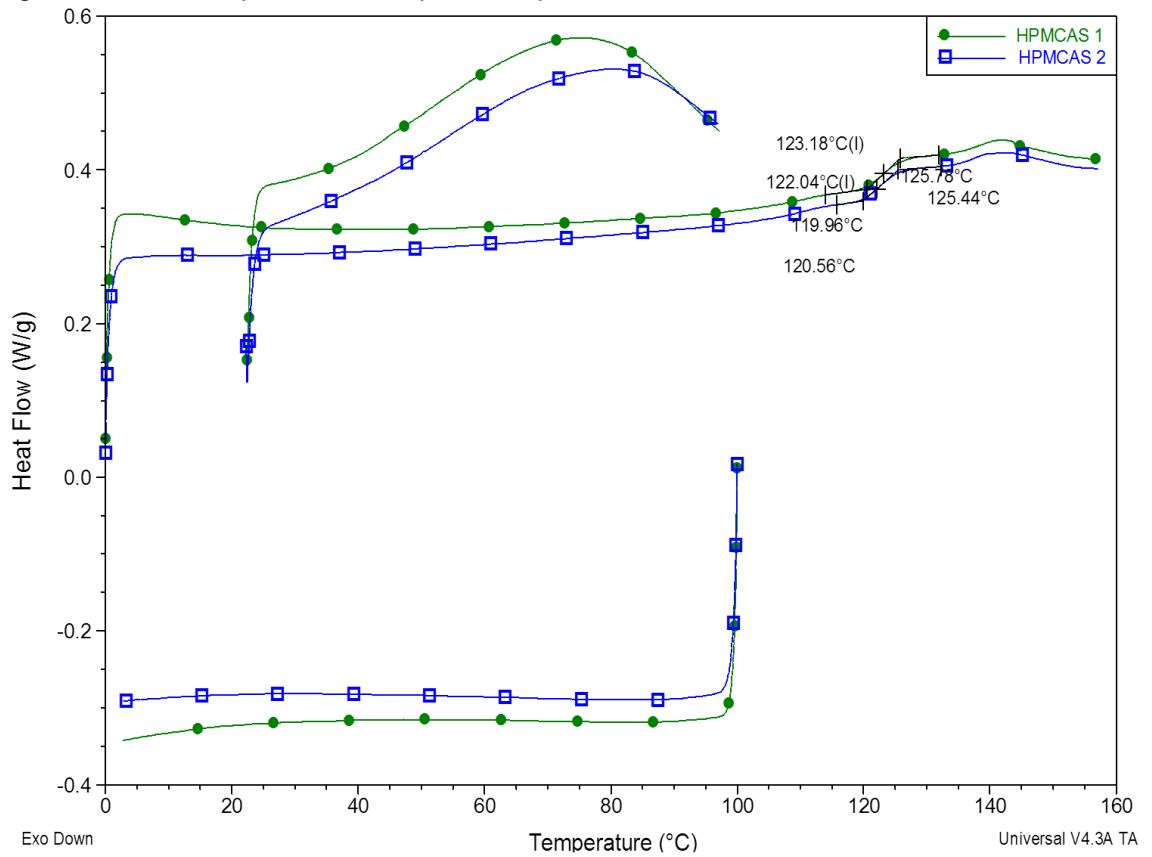


Figure AII.5. DSC duplicate scan of pure HPMCAS.

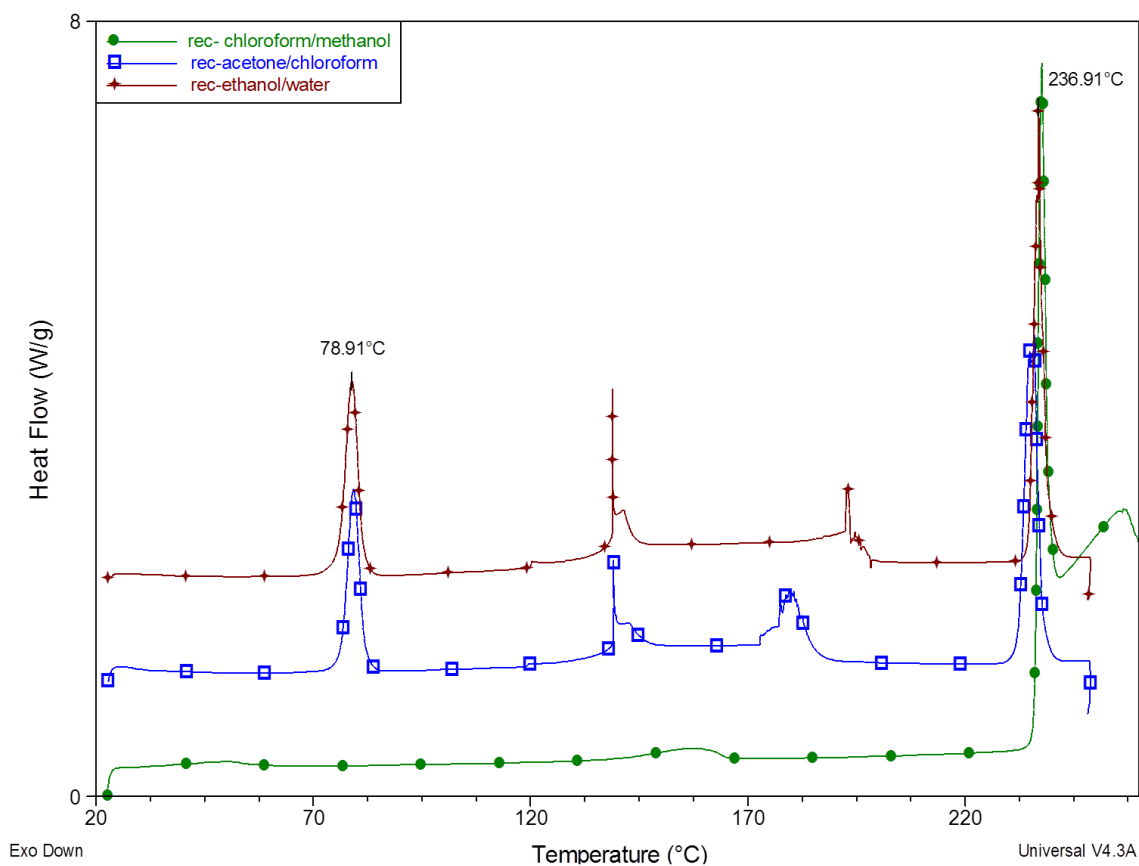


Figure AII.6. DSC scan of caffeine recrystallised with chloroform/methanol, acetone/chloroform, and ethanol water. First heating cycle.

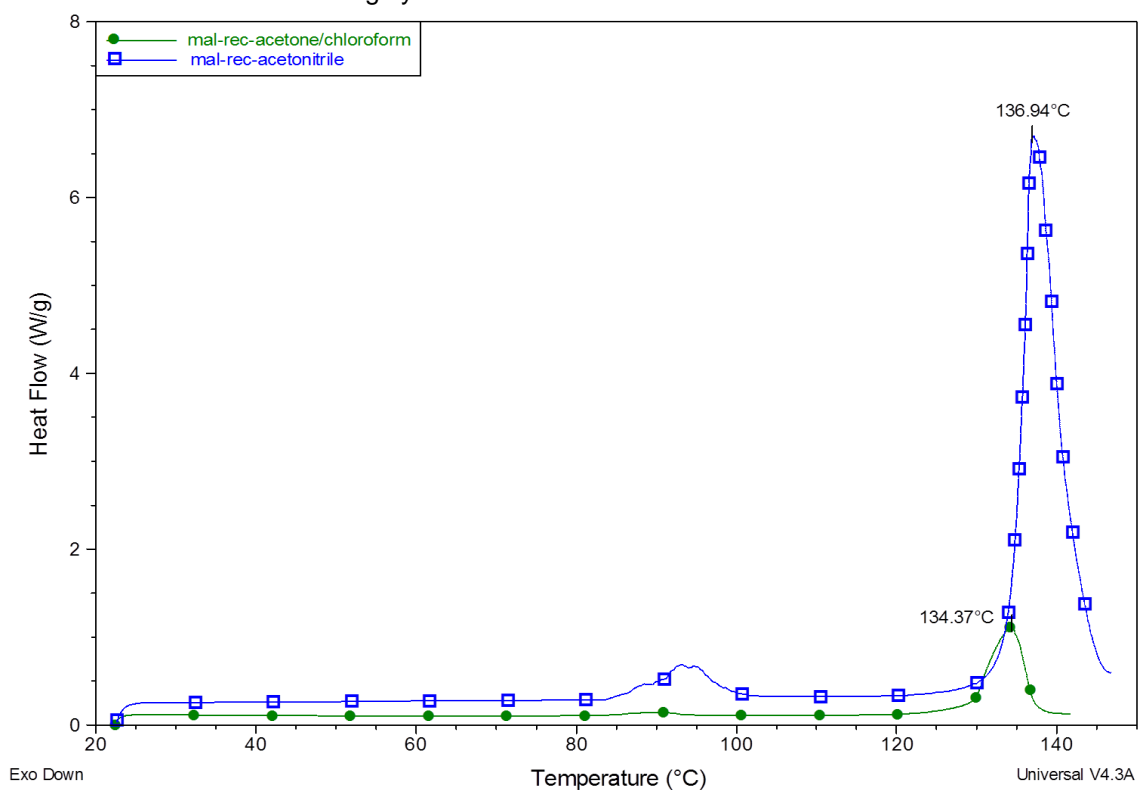


Figure AII.7. DSC scan of malonic acid recrystallised with acetone/chloroform and acetonitrile.

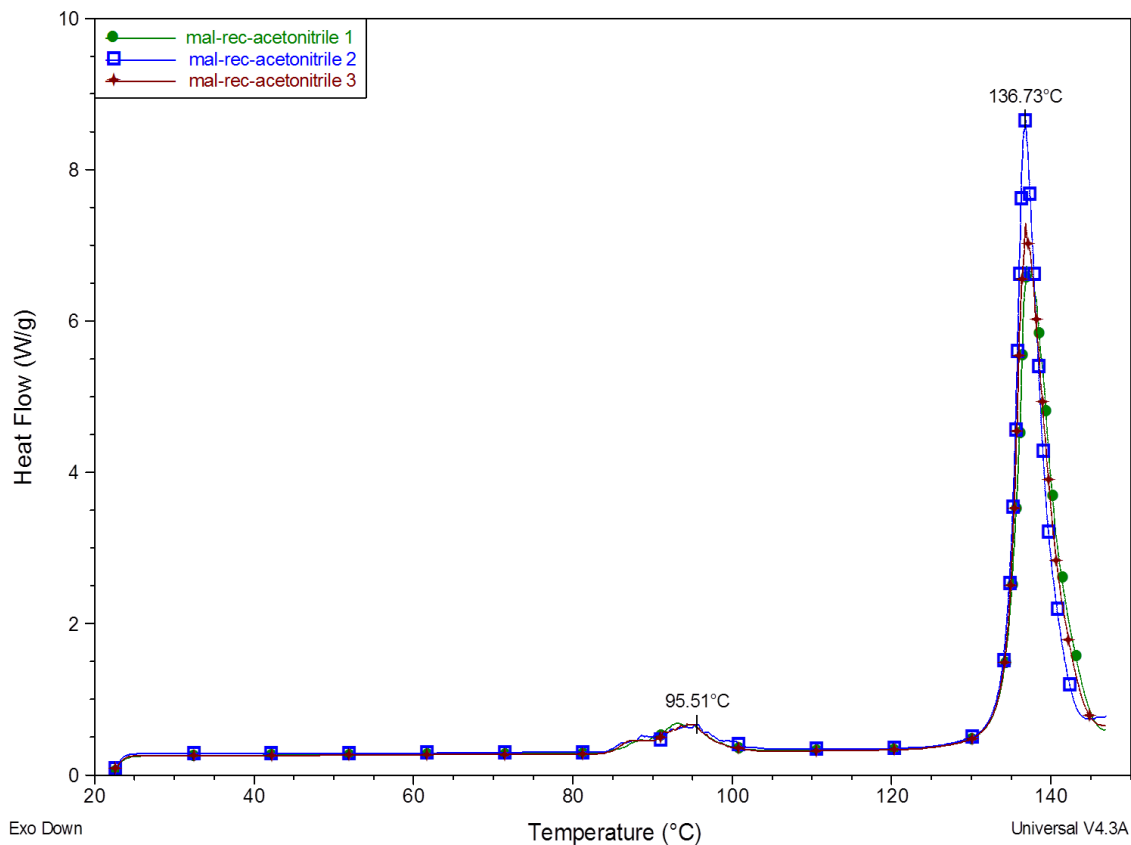


Figure All.8. DSC scan of malonic acid recrystallised with acetonitrile.

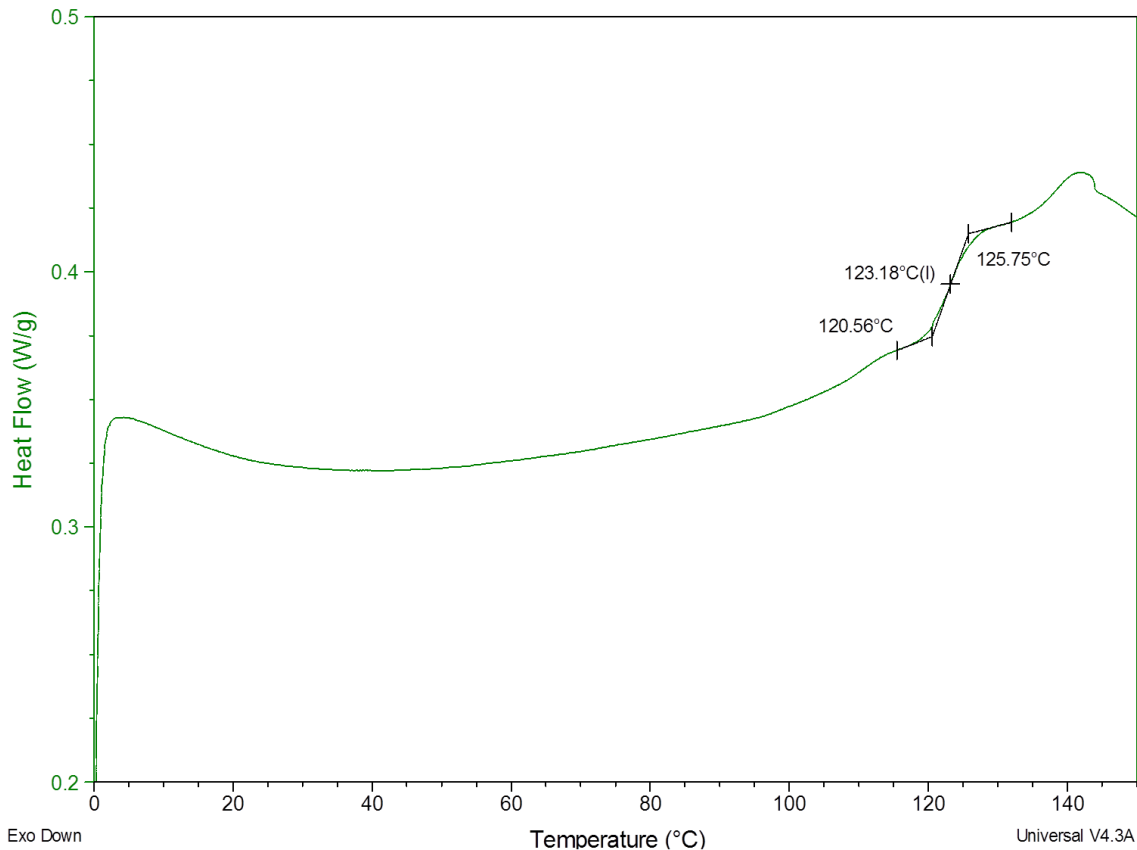


Figure All.9, DSC scan of pure HPMCAS showing the Tg of the pure material.

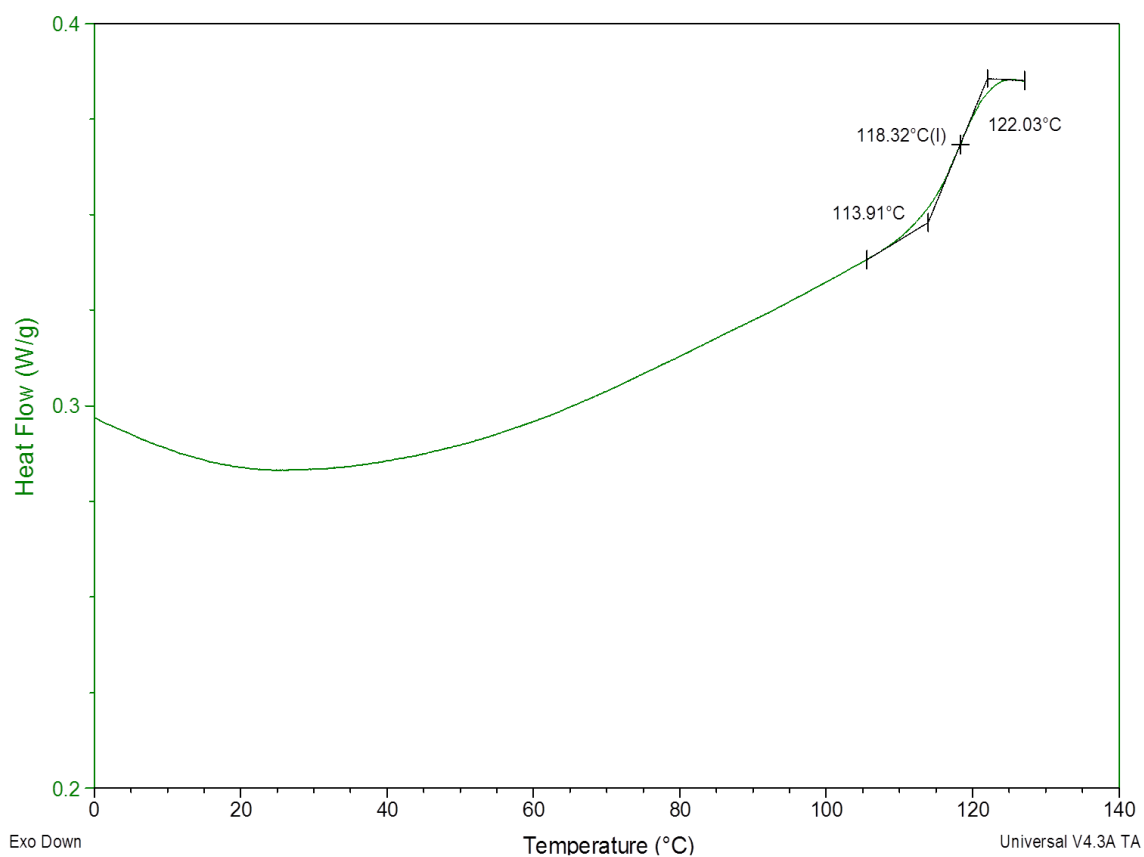


Figure All.10. DSC scan of cast HPMCAS film using acetonitrile for preparation.

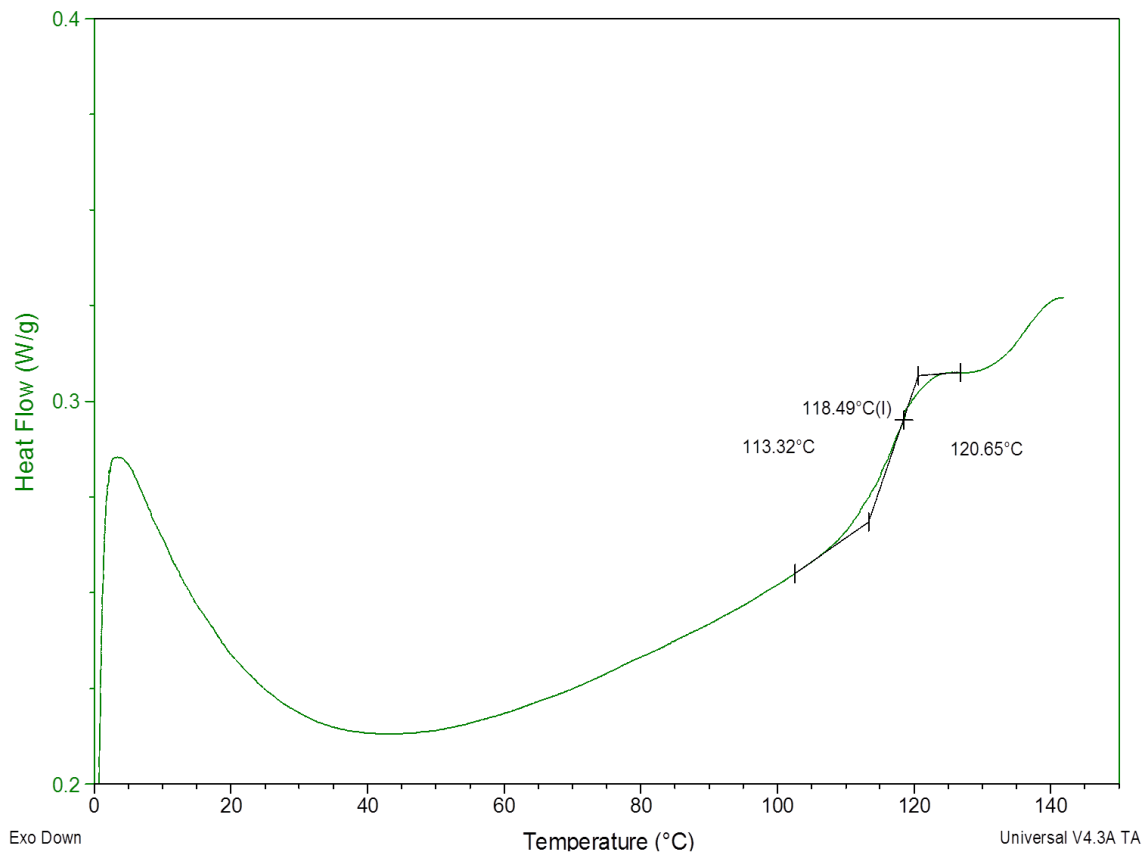


Figure All.11. DSC scan of cast HPMCAS film using ethanol/water for preparation.

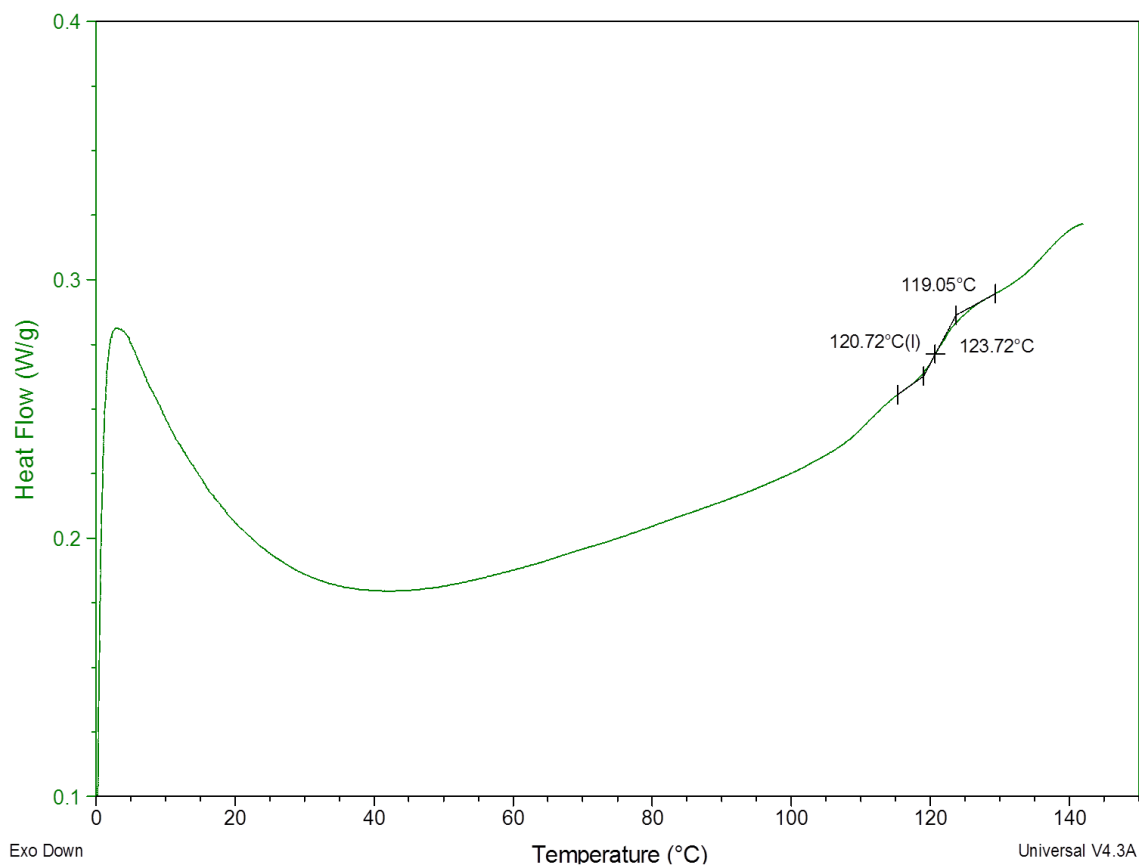


Figure All.12. DSC scan of cast HPMCAS film using acetone/chloroform for preparation.

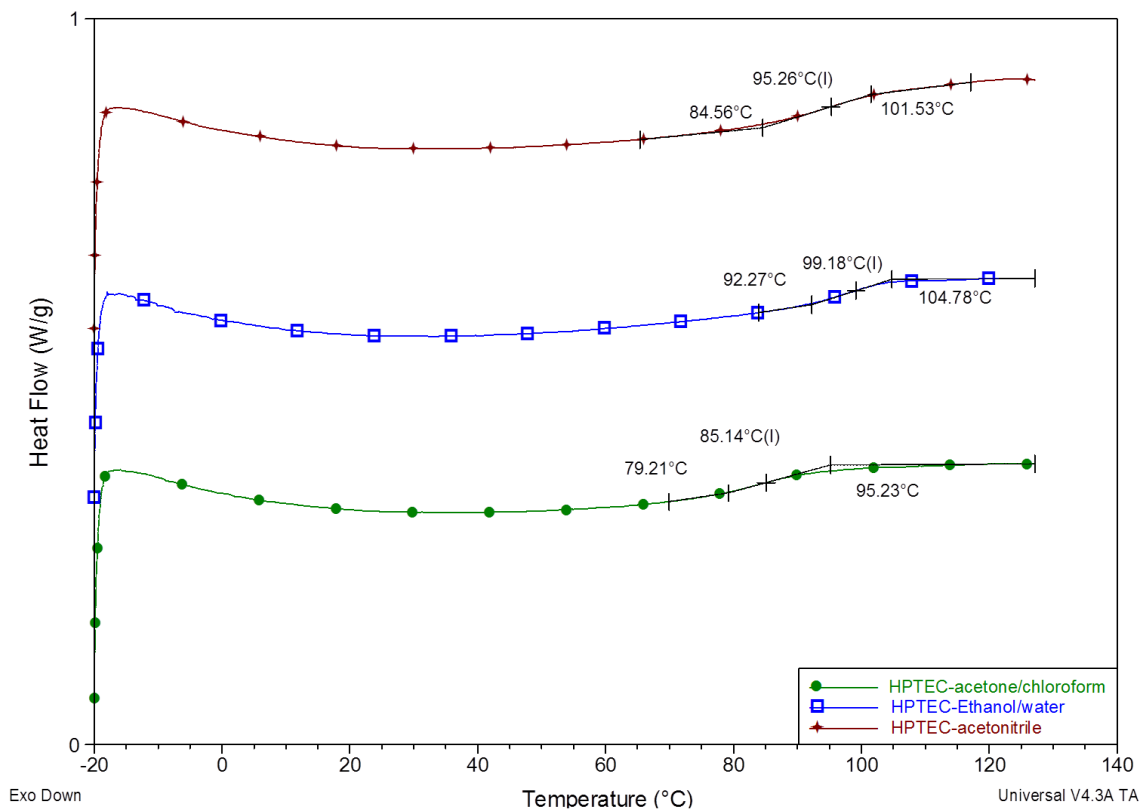


Figure All.13. DSC scan of three films of HPMCAS containing 5% TEC prepared with acetone/chloroform, ethanol/water, and acetonitrile.

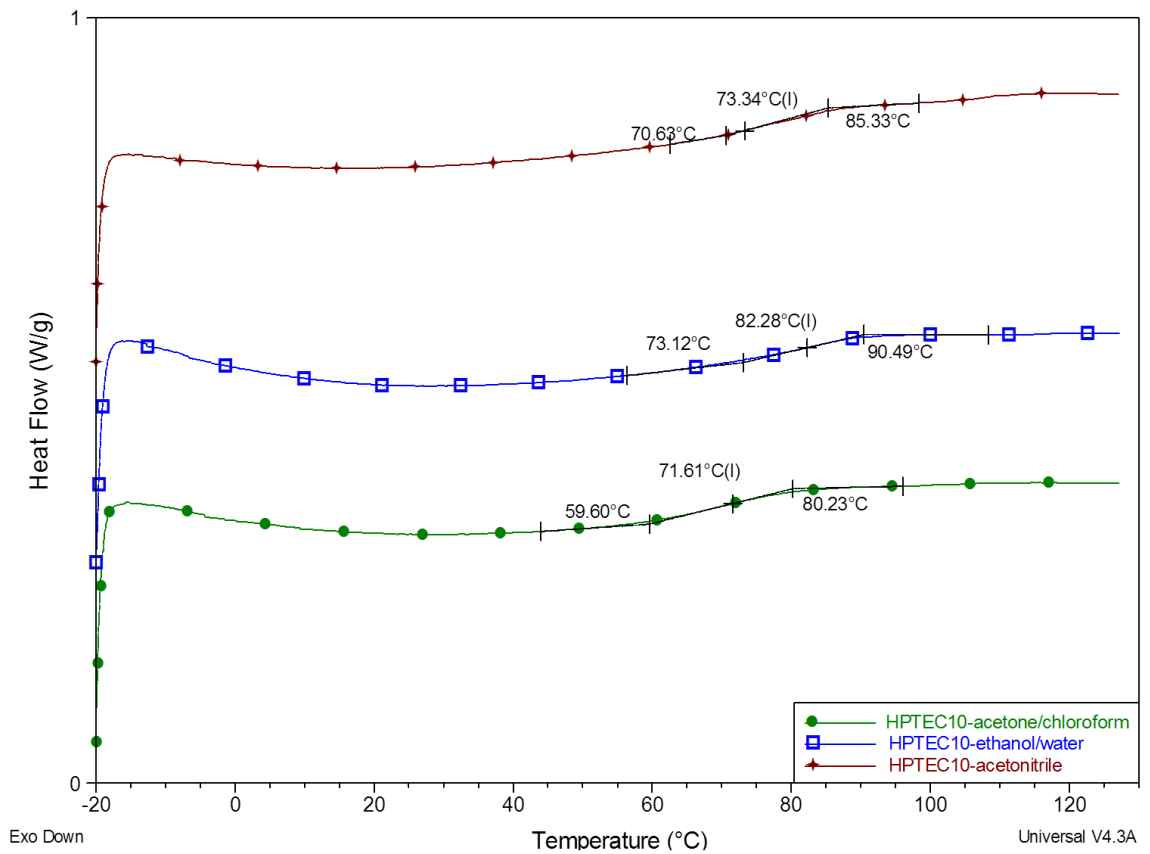


Figure AII.14. DSC scan of HPMCAS films containing 10% TEC prepared with acetone/chloroform, ethanol/water, and acetonitrile.

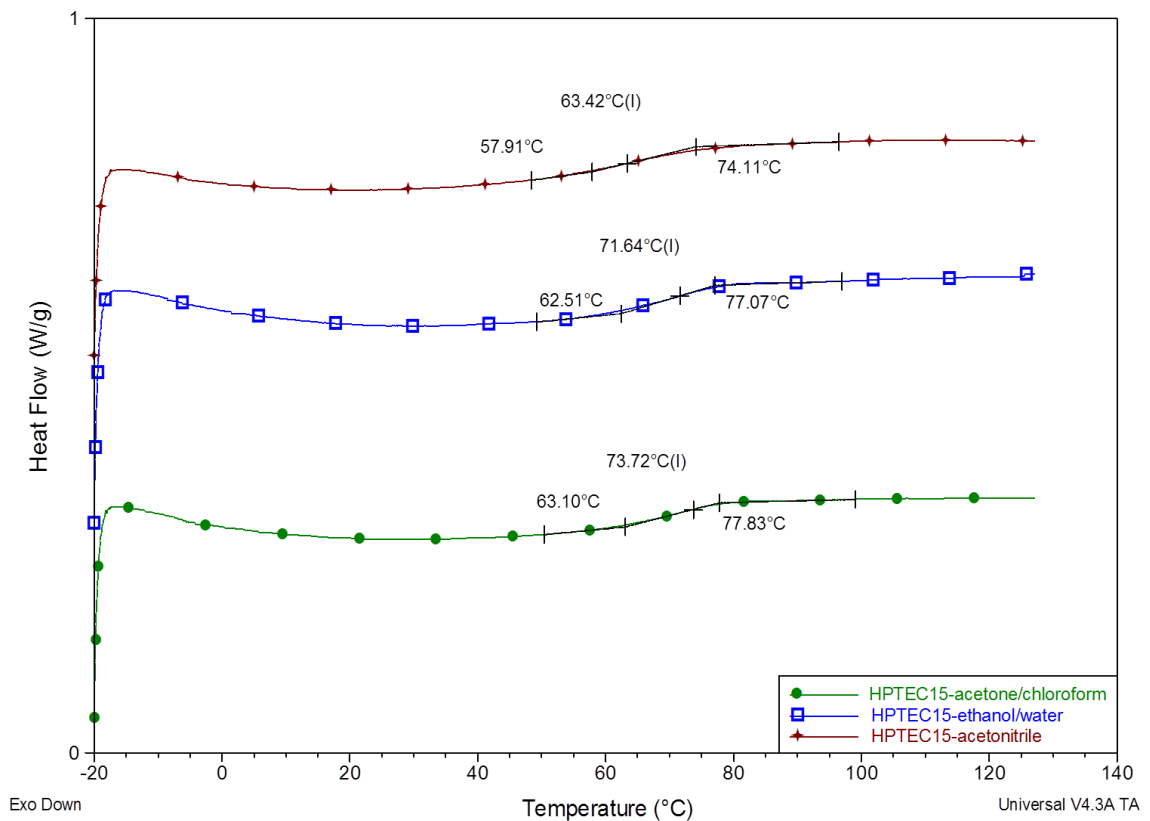


Figure AII.15. DSC scan of HPMCAS films containing 15% TEC prepared with acetone/chloroform, ethanol/water, and acetonitrile.



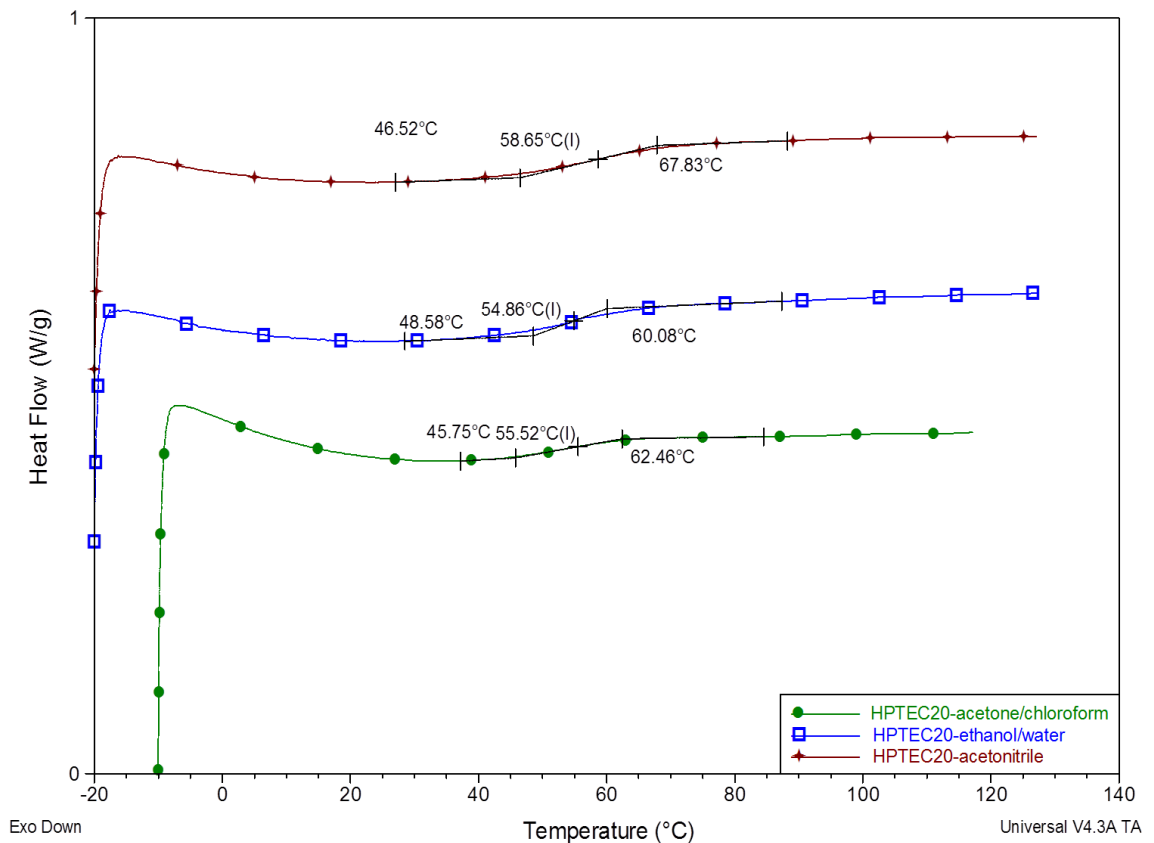


Figure AII.16. DSC scan of HPMCAS films containing 20% TEC prepared with acetone/chloroform, ethanol/water, and acetonitrile.

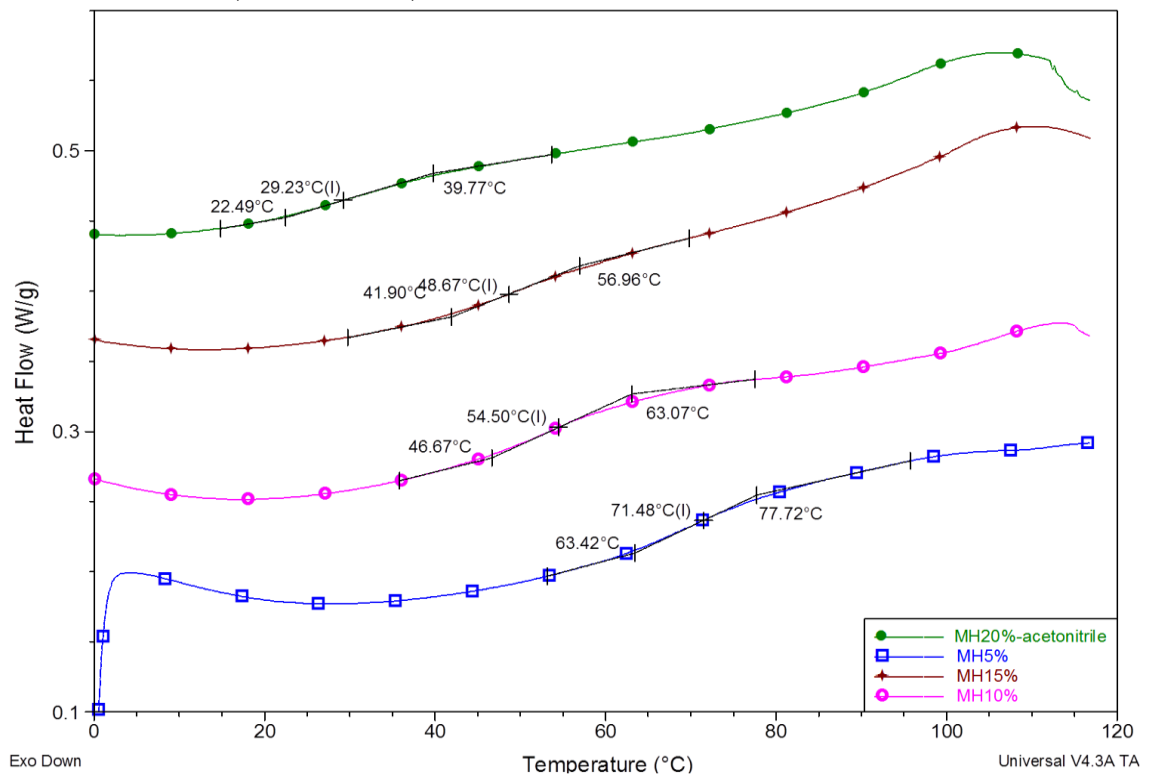


Figure AII.17. DSC scan of HPMCAS containing an ascending concentrations of malonic acid, prepared with acetonitrile.

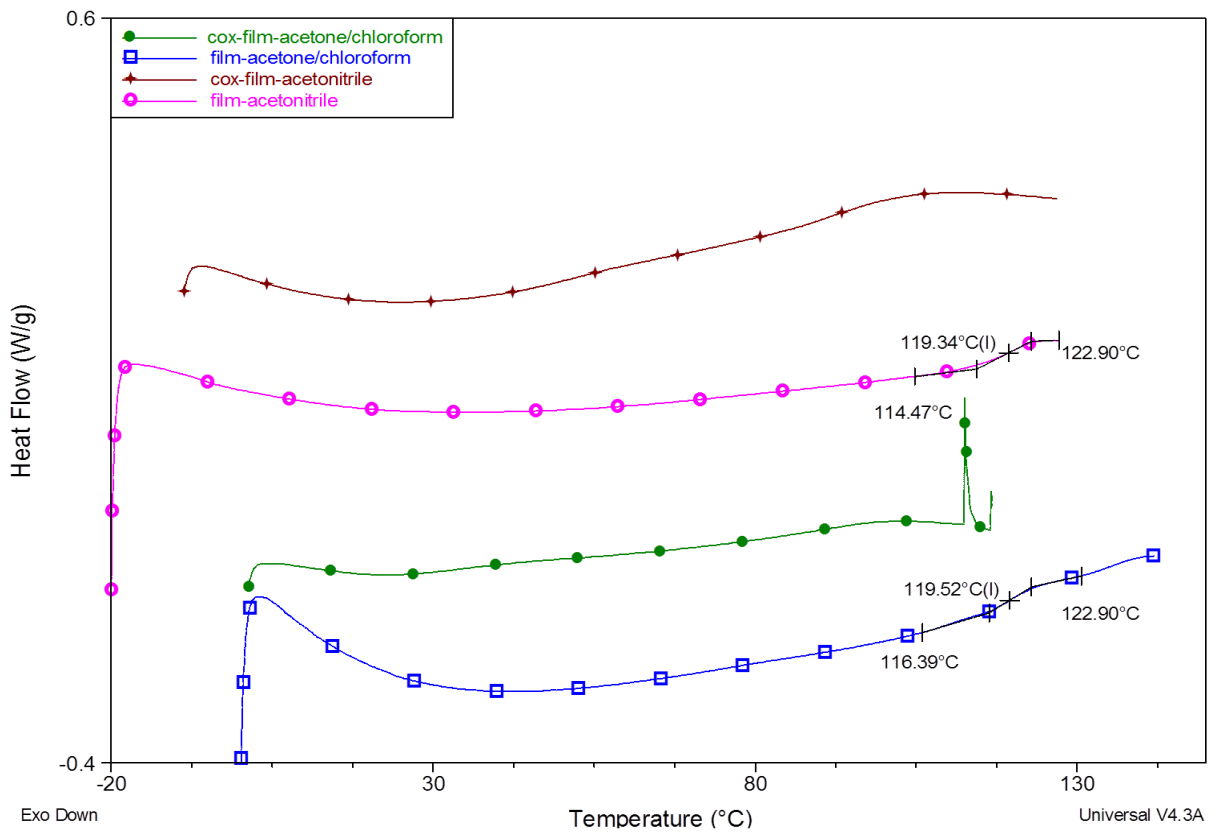


Figure AII.18. Representative DSC thermal profiles for a plain film prepared using acetonitrile (pink), a film prepared using acetone/chloroform (blue), a film containing co-crystals prepared using acetonitrile (red), and a film containing co-crystals prepared using acetone/chloroform (green).

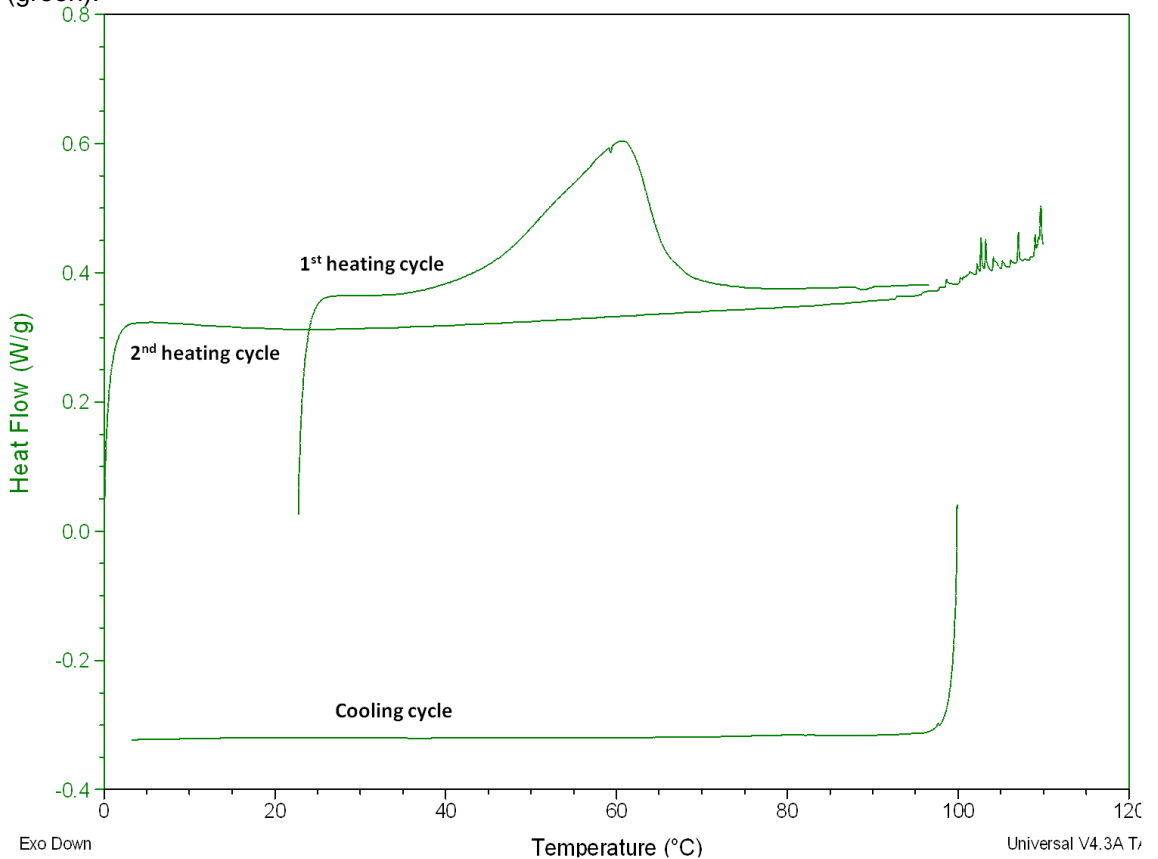


Figure All. 19. A representative of the thermal DSC profile for a film containing 3:4:10 ibuprofen/malonic acid/HPMCAS prepared using ethanol/water.

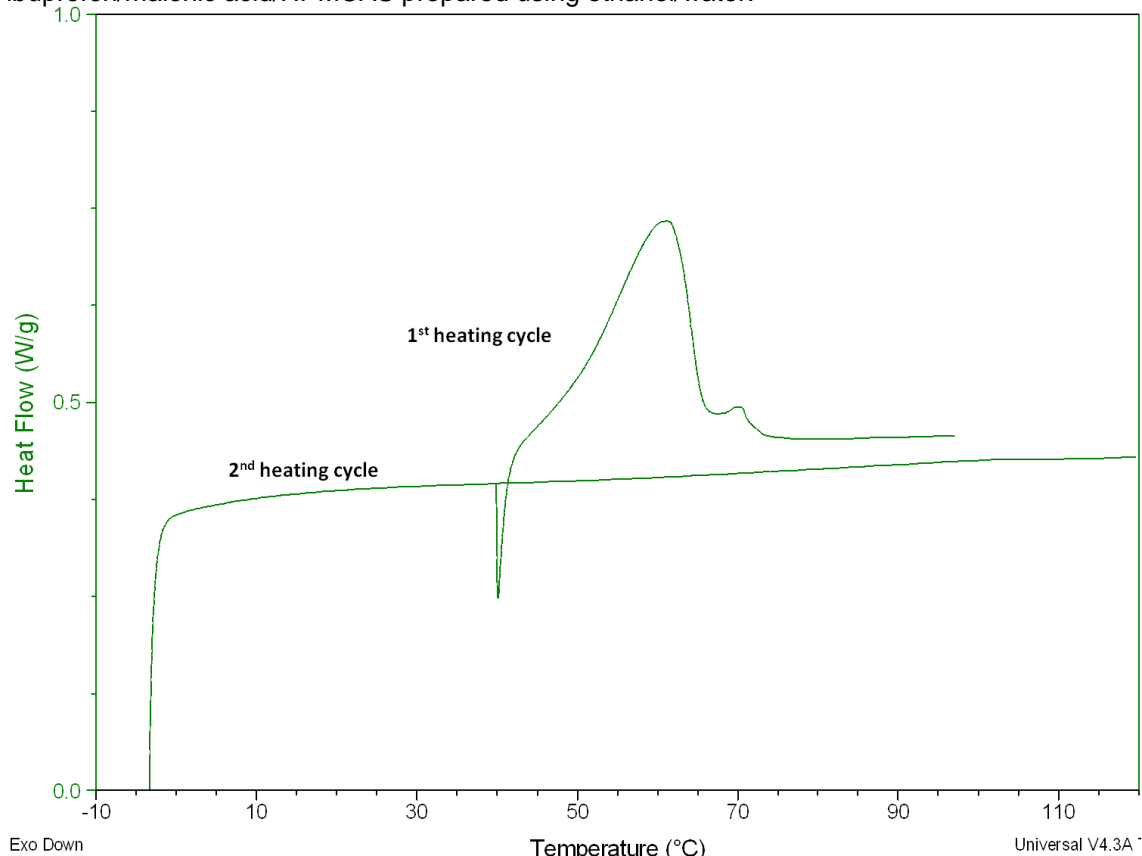


Figure All. 20. A representative thermal DSC profile for a film containing 3:2:10 w/w/w ibuprofen/malonic acid/HPMCAS prepared using acetonitrile.

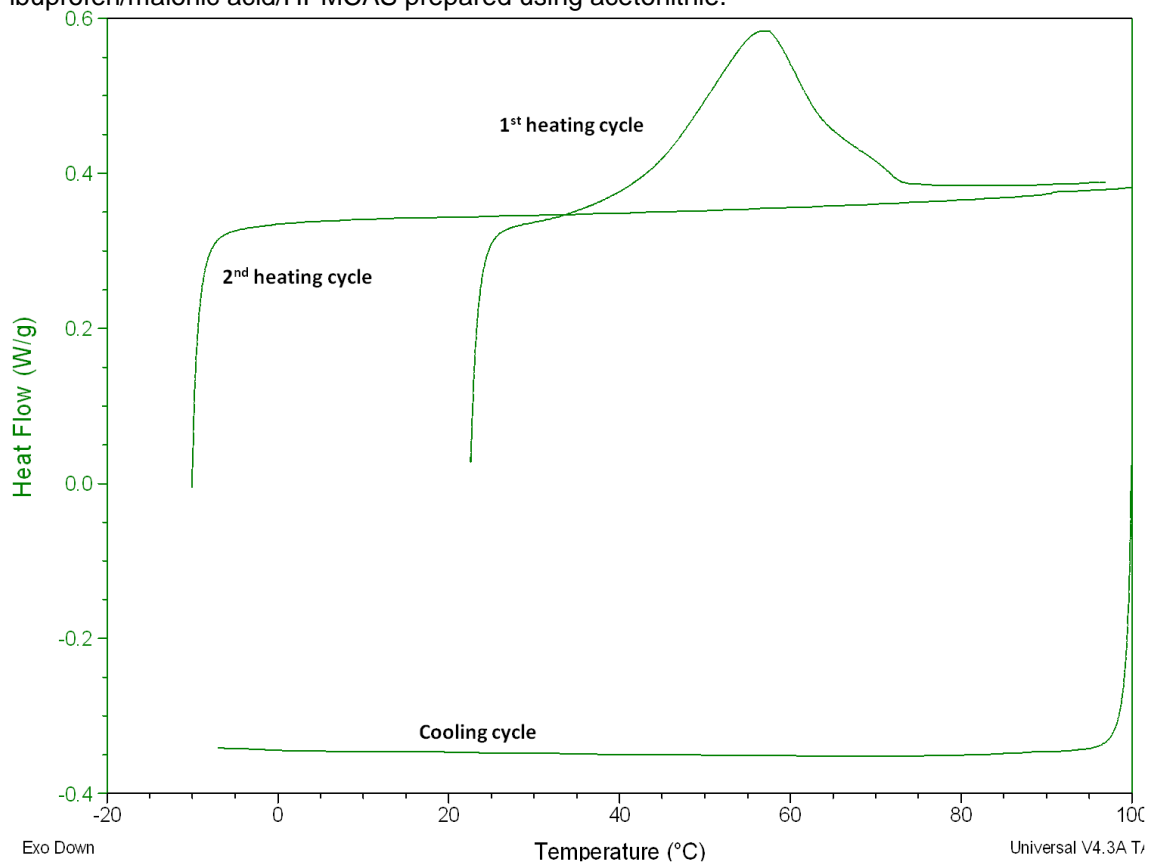


Figure All. 21. A representative thermal DSC profile for a film containing 3:2:10 w/w/w ibuprofen/malonic acid/HPMCAS prepared using acetone/chloroform.

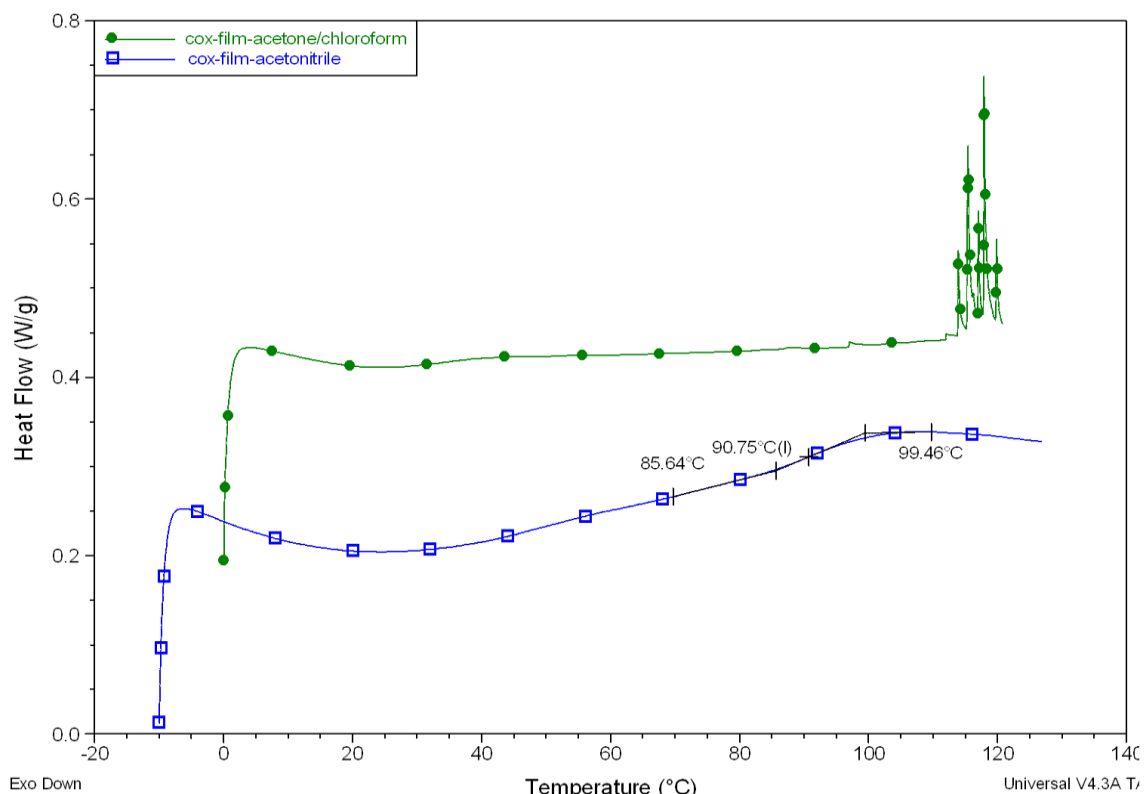


Figure All.22. Representative thermal DSC profiles for films containing caffeine-malonic acid co-crystals prepared using acetone/chloroform (green) and acetonitrile (blue).

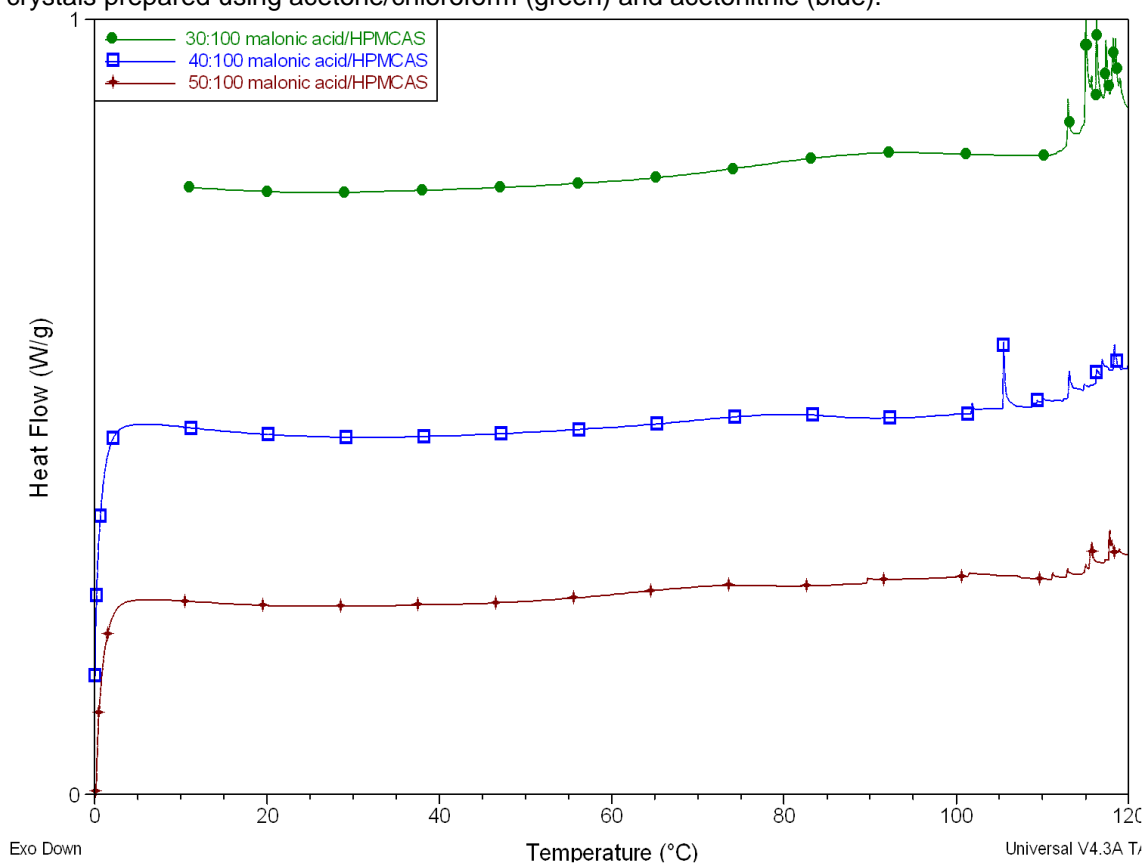


Figure All. 23. Representative thermal DSC profiles for films containing: 30:100 (green), 40:100 (blue), and 50:100 (red) w/w malonic acid/HPMCAS.

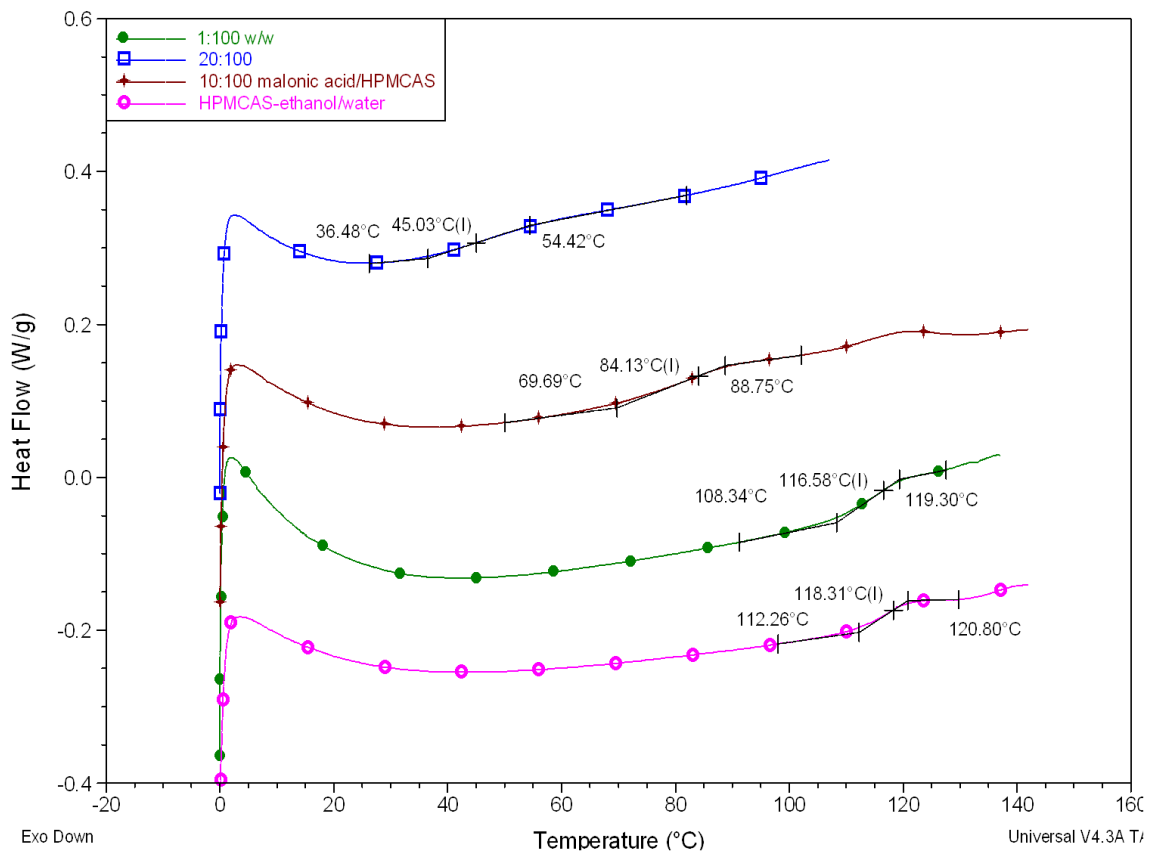


Figure All. 24. Representative thermal DSC profiles for films containing: 100% HPMCAS (pink), 1:100 w/w (green), 10:100 (red), and 20:100 (blue) w/w malonic acid/HPMCAS. all prepared using ethanol/water.

### Appendix III (Powder X-ray diffraction)

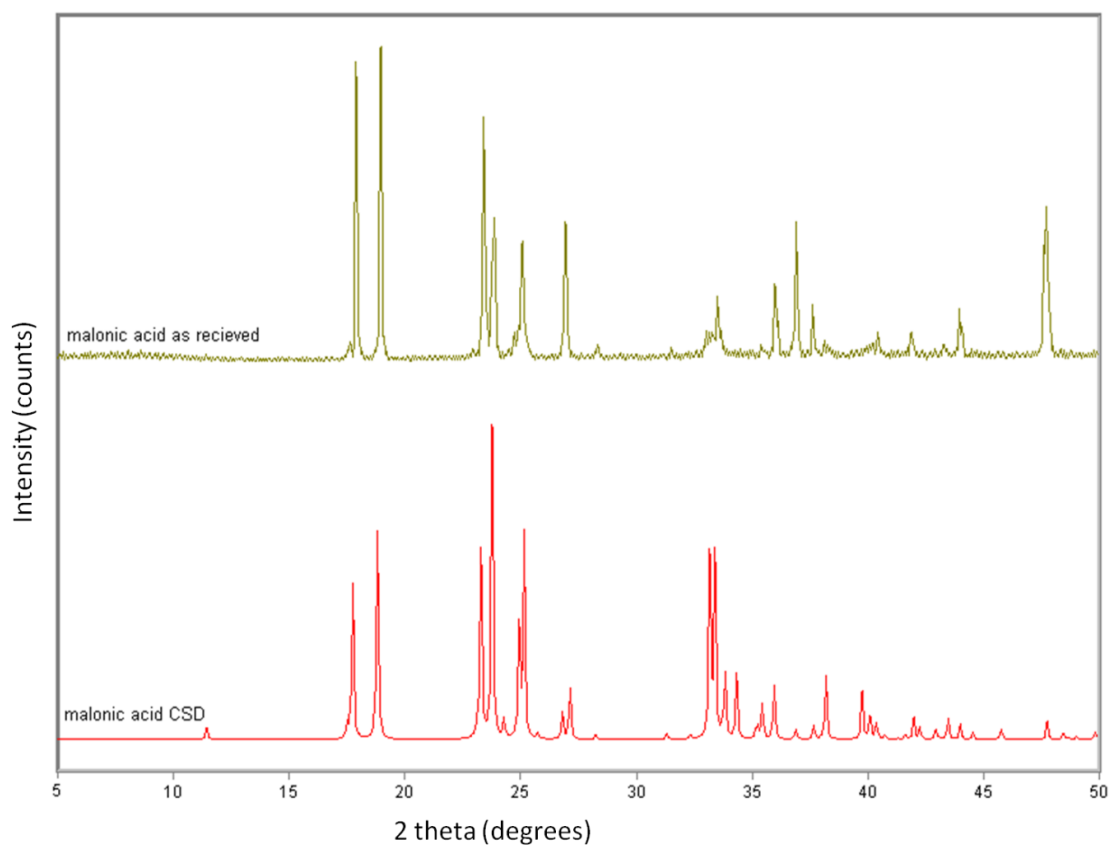


Figure AIII.1. X-ray scan of malonic acid as received (top) and the diffraction pattern of malonic acid obtained from CSD (bottom).

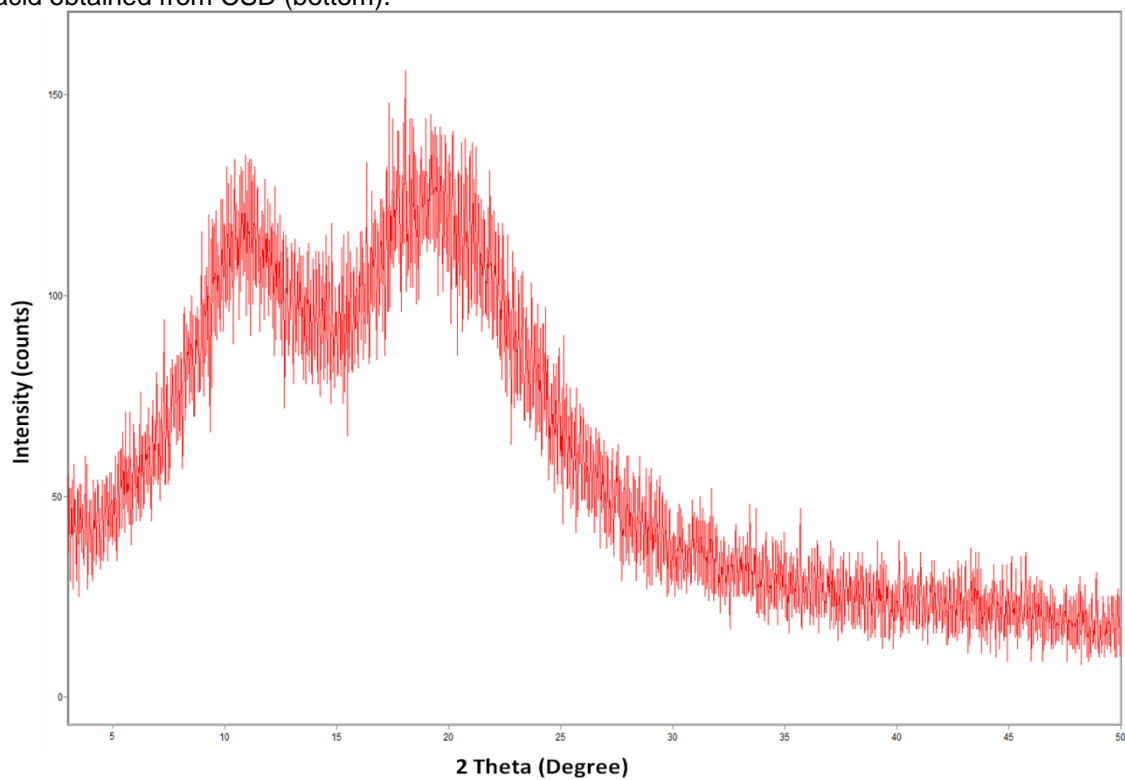


Figure AIII.2. X-ray scan of pure HPMCAS.

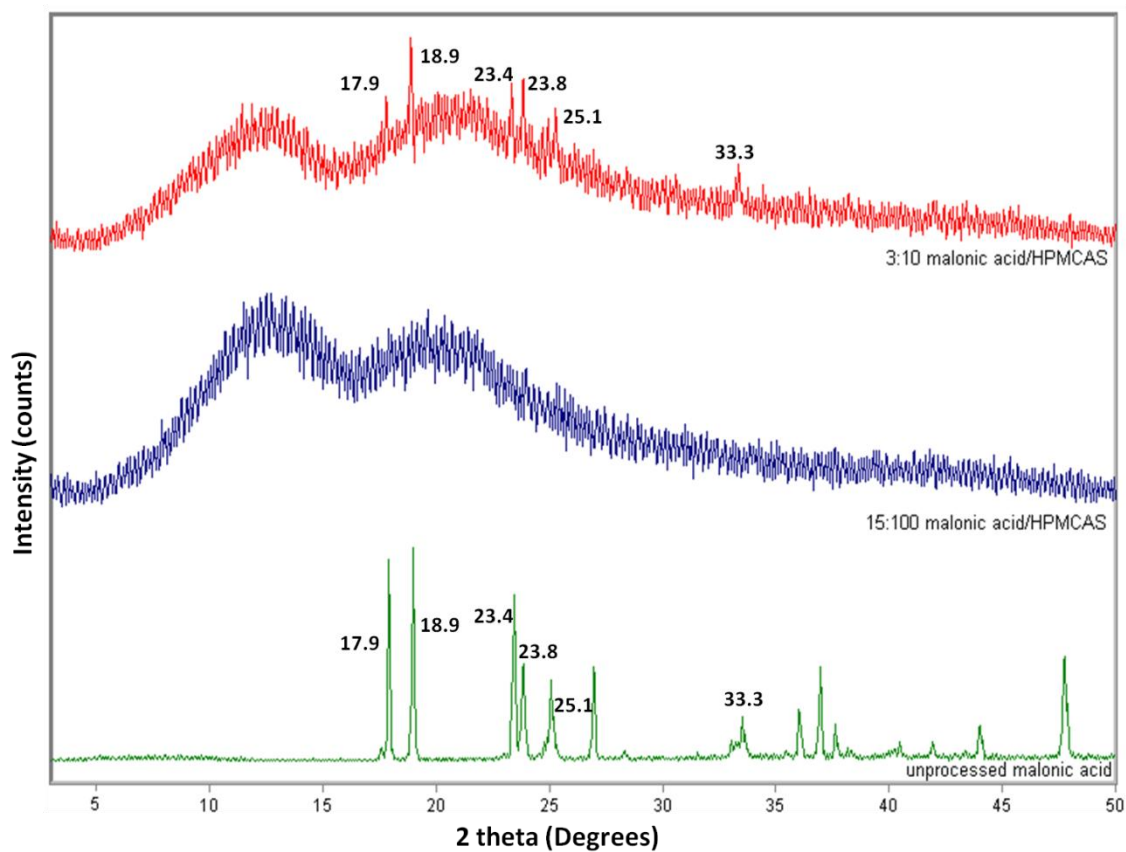


Figure AIII. 3. Representative powder x-ray diffraction patterns for unprocessed malonic acid (green), a film containing 15:100 malonic acid/HPMCAS (blue), and a film containing 3:10 malonic acid/HPMCAS (red)

## Appendix IV (FT-IR)

Assignment	malonic acid	ch5-2-	mh30-2-	CMX-2-	CMX-h-2-	cmx-h-2-	cmx-h-8-	HPMCAS 2
		8701	7701	8601	8502-8	8502-5	8602	
3114		3116		3121	3115			
	2992		2994					
2958		2934 wide		2951	2959	2941 multi+ wide		2934
2360	2362	2360	2363	2360	2362	2365		2365
2341	2342	2338	2340	2340	2342	2342		2338 + 2321

1738

1731

1730

C=N

1692

1698

1708

1694 wide

1698

1692

1702

1704



		wide			multi+wide		
C=O							
asymmetric	1644		1657		1656	1646	1657
C=C	1599		1600		1613	1601	
C=O							
symmetric	1547		1545		1545	1546	1551
	1480		1486		1503	1484	
	1455		1454		1453	1455	
(CH <sub>2</sub> , OH							
mal)	1429	1434	1431	1436	1432	1431	
	1402					1402	

(OH, C=O, C-C mal)	1396		1397			
					1372	1372
C-N	1358	1368 wide	1360	1359		
C-N	1326		1325	1325		
C-N	1285	1286	1279	1287	1286	
C-N	1237	1235	1227	1235	1235	1234
CH2	1215		1219			
C-N						
asymmetric	1188	1190 shallow	1179	1189		
CH2	1166		1168			
	1073	1052 very wide	1087 sh	not distin	not distin	

1025		not distin		1029	1027	1047 very wide	1047 very wide	1047 very wide
973		974		979	974	947 wide shal		974 wide shal
861		912 v wide		912 v wide				
758		770		759	770	759		763
742		744		748	743	746		749

Table AIV.1. FT-IR band assignment for film containing caffeine malonic acid co-crystals prepared with acetone/chloroform or acetonitrile.

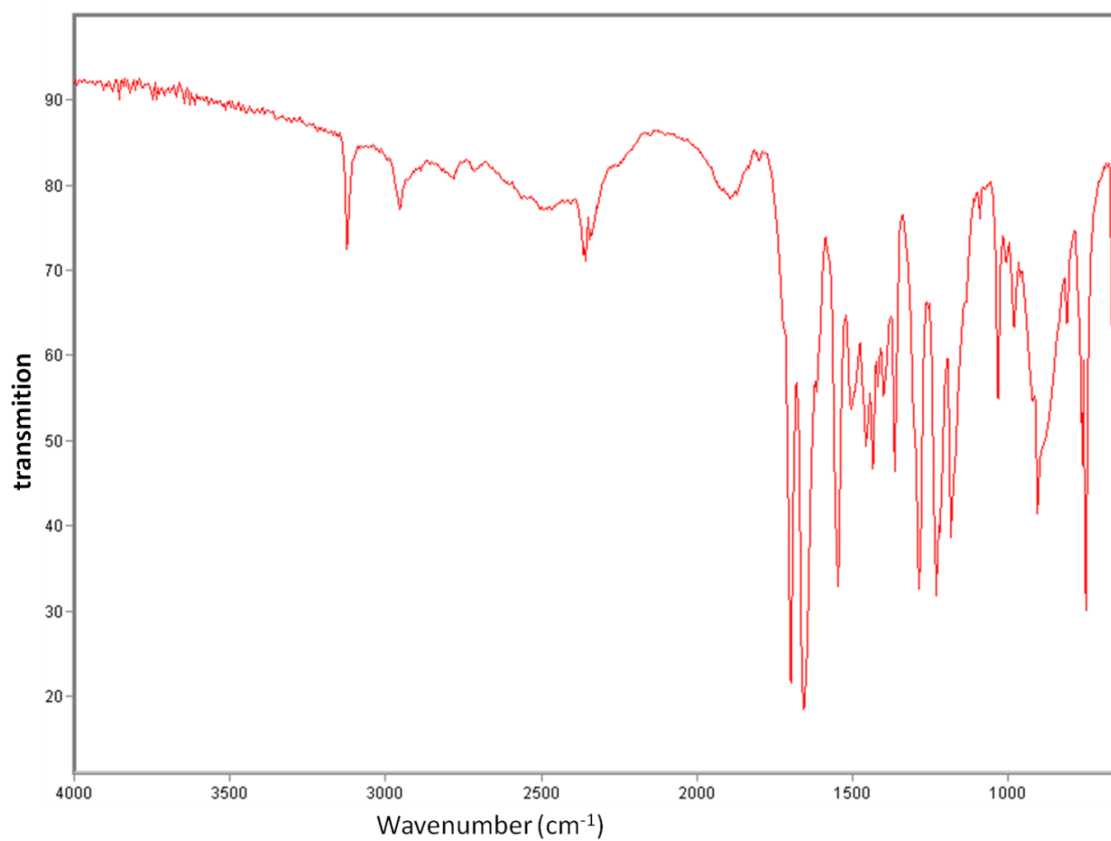


Figure AIV.1. a represent of FT-IR scan of malonic acid as received.

## Appendix V (SEM)

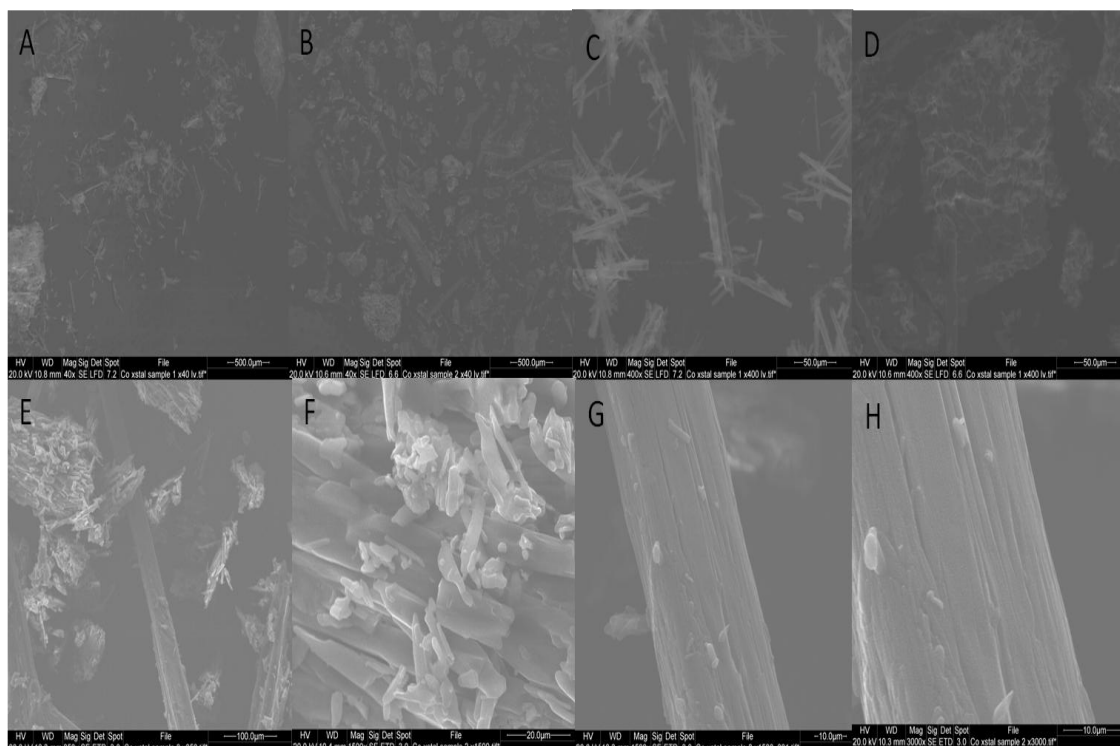


figure AV.1. SEM scan of caffeine-malonic acid co-crystals using different magnification powers. (A) and (B) 40X, (C) and (D) 400X, (E) 250, (F) and (G) 1500X, (H) 3000X.

## Appendix VI (Dissolution test)

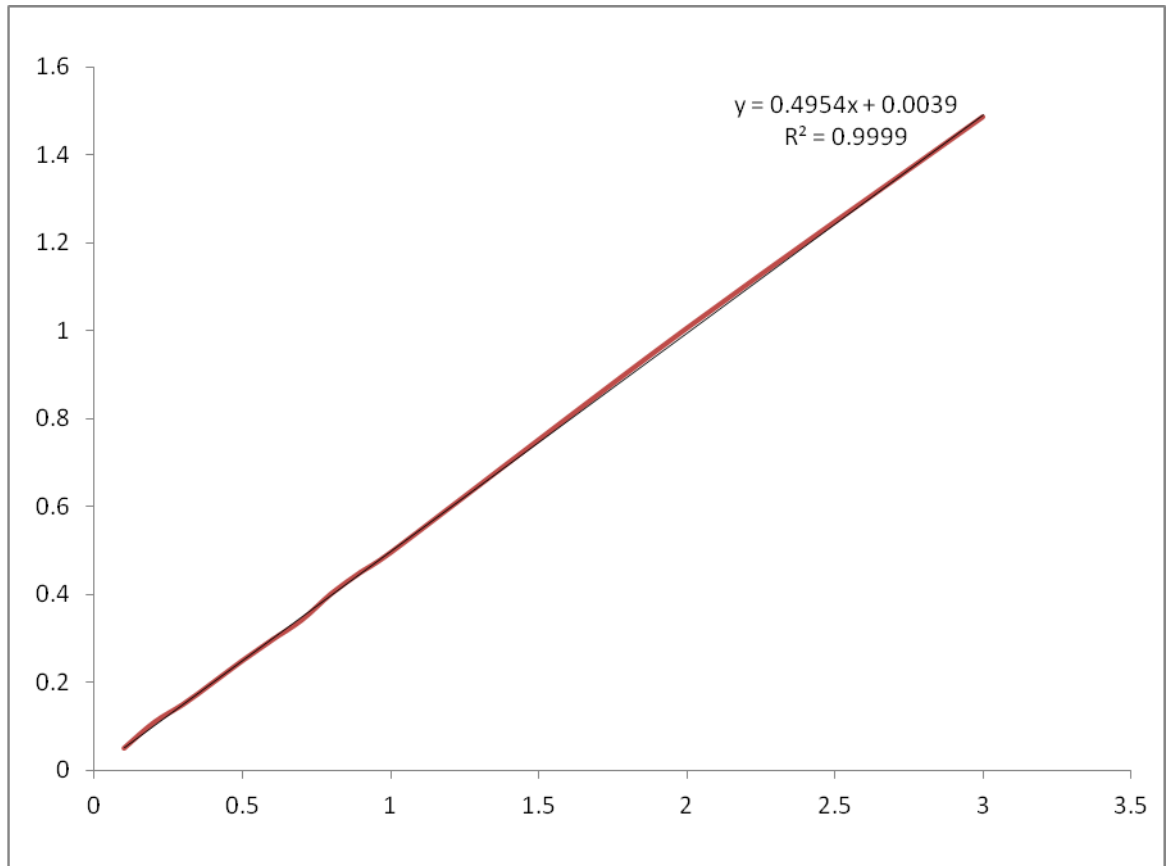


Figure AVI.1. standard curve for caffeine in distilled water.

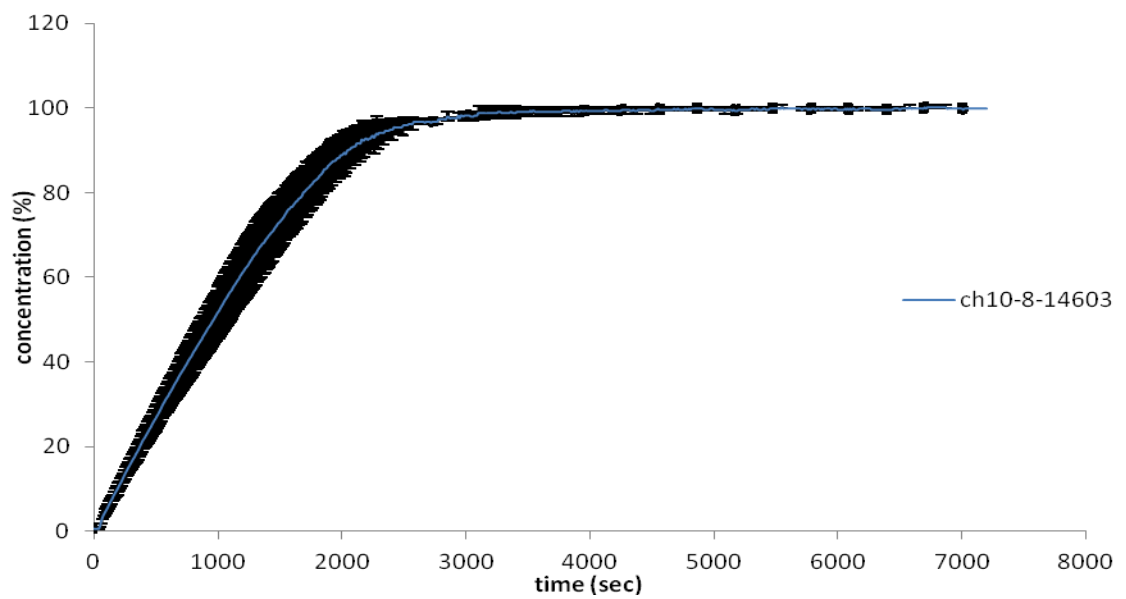


Figure AVI.2. the dissolution test of the film containing 10% w/w caffeine with error bars.

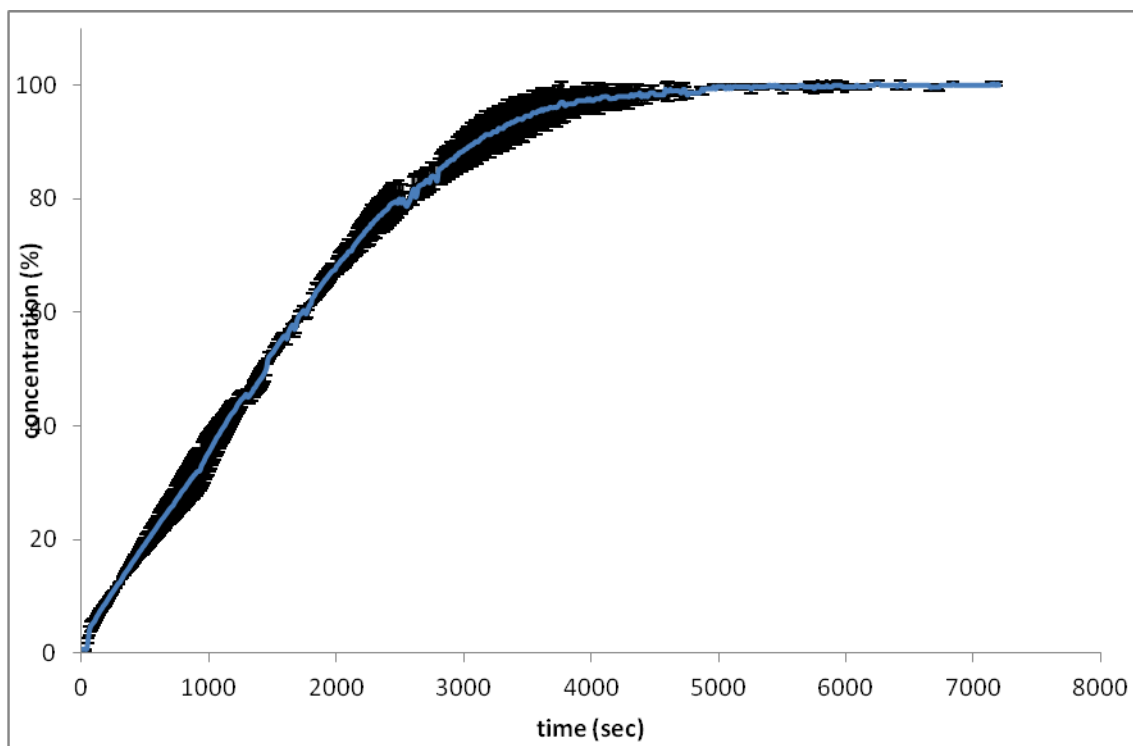


figure AVI.3. Drug release profile with error bars for films containing caffeine-malonic acid co-crystals prepared with acetone/chloroform.

## Appendix VII (Stability study)

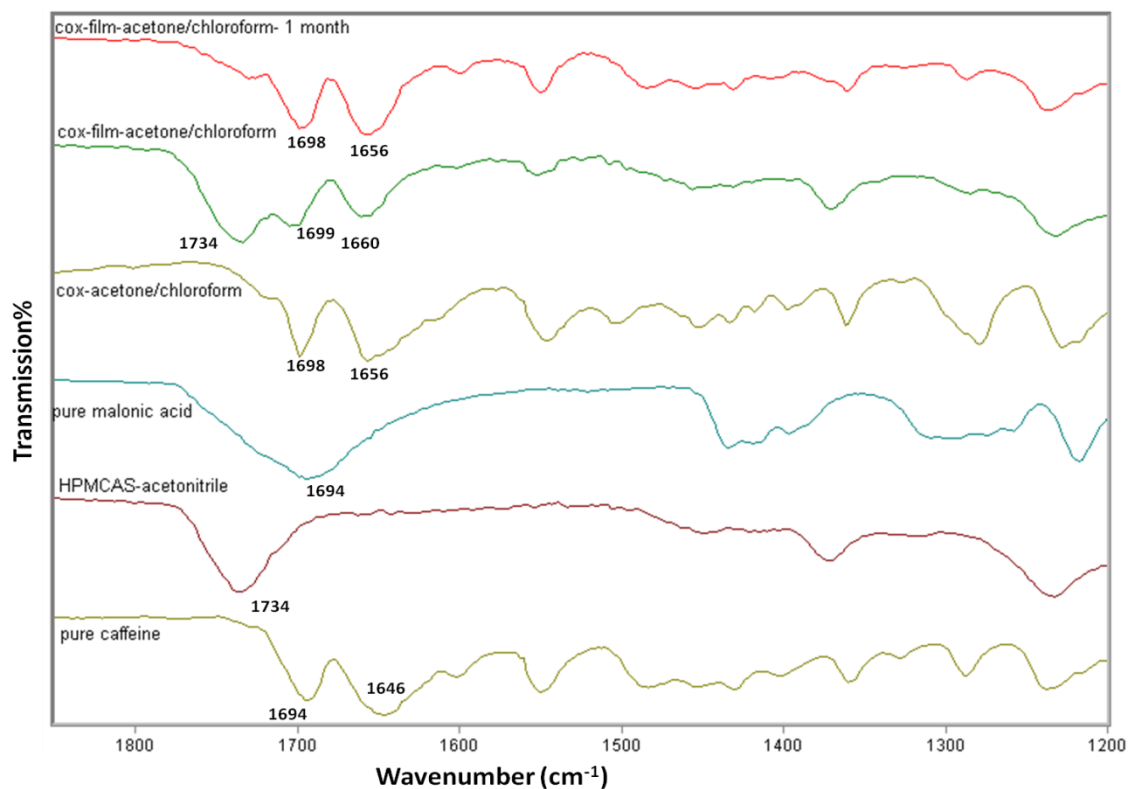


Figure AVII.1. FT-IR scan of co-crystals in a film after 1 month of storage. The film prepared with acetone/chloroform.

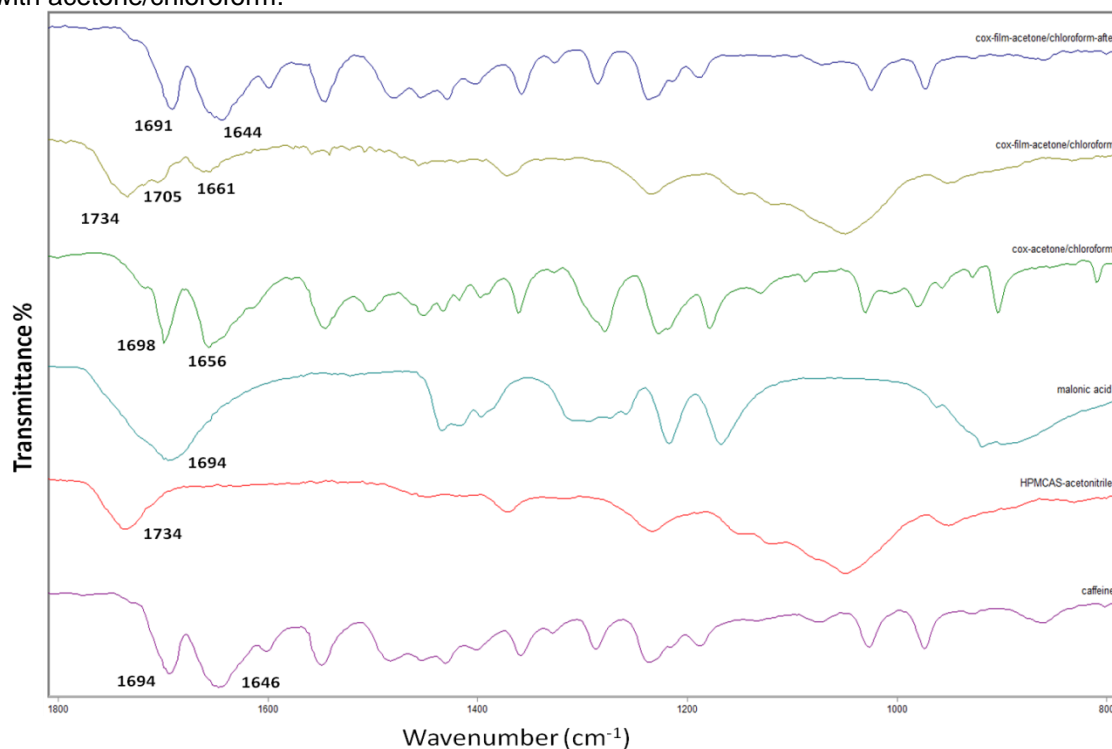


Figure AVII.2. FT-IR scan of co-crystals in a film after 1 month of storage. The film prepared with acetone/chloroform.



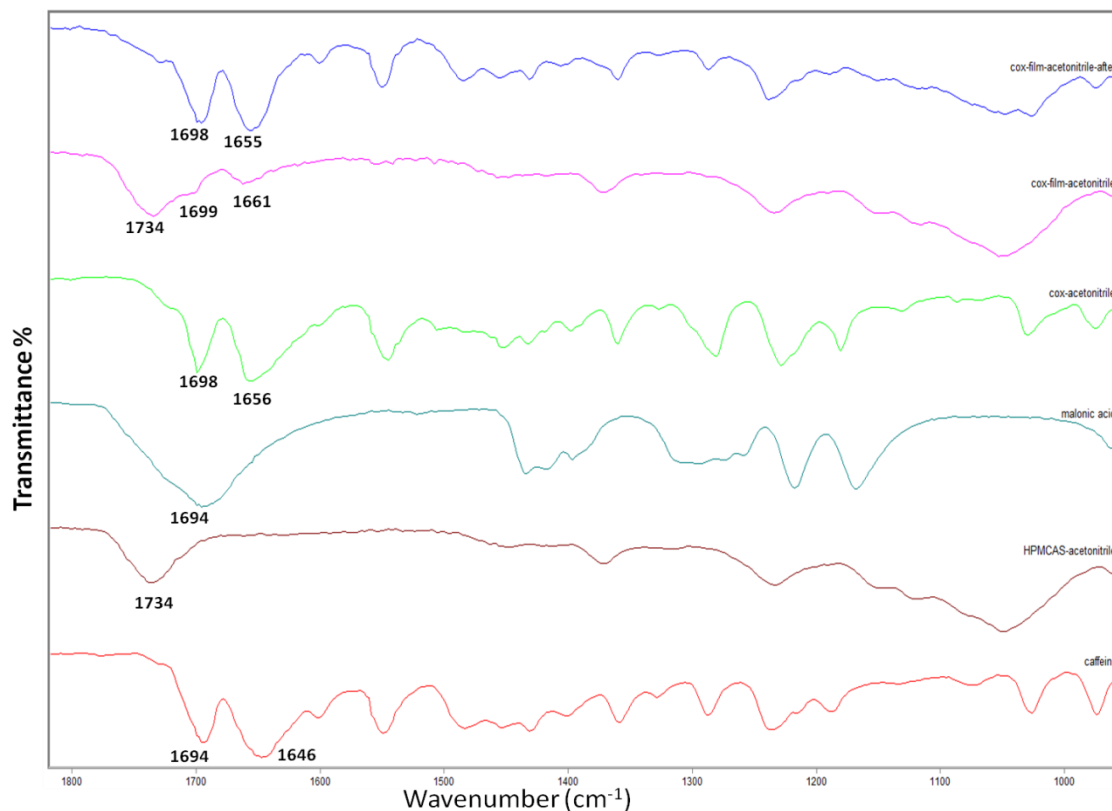


Figure AVII.3. FT-IR scan of co-crystals in a film after 1 month of storage. The film prepared with acetonitrile.

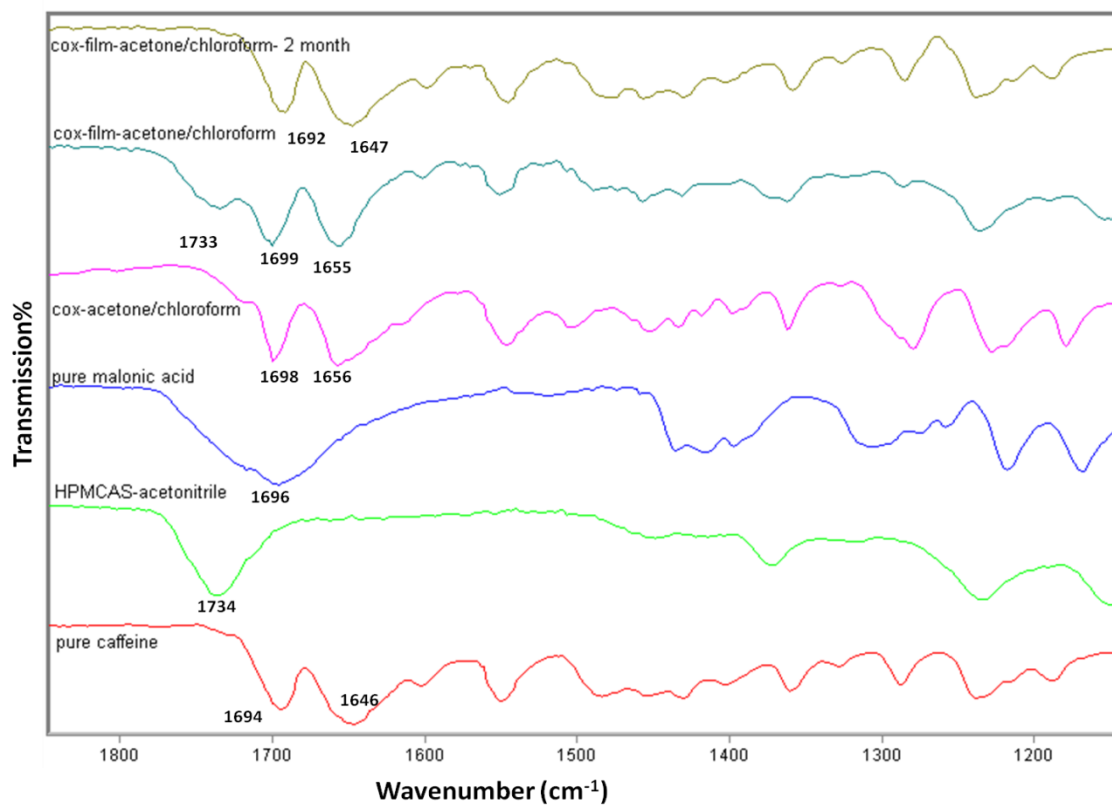


Figure AVII.4. FT-IR scan of co-crystals in a film after 2 month of storage. The film prepared with acetone/chloroform.

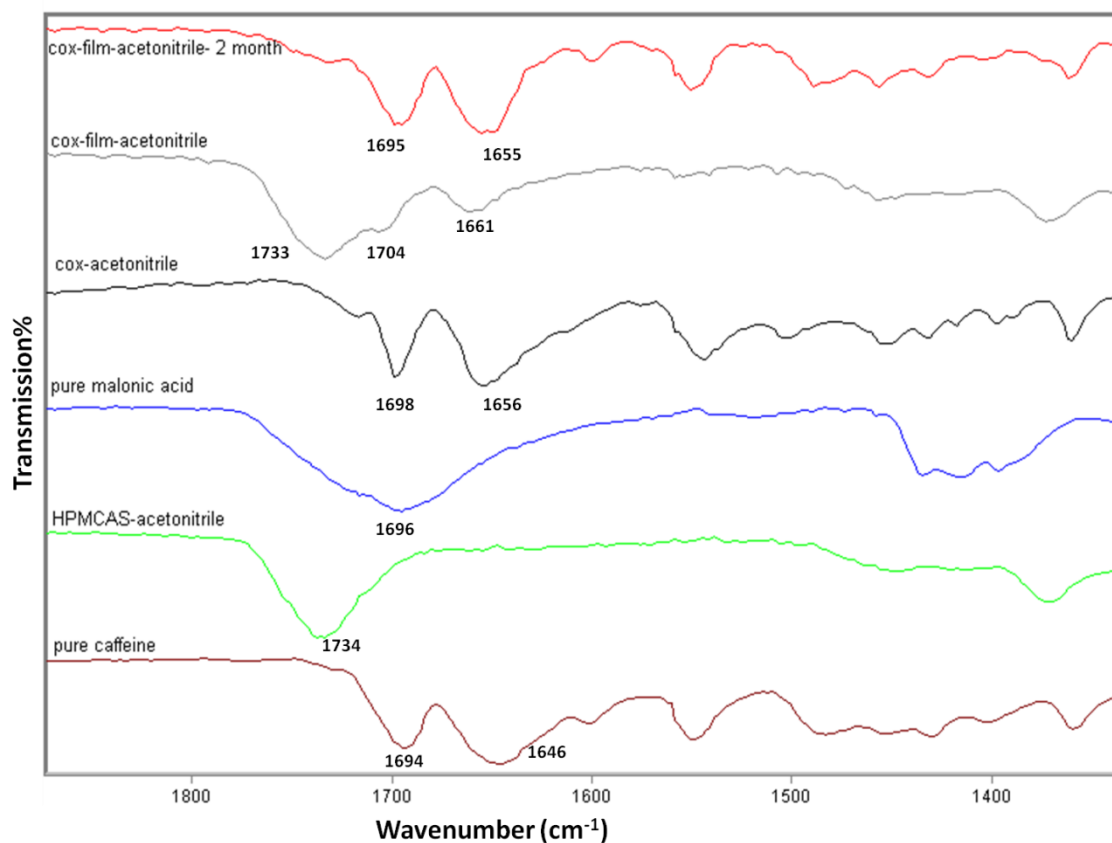


Figure AVII.5. FT-IR scan of co-crystals in a film after 2 month of storage. The film prepared with acetonitrile.

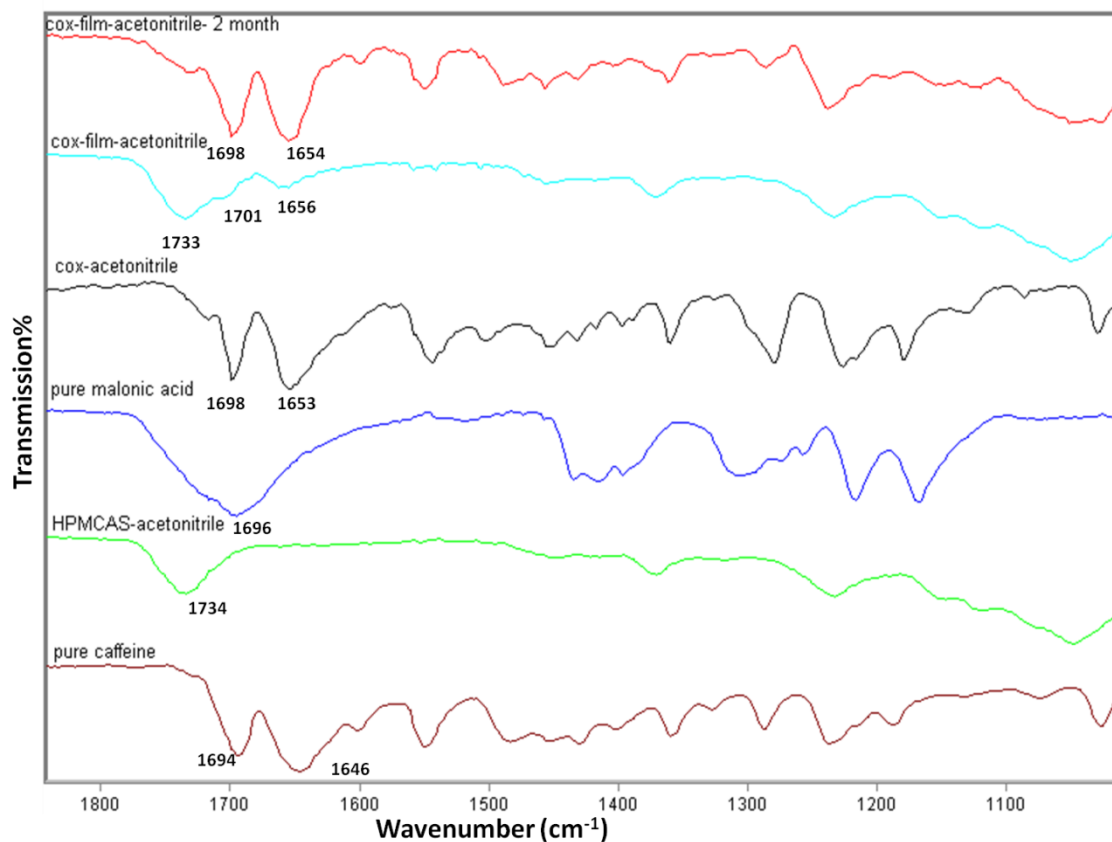


Figure AVII.6. FT-IR scan of co-crystals in a film after 2 month of storage. The film prepared with acetonitrile.

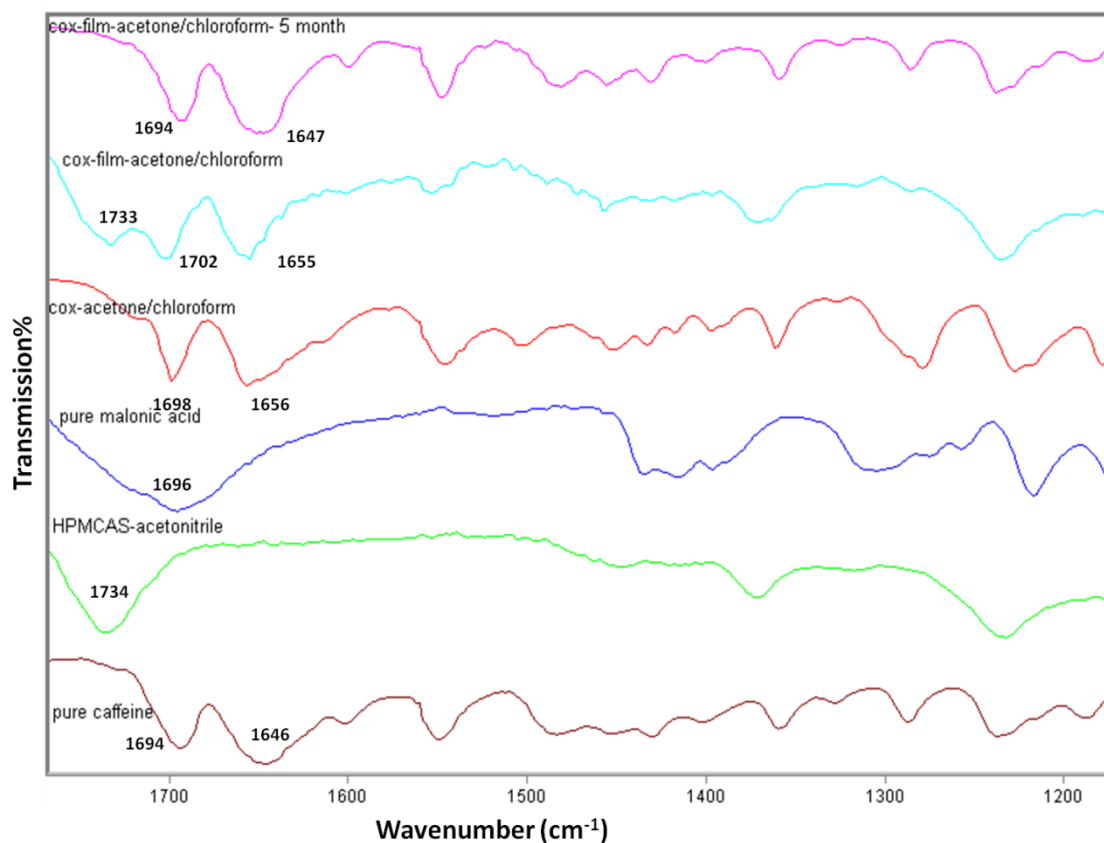


Figure AVII.7. FT-IR scan of co-crystals in a film after 4 month of storage. The film prepared with acetone/chloroform.

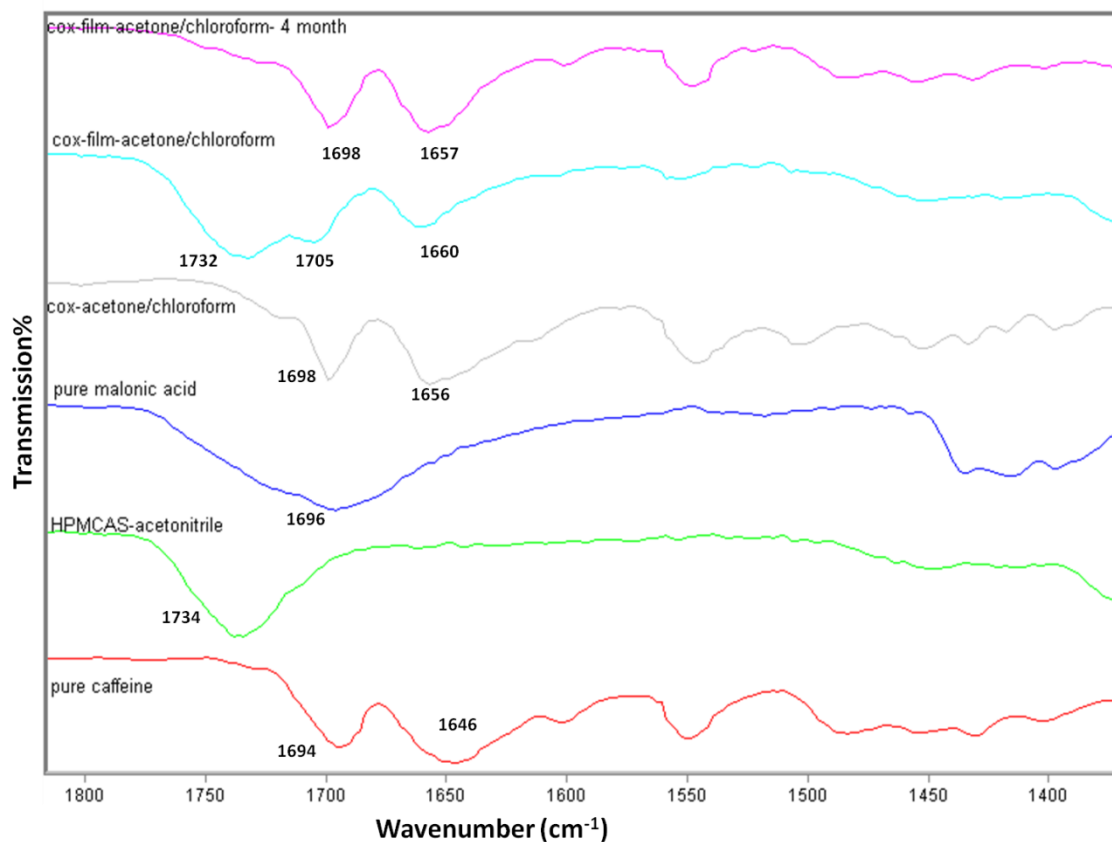


Figure AVII.8. FT-IR scan of co-crystals in a film after 4 month of storage. The film prepared with acetone/chloroform.

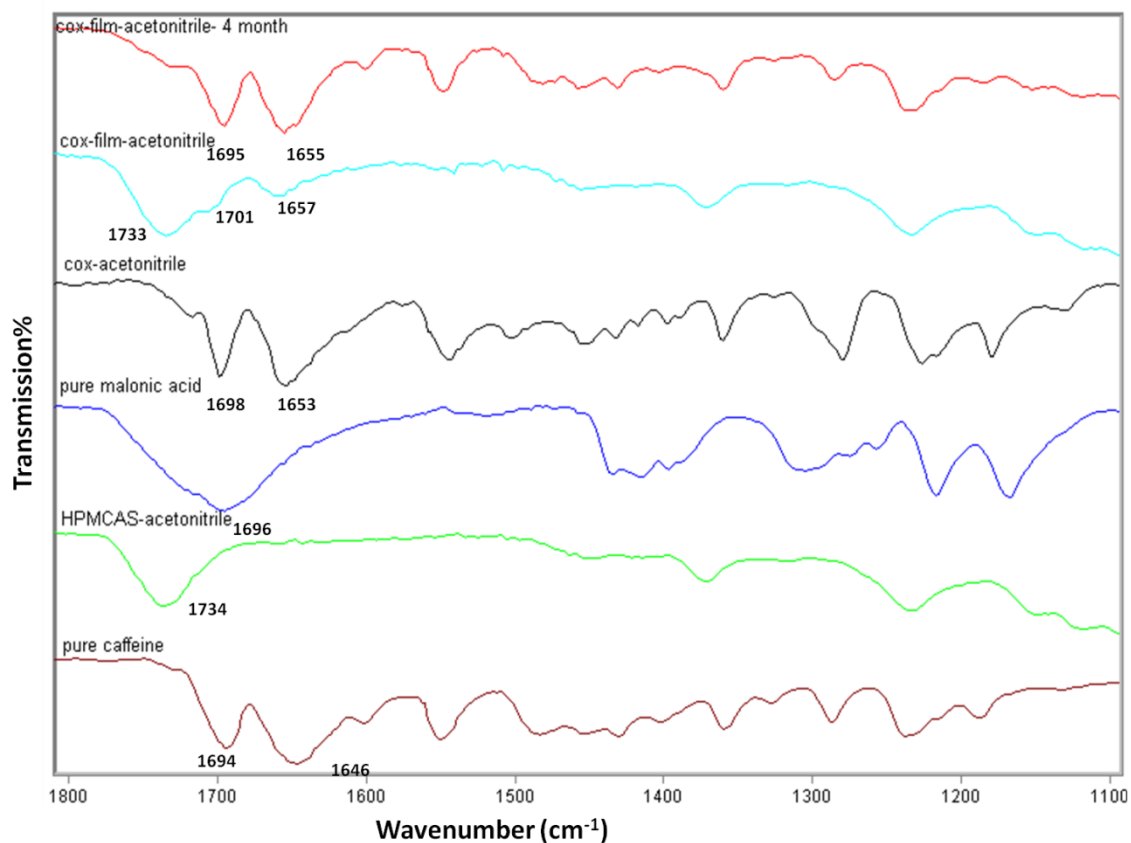


Figure AVII.9. FT-IR scan of co-crystals in a film after 4 month of storage. The film prepared with acetonitrile.

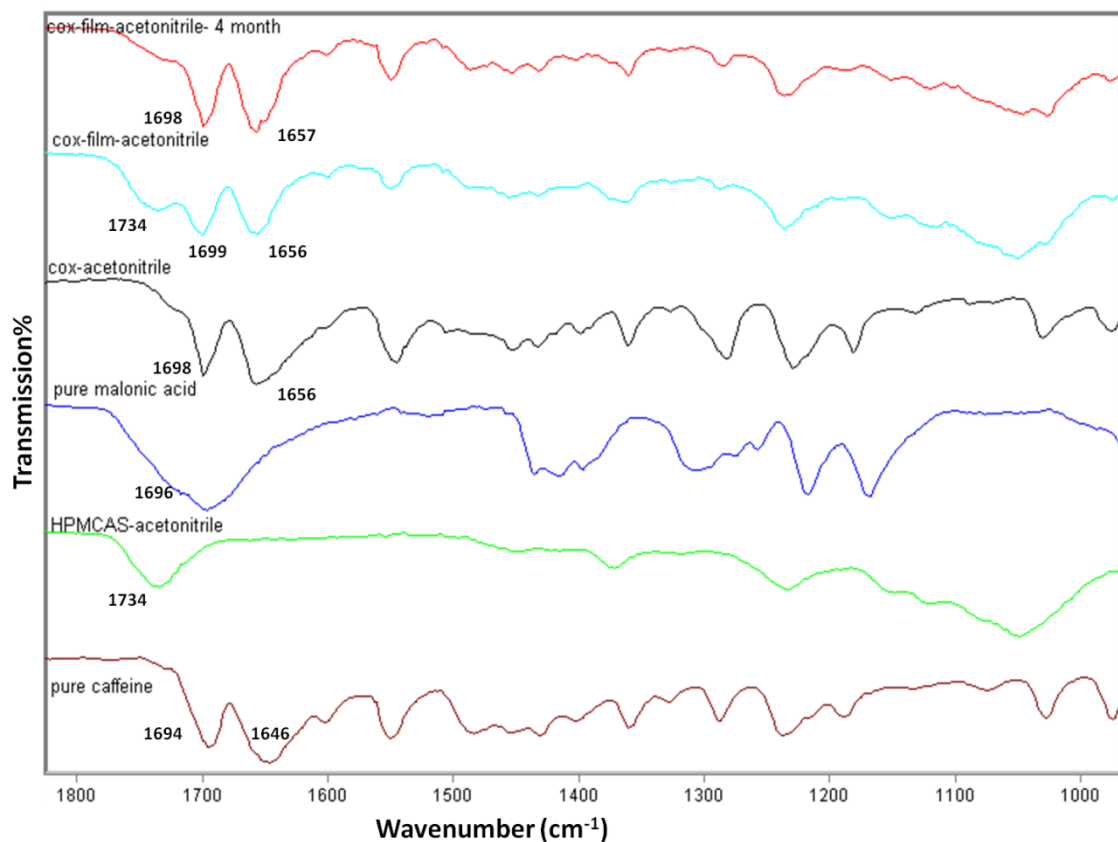


Figure AVII.10. FT-IR scan of co-crystals in a film after 4 month of storage. The film prepared with acetonitrile.

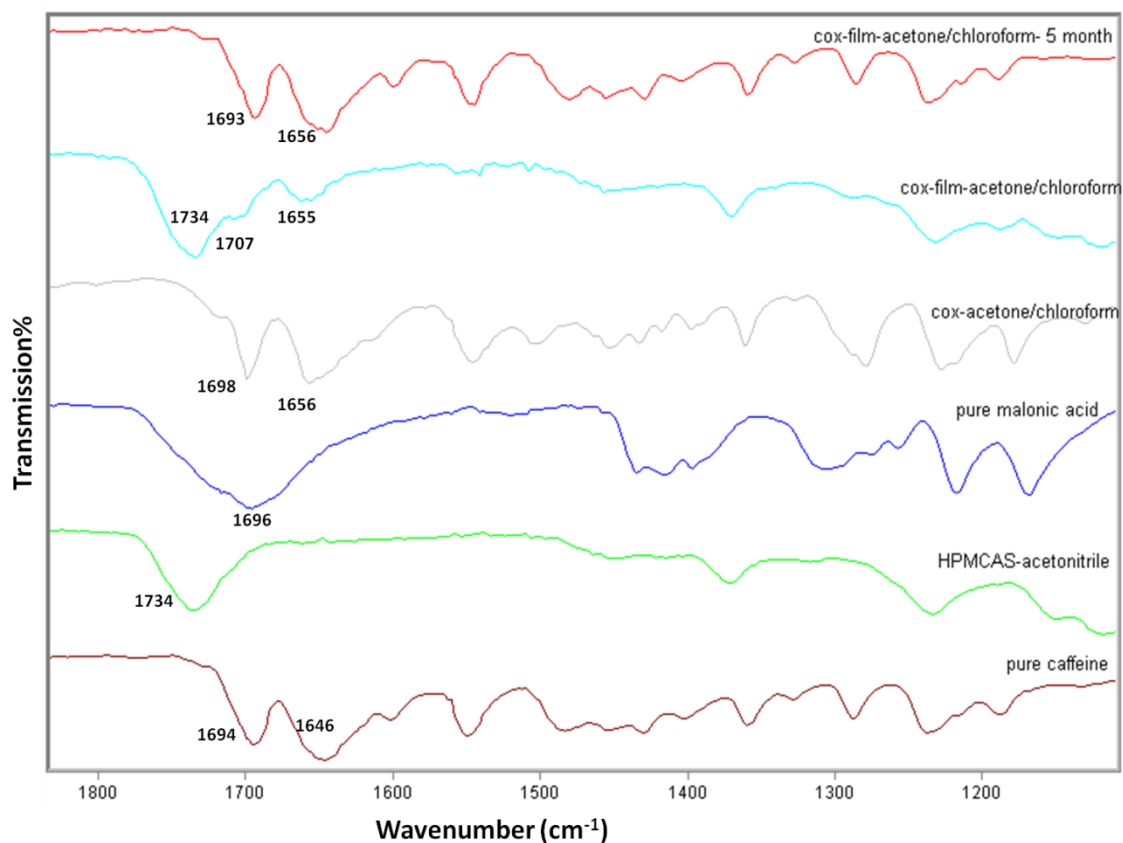


Figure AVII.11. FT-IR scan of co-crystals in a film after 5 month of storage. The film prepared with acetone/chloroform.

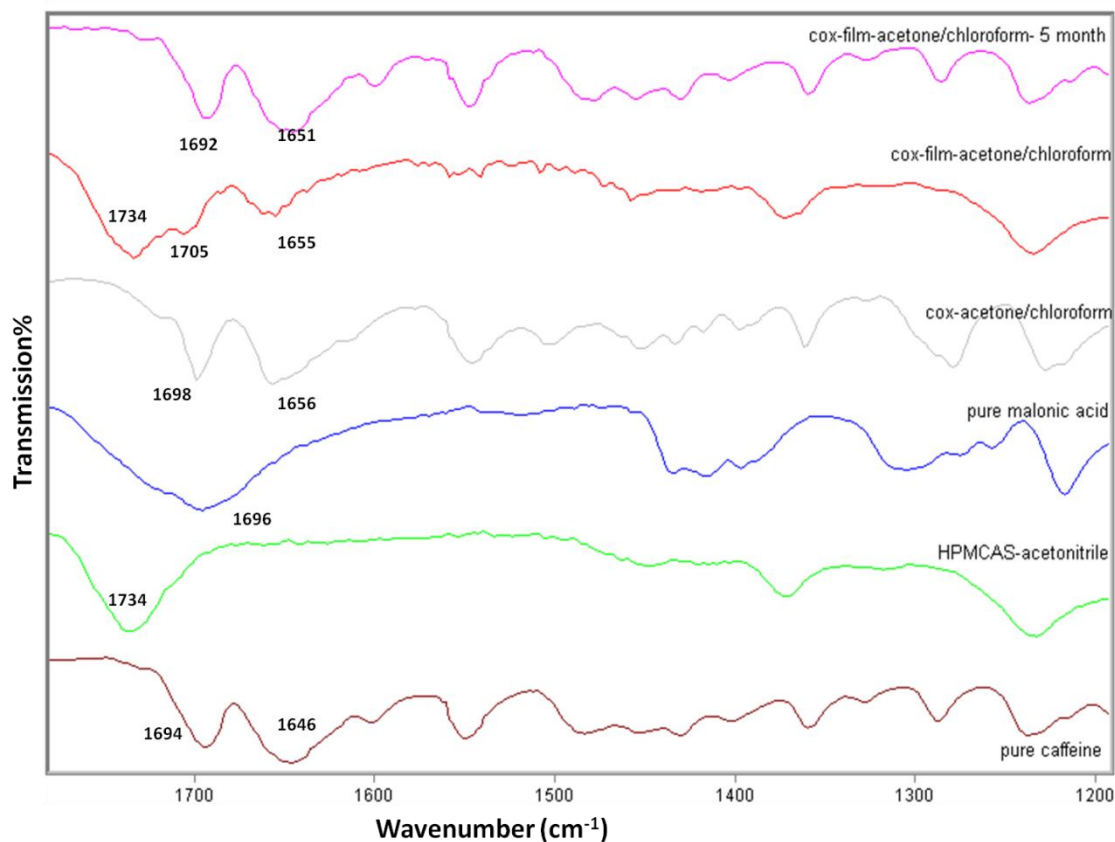


Figure AVII.12. FT-IR scan of co-crystals in a film after 5 month of storage. The film prepared with acetone/chloroform.

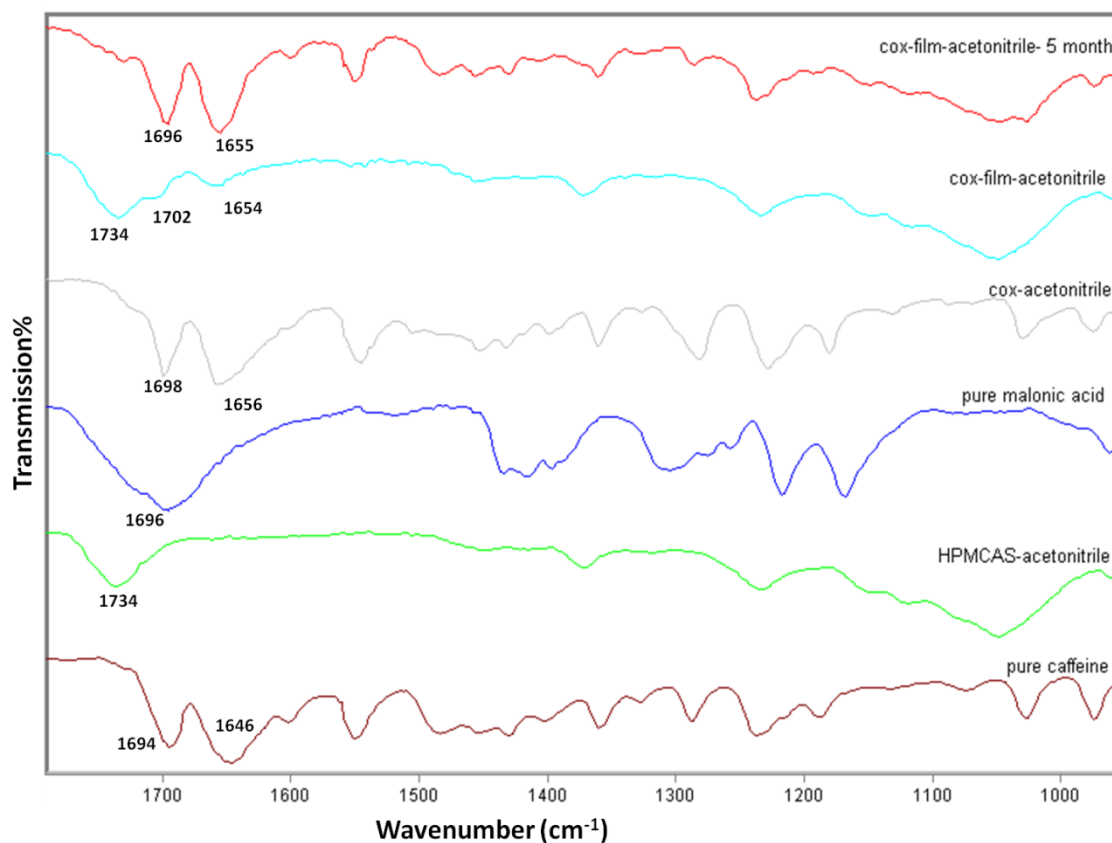


Figure AVII.13. FT-IR scan of co-crystals in a film after 5 month of storage. The film prepared with acetonitrile.

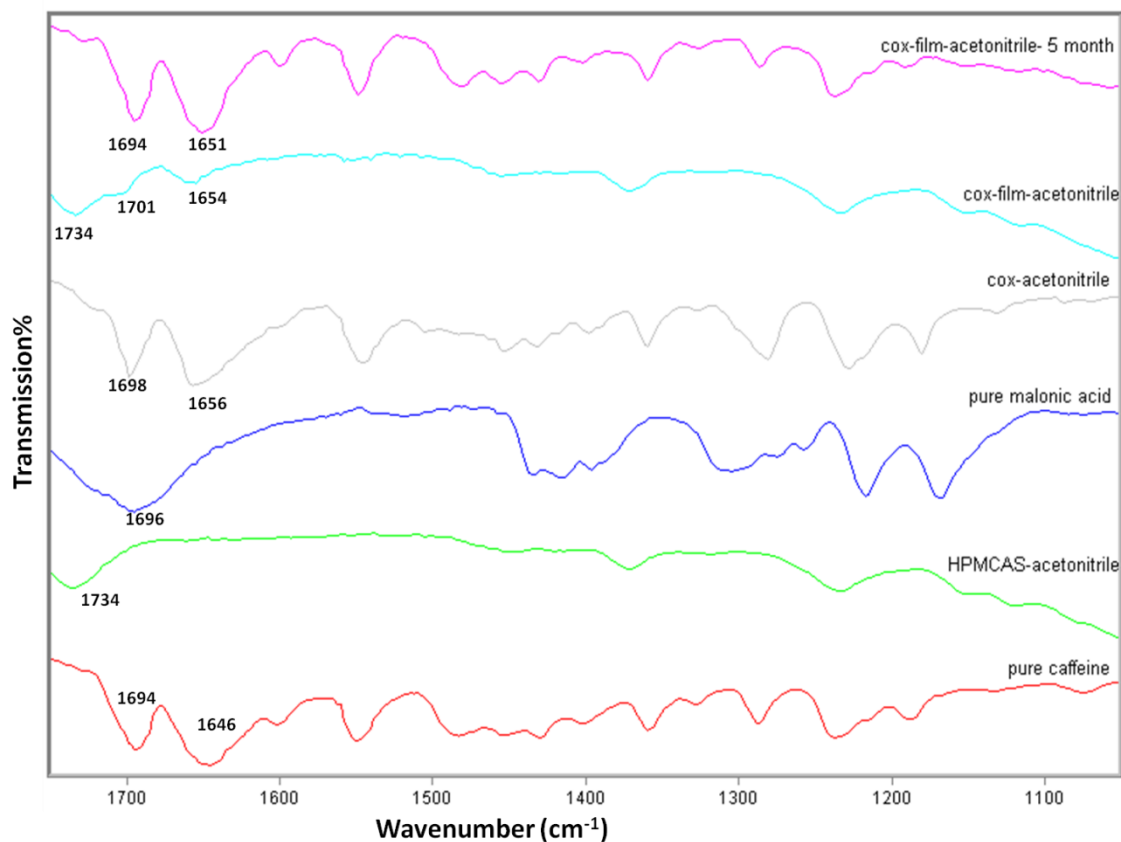


Figure AVII.14. FT-IR scan of co-crystals in a film after 5 month of storage. The film prepared with acetonitrile.

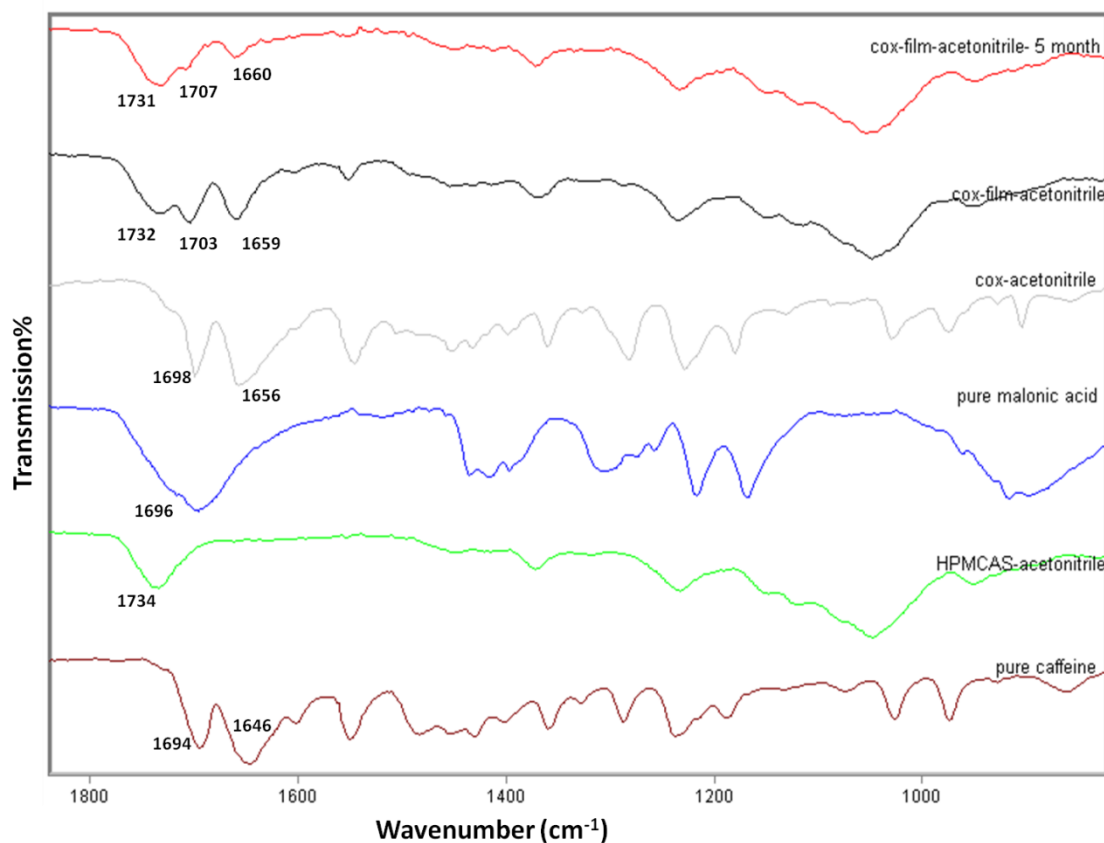


Figure AVII.15. FT-IR scan of co-crystals in a film after 5 month of storage. The film prepared with acetonitrile.

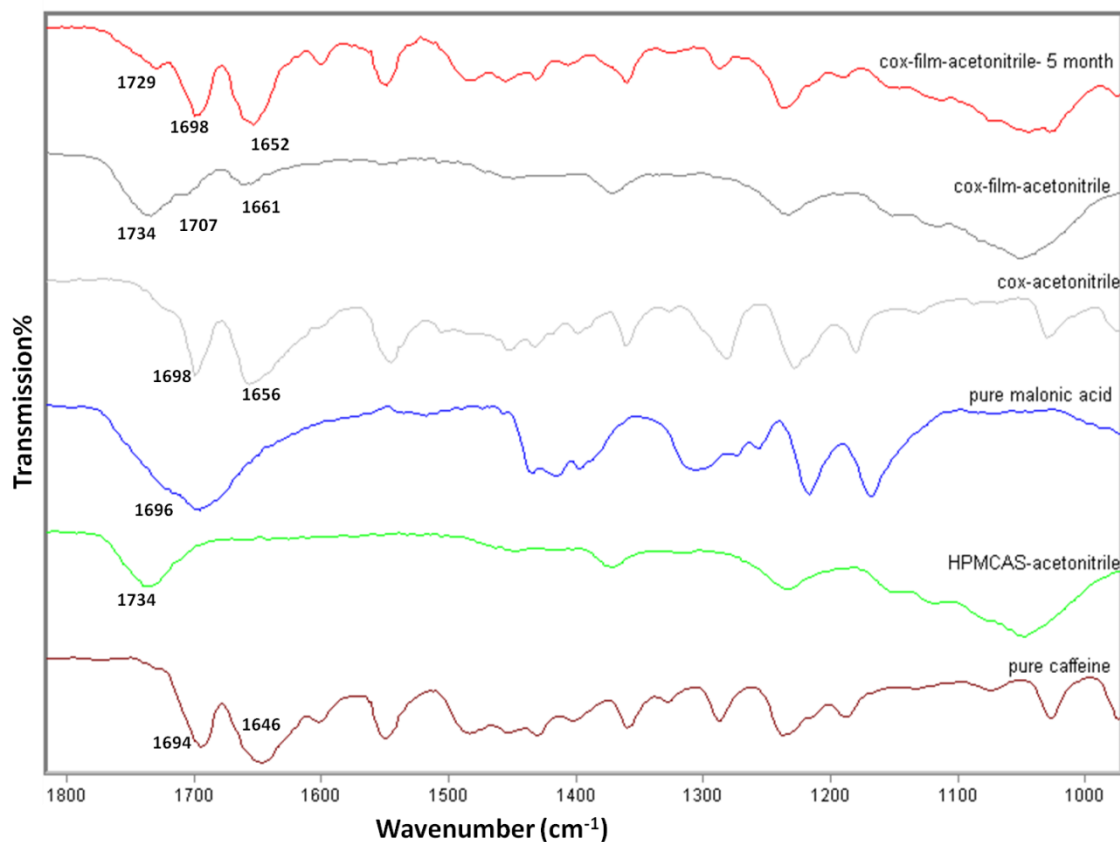


Figure AVII.16. FT-IR scan of co-crystals in a film after 6 month of storage. The film prepared with acetonitrile.

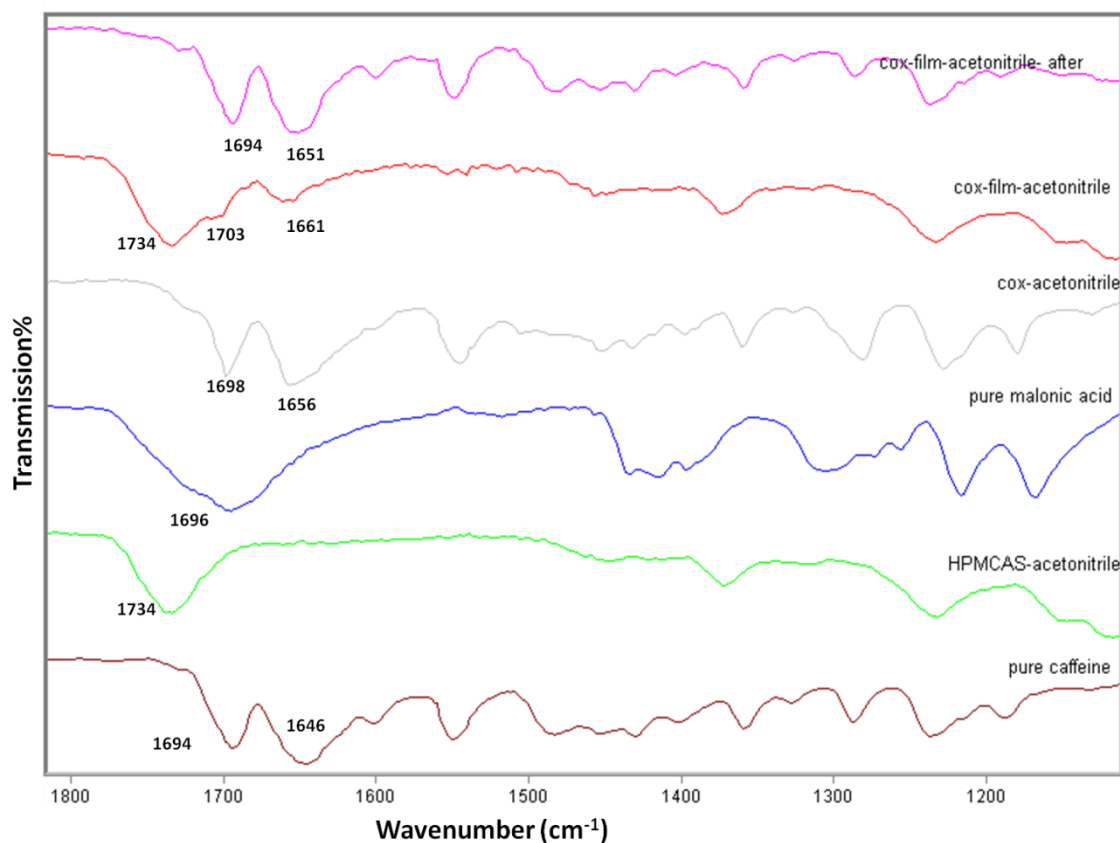


Figure AVII.17. FT-IR scan of co-crystals in a film after 6 month of storage. The film prepared with acetonitrile.

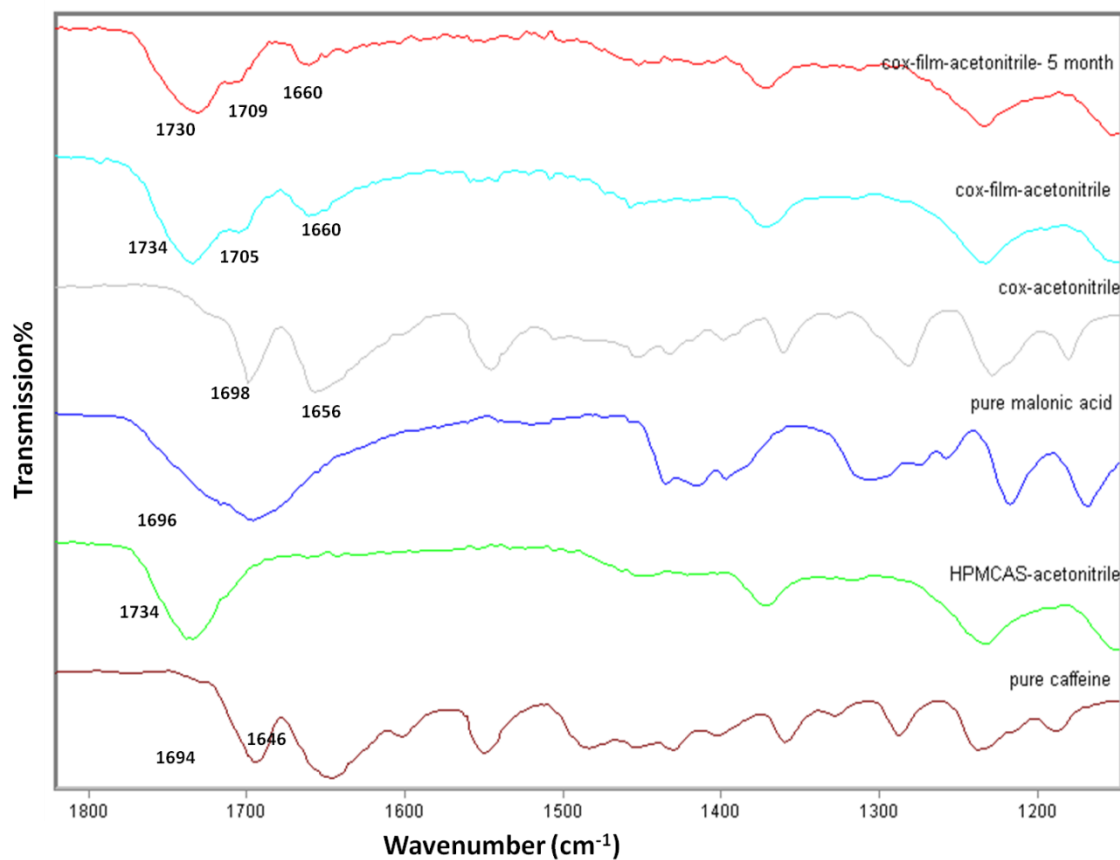


Figure AVII.18. FT-IR scan of co-crystals in a film after 6 month of storage. The film prepared with acetonitrile.



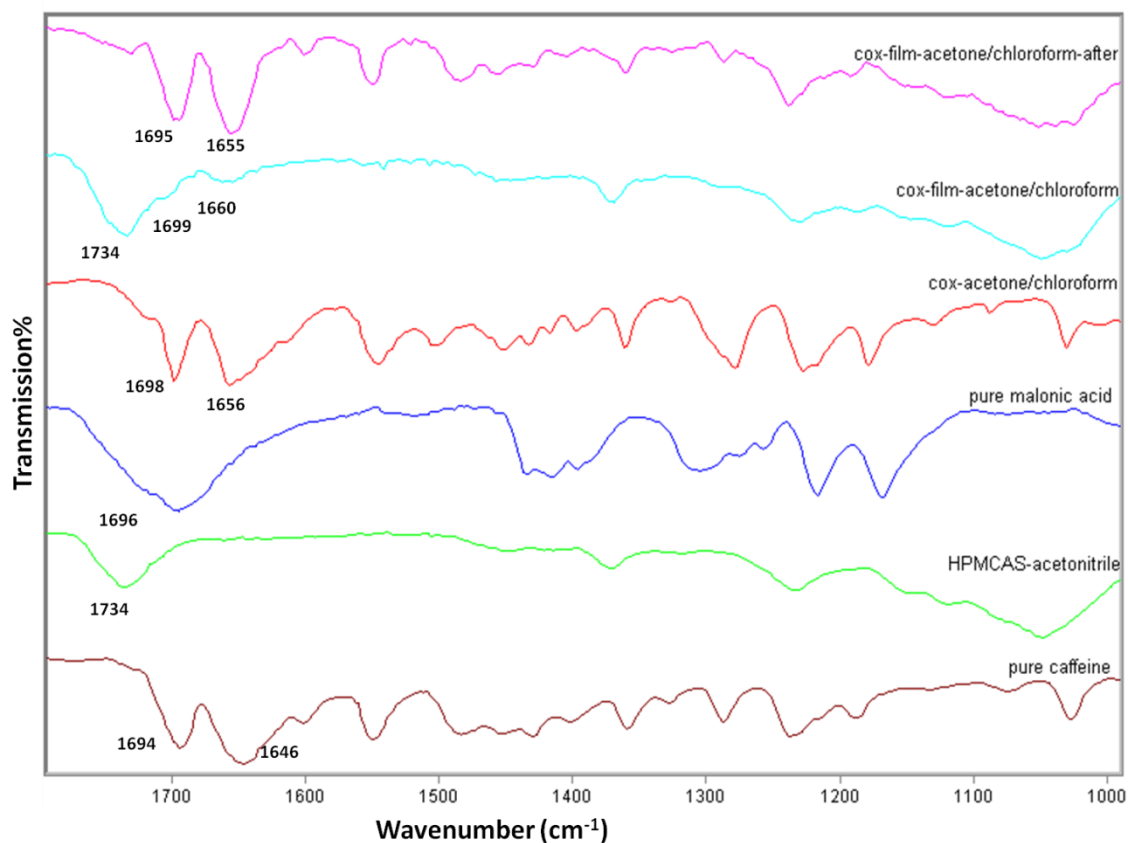


Figure AVII.19. FT-IR scan of co-crystals in a film after 7 month of storage. The film prepared with acetone/chloroform.

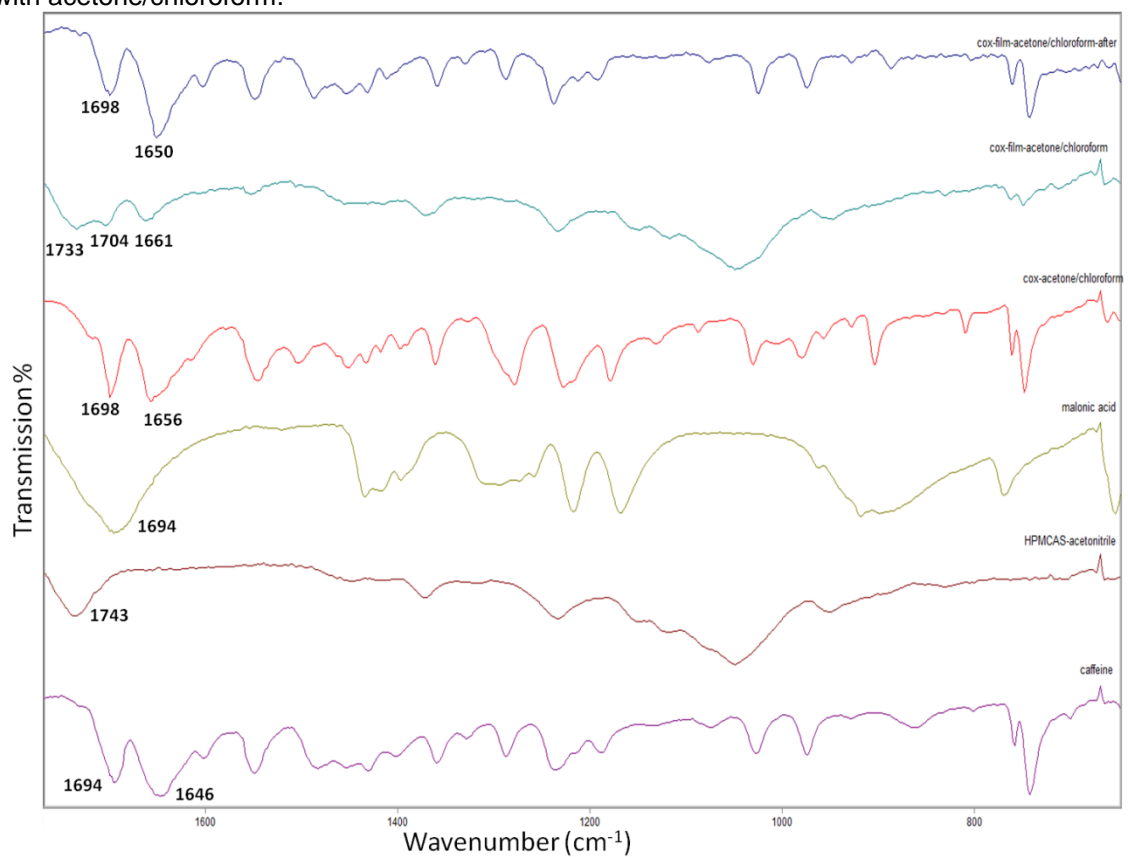


Figure AVII.20. FT-IR scan of co-crystals in a film after 7 month of storage. The film prepared with acetone/chloroform.

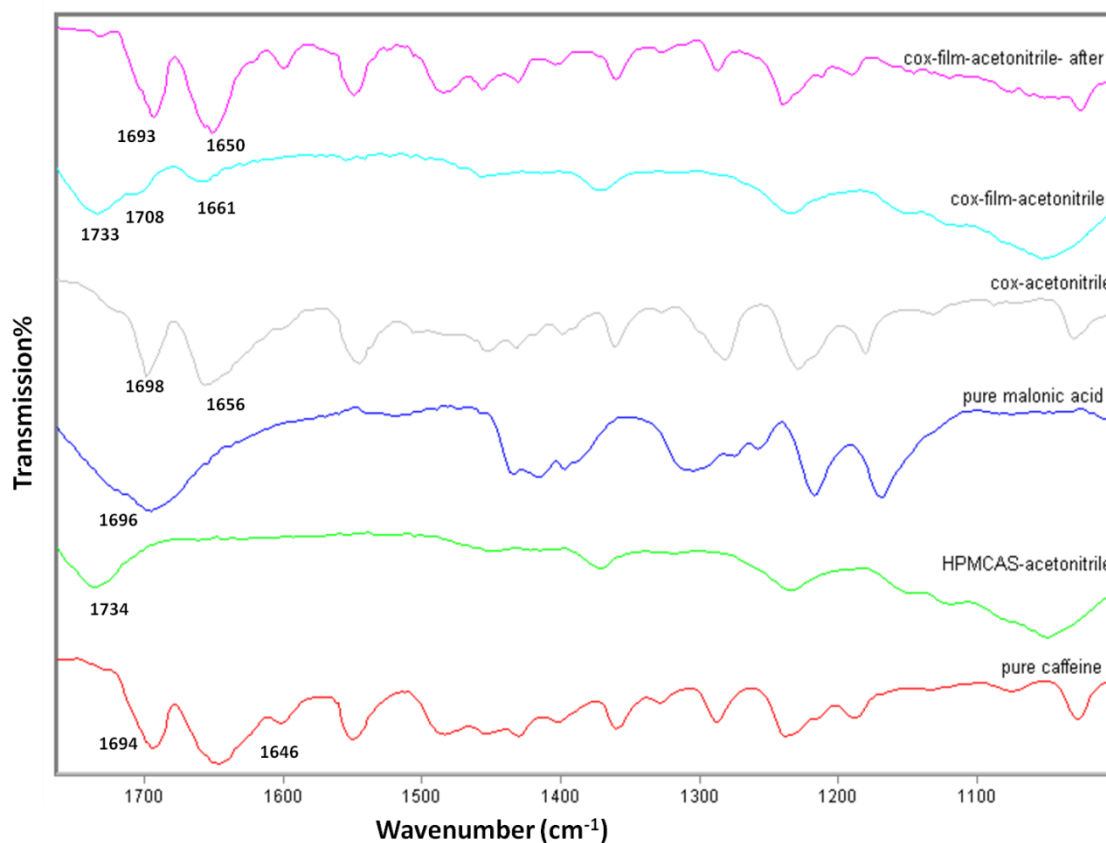


Figure AVII.21. FT-IR scan of co-crystals in a film after 7 month of storage. The film prepared with acetonitrile.

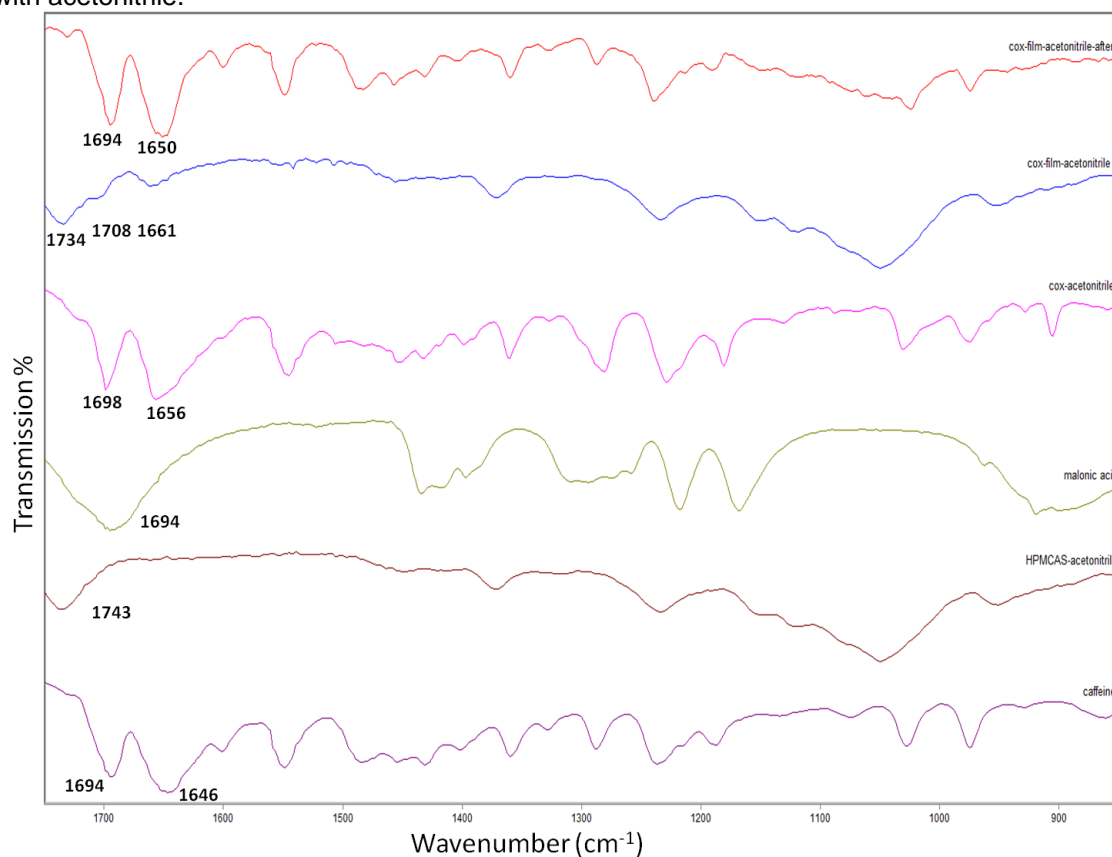


Figure AVII.22. FT-IR scan of co-crystals in a film after 7 month of storage. The film prepared with acetonitrile.

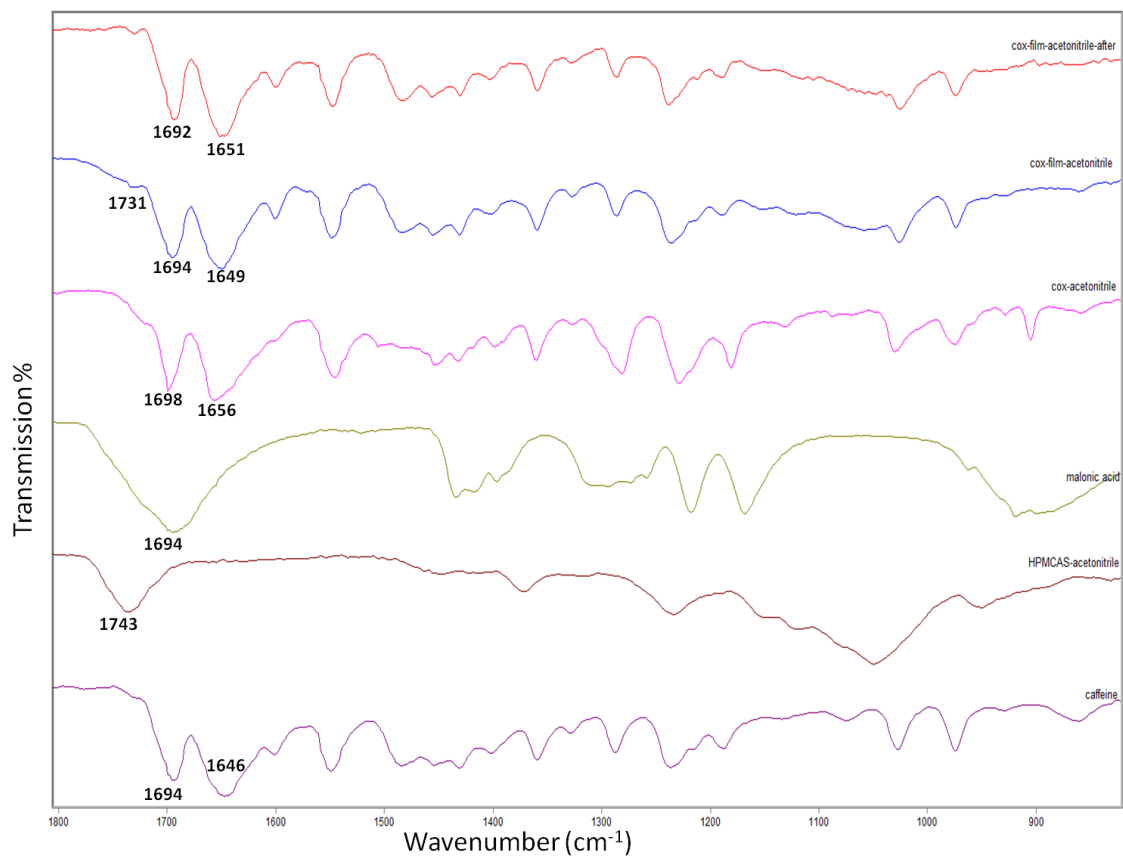


Figure AVII.23. FT-IR scan of co-crystals in a film after 7 month of storage. The film prepared with acetonitrile.